Characterisation of the Rrp5p/Noc1p/Noc2p protein complex and its function in ribosome biogenesis of *Saccharomyces cerevisiae*

DISSERTATION ZUR ERLANGUNG DES DOKTORGRADES DER NATURWISSENSCHAFTEN (DR. RER. NAT.)
DER FAKULTÄT FÜR BIOLOGIE UND VORKLINISCHE MEDIZIN
DER UNIVERSITÄT REGENSBURG

vorgelegt von

Thomas Hierlmeier aus Rottweil

im Januar 2013

Das Promotionsgesuch wurde eingereicht am: 15. Januar 2013

Die Arbeit wurde angeleitet von: Prof. Dr. Herbert Tschochner

Prüfungsausschuss:

Vorsitzender:	Prof. Dr. Thomas Dresselhaus
1. Prüfer:	Prof. Dr. Herbert Tschochner
2. Prüfer:	Prof. Dr. Gunter Meister
3. Prüfer:	Prof. Dr. Klaus Grasser

Tag der mündlichen Prüfung: 01.März 2013

Die vorliegende Arbeit wurde in der Zeit von Januar 2009 bis Januar 2013 am Lehrstuhl Biochemie III des Institutes für Biochemie, Genetik und Mikrobiologie der Naturwissenschaftlichen Fakultät III der Universität Regensburg unter Anleitung von Prof. Dr. Herbert Tschochner angefertigt.

Ich erkläre hiermit, dass ich diese Arbeit selbst verfasst und keine anderen als die angegebenen Quellen und Hilfsmittel verwendet habe. Diese Arbeit war bisher noch nicht Bestandteil eines Prüfungsverfahrens. Andere Promotionsversuche wurden nicht unternommen.

Thomas Hierlmeier
Regensburg, 15. Januar 2013

Table of Contents

1 Summary

Eukaryotic ribosome biogenesis is a very complex process that includes synthesis of the structural components (ribosomal RNAs (rRNAs) and proteins (r-proteins)), processing and folding of rRNA precursors, as well as assembly of the r-proteins onto the rRNA. Ribosome biogenesis starts with the transcription of the genes encoding the rRNAs (rDNA) in the nucleolus by RNA polymerase I and III, and includes transport of pre-ribosomal particles (pre-ribosomes) through the nucleus and export into the cytoplasm, where the final maturation steps occur. In addition to the structural components, these processes require the function of ~75 small nucleolar RNAs and of more than 150 non-ribosomal proteins termed biogenesis factors, which transiently interact with different pre-ribosomes. It could be shown that several subsets of biogenesis factors form protein modules, which are supposed to constitute building blocks of pre-ribosomes and/or to function together in ribosome biogenesis.

In this work, a protein complex consisting of the proteins Rrp5p, Noc1p and Noc2p from *Saccharomyces cerevisiae* could be reconstituted from heterologously expressed proteins. Noc1p and Noc2p are biogenesis factors of the large ribosomal subunit (LSU), whereas Rrp5p is required for maturation of both the large and the small ribosomal subunit (SSU). Analyses of pairwise interactions between the proteins, as well as negative stain electron microscopy of the purified complex provided further insights into architectural and structural features of the Rrp5p/Noc1p/Noc2p biogenesis factor module.

Ex vivo purifications of the module components and analyses of co-purified RNAs and proteins indicated that the Rrp5p/Noc1p/Noc2p module is predominantly associated with the first specific pre-LSU particles. In addition, Rrp5p, Noc1p and Noc2p showed association with early, common ribosomal precursor particles, which are formed before the pathways leading to the small and the large ribosomal subunit are separated. Furthermore, the module components co-purified specific regions of rDNA chromatin from cells treated with crosslinking reagents, and Rrp5p and Noc1p were identified as components of chromatin transcribed by RNA polymerase I. Accordingly, the Rrp5p/Noc1p/Noc2p module appeared to be associated with nascent rRNA precursor transcripts, providing further evidence that the module is recruited very early in ribosome biogenesis.

Individual inactivation or depletion of Rrp5p, Noc1p or Noc2p *in vivo* resulted in severely decreased levels of LSU specific pre-rRNA species and the appearance of aberrant pre-rRNA fragments. In addition, analyses of truncated *noc1* alleles indicated that impaired interactions of Noc1p with Noc2p, Rrp5p or pre-rRNA result in similar pre-rRNA processing phenotypes, suggesting that in absence of the Rrp5p/Noc1p/Noc2p module pre-ribosomes are destabilised and pre-rRNAs are prone to degradation. Furthermore, *in vivo* depletion of one module component and subsequent analyses of the association of the respective non-depleted proteins with pre-rRNA indicated a mutually independent binding of Rrp5p and Noc1p/Noc2p to pre-ribosomes. Accordingly, the module most probably has several binding sites on pre-ribosomal particles.

In summary, the results presented here suggest that formation of the Rrp5p/Noc1p/Noc2p module plays a role in the structural organisation of early LSU precursor particles and

thereby contributes to their stability, possibly by preventing inappropriate access of endo- and exonucleases to pre-rRNA. Besides, potential mechanisms of the Noc1p/Noc2p independent function of Rrp5p in SSU biogenesis, and a model for the recruitment of the Rrp5p/Noc1p/Noc2p module to pre-ribosomes are discussed.

Future studies will be required to determine the structure and architecture of this biogenesis factor module in detail. Furthermore, analyses of the RNA binding and folding activities of the module components, and of the impact of the module on the recruitment of r-proteins and/or other biogenesis factors to early pre-ribosomes will help to understand the precise molecular function of the Rrp5p/Noc1p/Noc2p module in ribosome biogenesis. As all three proteins have homologues in higher eukaryotes, it will be interesting to investigate if formation and function of this module are conserved in evolution.

Zusammenfassung

Die eukaryotische Ribosomenbiogenese ist ein hochkomplexer Prozess, der die Synthese der strukturellen Komponenten (ribosomale RNAs (rRNAs) und Proteine (r-Proteine)), Prozessierung und Faltung der rRNA Vorläufer, sowie die Assemblierung der r-Proteine auf der rRNA beinhaltet. Die Ribosomenbiogenese beginnt in einem spezialisierten Teil des Zellkerns, dem Nukleolus, mit der von den RNA Polymerasen I und III katalysierten Transkription der Gene, die die rRNAs (rDNA) codieren. Außerdem umfasst sie den Transport prä-ribosomaler Partikel (Präribosomen) durch den Zellkern und deren Export ins Cytoplasma, wo die finalen Reifungsschritte stattfinden. Zusätzlich zu den strukturellen Komponenten erfordern diese Prozesse die Funktion von etwa 75 kleinen nukleolären RNAs und von mehr als 150 nicht-ribosomalen Proteinen, die als Biogenesefaktoren bezeichnet werden und vorübergehend mit verschiedenen Präribosomen interagieren. Es konnte gezeigt werden, dass verschiedene Gruppen dieser Biogenesefaktoren Proteinkomplexe oder „Module“ bilden, die vermutlich vorgeformte Bausteine von Präribosomen darstellen und/oder in der Ribosomenbiogenese zusammenwirken.

In dieser Arbeit konnte ein Proteinkomplex, der aus den Proteinen Rrp5p, Noc1p und Noc2p der Hefe *Saccharomyces cerevisiae* besteht, aus heterolog exprimierten Proteinen rekonstruiert werden. Noc1p und Noc2p sind Biogenesefaktoren der großen ribosomalen Untereinheit (large ribosomal subunit, LSU), wohingegen Rrp5p sowohl für die Reifung der großen, als auch der kleinen ribosomalen Untereinheit erforderlich ist. Die Untersuchung paarweiser Wechselwirkungen zwischen diesen Proteinen, sowie elektronenmikroskopische Analysen der gereinigten und mit Schwermetall kontrastierten Proteinkomplexe lieferten zusätzliche Erkenntnisse bezüglich architektureller und struktureller Eigenschaften des Rrp5p/Noc1p/Noc2p Biogenesefaktormoduls.

Ex vivo Reinigungen der Modulkomponenten und Analysen der co-gereinigten RNAs und Proteine deuteten darauf hin, dass das Rrp5p/Noc1p/Noc2p Modul vor allem mit den ersten spezifischen Vorläufern der großen ribosomalen Untereinheit assoziiert ist. Daneben zeigten Rrp5p, Noc1p und Noc2p Assoziation mit früheren, gemeinsamen Vorläuferpartikeln der großen und kleinen ribosomalen Untereinheiten. Außerdem konnten aus Extrakten chemisch quervernetzter Hefezellen spezifische Bereiche des rDNA Chromatins zusammen mit den Modulkomponenten aufgereinigt werden, und Rrp5p und Noc1p wurden als Bestandteile von RNA Polymerase I transkribiertem Chromatin identifiziert. Demzufolge scheint das Rrp5p/Noc1p/Noc2p Modul mit naszierenden rRNA Vorläufertranskripten assoziiert zu sein, was einen weiteren Hinweis dafür liefert, dass das Modul sehr früh in der Ribosomenbiogenese rekrutiert wird.

In vivo Inaktivierung oder Depletion einzelner Proteine führte zu stark verringerten Mengen LSU spezifischer prä-rRNA Spezies und zur Bildung aberranter prä-rRNA Fragmente. Desweiteren wiesen Untersuchungen verschiedener verkürzter *noc1* Allele darauf hin, dass beeinträchtigte Interaktionen von Noc1p mit Noc2p, Rrp5p oder prä-rRNA zu einem ähnlichen prä-rRNA Prozessierungsphänotyp führen. Dies lässt vermuten, dass Präribosomen in Abwesenheit des Rrp5p/Noc1p/Noc2p Moduls destabilisiert sind und abgebaut werden. Außerdem lieferten Experimente, in denen eine Modulkomponente *in vivo*

depletiert wurde und anschließend die Assoziation der nicht depletierten Proteine mit prä-rRNA untersucht wurde, Hinweise dafür, dass Rrp5p und Noc1p/Noc2p unabhängig voneinander an Präribosomen binden können. Demzufolge hat das Modul aller Wahrscheinlichkeit nach mehrere Bindestellen an Präribosomen.

Zusammenfassend führen die hier geschilderten Ergebnisse zu der Schlussfolgerung, dass die Ausbildung des Rrp5p/Noc1p/Noc2p Moduls zur strukturellen Organisation früher LSU Vorläuferpartikel und somit zu deren Stabilisierung beiträgt, möglicherweise indem unerwünschter Zugang von Endo- und Exonucleasen zu prä-rRNA verhindert wird. Außerdem werden mögliche Mechanismen für die Noc1p/Noc2p unabhängige Funktion von Rrp5p in der Biogenese der kleinen ribosomalen Untereinheit und ein Modell für die Rekrutierung des Rrp5p/Noc1p/Noc2p Moduls an Präribosomen diskutiert.

Zukünftige Studien sind erforderlich um die Struktur und Architektur dieses Biogenesefaktormoduls im Detail aufzuklären. Außerdem sollten Untersuchungen bezüglich der RNA Bindungs- und Faltungsaktivitäten der Modulkomponenten, sowie des Einflusses des Moduls auf die Rekrutierung von r-Proteinen und/oder anderer Biogenesefaktoren an frühe Präribosomen dazu beitragen, die detaillierte molekulare Funktion des Rrp5p/Noc1p/Noc2p Moduls in der Ribosomenbiogenese zu verstehen. Da alle drei Proteine Homologe in höheren Eukaryoten haben, könnte die Ausbildung und Funktion des Moduls in der Evolution konserviert sein.

2 Introduction

2.1 The function and structure of ribosomes

Ribosomes are ribonucleoprotein particles that catalyse the translation of messenger RNA (mRNA) into proteins (Siekevitz, 1952, Wilson and Nierhaus, 2003; Schmeing and Ramakrishnan, 2009) and are conserved in all domains of life. They consist of a small ribosomal subunit (SSU) that binds the mRNA and contains the decoding centre, which facilitates codon-anticodon recognition between mRNA and tRNAs loaded with amino acids, and a large ribosomal subunit (LSU) that catalyses formation the peptide bond in the peptidyl transferase centre (Fig. 2-1). Notably, not only the interaction between the subunits, but also binding of mRNA, tRNA and formation of the peptide bond is predominantly mediated by the RNA components of the ribosome (ribosomal RNA, rRNA) (Ban et al., 2000; Carter et al., 2000; Wimberly et al., 2000; Yusupov et al., 2001; Ben-Shem et al., 2010, 2011), thus classifying the ribosome as a ribozyme (Cech, 2000). In contrast, the protein components (r-proteins) are mainly required to stabilise the structure of the subunits and for the interaction of the ribosome with translation factors (Stark et al., 2002; Wilson and Nierhaus, 2005), albeit some r-proteins also modulate codon-anticodon recognition (Ogle et al., 2001, 2002).

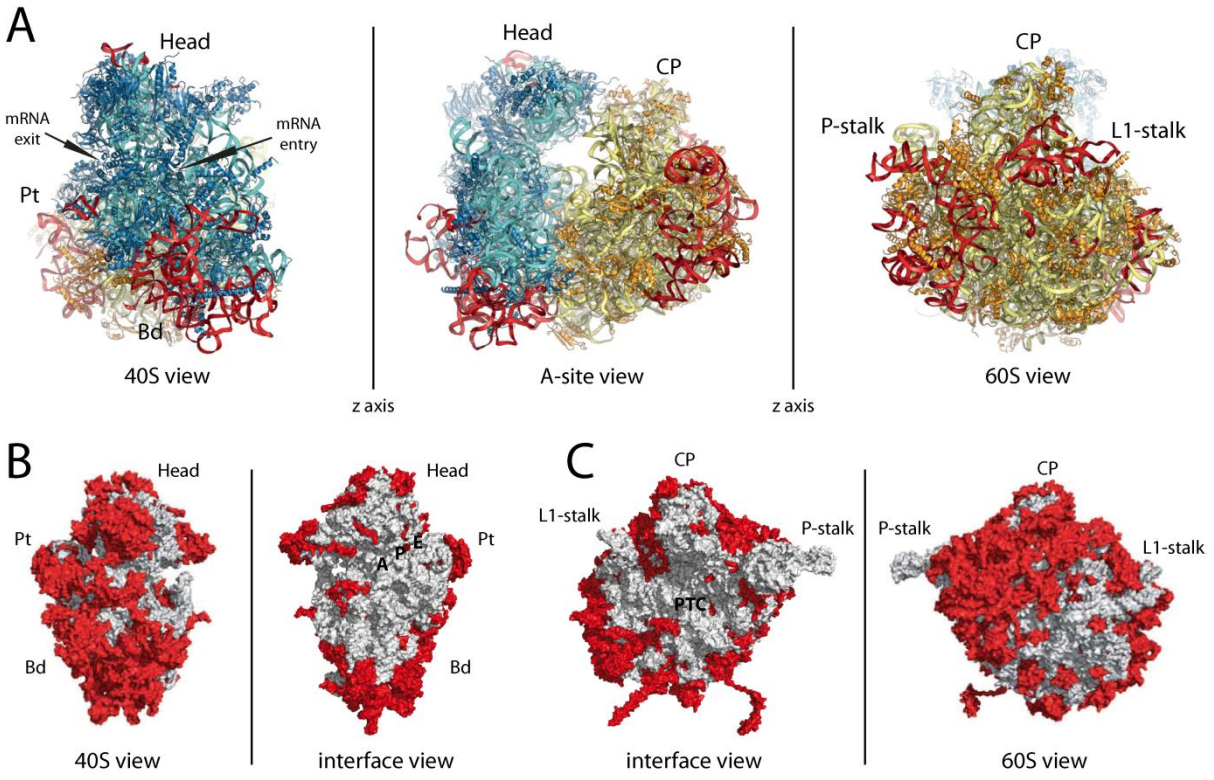

Fig. 2-1 Crystal structure of the 80S ribosome from *Saccharomyces cerevisiae*

A) The middle panel shows the ribosome from the 'side' along the mRNA tunnel viewed from the entry site/aminoacyl tRNA binding site (A-site). RNA and protein components of the SSU are coloured cyan and blue, those of the LSU in yellow and orange, respectively. Expansion segments of the eukaryotic rRNA are coloured red. The left and right panels show the 80S ribosome viewed from the 40S and 60S side and were obtained by rotating the middle structure by 90° and 270° along the z-axis, respectively. (continued on next page)

Fig. 2-1 (continued): Landmark structures of the SSU (head, platform (Pt), body (Bd)) and the LSU (central protruberance (CP), phospho-stalk (P-stalk), L1-stalk) are indicated. Adapted from Jenner et al. (2012) B, C) The large and the small ribosomal subunits are shown from the solvent side (40S view/60S view) or from the subunit interface. Conserved elements are depicted in gray, eukaryotic specific RNA and protein elements are coloured red. tRNA binding sites in the decoding centre (A-, P-, E-sites) and the peptidyl transferase centre (PTC) are indicated. Adapted from Ben-Shem et al. (2011).

Although the function and core structure of ribosomes is highly conserved in evolution, eukaryotic ribosomes are significantly larger (~ 40%) than their prokaryotic counterparts, and according to their sedimentation coefficient these are referred to as 80S and 70S ribosomes, respectively. The difference in size results from additional RNA elements inserted into the conserved rRNA regions, as well as ~ 25 additional ribosomal proteins (r-proteins) and extensions in conserved r-proteins (Spahn et al., 2001; Ben-Shem et al., 2010, 2011) found in eukaryotic ribosomes. These additional elements are predominantly located in solvent accessible regions of the 80S ribosome rather than in the subunit interface, the decoding centre or the peptidyl transferase centre (Fig. 2-1). This is consistent with the conserved, basal mechanism of translation and suggests a role of these additional elements in initiation, termination or regulation of translation, processes which are significantly different in prokaryotes and eukaryotes (Schmeing and Ramakrishnan, 2009; Sonenberg and Hinnebusch, 2009; Jackson et al., 2010).

In eukaryotes, the small, 40S subunit (30S in prokaryotes) contains the 18S rRNA and 32 r-proteins (rpS), whereas the large, 60S subunit (50S in prokaryotes) contains three ribosomal RNAs (5S, 5.8S, 25S/28S rRNAs) and 46 r-proteins (rpL) (Planta and Mager, 1998; Gerbasi et al., 2004). Notably, 5.8S and 25S/28S pre-rRNAs are homologous to the prokaryotic 23S rRNA (Jacq, 1981) and developed by insertion of a spacer sequence into the conserved rRNA region, which is removed during eukaryotic ribosome biogenesis. Consistently, 5.8S rRNA and 5' end of 25S rRNA form the same secondary structure ('domain I', Fig. 2-2) as the 5' part of 23S rRNA. In general, the conserved rRNA regions form highly similar secondary structures in prokaryotes and eukaryotes, which can be divided into three and six domains for the small and the large ribosomal subunit, respectively (Fig. 2-2 A + B). Notably, in case of the SSU the secondary structure domains (5'- , central, 3' domain) constitute distinct elements of the tertiary structure (body, platform, head), whereas the LSU shows a monolithic tertiary structure, in which all secondary structure domains are intertwined and establish multiple interactions (Fig. 2-2 C).

Fig. 2-2 Comparison of the secondary and tertiary structure organisation of the RNA components of the large and the small ribosomal subunit (next page)

A) Schematic presentation of the secondary structure of the prokaryotic 16S (left) and 23S (right) rRNA from *Thermus thermophilus*. Major secondary structure domains are indicated. Adapted from Ramakrishnan and Moore (2001). B) The conserved RNA elements of the eukaryotic 18S (left), 5.8S and 25S rRNAs (right) from *S. cerevisiae* are depicted in blue, black and yellow, respectively, and adopt a highly similar secondary structure as their prokaryotic counterparts. The domains are labelled in the same colour as in (A) and separated by black bars. Eukaryotic expansion segments are coloured red. For practical reasons, the LSU rRNA is split between domains III and IV (dashed line), and two expansion segments (a, b) are depicted separately. The dashed boxes mark the 'central pseudoknot' formed within the 16S/18S rRNA. C) Crystal structures of RNA components of the 40S and 60S subunits from *S. cerevisiae* viewed from the solvent side (40S view/60S view) and the subunit interface. The RNA is coloured according to the secondary structure domains in (B), 5S rRNA in magenta. While distinct tertiary structure elements of the 18S rRNA (body (bd), platform (pt), head) are correlated with the secondary structure domains, the LSU shows a monolithic tertiary structure, in which all secondary structure domains are intertwined and establish multiple interactions. (B) was adapted from Jenner et al. (2012), (C) was derived from the structure published in Ben-Shem et al. (2011).

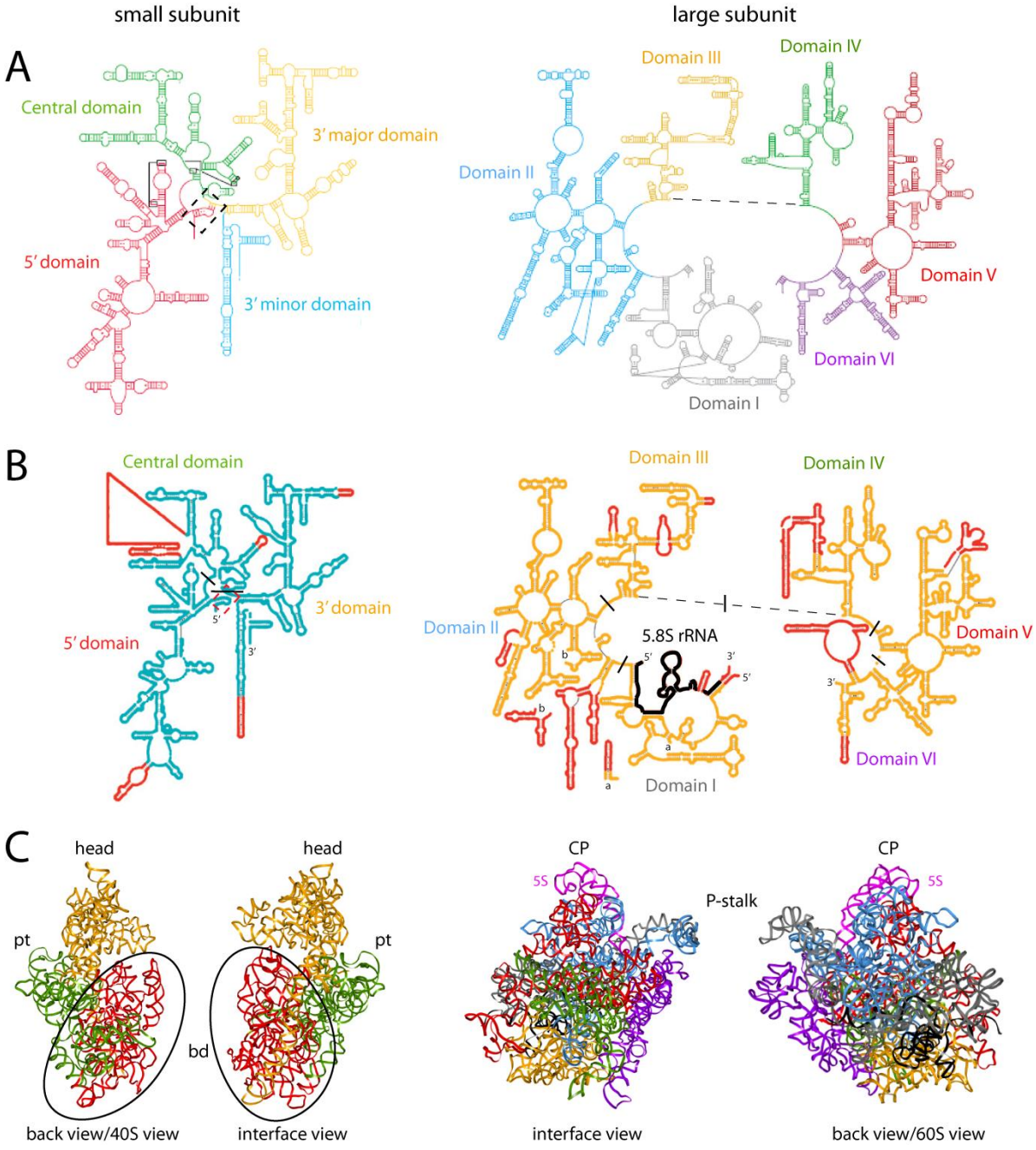

2.2 Ribosome biogenesis in eukaryotes

2.2.1 Overview

Ribosome biogenesis is a highly complex and energy consuming process that requires the action of all three eukaryotic RNA polymerases. In a rapidly growing yeast cell, 60% of total transcription is devoted to ribosomal RNA, and 50% of RNA polymerase II transcription and 90% of mRNA splicing are devoted to r-proteins to ensure the production of around 2000 ribosomes per minute (Warner, 1999). Ribosome biogenesis starts with the transcription of the genes encoding the rRNAs in a specialized nuclear compartment, the nucleolus, and ends with final maturation steps in the cytoplasm, where mature ribosomes translate mRNAs into proteins (Fig. 2-3). Amongst others, this process includes RNA modification, processing

and folding events, assembly of the r-proteins onto the rRNAs and transport and export of ribosomal precursor particles (pre-ribosomes) through/from the nucleus. In addition to the structural components, more than 70 small nucleolar RNAs (snoRNAs) and more than 150 proteins termed biogenesis factors, which transiently interact with different pre-ribosomes, are required to generate functional ribosomes. Most knowledge about eukaryotic ribosome biogenesis available today was obtained from studies in *Saccharomyces cerevisiae*, as this model organism is well accessible for genetic manipulations, cell biological techniques and biochemical approaches. Importantly, the majority of ribosome biogenesis factors are conserved in evolution, and a growing number of studies in higher eukaryotes indicate that ribosome biogenesis follows general mechanisms with some species specific differences (Henras et al., 2008). In this work, all statements are referred to the situation in *S. cerevisiae*, unless otherwise stated.

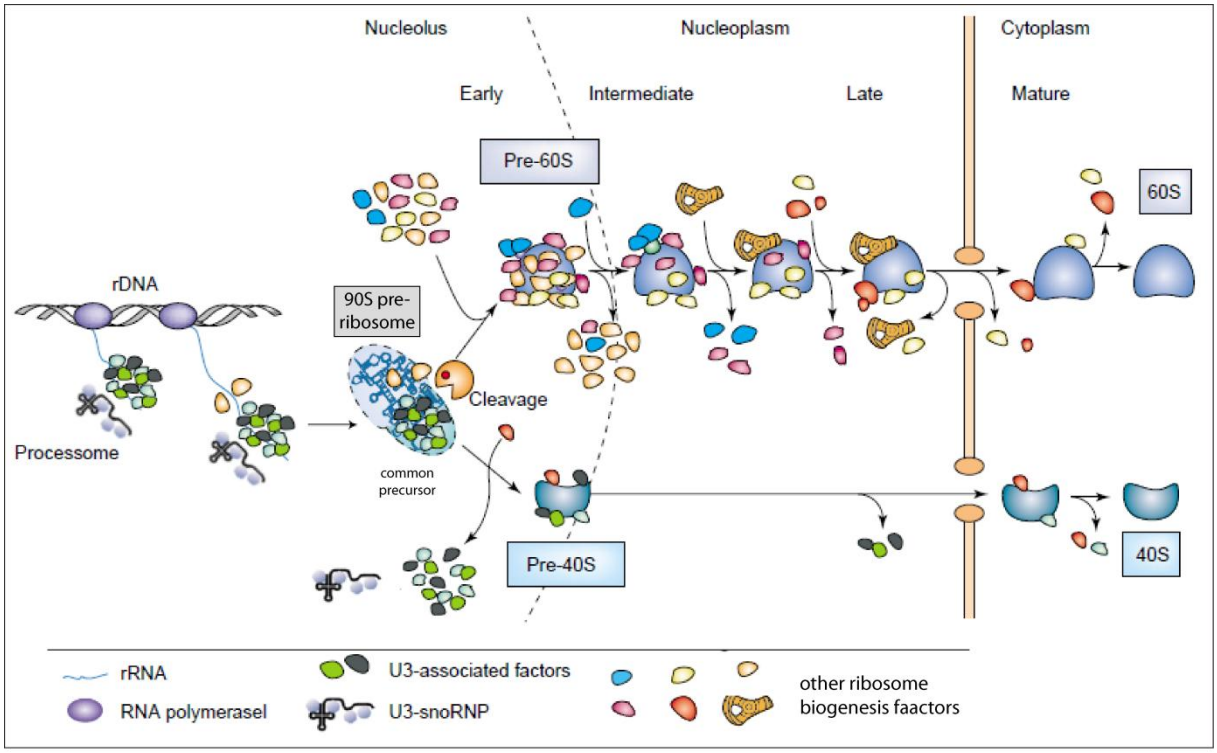

Fig. 2-3 Schematic overview of eukaryotic ribosome biogenesis

Ribosome biogenesis starts in the nucleolus with the transcription of rRNA genes yielding a common precursor particle. In the course of maturation, numerous ribosome biogenesis factors are associated with different pre-ribosomal particles, which are transported from the nucleolus through the nucleoplasm into the cytoplasm, where the mature subunits enter the translation cycle (see main text for details). Adapted from Tschochner and Hurt (2003).

2.2.2 The genes encoding the ribosomal RNAs are transcribed in the nucleolus

The nucleolus is a substructure within the nucleus that is visible in light microscopy as a dark spot in the nucleoplasm and is not separated by a membrane. Higher resolution analyses with electron microscopy identified three subcompartments of the nucleolus, the fibrillar centers (FC), dense fibrillar components (DFC) and granular components (GC) (for recent

reviews see (Raška et al., 2006, Hernandez-Verdun et al., 2010)) (Fig. 2-4). Further studies analysing DNA and protein composition of these nucleolar regions, as well as morphological studies in mutant yeast strains showed that these structures are linked to ribosome biogenesis (Oakes et al., 1998; Léger-Silvestre et al., 1999; Trumtel et al., 2000). In detail, there is evidence that the rRNA genes (rDNA) are localised in the FCs, whereas RNA polymerase I (Pol-I), which transcribes the rDNA, was detected at the boundary between FC and DFC. Accordingly, it was suggested that the DFC contains the nascent Pol-I transcripts as well as the earliest pre-ribosomal particles, which subsequently undergo further maturation steps in the GC before transport to the nucleoplasm and export to the cytoplasm.

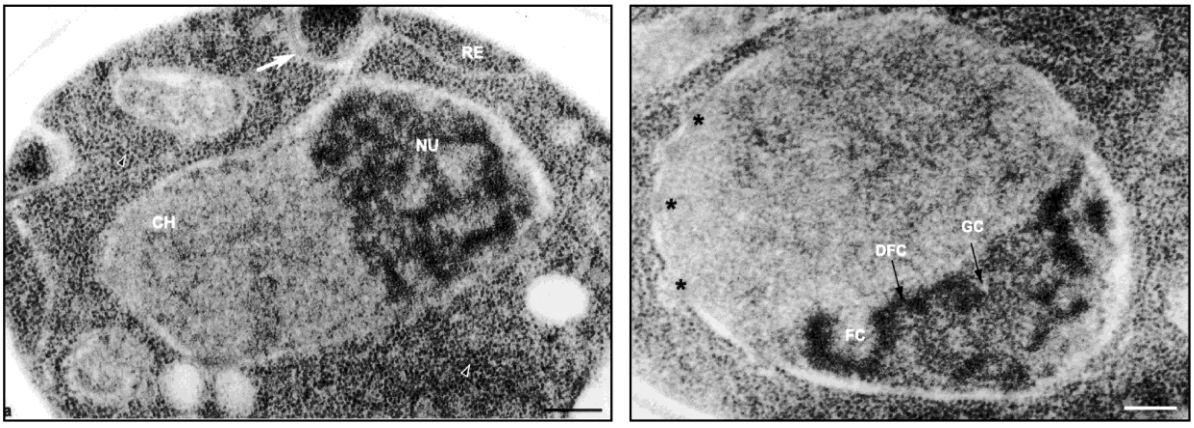

Fig. 2-4 Morphology of the nucleolus in *Saccharomyces cerevisiae*

Yeast cells were subjected to cryo-fixation and freeze substitution and subsequently analysed by transmission electron microscopy. Left panel: Overview of a yeast cell. The nucleus is surrounded by the nuclear envelope (bright line) and consists of a heavily contrasted region, the nucleolus (NU), and a brighter region (CH). An invagination of the plasma membrane (arrow) and part of the endoplasmatic reticulum (RE) are indicated. Right panel: A detailed view of the nucleus shows different substructures within the nucleolus, where different steps of ribosome biogenesis take place (see main text for details), namely the fibrillar centres (FC) near the nuclear envelope, the dense fibrillar components (DFC) surrounding the FCs and extending through the nucleolar region, and the granular components (GC) filling the remainder of the nucleolus. Nuclear pores are marked by asterisk. Scale bars correspond to 200 nm. Adapted from Léger-Silvestre et al. (1999).

In yeast, the genes encoding the ribosomal RNAs are organised in so called ‘rDNA repeats’ that are located in ~ 150 copies on chromosome XII (Petes, 1979; Long and Dawid, 1980) (Fig. 2-5 A). In each rDNA repeat, the 18S, 5.8S and 25S rRNA coding regions are arranged in an operon like structure, the 35S rDNA, which is separated from the 5S rDNA by a non-coding sequence termed intergenic spacer (IGS) (Philippsen et al., 1978). 35S and 5S rDNA are transcribed by RNA polymerase I (Pol-I) and RNA polymerase III (Pol-III), respectively (Sentenac, 1985). As RNA polymerase II (Pol-II), which synthesizes mRNAs, these enzymes are multi-subunit protein complexes, and all three polymerases have a common core of shared subunits but also several specific subunits (Paule and White, 2000). Note that in all eukaryotes the rRNA genes are arranged in multi-copy cluster(s) and 18S, 5.8S and 25S rRNA genes are generally organized in one transcription unit, probably to satisfy the high demand for ribosomal RNA and to ensure equal transcription levels, whereas strict co-localization with the 5S rRNA gene on one rDNA repeat is not observed in most other species, including *Schizosaccharomyces pombe* (Haeusler and Engelke, 2006).

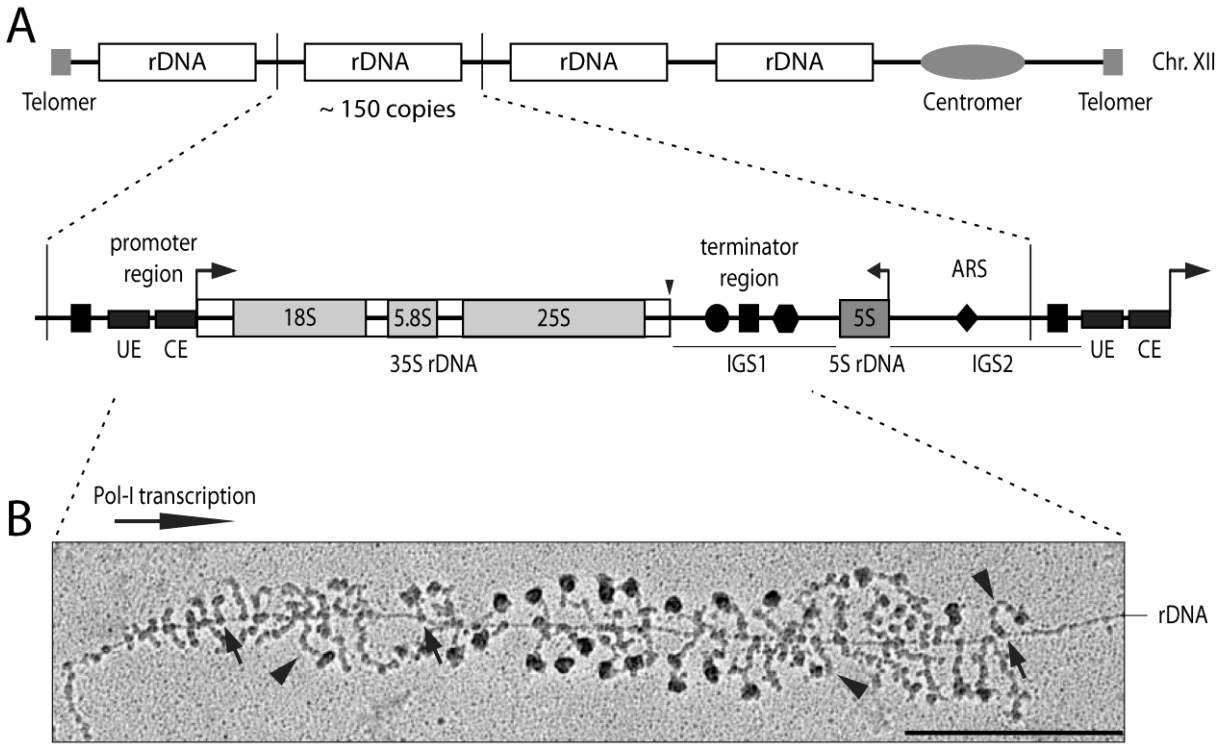

Fig. 2-5 The rRNA gene locus in *Saccharomyces cerevisiae*

A) The genes encoding the ribosomal RNAs are organised in so called 'rDNA repeats' that are located in ~ 150 copies on chromosome XII. In each rDNA repeat, the 18S, 5.8S and 25S rRNA coding regions are arranged in an operon like structure, the 35S rDNA, which is separated from the 5S rDNA by a non-coding sequence termed intergenic spacer (IGS1/2). The directions of Pol-I and Pol-III transcription are indicated by arrows, and positions of relevant DNA elements are marked. The 35S rDNA promoter contains the 'upstream element' (UE) and the 'core element' (CE), a sequence encoding a Rnt1p cleavage site (arrowhead) is located at the end of the 35S rDNA, IGS1 contains a T-rich element (circle), a Reb1 binding site (square) and the replication fork barrier (hexagon), and IGS2 contains an autonomous replication sequence (diamond) as well as another Reb1 binding site. B) Electron micrograph of a Miller chromatin spread showing a transcribed rDNA repeat. Pol-I molecules on the rDNA are marked by arrows, the nascent rRNA by arrowheads. Scale bar represents 0.5 µm. Adapted from Osheim et al. (2004).

Efficient initiation of Pol-I transcription *in vivo* requires the action of four transcription factors (core factor (CF), upstream activation factor (UAF), TATA box binding protein (TBP), Rrn3p) and two regulatory *cis* elements in the Pol-I promoter region, namely the core element (CE), locating to positions -28 to + 8 relative to the transcription start site (TSS) and the upstream element (UE; -146 to -51 relative to the TSS) (Musters et al., 1989; Kulkens et al., 1991) (Fig. 2-5 A). Rrn3p can bind to the Pol-I subunit Rpa43p, and only Pol-I molecules associated with Rrn3p are competent for transcription initiation *in vitro* (Yamamoto et al., 1996; Milkereit and Tschochner, 1998; Peyroche et al., 2000). CF, consisting of Rrn6p, Rrn7p and Rrn11p (Keys et al., 1994; Lalo et al., 1996), binds to the core element, and can recruit an Rrn3p-Pol-I complex to rDNA, possibly via direct interaction between Rrn6p and Rrn3p (Peyroche et al., 2000). UAF, consisting of Rrn5p, Rrn9p, Rrn10p and Uaf30p and the two histones H3 and H4 (Keys et al., 1996; Keener et al., 1997; Siddiqi et al., 2001), binds to the upstream element, and TBP can interact with Rrn6p and Rrn9p, thereby bridging CF and UAF, which appears to be required for stable association of CF with rDNA (Steffan et al., 1998). Accordingly, the current model for transcription initiation suggests that UAF, TBP and CF build a platform on the Pol-I promoter, to which an Rrn3p-Pol-I complex is recruited, resulting

in high level transcription of 35S rDNA. Besides, several other factors are described to play additional roles in Pol-I transcription, for instance Hmo1p, which maintains an accessible rDNA structure (Gadal et al., 2002a) or elongation factors as Fcp1p, Spt4p, Spt5p or Paf1C (Fath et al., 2004; Schneider et al., 2006; Zhang et al., 2009, 2010). Termination of Pol-I transcription termination depends on several *cis* elements downstream of the 3' end of the 35S rRNA coding region (T-rich element, Reb1-binding site, replication fork barrier; Fig. 2-5 A) (Lang and Reeder, 1993, 1995; Lang et al., 1994; El Hage et al., 2008), and on trans acting factors that bind to these elements (Nsi1p, Fob1p) (Prescott et al., 2004; Huang et al., 2006; El Hage et al., 2008; Reiter et al., 2012). Furthermore, release of the 35S rRNA by endonucleolytic cleavage of the nascent transcript by Rnt1p or an alternative, unknown nuclease, and subsequent exonucleolytic degradation of the downstream transcript could also contribute to the dissociation of Pol-I from the rDNA (Prescott et al., 2004; El Hage et al., 2008; Kawauchi et al., 2008).

Notably, even in exponentially growing cells only ~ 50% of the 35S rDNA repeats are actively transcribed, whereas the other half is transcriptionally silent and packaged into nucleosomes, which appears to be important for the integrity of the rDNA locus (Ide et al., 2010). Active repeats are simultaneously transcribed by a large number of Pol-I molecules (up to 120 molecules per 35SrDNA (Osheim et al., 2009)), which can be visualized in Miller chromatin spreads (Miller and Beatty, 1969) by electron microscopy (Fig. 2-5 B).

2.2.3 Processing and modification of ribosomal RNAs

The primary transcript of Pol-I contains the sequences of the 18S, 5.8S and 25S rRNAs, separated by two internal transcribed spacer (ITS1, ITS2) regions and flanked by external transcribed spacer regions (5' ETS, 3' ETS), which are sequentially removed via a complex series of endo- and exonucleolytic processing events to generate the mature rRNAs (Fig. 2-6).

Endonucleolytic cleavage in the 3'ETS region at site B0 by Rnt1p releases the 35S pre-rRNA, and endonucleolytic cleavages at sites A0 and A1 by so far unknown nucleases generate the 5' end of 18S rRNA. Then, cleavage at site A2, possibly by Rcl1p (Horn et al., 2011), separates the SSU specific 20S pre-rRNA from the LSU specific 27SA2 pre-rRNA. Cleavage of the 20S pre-rRNA at site D by the endonuclease Nob1p in the cytoplasm removes the remainder of the ITS1 sequence and generates the 3' end of mature 18S rRNA (Udem and Warner, 1973; Fatica et al., 2003; Lamanna and Karbstein, 2009, 2011; Pertschy et al., 2009). Further processing of the 27SA2 pre-rRNA occurs via two mutually exclusive pathways, both resulting in the same 25S rRNA sequence, but yielding alternative forms of 5.8S rRNA that differ in length by 6 nucleotides at the 5' end ($5.8S_S$/$5.8S_L$). Accordingly, eukaryotic cells possess at least two different populations of ribosomes that contain either $5.8S_S$ or $5.8S_L$ rRNA, which might play a role in transcribing different mRNAs, but so far no specific functions could be demonstrated. The major pathway (~ 80%), resulting in the 5' end of $5.8S_S$ rRNA, involves endonucleolytic cleavage at site A3 by RNase MRP (Schmitt and Clayton, 1993; Chu et al., 1994; Lygerou et al., 1996) yielding 27SA3 pre-rRNA, and subsequent exonucleolytic trimming to site B1S by Rat1p or Rrp17p (Henry et al., 1994;

Oeffinger et al., 2009). Alternatively, processing at site B1L, most likely by a so far unknown endonuclease (Faber et al., 2006), generates the 5' end of $5.8S_L$ rRNA. Concomitant with the formation of the 5' ends of the 5.8S rRNAs, the 3' end of 25S rRNA is formed by exonucleolytic trimming involving Rex1p (Kempers-Veenstra et al., 1986; van Hoof et al., 2000), yielding the alternative $27SB_S$/$27SB_L$ pre-rRNAs that are further on processed in the same way. First, endonucleolytic cleavage at site C2 by an unknown nuclease separates $7S_{L/S}$ and 26S pre-rRNAs that are subsequently converted to $5.8S_{L/S}$ and 25S rRNA by exonucleolytic trimming. Formation of the 5' end of 25S rRNA by Rat1p and/or Rrp17p appears to be completed in the nucleus (Geerlings et al., 2000; Oeffinger et al., 2009), whereas formation of the 3' end of 5.8S rRNA apparently includes nuclear steps as well as a final, cytoplasmic trimming event. The former involve the exosome (Allmang et al., 1999b), a ubiquitous multi-subunit complex with 3'->5' exonuclease activity provided by Rrp44p, as well as Rrp6p, a component specific for nuclear exosomes, and Rex1p, whereas the latter requires only Ngl2p (Briggs et al., 1998; Allmang et al., 1999a; van Hoof et al., 2000; Faber et al., 2002; Thomson and Tollervey, 2010). Note that in yeast processing at sites A0, A1 and A2 frequently occurs co-transcriptionally on the nascent 35S pre-rRNA (Kos and Tollervey, 2010), releasing 20S pre-rRNA while the LSU specific rDNA is still transcribed by Pol-I (see also section 2.2.5). In this case, Rnt1p cleavage releases 27SA pre-rRNA which subsequently undergoes the same maturation as described above.

In an alternative, minor pathway (Fig. 2-6 C), A3 processing can occur first, resulting in the formation of 27SA3 pre-rRNA, which subsequently undergoes normal maturation, and 23S pre-rRNA, which can then be processed at sites A0, A1 and A2 to yield 22S, 21S and 20S pre-rRNAs, respectively.

In addition to pre-rRNA processing events, numerous modifications, predominantly pseudouridinylations and 2'-O-methylations, are introduced at specific sites of the rRNA sequences early during ribosome biogenesis (Retèl et al., 1969; Brand et al., 1977; Kos and Tollervey, 2010). These reactions are catalysed by two different classes of small nucleolar ribonucleoprotein particles (snoRNPs), box H/ACA snoRNPs (Ganot et al., 1997; Ni et al., 1997) and box C/D snoRNPs (Cavaillé et al., 1996; Tycowski et al., 1996), respectively. The snoRNPs consist of a variable snoRNA that guides the snoRNP to a specific modification site by base pairing with rRNA, and of common protein components specific for each class. For box H/ACA snoRNPs, these are the catalytic subunit Cbf5p as well as the core proteins Gar1p, Nhp2p and Nop10p, and box C/D snoRNPs contain the catalytic subunit Nop1p/fibrillarin as well as Nop56p, Nop58p and Snu13p. Although single modifications are not essential, there is growing evidence that the sum of modifications is important for the function of the ribosome, and also affects ribosome biogenesis (King et al., 2003; Liang et al., 2007, 2009).

Fig. 2-6 (continued from next page): C) Alternative pre-rRNA processing pathways bypassing A2-site processing and yielding 27SA3 and 23S or 21S pre-rRNA (see main text for details). Normally, 27SA3 is subsequently processed via the B1s pathway yielding 25S and 5.8Ss rRNAs. However, mutant analyses indicated that 27SA3 pre-rRNA can also be substrate for processing site B1L (dashed line), yielding 25S and $5.8S_L$ rRNAs (e.g.Torchet and Hermann-Le Denmat, 2000). Adapted from Hierlmeier et al. (2012).

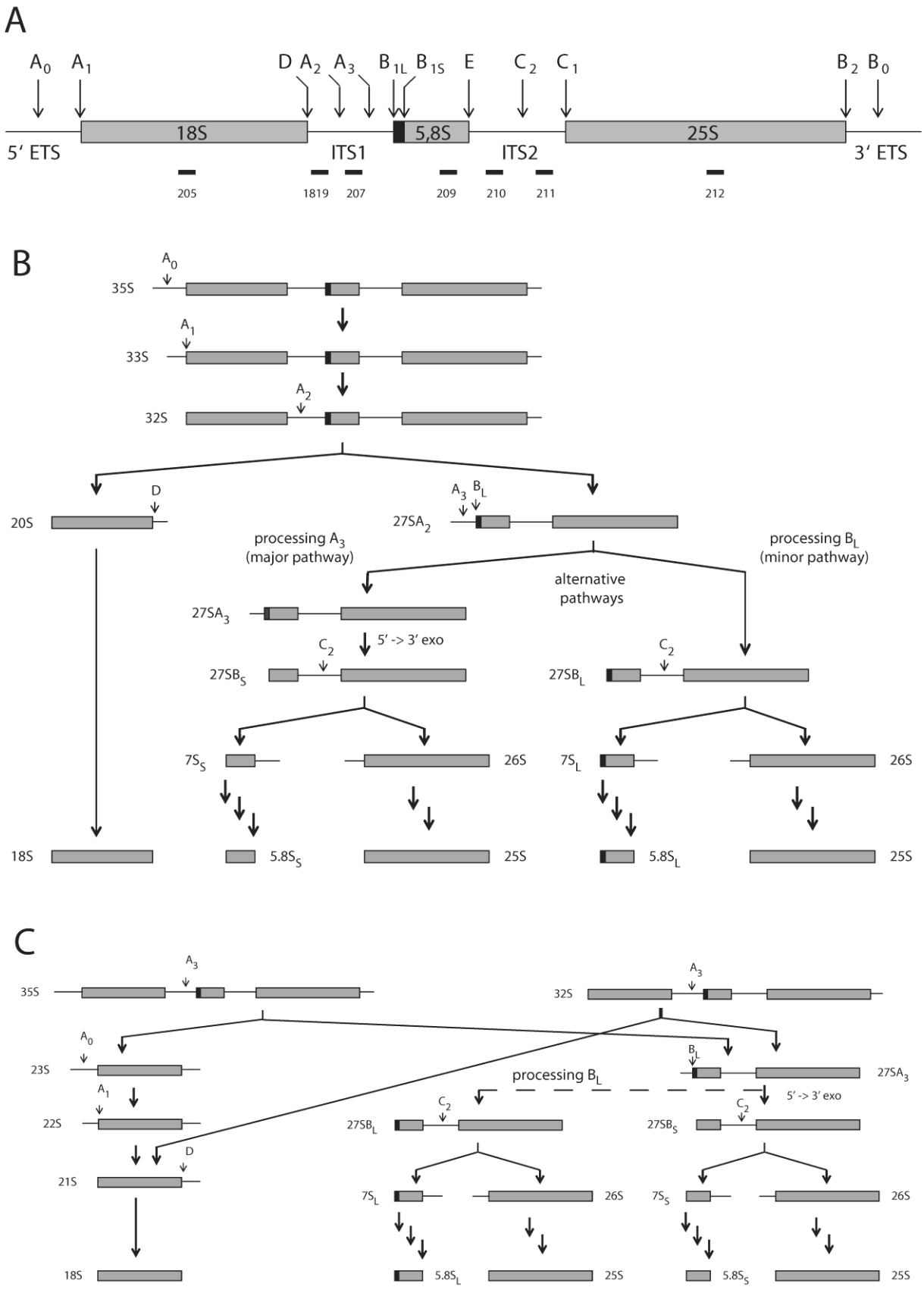

Fig. 2-6: pre-rRNA processing in *Saccharomyces cerevisiae*

A) The 35S rRNA gene contains the sequences of 18S, 5.8S and 25S rRNAs separated by two internal transcribed spacer (ITS1, ITS2) regions and flanked by external transcribed spacer regions (5'-ETS, 3'-ETS). Processing sites of precursor rRNAs are indicated (A0, A1, etc.). Positions of antisense oligo probes (o205, etc.) used for Northern hybridisation and primer extension analyses are indicated with bars. B) Canonical pre-rRNA processing pathways (see main text for details). (continued on previous page)

2.2.4 Nuclear surveillance of ribosome biogenesis and degradation of aberrant ribosomal precursor RNAs

To ensure that only functional ribosomes are produced, and to prevent that ribosome biogenesis factors are sequestered into aberrant pre-ribosomal particles, which would result in a rapid block of ribosome biogenesis, these are efficiently degraded in the nucleus by different nucleases (for recent reviews see Houseley et al., 2006; Vanacova and Stefl, 2007; Houseley and Tollervey, 2009). The major quality control mechanism involves the TRAMP complex and the nuclear exosome, which is also involved in formation of the 3' end of 5.8S rRNA (section 2.2.3). The TRAMP (Trf/Air/Mtr4 polyadenylation) complex polyadenylates aberrant pre-rRNAs (Fang et al., 2005; LaCava et al., 2005; Vanácová et al., 2005), which is the signal for subsequent degradation by the nuclear exosome (Mitchell et al., 1997; Allmang et al., 2000). TRAMP complexes contain one of the poly-A polymerases Trf4p (TRAMP4) or Trf5p (TRAMP5), one of the Zn-knuckle proteins Air1p or Air2p, and the putative RNA helicase Mtr4p. Recently it could be shown that Air2p binds to RNA and bridges between Trf4p and Mtr4p, which is crucial for the activation of the exosome (Holub et al., 2012). Notably, the different TRAMP4/5 complexes appear to act on aberrant LSU and SSU pre-rRNAs, respectively (Dez et al., 2006, 2007; Houseley et al., 2006; Wery et al., 2009). Although, the mechanism how TRAMP complexes distinguish aberrant from productive pre-rRNA species is still unknown, a kinetic discrimination model was suggested, according to which biogenesis factors that are not appropriately released from aberrant pre-ribosomal particles could recruit the TRAMP complex (Dez et al., 2007).
Furthermore, Rat1p, the 5'->3' exonuclease involved in formation of the 5' ends of $5.8S_S$ and 25S pre-rRNAs (section 2.2.3) and removal of excised 5'ETS and ITS1 sequences (Petfalski et al., 1998), also functions in the degradation of aberrant pre-rRNAs (Fang et al., 2005), raising the question, how the processing and degradation functions are regulated. Recently, it was suggested that trimming of the ITS1 sequence by Rat1p could be precisely stopped at site $B1_S$ by formation of a defined RNA structure stabilised by RNA-protein interactions ((Pöll et al., 2009; Sahasranaman et al., 2011); see also section 2.2.6 for more details). In this way, pre-rRNA processing could switch to degradation of aberrant pre-ribosomes if this structure cannot be formed. In general, all exonucleases involved in rRNA processing act on several substrates (section 2.2.3), indicating that they have no pronounced sequence specificity. Accordingly, access of the nucleases to pre-rRNA has to be tightly controlled to prevent unspecific degradation. This could be achieved by the structural organisation of pre-ribosomes, resulting in inaccessible 5' and 3' RNA ends by base-pairing, protein binding and/or orientation to the core of the particles.

2.2.5 Maturation of the small ribosomal subunit

Besides the nucleases involved in pre-rRNA processing and the snoRNP protein components (section 2.2.3), a large number of additional biogenesis factors, which transiently interact with different pre-ribosomal particles, is required for the formation of mature ribosomal subunits. However, to date, the precise molecular function of most of those remains elusive. Many ribosome biogenesis factors, in particular those associated with early

pre-ribosomes, are supposed to play a role in the structural organisation of pre-ribosomes and thus to stabilise pre-rRNAs and to facilitate RNA processing and folding, as well as r-protein assembly (see below and section 2.2.6 for details). Furthermore, a few biogenesis factors are homologous to r-proteins and are thus supposed to act as place holders in pre-ribosomes until the respective r-proteins are incorporated (e.g. Rlp24p (Saveanu et al., 2001), Mrt4p (Rodríguez-Mateos et al., 2009)). In addition, some biogenesis factors function as export adaptors and are required for the transport of LSU and/or SSU precursors through the nuclear pore. Only a subset of biogenesis factors has predicted enzymatic functions like GTPase, ATPase or helicase activity (reviewed in Kressler et al., 2010), and just in few cases this was experimentally validated. In this chapter, the focus is set on early, nucleolar SSU maturation events, whereas later nucleoplasmic and cytoplasmic biogenesis events as well as nuclear export are just briefly summarised (reviewed in detail in (Henras et al., 2008; Panse and Johnson, 2010; Karbstein, 2011).

Initial studies by Trapman and Planta (1975) identified a particle showing a sedimentation coefficient of 90S and containing 35S pre-rRNA as the common precursor to the large and the small ribosomal subunits. To generate the SSU specific 20S pre-rRNA from the 35S pre-rRNA by processing at sites A0, A1 and A2, the function of ~ 50 biogenesis factors (see below) and three snoRNAs (U3 (Kass et al., 1990; Savino and Gerbi, 1990; Hughes and Ares, 1991), U14 (Zagorski et al., 1988; Li et al., 1990), snR30 (Morrissey and Tollervey, 1993)), as well as the presence of many r-proteins of the small subunit (Ferreira-Cerca et al., 2005) are required.

Of these snoRNAs, which belong to the box C/D (U3, U14) and box H/ACA (snR30) snoRNAs, only U14 guides a RNA modification, but all of them can form base pairing interactions with pre-rRNAs in regions where no RNA modifications are introduced, which is supposed to facilitate correct processing and folding of pre-rRNA (Beltrame and Tollervey, 1995; Liang and Fournier, 1995; Borovjagin and Gerbi, 2000; Karbstein, 2011). This has been most extensively studied for U3 snoRNA, which has several binding sites within the 5' ETS region as well as in the 18S rRNA sequence (Fig. 2-7; (Beltrame and Tollervey, 1992, 1995; Hughes, 1996; Méreau et al., 1997; Sharma and Tollervey, 1999; Dutca et al., 2011; Kudla et al., 2011). The former appear to be crucial for initial binding to pre-rRNA, whereas the latter are incompatible with the base pairings found in the 'central pseudoknot', a characteristic RNA structure of the mature SSU, which involves base pairing between distant regions of the 18S rRNA (Fig. 2-7 A). Accordingly, U3 snoRNA (Fig. 2-7 B) prevents premature formation of secondary and tertiary rRNA structure elements found in mature ribosomes (Fig. 2-7C), and could hence maintain the pre-rRNA accessible for the assembly of r-proteins. In addition, snoRNAs could specifically recruit biogenesis factors (e.g. helicases, nucleases) to distinct regions of the pre-rRNA as suggested for snR30 (Fayet-Lebaron et al., 2009), and establish RNA structures required for processing events.

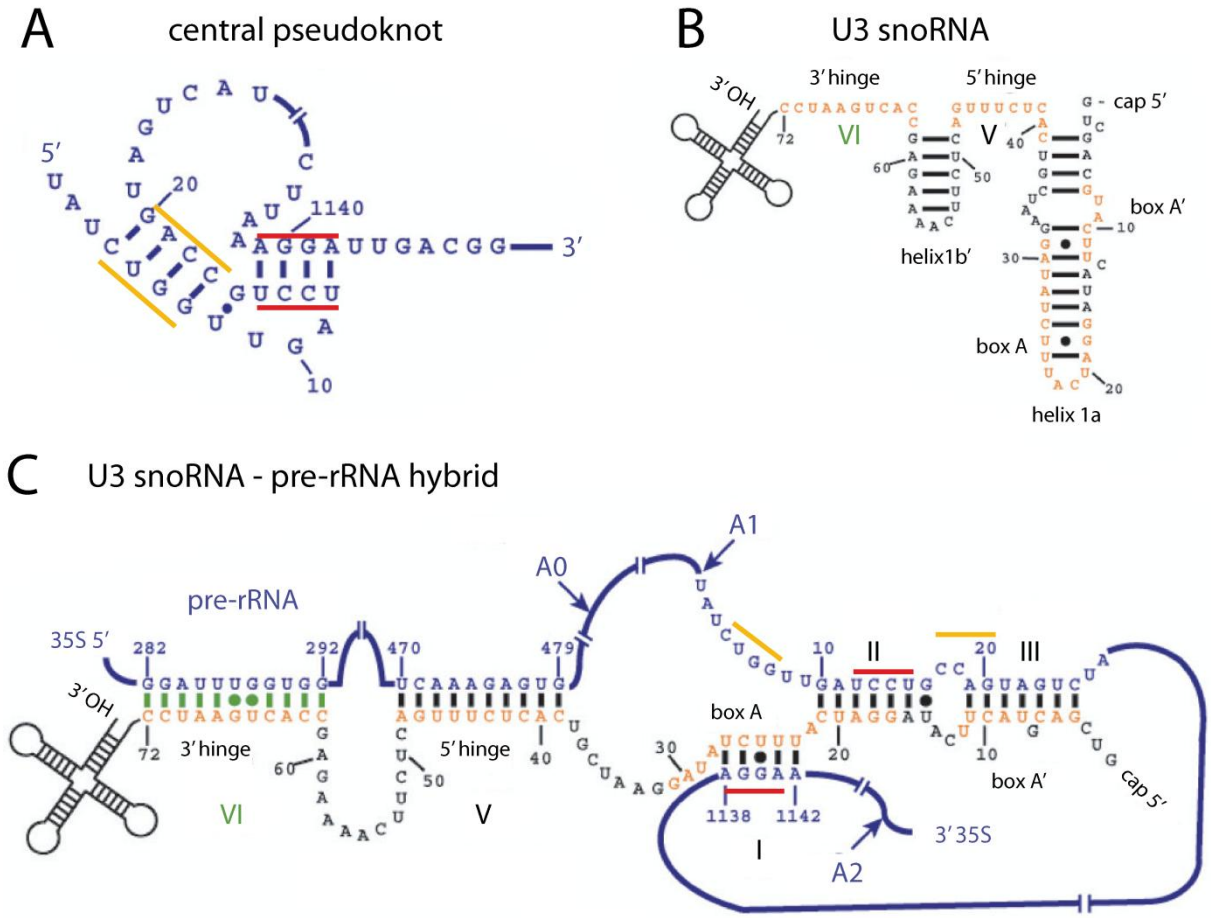

Fig. 2-7: The function of the U3 snoRNA in ribosome biogenesis

A) The 5' end of the 18S rRNA forms a structure termed 'central pseudoknot' with the central region of 18S rRNA by base pairing interactions (see also Fig. 2-2). Nucleotide positions are numbered from the 5' end of 18S rRNA. B) Schematic view of the of the U3 snoRNA secondary structure. C) Predicted base pairing interactions of U3 snoRNA with pre-rRNA in the 5' ETS region and in the 18S rRNA sequence, which are not compatible with the formation of the central pseudoknot. Note that not all U3-rRNA interactions are experimentally validated. Yellow and red lines mark nucleotides involved in formation of the central pseudoknot. Nucleotide positions in the 5' ETS region are numbered from the 5' end of 35S pre-rRNA. Processing at site A1 generates the 5' end of 18S rRNAan numbering of 18S rRNA nucleotides is as in (A). Adapted from Henras et al. (2008).

Already two decades ago, it was proposed that in analogy to the spliceosome, binding of the snoRNAs and other factors to 35S pre-rRNA could form a large RNP complex, a 'processome' facilitating ribosome biogenesis (Fournier and Maxwell, 1993). Ten years later, the Baserga group purified a large RNP containing the U3 snoRNA, which sedimented at ~80S and contained, besides ten known U3 snoRNA interacting proteins, a set of 17 previously unknown proteins (named 'U three proteins'; Utps) that also affect SSU maturation, as well as some rpS, and hence referred to it as the 'SSU processome' (Dragon et al., 2002). In parallel, using several affinity tagged biogenesis factors the Hurt group (Grandi et al., 2002) isolated early pre-ribosomal particles which sedimented at ~ 90S and contained U3 snoRNA and pre-rRNAs containing the 5'ETS sequence. However, since pre-rRNAs were just analysed in distinct primer extension reactions, it remained unclear, whether, and in which ratios, these particles contain 35S and/or 23S pre-rRNAs, and thus if a single precursor or a mixture of several, subsequent pre-ribosomes was isolated. Furthermore, several rpS, but only few rpL, were identified in these particles, as well as 35 non-ribosomal proteins, which were largely overlapping with the ones identified in the 'SSU

processome'. Notably, the additional non-ribosomal proteins found in these particles were in a later report also classified as SSU processome components, as they localise to the nucleolus, co-purify the SSU processome components U3 snoRNA and Mpp10p, and affect 18S synthesis (Bernstein et al., 2004). Accordingly the particles identified by the Baserga and Hurt laboratories could represent the same, common 90S precursor to the large and small ribosomal subunits described by Trapman and Planta (1975).

Remarkably, formation of the SSU processome occurs already co-transcriptionally on the nascent 35S pre-rRNA (Mougey et al., 1993; Osheim et al., 2004; Wery et al., 2009), which can be visualized in electron micrographs of Miller chromatin spreads as knob like structures at the ends of the nascent transcripts (Miller and Beatty, 1969) (see below; Fig. 2-9). These 'terminal balls' or 'terminal knobs' are not formed when the 5'ETS region is mutated or when U3 snoRNA or other SSU processome components are depleted in the cells (Mougey et al., 1993; Dragon et al., 2002; Osheim et al., 2004). Furthermore, in cells depleted of SSU processome components, levels of 35S and 23S pre-rRNA are elevated, whereas levels of 32S, 20S and 27SA2 are reduced, indicating impaired processing of sites A0, A1, A2 and alternative processing of 35S pre-rRNA at site A3 (Baudin-Baillieu et al., 1997; Dunbar et al., 1997; Venema et al., 2000; Bernstein et al., 2004; Gallagher et al., 2004). In addition, pre-rRNAs appear to be destabilized and degraded via the TRAMP/exosome pathway in these conditions (Dez et al., 2007; Wery et al., 2009).

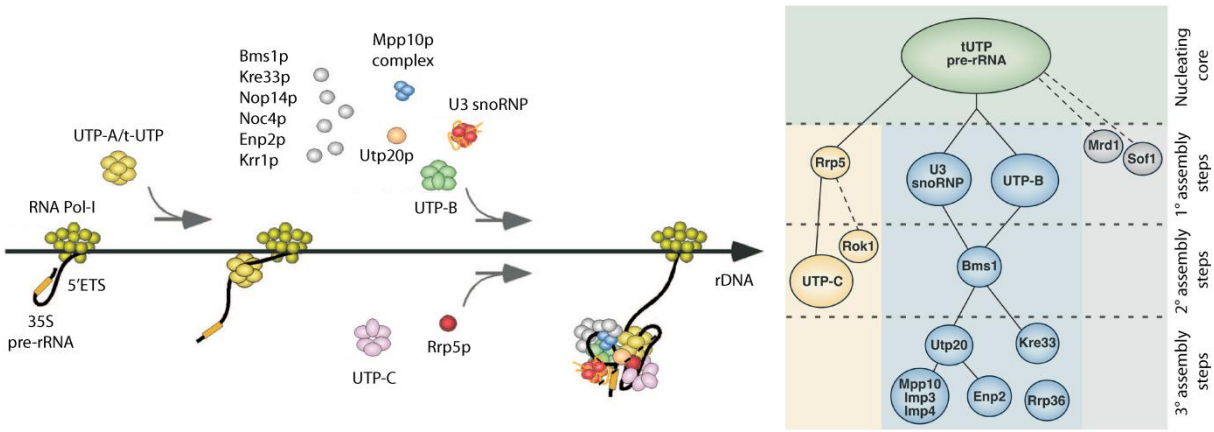

Fig. 2-8: Model for the assembly of the SSU processome on pre-rRNA

The UTP-A/t-UTP complex can bind independent of all other analysed SSU processome components to nascent pre-rRNA. This facilitates subsequent assembly of other SSU processome components in different branches via hierarchical and cooperative pathways. See main text for details. Left and right panels are adapted from Pérez-Fernández et al. (2007; 2011), respectively.

Many components of the SSU processome form 'modules', which can be isolated from cell extracts independent of pre-ribosomal particles after these have been sedimented by high speed centrifugation. These modules, e.g. the 'U three protein complexes' UTP-A (containing Utp4p, Utp5p, Utp8p, Utp9p, Utp10p, Utp15p, Utp17p/Nan1p), UTP-B (Utp1p/Pwp2p, Utp6p, Utp12p/Dip2p, Utp13, Utp18p, Utp21p) and UTP-C (Utp22p, Rrp7p, Cka1p, Cka2p) (Dosil and Bustelo, 2004; Gallagher et al., 2004; Krogan et al., 2004), the U3 snoRNP (U3 snoRNA, Nop1p, Nop56p, Nop58p, Snu13p, Rrp9p) (Venema et al., 2000), and other complexes like Mpp10p/Imp3p/Imp4p (Granneman et al., 2003), Noc4p/Nop15p (Milkereit et al., 2003; Kühn

et al., 2009) and Rcl1p/Bms1p (Wegierski et al., 2001), are supposed to constitute building blocks of 90S/SSU processome particles. Furthermore, it could be shown that binding of these modules to pre-ribosomes follows, at least in part, a hierarchical order, albeit parallel pathways exist and stable association of the modules with pre-ribosomes apparently involves additional cooperative effects (Fig. 2-8). Accordingly, binding of UTP-A to pre-rRNA is required for recruitment of all other analysed components, followed by different binding branches (Pérez-Fernández et al., 2007). In one, UTP-B and U3 snoRNP bind in a cooperative manner (Dosil and Bustelo, 2004) and enable subsequent binding of Bms1p, Mpp10p/Imp3p/Imp4p and other factors (Pérez-Fernández et al., 2011). In an alternative branch, Rrp5p binds first to enable recruitment of UTP-C and Rok1p (Vos et al., 2004a; Pérez-Fernández et al., 2011), and other factors like Sof1p and Mrd1p apparently enter in Rrp5p and U3 snoRNP independent branches (Bax et al., 2006b; Segerstolpe et al., 2008). Furthermore, there is evidence that other factors required for A0, A1 and A2 processing as Utp23p and snR30 snoRNA could bind independent of UTP-A to pre-rRNA (Hoareau-Aveilla et al., 2012). Distinct regions of snR30 are either involved in base pairing interactions with pre-rRNA or likely to mediate interactions with proteins, respectively, suggesting that snR30 might recruit SSU processome components to pre-rRNA (Fayet-Lebaron et al., 2009). As described above, snoRNAs are also supposed to maintain the pre-rRNA accessible for the assembly of r-proteins. Congruently, a subset of r-proteins that bind to the 5' (body) and central (platform) domain of the 18S rRNA (Fig. 2-2) and whose depletion causes similar pre-rRNA processing phenotypes as depletion of SSU pocessome components (Ferreira-Cerca et al., 2005), is also associated with 90S/SSU processome particles, although much weaker than with mature 40S subunits (Ferreira-Cerca et al., 2007). While these r-proteins have no impact on the binding of the UTP-A and UTP-B complexes to pre-rRNA, some platform binding r-proteins are required to recruit the biogenesis factor Noc4p to pre-ribosomes (Jakob et al., 2012). Noc4p in turn is required for the assembly of r-proteins bound to the 3' domain (head) of 18S rRNA (Fig. 2-2), which only affect later maturation steps (Ferreira-Cerca et al., 2005). Furthermore, the association of some early binding SSU processome modules with pre-ribosomes appeared to be stabilized by later binding factors (Pérez-Fernández et al., 2011). Accordingly, a complex interaction network between biogenesis factors, snoRNAs, pre-rRNA and r-proteins in combination with structural rearrangements during formation of the SSU processome could enable the structural organisation of the pre-rRNA to stabilise pre-ribosomal particles and to facilitate processing at sites A0, A1 and A2 as well as assembly of r-proteins onto the pre-rRNA.

As mentioned above, co-transcriptional formation of the SSU processome can be observed in electron micrographs of Miller chromatin spreads as 'terminal knobs' on the nascent transcripts, and these structures are not formed when the 5'ETS region is mutated or when U3 snoRNA or other SSU processome components are depleted in the cells. Congruently, SSU processome components were shown to be associated with rDNA in an RNA dependent manner (Wery et al., 2009). Based on this and kinetic analyses of pre-rRNA processing in UTP-A mutant strains (Dez et al., 2007) it seems unlikely that the UTP-A/t-UTP complex binds directly to rDNA and affects Pol-I transcription in yeast, as previously suggested by Gallagher and co-workers (2004). Remarkably, human homologs of UTP-A

components apparently have adopted such functions (Prieto and McStay, 2007; Freed et al., 2012). Co-transcriptional binding of (some) SSU processome components to pre-rRNA appears to be conserved in all eukaryotes, as formation of the terminal balls was observed in algae, fungi, insects, amphibians and mammals (Herbert Spring, 1974; Trendelenburg, 1974; McKnight and Miller Jr., 1976; Trendelenburg and Gurdon, 1978; Saffer and Miller, 1986; Scheer and Benavente, 1990). In all analysed species except *S. cerevisiae*, terminal knobs of similar size are observed on all nascent transcripts that increase in length along the rDNA repeat (Fig. 2-9 A). In yeast, however, transcripts located in the middle third of rDNA repeats show a larger knob than transcripts in the last third, most of which are, in addition, shorter than expected for the full length 35S rDNA transcript (Fig. 2-9 B) (Osheim et al., 2004). These observations are interpreted in a way that the SSU processome is fully assembled on the nascent pre-rRNA, resulting in its compaction into large 'SSU knobs' and facilitating rRNA processing at sites A0, A1 and A2 (Osheim et al., 2004; Wery et al., 2009). In this way, pre-40S particles are separated from the LSU specific nascent transcripts, which subsequently also form terminal balls ('LSU knobs') that are supposed to contain LSU biogenesis factors (Fig. 2-9 C). However, to date this was experimentally validated for only two factors, Nop53p (Granato et al., 2008) and Nop15p (Wery et al., 2009).

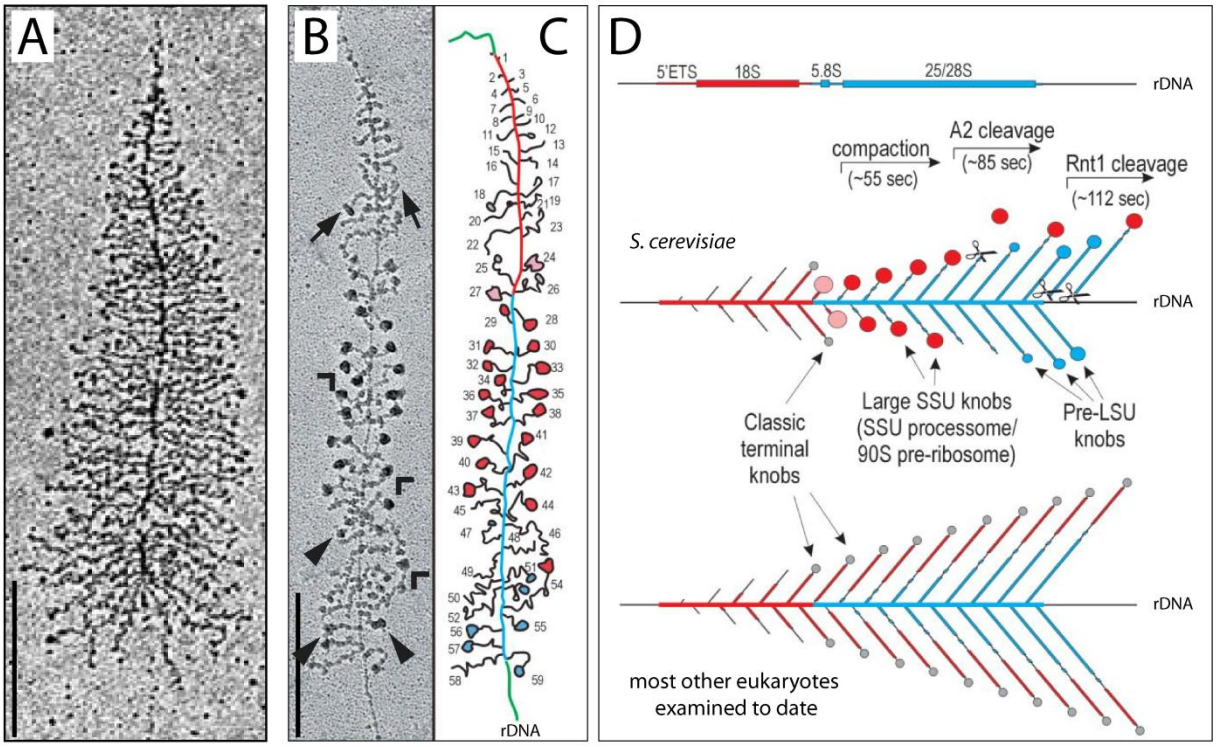

Fig. 2-9: pre-rRNA processing can occur co-transcriptionally in *Saccharomyces cerevisiae*

A) Electron micrograph of a Miller chromatin spread showing a transcribed rDNA repeat from *Xenopus*. The transcripts increase in length along the gene and small particles are visible at their ends. B, C) Electron micrograph of a Miller chromatin spread showing a transcribed rDNA repeat from *S. cerevisiae* (same as in Fig. 2-5) and schematic tracing thereof. Transcripts in the first third of the gene increase in length and show small particles on their ends (indicated by arrows (B)/in gray (C)). Transcripts in the middle part of the gene appear shorter than expected and large particles (arrowheads/red) are visible at their ends. In contrast, transcripts in the last third of the gene exhibit smaller particles (triangles/blue) at their ends. D) Schematic interpretation of the data in (A, B), see main text for details. Scale bars correspond to 1 µm (A) and 0.5 µm (B). (A) was adapted from Raška et al. (2006), (B-D) was adapted from Osheim et al. (2004).

Co-transcriptional pre-rRNA processing could be confirmed by rapid metabolic labelling techniques (Kos and Tollervey, 2010). These experiments showed that in exponentially growing yeast cells ~ 70% of the transcripts are co-transcriptionally cleaved, and furthermore that 2'-O-methylation also frequently occurs co-transcriptionally, indicating co-transcriptional binding of the respective guide snoRNAs. Accordingly, pre-40S particles are generated either by co-transcriptional cleavage of the nascent pre-rRNA or from common, 35S pre-rRNA containing, 90S pre-ribosomes in case that processing starts only after Pol-I transcription has been completed. In either case, the SSU processome components dissociate rapidly from the pre-40S particles (Schäfer et al., 2003).

The subsequent maturation events yielding mature 40S subunits, which largely occur in the cytoplasm, are briefly summarized in the following paragraph (for more detailed reviews see (Henras et al., 2008; Karbstein, 2011)). Only a few (~ 10) biogenesis factors are required for these steps, including Enp1p, the D site nuclease Nob1p (Lamanna and Karbstein, 2009, 2011) and its associated proteins Pno1p/Dim2p, Dim1p that catalyses methylation of two adenosine residues at the 3' end of the 18S rRNA (Lafontaine et al., 1994), the potential export factors Ltv1p and Rrp12 (Ito et al., 2001; Oeffinger et al., 2004; Seiser et al., 2006), the kinases Rio1p and Rio2p and a GTPase-like protein Tsr1p. Notably, most of these factors are already associated with 90S pre-ribosomes (Chen et al., 2003; Schäfer et al., 2003), and Enp1p, Pno1p and Dim1p are essential for early pre-rRNA processing events (Lafontaine et al., 1995; Fatica et al., 2003; Vanrobays et al., 2004). Mapping of binding sites on pre-rRNAs by cross-linking studies (Granneman et al., 2010) and cryo-EM studies (Strunk et al., 2011) indicated that the late acting SSU biogenesis factors are placed on the pre-40S particles containing 20S pre-rRNA in a way that prevents premature translation initiation. Recently, two independent studies provided evidence that a specific translation initiation factor (eIF5B/Fun12p) is required for processing of site D to generate the 3' end of 18S rRNA (Lebaron et al., 2012; Strunk et al., 2012), and suggested that the final SSU maturation steps could involve a translation like cycle as a quality control mechanism for the newly synthesized subunits.

2.2.6 Maturation of the large ribosomal subunit

In contrast to the pre-40S maturation pathway, LSU maturation proceeds via several distinct pre-60S particles that are characterised by the different pre-rRNA species (see Fig. 2-6) as well as by the set of associated biogenesis factors. Analyses of pre-rRNA processing phenotypes in yeast strains that depend on conditional alleles of the different biogenesis factors helped to understand for which maturation steps the respective factors are required, but nevertheless, the molecular function of most factors remains elusive. Over the last decade, tandem-affinity purification approaches combined with mass spectrometric analyses (Rigaut et al., 1999) were extensively used to analyse the composition of the different LSU precursors, and identified probably most of the required biogenesis factors. These results, in combination with intracellular localisation studies of immuno-gold labelled biogenesis factors by electron microscopy provided insights into the migration of pre-ribosomes from the nucleolus to the cytoplasm. Accordingly, the first specific pre-60S particles containing 27SA2

pre-rRNA and the diagnostic biogenesis factor Npa1p (Dez et al., 2004) are localised in the nucleolus at the border between DFC and GC (see Fig. 2-4), consistent with the localisation of snoRNP core proteins, which predominantly act on nascent pre-rRNA or 90S particles, in the DFC (Léger-Silvestre et al., 1999). Subsequent maturation steps including cleavage at site C2 are likely to occur in the GC, where Rlp7p, a factor required for this step is localised (Gadal et al., 2002b), followed by transport into the nucleoplasm, where pre-ribosomes accumulate when late acting biogenesis factors like Nog2p are inactivated (Saveanu et al., 2001) and export into the cytoplasm is impaired. However, just few biogenesis factors are associated only with pre-ribosomes containing a specific pre-rRNA (e.g. Npa1p (27SA2) (Dez et al., 2004), Nsa1p (27SB) (Kressler et al., 2008)), whereas most stay associated with subsequent intermediates and some even from very early nucleolar to late nucleoplasmic or cytoplasmic pre-60S particles (e.g. Nsa3p (Nissan et al., 2002), Nog1p (Saveanu et al., 2003)). In addition, the different pre-rRNA species have rather long life times (15-95 sec (Kos and Tollervey, 2010)). Hence it is complicated to precisely determine the composition of subsequent precursor particles. Nevertheless, numerous studies suggest that different groups of biogenesis factors are specifically associated with early, intermediate and late pre-60S particles and indicated that the complexity of pre-ribosomes in terms of biogenesis factor composition decreases in the course of maturation (e.g. Fatica et al., 2002; Nissan et al., 2002, 2004; Saveanu et al., 2003; Dez et al., 2004; Lebreton et al., 2008).

In this chapter, the focus is set on early, nucleolar LSU maturation steps, which are most important within the scope of this work, whereas intermediate and late maturation steps are just briefly summarised (for more detailed reviews see Henras et al., 2008; Kressler et al., 2010; Panse and Johnson, 2010).

Only few LSU biogenesis factors have been found to co-purify 35S pre-rRNA or SSU processome components (see below) or were identified as components of 90S/SSU processome particles (Grandi et al., 2002). While this is not surprising in case that co-transcriptional processing occurs (~ 70% of transcripts (Kos and Tollervey, 2010)), it indicates that LSU biogenesis factors bind either just weakly and/or immediately before A2 site cleavage to 90S pre-ribosomes, or exclusively to the resulting pre-60S particles. This would be consistent with the general assumption that the delay of the early, SSU maturation specific cleavage events at sites A0, A1 and A2 observed in mutants of most LSU biogenesis factors is an indirect effect, possibly due failure of recycling of biogenesis factors required for these steps (Venema and Tollervey, 1999).

Some of the LSU biogenesis factors that are apparently already associated with 90S pre-ribosomes are Npa1p, Ssf1p, Ytm1p, Erb1p, Nop7p, Rpf2p and Rrs1p (Fatica et al., 2002; Dez et al., 2004; Zhang et al., 2007; Sahasranaman et al., 2011). The latter two are required for the assembly of 5S rRNA, rpL5 and rpL11 into pre-ribosomes, which can apparently occur very early during ribosome biogenesis, as rpL5 and rpL11 co-purify a pre-rRNA containing the 5'ETS region and are thus *bona fide* components of 90S pre-ribosomes (Zhang et al., 2007). Rpf2p, Rrs1p, rpL5 and rpL11 interact directly with each other and can be isolated as a complex with 5S rRNA from cells defective in ribosome biogenesis, but it remains unclear if this RNP is recruited *en bloc* to, or is formed on pre-ribosomes. The earliest pre-60S particles purified via Npa1p (Dez et al., 2004) contain amongst others a

group of factors whose depletion causes reduced levels of all LSU specific pre-rRNAs (e.g. Nop4p/Nop77p (Bergès et al., 1994), Noc1p, Noc2p (Milkereit et al., 2001)), as well as several factors that affect specific maturation steps, e.g. conversion of 27SA3 to $27SB_S$ pre-rRNA generating the 5' end of $5.8S_S$ rRNA ('A3-factors', see below) or separation of 5.8S and 25S precursors by processing of 27SB pre-rRNAs in the ITS2 region ('B-factors', see below).

While few is known about the initial processing at site A3 by RNAse MRP or the minor pathway starting with processing of site $B1_S$, the role of the 'A3-factors' (Ytm1p, Erb1p, Nop7p, Rlp7p, Nsa3p/Cic1p, Nop15p, Rrp1p) has been extensively studied (Dunbar et al., 2000; Pestov et al., 2001; Adams et al., 2002; Oeffinger et al., 2002; Fatica et al., 2003; Oeffinger and Tollervey, 2003; Horsey et al., 2004; Miles et al., 2005; Sahasranaman et al., 2011; Granneman et al., 2011; Jakovljevic et al., 2012). These analyses provided insights into several aspects of ribosome biogenesis, for instance (i) how biogenesis factors interact with pre-ribosomes, (ii) the interplay between r-protein assembly and rRNA processing and (iii) regulation of nuclease activity, which are likely to represent general mechanisms that also play a role in other maturation steps. In absence of each individual 'A3-factor', levels of $27SB_S$ pre-rRNA, which is generated by exonucleolytic trimming by Rat1p and/or Rrp17p (section 2.2.3), are severely reduced and shorter fragments thereof are detected (Sahasranaman et al., 2011). For four 'A3-factors', as well as for Nop4p/Nop77p, binding sites on pre-rRNA could be mapped in a UV cross linking approach (Granneman et al., 2011), which locate to the ITS2 region (Nop15p, Nsa3p/Cic1p) and domains I (Erb1p), III (Nop7p) and both II and III (Nop4p/Nop77p) of 25S rRNA, respectively, and partially overlap with r-protein binding sites (Fig. 2-10 B). In mature ribosomes, 5.8S rRNA and domain I of 25S rRNA form base pairing interactions involving both their 5' and 3' regions, and domain III is in close contact to domain I (Fig. 2-10 A + D; see also Fig. 2-2) (Ben-Shem et al., 2010, 2011). Six of the seven 'A3-factors' (except Rrp1p) show interdependent binding to pre-ribosomes (Sahasranaman et al., 2011), indicating proximity of these factor on pre-ribosomes, and Ytm1p, Erb1p and Nop7p form a protein complex that can be isolated from cells and reconstituted *in vitro* (Krogan et al., 2004; Miles et al., 2005; Tang et al., 2008). In addition, these six 'A3-factors' require for stable association with pre-ribosomes prior assembly of rpL7 and rpL8 (Jakovljevic et al., 2012), which are bound to domains II and I of 25S rDNA (Fig. 2-10 D), respectively, and depletion of which phenocopies the rRNA processing defects of the 'A3-factors' (Pöll et al., 2009). Furthermore, rpL7 and rpL8 are also required for stable assembly of several other r-proteins (Jakovljevic et al., 2012). Both affect binding of four r-proteins bound to domain I (rpL17, rpL26, rpL35, rpL37; Fig. 2-10 E), and in addition, rpL7 and rpL8 specifically affect stable assembly of four and six other r-proteins of domains II and I, respectively. Rlp7p, and thus probably also the other interdependent 'A3-factors', also affect assembly of rpL17, rpL26, rpL35, rpL37 to pre-ribosomes (Sahasranaman et al., 2011). Hence, rpL7 and rpL8 appear to be important for the formation of domains II and I, respectively, and the 'A3-factors' provide an example how r-protein assembly and the function of biogenesis factors can be interconnected.

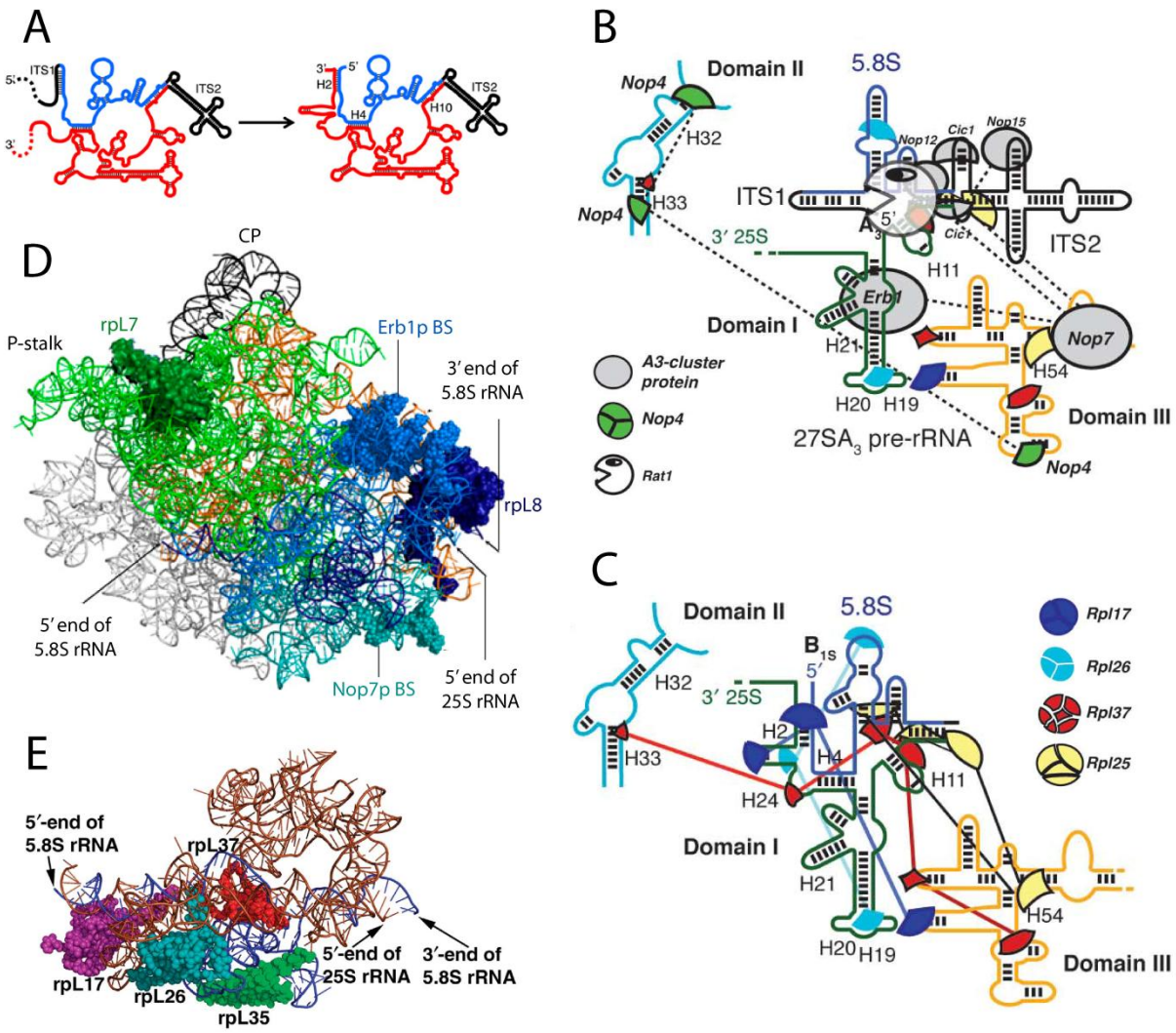

Fig. 2-10 The role of the 'A3-factors' in ribosome biogenesis

A) In pre-rRNAs containing the ITS1 region, the 5' region of the 5.8S rRNA sequence (blue) is predicted to base pair with the 3' part of ITS1 (left), which prevents interaction with domain I of 25S rRNA (red) as found in the mature ribosome (right; see also Fig. 2-2). B, C) The binding sites of Rat1p, Nop4p/Nop77p and the 'A3-factors' Nop7p, Erb1p, Nop15p and Cic1p/Nsa3p on 5.8S rRNA, 25S rRNA (domains I, II, III) and in the ITS2 region as determined by CRAC analyses (Granneman et al., 2011) are schematically depicted. In addition, the binding sites of 4 r-proteins as found in mature 80S ribosomes are marked (Ben-Shem et al., 2011). Dashed lines in (B) indicate (potential) interactions within pre-ribosomes mediated by the biogenesis factors, solid lines in (C) indicate interactions between domains I, II and III in the mature ribosome that are stabilized by the respective r-proteins. The different secondary structures of the 5' end of 5.8S rRNA are indicated. D) Crystal structure of the RNA components of 60S subunits from *S. cerevisiae* viewed from the solvent side (as in Fig. 2-2). 5S rRNA is coloured in black, 5.8S rRNA in dark blue, domains I, II, III and V of 25S rRNA in light blue, green, cyan and orange, respectively. rpL7 and rpL8 are shown as space filling models in dark green and dark blue, respectively, and binding sites of Erb1p and Nop7p (see also (B)) on domains I and III are highlighted. D). Positions of the indicated r-proteins on 5.8S rRNA (blue) and domain I of 25S rRNA (brown) in the mature ribosome. (A, D) are adapted from Jakovljevic et al. (2012), (B, C) from Granneman et al. (2011), (E) from Sahasranaman et al. (2011). See main text for details.

In addition, formation of 27SB pre-rRNA apparently requires rearrangements within the ITS1/5.8S region, as there is evidence that in 35S/27SA pre-rRNAs the 5' end of 5.8S rRNA forms a stable structure with the 3' part of ITS1 (Yeh et al., 1990; Henry et al., 1994; van Nues et al., 1994), which has to be released to allow base pairing with domain I of 25S rRNA as found in mature ribosomes (Fig. 2-10 A) (Ben-Shem et al., 2010, 2011). The proteins rpL17, rpL26, rpL35 and rpL37 make contacts to both domain I and 5.8S rRNA, and rpL17,

rpL35 and rpL37 make additional contacts with domains II and/or III (Fig. 2-10 E). In this way, these (and other) r-proteins probably stabilise the 5.8S/25S hybrid and organise the relative positioning of domains I, II and III in mature ribosomes (Fig. 2-10 C). Based on the results described above, it was suggested that the 'A3-factors' and Nop4p/Nop77p, amongst others, could establish these RNA structures in early pre-ribosomes by forming an extensive interaction network (Fig. 2-10 B) and thereby facilitate assembly of the r-proteins, which then take over the function in stabilisation of tertiary rRNA structures (Fig. 2-10 C) (Granneman et al., 2011; Sahasranaman et al., 2011).

Formation of a stable 5.8S/25S hybrid at the 5' end of 5.8S rRNA (Fig. 2-10 E) was proposed to precisely stop exonucleolytic trimming by Rat1p or Rrp17p at site $B1_S$ (Pöll et al., 2009; Sahasranaman et al., 2011). As Rat1p is also involved in degradation of aberrant pre-rRNAs (Fang et al., 2005), this provides a potential link between r-protein assembly, rRNA processing and surveillance pathways (Sahasranaman et al., 2011; Jakovljevic et al., 2012). Notably, binding of Rat1p, but not of Rrp17p, to pre-ribosomes appeared to be independent of 'A3-factors', and Rat1p and Rrp17p were found to be associated predominantly with pre-60S particles containing 27SA2 or 27SB pre-rRNA, respectively (Oeffinger et al., 2009; Sahasranaman et al., 2011). Major binding sites of Rat1p were mapped to the 5.8S rRNA (Fig. 2-10 B), the 5' part of ITS2 and domain I of 25S rRNA, rather than to the Rat1p substrate regions between A3-$B1_S$ or C2-C1, but no binding sites could be mapped for Rrp17p (Granneman et al., 2011). Accordingly, Rat1p is supposed to be recruited prior to its time of action to pre-ribosomes, waiting for a trigger event, and then to rapidly degrade its substrates. In contrast, Rrp17p is apparently only recruited to pre-60S particles containing 27SA3 pre-rRNA, which are ready for exonucleolytic trimming, and subsequently stays associated with pre-ribosomes containing 27SB pre-rRNA until processing at site C2 occurs, which provides the next substrate for Rrp17p (see section 2.2.3).

The subsequent nuclear and cytoplasmic LSU maturation steps are briefly summarized in the following paragraphs (for more detailed reviews see Henras et al., 2008; Kressler et al., 2010; Panse and Johnson, 2010). Endonucleolytic cleavage of 27SB pre-rRNA within the ITS2 sequence requires the function of at least 14 biogenesis factors ('B-factors'), which are recruited to pre-ribosomes in part in a hierarchical manner and/or are mutually interdependent for stable association with pre-ribosomes (Saveanu et al., 2003, 2007; Talkish et al., 2012). Accordingly, Nop2p and Nip7p, which are part of very early pre-60S particles associated with Npa1p (Dez et al., 2004), are required to enable binding of Rpf2p, Rrs1p and Spb4p in one branch, and for instance Rlp24p, Nog1p, Nsa2p in a second branch. Both branches are required for binding of Nog2p to pre-ribosomes, which was suggested to provide a check point in LSU maturation and to trigger processing at site C2 (Talkish et al., 2012). However, this remains a matter of debate, since in cells depleted of Nog2p not only 27SB, but also 7S pre-rRNAs are accumulated (Saveanu et al., 2001). Thus delay of C2 cleavage in absence of Nog2p could be a secondary effect due to impaired release other 'B-factors' from later pre-ribosomes in these conditions. Consistent with this, prior to or concomitant with the conversion of 27SB in 7S and 26S pre-rRNA, most biogenesis factors that have been associated with the early pre-60S particles are released and a set of new factors, for instance Rea1p, Rix1p, Ipi1p, Ipi3p and Arx1p (Nissan et al., 2002, 2004; Krogan

et al., 2004) is recruited. There is evidence that some of these release events are energy dependent processes that require the functions of the AAA-type ATPases Rix7p and Rea1p (Kressler et al., 2008; Ulbrich et al., 2009; Bassler et al., 2010).

The remaining steps in LSU biogenesis include formation of the 3' and 5' ends of 5.8S and 25S rRNA (see section 2.2.3), transport of the precursor particles through the nuclear pores into the cytoplasm involving export factors like Nmd3p, Mex67p-Mtr2p or Arx1p (Ho and Johnson, 1999; Ho et al., 2000; Gadal et al., 2001; Bradatsch et al., 2007; Yao et al., 2007, 2008; Hung et al., 2008), assembly of lacking r-proteins (e.g. 'phospho-stalk' proteins, see below) and some structural rearrangements to acquire the mature 60S structure. The latter could be recently confirmed in cryo-EM analyses of pre-60S particles purified via Arx1p (Bradatsch et al., 2012), which predominantly represent the latest nucleoplasmic and early cytoplasmic LSU precursors. The overall structure of the 'Arx1 particles' is similar to mature 60S subunits, albeit some landmark structures as the 'central protuberance' or the 'phospho stalk' (see Fig. 2-1), which mediates interaction with translation factors in mature ribosomes (e.g. eEF2 (Bargis-Surgey et al., 1999); for a review see (Gonzalo and Reboud, 2003)), are not (fully) established. Furthermore, additional densities were observed at several regions relevant for the function of mature 60S subunits, which could be in part assigned to biogenesis factors, e.g. Arx1p being located in front of the peptide exit tunnel and Tif6p in the subunit interface, where the export adaptor Nmd3p is also supposed to bind (Sengupta et al., 2010). The binding site of Arx1p was confirmed in cryo-EM analyses of *in vitro* assembled complexes of mature 60S subunits with recombinantly expressed late acting biogenesis factors (Greber et al., 2012), which could also define nearby binding sites of the Arx1p release factors Rei1p and Jjj1p (Hung and Johnson, 2006; Meyer et al., 2010). In summary, these results strongly suggest that cytoplasmic pre-60S particles are not competent for translation.

To obtain functional 60S subunits, the remaining biogenesis factors are removed in a coordinated way involving several ATPases and GTPases (Lebreton et al., 2006; Lo et al., 2010), and lacking r-proteins are assembled (rpL24 (Kruiswijk et al., 1978); 'phospho stalk' proteins (Krokowski et al., 2005; Kemmler et al., 2009; Lo et al., 2009; Rodríguez-Mateos et al., 2009). As one of the last steps downstream of the 'phospho-stalk' assembly requires the action the GTPase Efl1p (Elongation factor 2 like protein), it was hypothesized that this could be a translation like event, providing a quality control step at the end of LSU biogenesis, analogous to the final SSU maturation steps (see section 2.2.5). However, and in contrast to the surveillance and degradation of aberrant nuclear pre-rRNAs (see section 2.2.4), to date only few is known about the degradation of non-functional (pre-) ribosomes in the cytoplasm. The cytoplasmic exosome appears to be involved in degradation of both aberrant SSU and LSU (precursor) particles, and the former is suggested to occur by a similar translation dependent mechanism as in the 'no go decay' of mRNAs, on which ribosomes are stalled due to structural barriers (Cole et al., 2009; Soudet et al., 2010). In contrast, aberrant (pre-) 60S particles seem to be trapped near the nuclear envelope and degraded independent of translation (LaRiviere et al., 2006; Cole et al., 2009).

2.2.7 The role of Rrp5p, Noc1p and Noc2p in ribosome biogenesis

Rrp5p, which is a component of 90S/SSU processome particles (Dragon et al., 2002; Grandi et al., 2002) and required for the recruitment of the UTP-C complex (Pérez-Fernández et al., 2007), is one of only few biogenesis factors described to affect both the maturation of the large and the small ribosomal subunits, besides for instance Rrp12p (Oeffinger et al., 2004) or Prp43p (Lebaron et al., 2005; Combs et al., 2006; Leeds et al., 2006). Rrp5 was initially identified in a screen for genes being synthetic lethal with snR10 (Venema and Tollervey, 1996), an unessential snoRNA affecting pre-rRNA processing at sites A1 and A2 (Tollervey and Guthrie, 1985; Tollervey, 1987). This study showed that Rrp5p is not only required for processing at sites A0, A1 and A2 yielding the 18S rRNA precursor, but also for A3 processing and hence for formation of the 5' end of $5.8S_S$ rRNA (Venema and Tollervey, 1996). Rrp5p shows a distinct bipartite structure with the N-terminal part containing twelve repeats of the S1 RNA binding motif (Bycroft et al., 1997) and the C-terminal part containing seven tetratricopeptide repeat (TPR) motifs (Fig. 3-6), which often mediate protein-protein interactions (Lamb et al., 1995). Interestingly, the function of Rrp5p in LSU and SSU maturation pathways could be pinpointed to its N- and C-terminal parts, respectively, and *in vivo* co-expression of the respective Rrp5p variants complements the essential function of Rrp5p (Torchet et al., 1998; Eppens et al., 1999). In addition, *in vitro* studies showed that Rrp5p can directly interact with RNA and suggested binding sites of Rrp5p within the ITS1 region of pre-rRNA, in particular between processing sites A2 and A3, but also upstream of A2 (De Boer et al., 2006; Young and Karbstein, 2011). As expected, the S1 motifs are crucial for stable RNA interaction *in vitro* (De Boer et al., 2006), but interestingly they appeared to have distinct functions, since the N-terminal part of Rrp5p containing the first nine S1 motifs bound RNA with high affinity but unspecifically, whereas the C-terminal part containing the last three S1 motifs and the TPR repeats showed specific RNA binding but with low affinity (Young and Karbstein, 2011).

In contrast to Rrp5p, Noc1p/Mak21p and Noc2p specifically affect the maturation of the large ribosomal subunit (Edskes et al., 1998; Milkereit et al., 2001). Noc2p was identified in a screen for factors that influence export of pre-ribosomes from the nucleus to the cytoplasm and found to form heteromeric complexes with Noc1p and Noc3p, which can be isolated under high salt conditions from yeast cell extracts (Milkereit et al., 2001). All three proteins have homologs in higher eukaryotes (see below), and Noc1p and Noc3p contain a highly conserved region of ~ 45 amino acids, the 'NOC domain', which is also found in Noc4p, a component of the SSU processome (Milkereit et al., 2001). Noc4p forms a protein complex with Nop14p/Noc5p (Milkereit et al., 2003), and the interaction was shown to depend on a part of Noc4p containing the 'NOC domain' (Kühn et al., 2009). Noc1p is predominantly localised in the nucleolus and co-sediments on sucrose gradients with 35S and 27S pre-rRNA, whereas Noc3p shows mainly nucleoplasmic localisation and co-sediments with 27S and 7S pre-rRNA (Milkereit et al., 2001). Noc2p shows an intermediate distribution both within the nucleus and on sucrose gradients, and synthetic lethal effects between mutant *noc2/noc1* and *noc2/noc3*, but not between *noc1/noc3* alleles are observed. Hence, it was suggested that Noc1p/Noc2p and Noc2p/Noc3p complexes act on early, nucleolar and later,

nucleoplasmic pre-60S particles, respectively (Milkereit et al., 2001), which is supported by several studies analysing the protein composition of LSU precursors of different maturation states (Nissan et al., 2002; Dez et al., 2004; Kressler et al., 2008). Consistently, in conditional *noc1*, *noc2* and *noc3* mutant strains pre-60S particles are accumulated in the nucleolus (*noc1*, *noc2* mutants) and/or in the nucleoplasm (*noc2*/*noc3* mutants) (Milkereit et al., 2001). Analyses of the pre-rRNA processing phenotypes in these mutant strains showed decreased levels of all LSU precursor RNAs and no apparent processing block at a specific maturation step. In addition, overexpression of the 'NOC domain' in wild type cells, which abolishes cell growth, had no apparent effect on pre-rRNA processing, but resulted in nuclear accumulation of pre-60S particles (Milkereit et al., 2001). Hence, it was concluded that the Noc1/2/3p proteins have no direct effect on pre-rRNA processing, but rather are required for intranuclear transport and export of pre-60S particles and/or for other maturation events that facilitate transport of pre-60S particles. When the functions of the Noc1/2/3p proteins are impaired, LSU precursors are apparently prone to degradation.

Rrp5p, Noc1p and Noc2p have homologs in higher eukaryotes (Venema and Tollervey, 1996; Milkereit et al., 2001) and the human homologs have been identified as nucleolar components in a large scale proteome analysis of human nucleoli (Andersen et al., 2002). In addition, for human (h)Rrp5p/NFBP (Sweet et al., 2008) and hNoc2p/NIR (Wu et al., 2012) a function in ribosome biogenesis could be shown, as well as association with precursor RNA and U3 snoRNA (Turner et al., 2009; Wu et al., 2012). Besides, all human homologs adopted additional functions, as it is reported that hRrp5p/NFBP interacts with NF-KB (Sweet et al., 2003, 2005), that hNoc1p/CBP stimulates transcription from the hsp70 promoter (Lum et al., 1990, 1992, Imbriano et al., 2001) and that hNoc2p/NIR acts as an inhibitor of acetyl transferases and modulates p53 and TAp63 activity (Hublitz et al., 2005; Heyne et al., 2010). Hence, hNocp2/NIR could add another link between the p53 stress response pathway and ribosome biogenesis in higher eukaryotes (for reviews, see Deisenroth and Zhang, 2010; Chakraborty et al., 2011).

2.3 Objectives

In contrast to the early SSU maturation steps, which require formation of the SSU processome from its modular building blocks, knowledge about the earliest LSU specific maturation events in terms of both recruitment and function of the respective biogenesis factors is still very limited (see sections 2.2.5, 2.2.6). As described above in detail (section 2.2.7), Rrp5p, Noc1p and Noc2p affect very early LSU maturation steps and/or appear to be associated with early pre-60S particles. In addition, a recent study, in which interactions between ribosome biogenesis factors after shut down of Pol-I transcription were analysed, indicated that Noc1p could form a protein complex with Noc2p and Rrp5p independent of pre-ribosomal particles (Merl et al., 2010). Hence, a Rrp5p/Noc1p/Noc2p module might act as an entity in early steps of LSU biogenesis.

One goal of this work was to verify if Rrp5p, Noc1p and Noc2p can in fact form a protein complex. To this end, the baculo virus/SF21 insect cell expression system was employed, which enables co-expression of recombinant proteins in the context of eukaryotic cells. The

reconstituted complex was further characterised by size exclusion chromatography and electron microscopy to obtain first insights into its architecture and structure.

To study the physiological relevance and function of the Rrp5p/Noc1p/Noc2p module, the following aspects were analysed *in vivo,* employing different genetic, cell biological and biochemical approaches. First, to determine if the module components affect the same maturation steps, the impact of the individual proteins on ribosome biogenesis was directly compared in conditional *noc1*, *noc2* and *rrp5* mutant strains by analysing the resulting pre-rRNA processing phenotypes. Second, the RNA and protein composition of pre-ribosomes associated with the module components was analysed to elucidate if Rrp5p, Noc1p and Noc2p act on the same or on different pre-ribosomal particles. Third, the binding interdependencies between the module components to pre-ribosomal particles was investigated, to determine which proteins directly interact with pre-ribosomes and to establish a potential binding hierarchy. Fourth, to address if the module components are already co-transcriptionally recruited to pre-rRNA, the association of Rrp5p, Noc1p and Noc2p with rDNA chromatin was analysed. Finally, the obtained results were combined to infer the function of the Rrp5p/Noc1p/Noc2p module in the maturation of the large ribosomal subunit.

3 Results

3.1 Ribosomal precursor RNAs are destabilised in absence of functional Noc1p, Noc2p or Rrp5p

3.1.1 Processing of pre-rRNA is differently affected in temperature sensitive *noc1* and *noc2* than in *noc3* mutant strains

Initial characterisation of the yeast proteins Noc1p, Noc2p and Noc3p indicated that a Noc1p/Noc2p complex is associated with early, nucleolar pre-ribosomes, whereas a Noc2p/Noc3p complex is associated with later, nucleolar and nucleoplasmic pre-ribosomes (section 2.2.7; (Milkereit et al., 2001)). These findings were further supported by studies analysing the protein composition of pre-ribosomes of different maturation states (Nissan et al., 2002; Kressler et al., 2008). However, in temperature sensitive (ts) *noc1-1*, *noc2-1* and *noc3-1* mutant strains pre-rRNA processing was apparently not blocked at different stages, but rather steady state levels of pre-rRNAs appeared to be similarly affected, possibly due to secondary effects, e.g. impaired release of biogenesis factors from aberrant pre-ribosomes (Milkereit et al., 2001).

To test, if *noc1*, *noc2* or *noc3* specific effects have been masked in steady state analysis, pre-rRNA processing was kinetically analysed by metabolic labelling of RNAs in yeast strains that depend on chromosomally encoded temperature sensitive *noc1-6, noc1-7 or noc2-1 alleles* (TY2068, TY2069, TY23; listed in section 5.1.1), or on a plasmid encoded *ProteinA-noc3-1* allele (TY71). The *noc1-6* and *noc1-7* alleles were obtained from the same plasmid library of random *noc1* mutant alleles as *noc1-1* (Milkereit et al., 2001) and integrated at the endogenous *NOC1* gene locus by homologous recombination (sections 5.2.2.4/5). For unknown reasons, this approach was not successful for the *noc1-1* and the *noc3-1* alleles, and the protein A epitope appeared to be essential for the ts phenotype of the *noc3-1* allele (data not shown). Compared to the respective wild type strains, these strains showed normal growth at 24°C, but significantly impaired growth at higher temperatures, although with allele specific differences (Fig. 3-1 A + B). For metabolic labelling, cultures of the respective mutant or wild type control strains (TY543, TY772) were shifted for 1h from permissive (24°C) to restrictive temperature (37°C) and transferred to minimal medium containing ^{3}H-uracil to radiolabel newly synthesized RNAs (pulse), followed or not by incubation with excess unlabelled uracil (chase) to monitor processing of labelled RNAs (section 5.2.5.9). Total RNA was isolated from the cells, separated by gel electrophoresis and analysed by autoradiography.

In wild type strains, most of the radioactivity was incorporated in mature 25S, 18S, 5.8S and 5S rRNAs and tRNAs after 15 min of ^{3}H-uracil labelling (Fig. 3-1 C + D, lanes 1, 16). Besides, substantial amounts of the common 35S pre-rRNA, as well as the LSU specific 27S pre-rRNA and the SSU specific 20S pre-rRNA were detected, which were almost completely converted to mature rRNAs after 30 min of chase with unlabelled uracil (Fig. 3-1 C, lanes 1-3, 16-18; see Fig. 2-6 for a rRNA processing scheme).

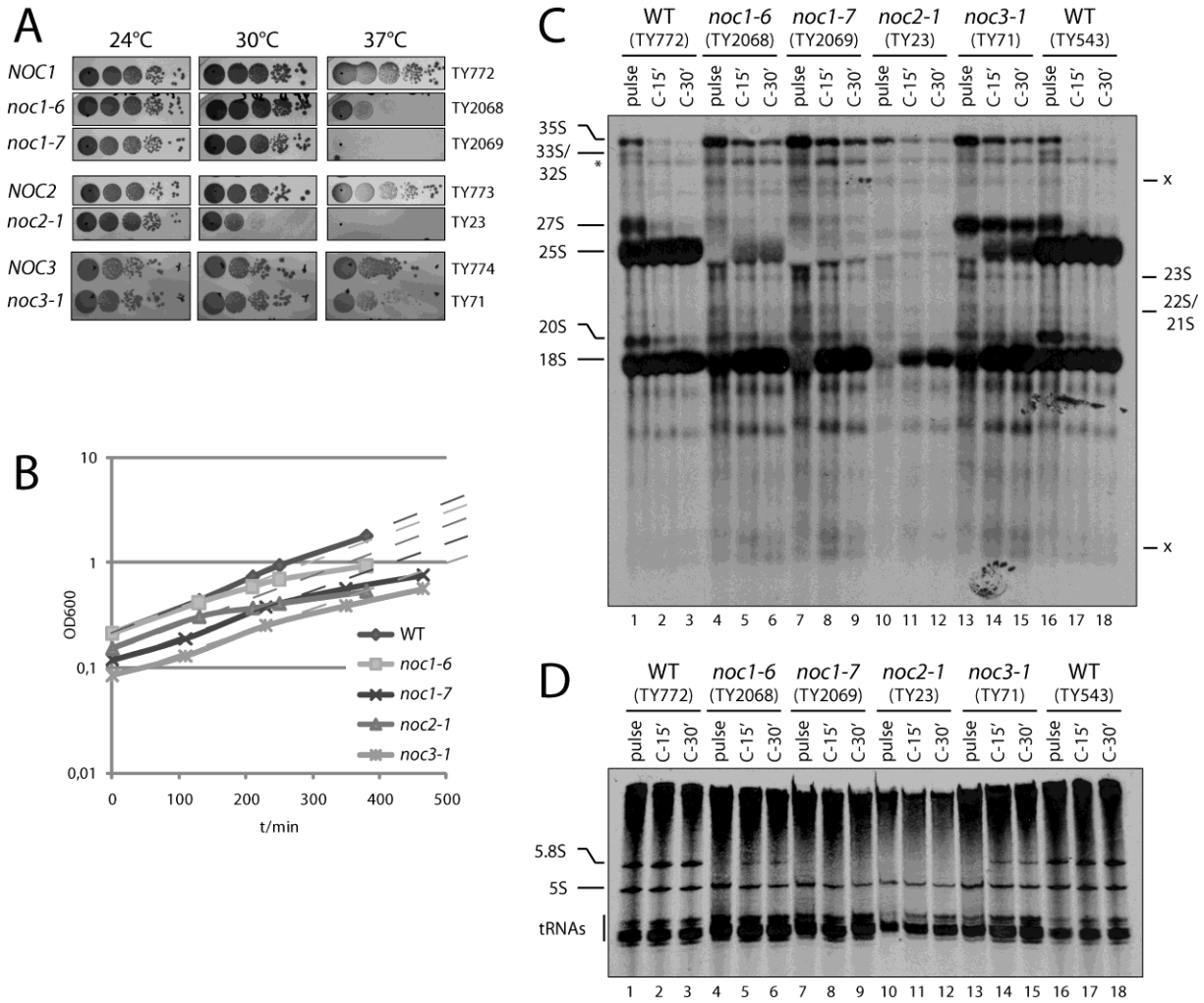

Fig. 3-1: Kinetic analysis of pre-rRNA processing in temperature sensitive *noc1, noc2* and *noc3* mutant strains

A) The effect of the indicated genomic (*noc1-6, noc1-7 and noc2-1)* or ectopic *(ProtA-noc3-1)* mutant alleles (see main text for details) on cell growth at different temperatures was analysed in comparison to the respective wild type alleles. Therefore, exponentially growing cultures of the indicated strains (24°C, YPD) were adjusted to OD600 = 1, and 10-fold serial dilutions thereof were spotted on YPD plates and incubated for three days at the indicated temperatures (section 5.2.2.6). B) Exponentially growing cultures (24°C, YPD) of the indicated strains were adjusted to OD600 = 0.1 – 0.2 and shifted to 37°C. Cell growth was followed by measuring OD600 for 6-7 h (section 5.2.2.7) and is shown in semi-logarithmic scale. Dashed lines are extrapolations of the initial growth rates at 37°C. C, D) Yeast strains bearing the indicated *noc1, noc2* and *noc3* mutant alleles as well as two different wild type (WT) strains were grown to exponential phase (OD600 = 0.3 – 0.4) in YPDA at 24°C and then shifted to 37°C for 1h. Subsequently, aliquots of cells were incubated with ^{3}H-uracil containing medium (15 min, 37°C; pulse) to radiolabel newly synthesized RNAs, followed or not by incubation with medium containing excess of unlabelled uracil (15 or 30 min, 37°C; chase (C); see section 5.2.5.9 for details). Total RNA was isolated from the cells and the incorporated activity was determined using a scintillation counter. Aliquots of RNA corresponding to 200,000 cpm (100,000 in case of TY23) were separated on an agarose gel (C) or a poly-acrylamide gel (D), transferred to positively charged membranes and analysed by autoradiography. Bands corresponding to mature rRNAs, tRNAs and major pre-rRNA species are indicated on the left, bands predominantly detected in the mutant strains are indicated on the right. A band of unclear origin that is stable over the entire chase period in WT and mutant strains is marked by asterisk.

In *noc1*, *noc2* and *noc3* mutant strains, production of 18S rRNA was slightly delayed, but finally reached similar levels as in the wild type strains. In contrast, production of 25S and 5.8S rRNAs was severely impaired, as even after 30 min chase no (*noc1-7, noc2-1*) or only minor amounts (*noc1-6, noc3-1*) of these rRNAs could be detected (Fig. 3-1 C + D, compare lanes 4-6/7-9/10-12/13-15 with 1-3/16-18), in agreement with the essential function of Noc1p, Noc2p and Noc3p in LSU maturation (Edskes et al., 1998; Milkereit et al., 2001).

Furthermore, in all mutant strains radiolabelled 35S pre-rRNA was initially accumulated compared to the wild type strains, and substantial amounts were still detected after 30 min chase, indicating that Pol-I transcription was not directly affected and/or that 35S processing was delayed. Levels of 20S pre-rRNA were slightly reduced and several additional bands migrating between the 25S and 20S (pre-)rRNA bands were detected, most likely corresponding to 23S, 22S, 21S pre-rRNAs resulting from delayed processing of A0, A1 and A2 sites (Fig. 3-1 C + D, compare lanes 4/7/10 with 1/16). In contrast, levels of 27S pre-rRNA were severely reduced in *noc1* and *noc2*, but not in the *noc3* mutant strains (Fig. 3-1 C + D, compare lanes 4-6/7-9/10-12 and 13-15 with 1-3/16-18). This indicated that processing of 27SB pre-rRNA in the ITS2 sequence at site C2 is specifically impaired in the *noc3* mutant strain, and that the respective pre-ribosomes are relatively stable. A similar phenotype is frequently observed in mutants of biogenesis factors associated with intermediate pre-ribosomes containing 27SB pre-rRNA (e.g. Spb4p (De la Cruz et al., 1998; García-Gómez et al., 2011b), Nog1p, Rlp24p, Nsa2p (Saveanu et al., 2003, 2007)), with which Noc3p is also supposed to be associated (Milkereit et al., 2001; Nissan et al., 2002; Kressler et al., 2008). Some additional bands in the high and low molecular weight range were also observed in all mutant strains, possibly due to turnover of aberrant pre-rRNAs.
In summary, these results indicated that in absence of functional Noc1p and Noc2p no stable LSU precursors are formed and the pre-rRNAs are rapidly degraded, as suggested previously (Milkereit et al., 2001). Furthermore, these experiments provided clear evidence that inactivation of Noc3p affects pre-rRNA processing at later steps than inactivation of Noc1p and Noc2p. These differences in the pre-rRNA processing phenotypes of *noc3* mutants versus *noc1* and *noc2* mutants could not be detected in previous work (Milkereit et al., 2001), but correlate very well with the described association of a Noc1p/Noc2p complex with pre-ribosomes of an earlier maturation state than a Noc3p/Noc2p complex (Milkereit et al., 2001; Nissan et al., 2002; Kressler et al., 2008). As the *noc3-1* strain showed still significant growth at 37°C, different *noc3* mutant alleles and/or strains expressing NOC3 under control of a conditional promoter should be analysed in future studies to clarify the function of Noc3p in LSU biogenesis.

3.1.2 Levels of rRNA precursors are significantly reduced after *in vivo* depletion of Noc1p, Noc2p or Rrp5p

Previous studies indicated that Rrp5p could form together with Noc1p and Noc2p a protein module that exists in cells independent of pre-ribosomal particles (Merl et al., 2010). Furthermore, *in vivo* depletion of Rrp5p resulted in severely reduced levels of all pre-rRNAs (Venema and Tollervey, 1996), similar as observed in the temperature sensitive *noc1* and *noc2* strains (Milkereit et al., 2001), indicating that Noc1p, Noc2p and Rrp5p might function together in LSU biogenesis. To directly compare the effect of the respective proteins on ribosome biogenesis, rRNA processing was analysed in yeast strains, in which expression of the individual proteins is regulated by the galactose inducible/glucose repressible *GAL1/10* promoter (pGAL). These strains (TY775, TY776, TY2299) grew equally well as the corresponding wild type strains on plates containing galactose as carbon source, but did not

grow on glucose containing plates (Fig. 3-2 A). More detailed growth analysis showed that growth rates in glucose containing medium were similar in wild type and pGAL-*NOC1*/-*NOC2*/-*RRP5* strains during the first nine hours of cultivation, but were significantly decreased after twelve hours of cultivation (Fig. 3-2 B). Consistent with this, levels of Noc1p and Noc2p were reduced to ~ 1/3 and ~ 1/10 of the endogenous levels after nine and 13 hours cultivation in glucose and further decreased with longer depletion times, whereas the levels of other proteins were not or significantly less affected (Fig. 3-2 C, compare signal intensities of Noc2p and of the cross reacting protein; see also lower panel showing the Poinceau stained membrane).

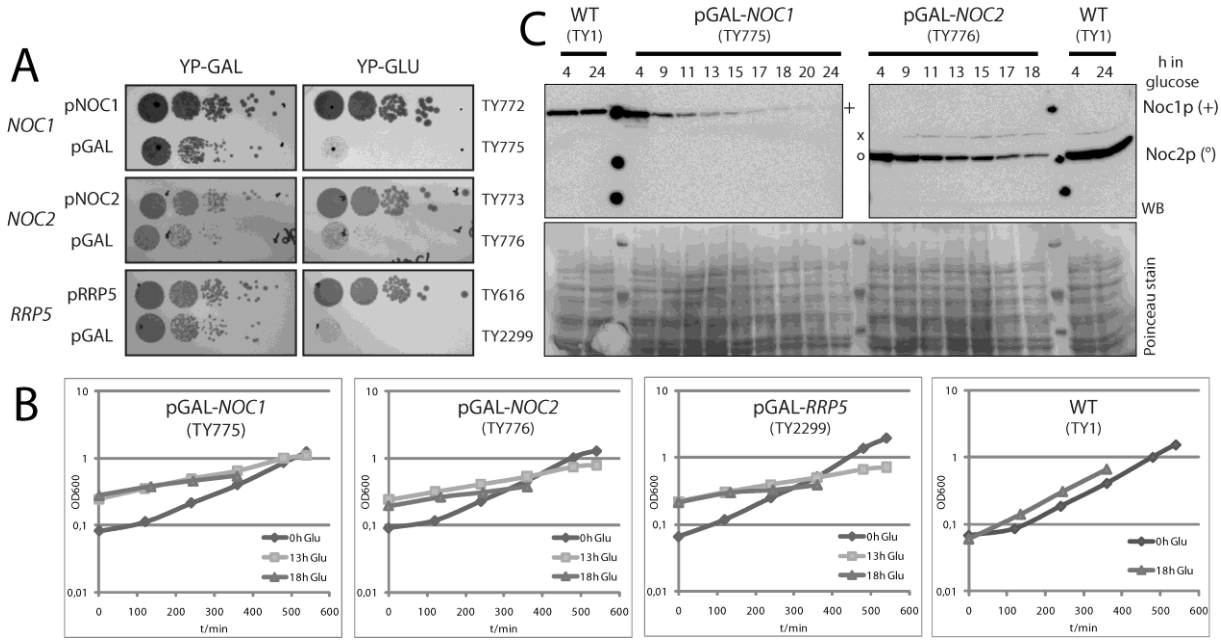

Fig. 3-2: Analysis of growth defects resulting from *in vivo* depletion of Noc1p, Noc2p and Rrp5p

Yeast strains in which the indicated genes are under control of their endogenous promoter or of the galactose inducible/glucose repressible *GAL1/10* promoter (pGAL) were grown to exponential phase in galactose containing full medium (YPGA) at 30°C. A) For growth tests, 1 OD of cells was resuspended in 1 ml sterile H_2O and 10-fold serial dilutions thereof were spotted on the indicated plates containing glucose or galactose as carbon source and incubated for three days at 30°C. B) Alternatively, the indicated strains were shifted to glucose containing medium (YPDA) for 0, 13 or 18 h, diluted to OD600 ~ 0.1 - 0.2 in YPDA and incubated at 30°C. Cell growth was followed by measuring OD600 for 6-9 h and is shown in semi-logarithmic scale. The wild type strain TY1 was included as a control. At several time points after shift to YPDA medium, two aliquots corresponding to 2OD of cells were harvested for protein and RNA analyses (see Fig. 3-3). C) Proteins were isolated by denaturing protein extraction (section 5.2.6.4), protein amounts corresponding to 0.5 OD cells were separated by SDS-PAGE (section 5.2.6.5) and analysed by Western blotting (section 5.2.6.7) using purified anti-Noc1 (upper left panel) and anti-Noc2 (upper right panel) antibodies, respectively. The anti-Noc2 antibody showed cross reaction with another protein (marked by a cross), levels of which were unchanged over the time course of Noc2p depletion. Prior to detection, membranes were stained with Poinceau S solution to check protein loading (lower panel). Depletion of Rrp5p was not analysed since no anti-Rrp5 antibody was available.

Steady state levels of pre-rRNAs in the pGAL-*NOC1*/-*NOC2*/-*RRP5* and in a wild type control strain were analysed by Northern blotting at several time points after shift to glucose containing medium. The pre-rRNA processing phenotypes in the pGAL-*NOC1* and pGAL-*NOC2* strains were virtually identical. During the first 13-15 h of cultivation in glucose containing medium, levels of 35S pre-rRNA were strongly accumulated relative to the wild type control, accompanied by elevated levels of 23S pre-rRNA, indicating a delay in early pre-rRNA processing events at A0, A1 and A2 (Fig. 3-3 A + B). This effect was observed

before in numerous mutants affecting the LSU maturation pathway (Venema and Tollervey, 1999; Van Beekvelt et al., 2001, and discussion therein; (Pöll et al., 2009); see also Wild et al., 2010). All LSU precursor species (27SA2, 27SB and 7S pre-rRNAs) were drastically reduced, whereas decrease in 20S pre-rRNA was less severe (Fig. 3-3 A-C, E). Consequently, levels of mature LSU components 25S and 5.8S rRNA were significantly diminished, whereas levels of the mature SSU component 18S rRNA showed only moderate reduction (Fig. 3-3 D + F). After 20 - 24h cultivation in glucose containing medium, levels of 35S pre-rRNA were still higher than in the wild type strain, whereas all other pre-rRNA species could hardly be detected (Fig. 3-3 A-C). Altogether, and consistent with the analysis of temperature sensitive *noc1* and *noc2* mutants (section 3.1.1; Milkereit et al., 2001), these experiments indicated a pronounced destabilization of LSU precursors after depletion of Noc1p and Noc2p with secondary effects on SSU pre-rRNAs, whereas synthesis of the primary Pol-I transcript was apparently not directly affected.

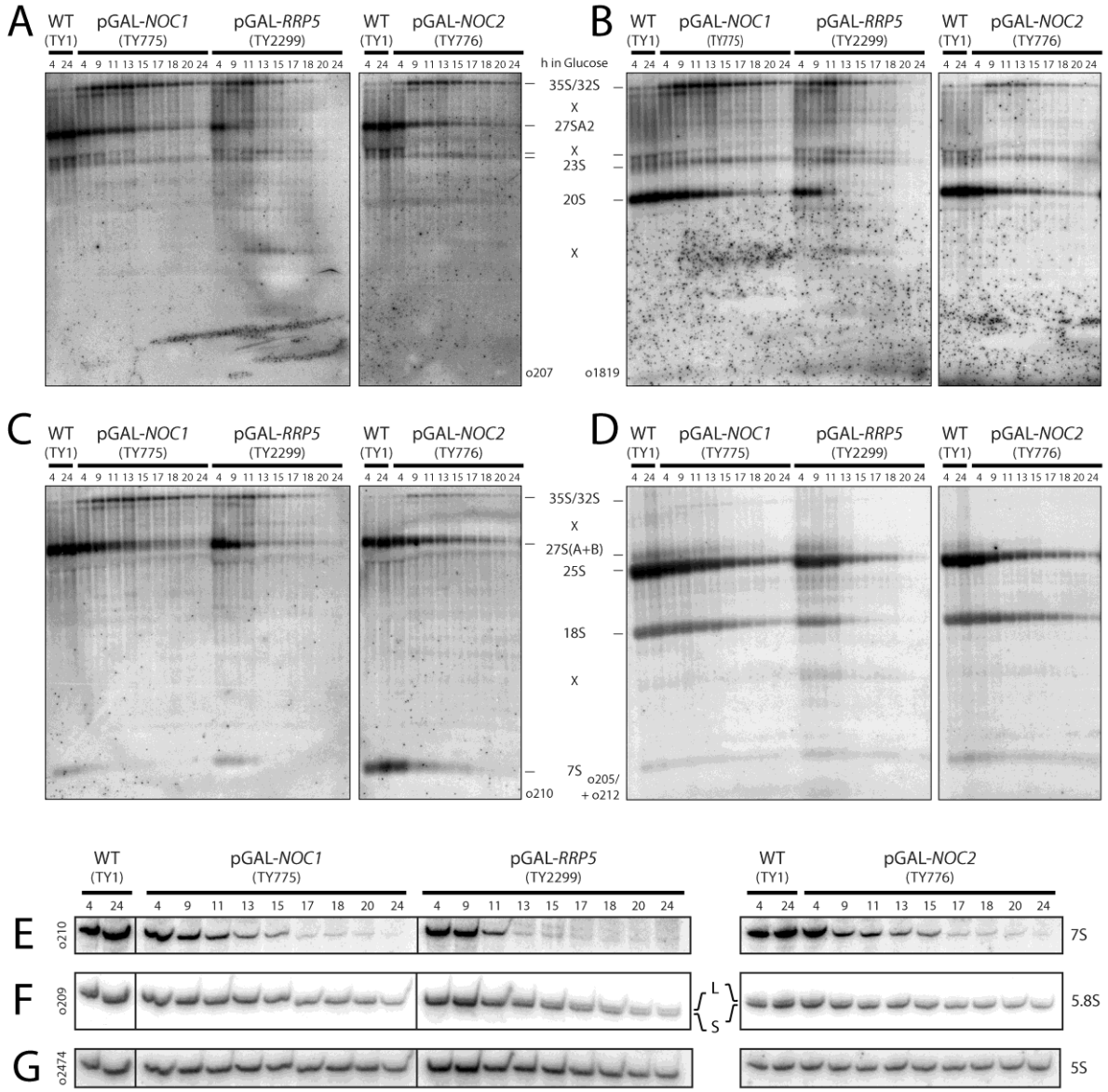

Fig. 3-3: Analysis of pre-rRNA processing defects resulting from *in vivo* depletion of Noc1p, Noc2p and Rrp5p (see next page)

Fig. 3-3 (continued from previous page): The indicated strains were grown in YPDA medium for 24 h and aliquots of cells were harvested at the indicated time points as described in Fig. 3-2. Total RNA was isolated by phenol-chloroform extraction (section 5.2.5.1), separated on agarose (A-D) or acryl amide (E-G) gels (sections 5.2.5.2/3) and analysed by Northern blotting by sequential hybridization with the indicated probes (sections 5.1.5, 5.2.5.4/5/7; for binding sites of o202 – o2474 see Fig. 2-6, 3-7). RNA amounts corresponding to 0.07 and 0.14 OD cells were analyzed on acryl amide and agarose gels, respectively. Bands corresponding to mature rRNAs and major pre-rRNA species are indicated. Bands specifically appearing after depletion of biogenesis factors are marked with a cross.

Depletion of Rrp5p caused initial accumulation of 35S and 23S pre-rRNA and drastically reduced levels of 27S(A+B), 7S, but also of 20S pre-rRNAs (Fig. 3-3 A-C, E), and consistently levels of 25S and 18S rRNAs were equally reduced (Fig. 3-3 D + F), confirming the previously described role of Rrp5p in LSU and SSU biogenesis (Venema and Tollervey, 1996). Furthermore, and in contrast to Noc1p and Noc2p depletion, levels of $5.8S_S$ pre-rRNA were specifically reduced relative to $5.8S_L$ pre-rRNA (Fig. 3-3 F), reflecting the described influence of Rrp5p on processing of site A3 (Venema and Tollervey, 1996). Besides, several aberrant pre-rRNA fragments were detected, most likely resembling the described 31S', 30S', 24S, 17S', 12S' RNAs (Fig. 3-3 A-D). After 20-24h cultivation in glucose containing medium, levels of all (precursor) rRNAs including 35S pre-rRNA were more strongly reduced than after depletion of Noc1p and Noc2p. This could either be due to different depletion kinetics of the proteins or, alternatively, reflect an additional role of Rrp5p in stabilisation of the 35S pre-rRNA.

In summary these experiments showed that *in vivo* depletion of Noc1p, Noc2p and Rrp5p resulted in severely reduced levels of LSU pre-rRNAs indicating that each individual protein is required to form stable pre-LSU particles. In addition, and in agreement with previous studies, Rrp5p specifically influenced A3 site processing in the LSU maturation pathway, and showed a pronounced effect on SSU biogenesis.

3.2 Reconstitution and characterisation of a Rrp5p/Noc1p/Noc2p protein complex

3.2.1 Noc1p, Noc2p and Rrp5p form protein complex

To directly test if Rrp5p can form a protein module with Noc1p and Noc2p as it was indicated by previous studies (Merl et al., 2010), the complex should be reconstituted from proteins co-expressed proteins in SF21 insect cells using recombinant baculo viruses (Berger et al., 2004; Fitzgerald et al., 2006). Furthermore, pair wise interactions between the proteins should be analysed to determine architectural features of the potential complex. Therefore, recombinant baculo viruses encoding combinations of yeast *NOC1*, *NOC2* and *RRP5* genes with always one gene being fused to the sequence coding for the Flag epitope were generated (described in section 5.2.1) and used to co-express the respective proteins in SF21 insect cells. Flag-tag fusion proteins were affinity purified from the respective cell extracts (section 5.2.7.1), and (co-)purified proteins in the final elution fractions were separated by SDS-PAGE followed by Coomassie staining and mass spectrometric analysis. In addition, cell lysates and purified fractions were analysed by Western blot to monitor protein expression and purification efficiencies. These analyses showed that all viruses

induced expression of the expected proteins (Fig. 3-4 B, compare lanes 1, 4, 7, 10, 13) and indicated similar purification efficiencies of the bait proteins in all experiments (Fig. 3-4 B, compare eluate/lysate signal ratios).

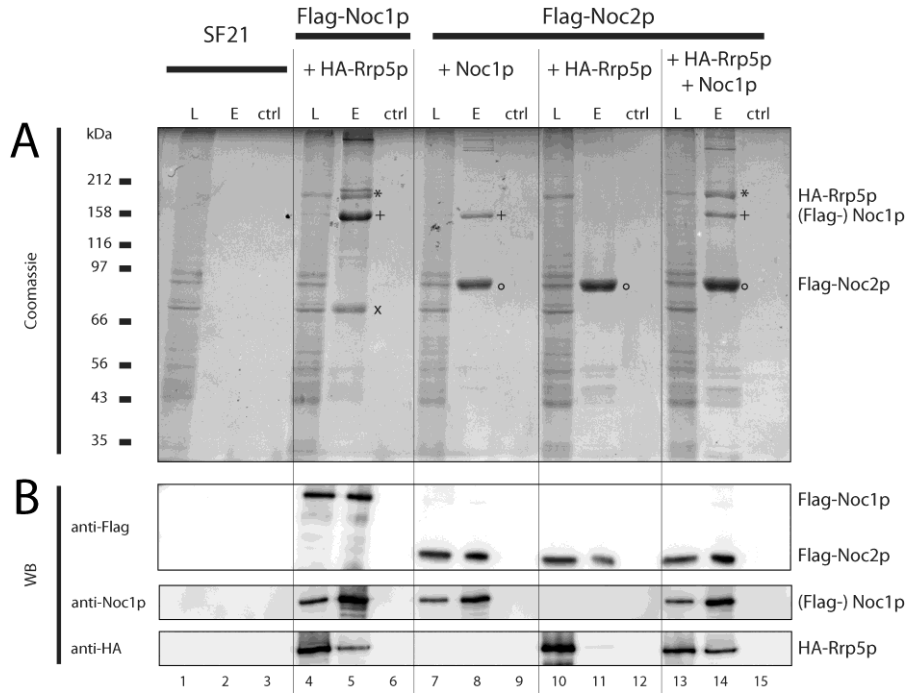

Fig. 3-4: Reconstitution of the Rrp5p/Noc1p/Noc2p module from proteins co-expressed in insect cells

The indicated combinations of Flag-tagged bait proteins and potential interaction partners were co-expressed in SF21 insect cells infected with recombinant baculo viruses containing the plasmids K1232, K1504, K1658 or K1677 (section 5.1.4). Cleared lysates of 50 x 10^6 infected cells and uninfected control cells (SF21) were split in two aliquots and incubated either with anti-Flag affinity matrix or with IgG coupled sepharose. After washing, bound material was eluted with buffer containing Flag peptide (see section 5.2.7.1 for details). Aliquots of the lysates (L), the eluates from the anti-Flag matrix (E) and the IgG sepharose (ctrl.) were analysed by (A) Coomassie stained SDS-PAGE (0.05 % of lysates and 23 % of the eluted material were loaded on the gel) or (B) Western Blotting using anti-Flag (0.015 % L, 0,3 % E/ctrl), anti-Noc1p and anti-HA antibodies (0.006 % L, 1.2 % E/ctrl). Coomassie stained proteins were identified by mass spectrometry and indicated as follows: *: HA-Rrp5p; °: Flag-Noc2p; +: (Flag-) Noc1p; x: N-terminal Flag-Noc1p fragment.

When Flag-Noc2p was co-expressed with Noc1p and HA-Rrp5p, all three proteins were efficiently enriched in the elution fraction after anti-Flag affinity purification but not in the control purification (Fig. 3-4, lanes 13-15), indicating direct interactions between the proteins and potential formation of a Rrp5p/Noc1p/Noc2p complex. When pairs of proteins were expressed, Flag-Noc2p efficiently co-purified Noc1p (Fig. 3-4, lanes 7-9), but not HA-Rrp5p (Fig. 3-4, lanes 10-12) from cell extracts, suggesting that Noc2p cannot stably interact with Rrp5p in absence of Noc1p. In contrast, HA-Rrp5p was efficiently enriched together with affinity purified Flag-Noc1p (Fig. 3-4, lanes 4-6). In summary, these experiments could not only confirm that Noc1p interacts with Noc2p in a robust and specific way (Milkereit et al., 2001), but also suggested that Noc1p can directly interact with Rrp5p. In this way, Noc1p can bridge between Noc2p and Rrp5p to form a hetero-trimeric protein complex, which might act as a functional entity in ribosome biogenesis.

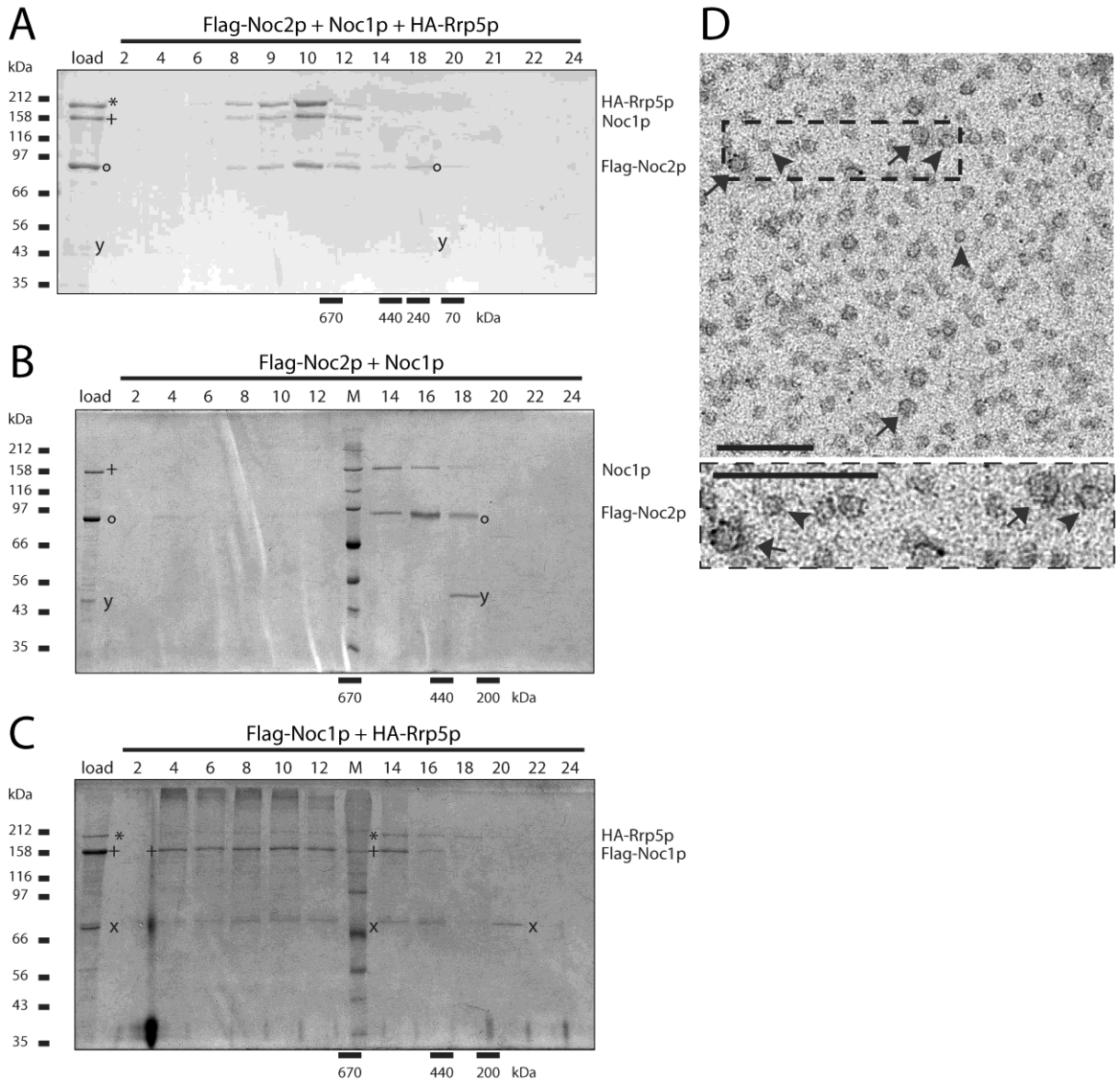

Fig. 3-5: Analyses of reconstituted biogenesis factor modules by gel filtration and electron microscopy

Affinity purified Flag-Noc2p-Noc1p-Rrp5p (A), Flag-Noc2p-Noc1p (B) and Flag-Noc1p-Rrp5p (C) complexes (obtained as in Fig. 3-4) were applied on a Superose 6 gel filtration column, and after washing with 800 µl (A) or 700 µl (B, C) buffer, 50 µl fractions were collected (see section 5.2.7.2 for details). Aliquots of the eluates applied to the column (load; 20% in A, 5% in B and C) and of the chromatography fractions (2-24; 40%) were analysed by Coomassie stained SDS-PAGE (*: HA-Rrp5p; °: Flag-Noc2p; +: (Flag-) Noc1p; x/y: N-terminal Flag-Noc1p/Flag-Noc2p fragments). Elution of marker proteins in independent gel filtration runs is indicated at the bottom of the panels. D) Electron micrograph of an uranyl acetate stained aliquot of the Flag-Noc2p-Noc1p-Rrp5p complex after Superose 6 gel filtration (fraction 10 in (A); for experimental details see section 5.2.7.3). Arrows and arrowheads indicate particles of 12 nm and 8 nm diameter, respectively. The lower panel shows an enlarged view of the boxed area. Scale bars are 70 nm.

For further characterisation, the affinity purified Flag-Noc2/Noc1p/HA-Rrp5p complex was applied onto a Superose 6 size exclusion column. Analysis of the gel filtration fractions by SDS-PAGE and Coomassie staining showed that the bait protein was purified in excess over Rrp5p and Noc1p. Free Flag-Noc2p (Fig. 3-5 A, frct. 18+20) was well separated from a complex bound population of Flag-Noc2p (theoretical MW (Noc2p) = 81 kDa) that co-eluted with Noc1p (theoretical MW = 116 kDa) and HA-Rrp5p (theoretical MW (Rrp5p) = 193 kDa)

at an apparent MW of > 670 kDa (Fig. 3-5 A, frct. 8-12), indicating that the complex could contain some proteins in a higher order stoichiometry.
To address this question, affinity purified Flag-Noc2p/Noc1p and Flag-Noc1p/HA-Rrp5p subcomplexes were also analysed by gel filtration on a Superpose 6 column. In the former case, both Flag-Noc2p and Noc1p eluted in fractions 14-18, but in different ratios (Fig. 3-5 B, compare band intensities of Noc1p and Flag-Noc2p). Besides, an N-terminal fragment of Flag-Noc2p exclusively eluted in fraction 18. These findings indicated that elution of the Flag-Noc2p/Noc1p complex peaked in fractions 14-16 (MW_{app} ~ 440 – 670 kDa), whereas excess, free Flag-Noc2 and fragments thereof peaked in fractions 16-18 (MW_{app} ~ 200 – 440 kDa), compatible with formation of Flag-Noc2p homo-oligomers and a potential higher order stoichiometry of Noc1p in the Flag-Noc2p/Noc1p complex. In case of the Flag-Noc1p/HA-Rrp5p complex, results were less clear, since both proteins eluted over a large range of fractions. However, HA-Rrp5p predominantly eluted in fraction 14 – 16 (MW_{app} ~ 440 – 670 kDa) together with a subpopulation of Noc1p, possibly representing the Flag-Noc1p/HA-Rrp5p subcomplex. In contrast, fractions 4 – 12 predominantly contained Flag-Noc1p and just minor amounts of HA-Rrp5p, indicating large excess of the bait protein in the affinity purified fraction and formation of large Flag-Noc1p homo-oligomers of undefined size (MW_{app} > 670 kDa), which showed only minor association with Rrp5p. The tendency of Noc1p to form homooligomers and aggregates could be confirmed when Flag-Noc1p was expressed alone, and was also observed for Flag-Noc2p and Flag-Rrp5p in absence of their genuine interaction partners (data not shown), which prevented clear conclusions about the oligomerisation state of the single proteins in the respective (sub-)complexes.
Analysis of the Flag-Noc2p/Noc1p/Rrp5p complex after gel filtration by electron microscopy showed particles of ~ 8 nm and ~ 12 nm in diameter (Fig. 3-5 D), the latter of which is well compatible with the apparent molecular weight of ~ 670 kDa of the complex estimated by size exclusion chromatography. However, it remained unclear whether the differently sized particles represent different orientations of the complex on the grid, or particles differing in protein composition.
In summary, these experiments provide strong evidence that Rrp5p, Noc1p and Noc2p form a large hetero-oligomeric protein complex. Clearly, further experiments will be necessary to determine in detail the structure of the complex and the stoichiometry of its components.

3.2.2 The N-terminus of Rrp5p mediates stable interaction with Noc1p

Previous studies showed that the function of Rrp5p in LSU and SSU biogenesis can be separated into its N- and C-terminal parts, respectively, and that co-expression of the respective Rrp5p variants can complement for deletion of *RRP5* (Torchet et al., 1998; Eppens et al., 1999). Since Rrp5p can directly interact with Noc1p (see above; Fig. 3-4) and both proteins affect LSU maturation (Fig. 3-3; (Venema and Tollervey, 1996; Edskes et al., 1998; Milkereit et al., 2001)), the Rrp5p-Noc1p interaction might also be mediated by the N-terminal part of Rrp5p. To test this hypothesis, different truncated HA-Rrp5p variants (Fig. 3-6 A) were co-expressed with Flag-Noc1p in SF21 cells and analysed for co-purification with Flag-Noc1p. Cell lysates and elution fractions after anti-Flag affinity purification were

analysed by SDS-PAGE followed by Western blotting or Coomassie staining to monitor expression of the respective protein variants and (co-)purification efficiencies.

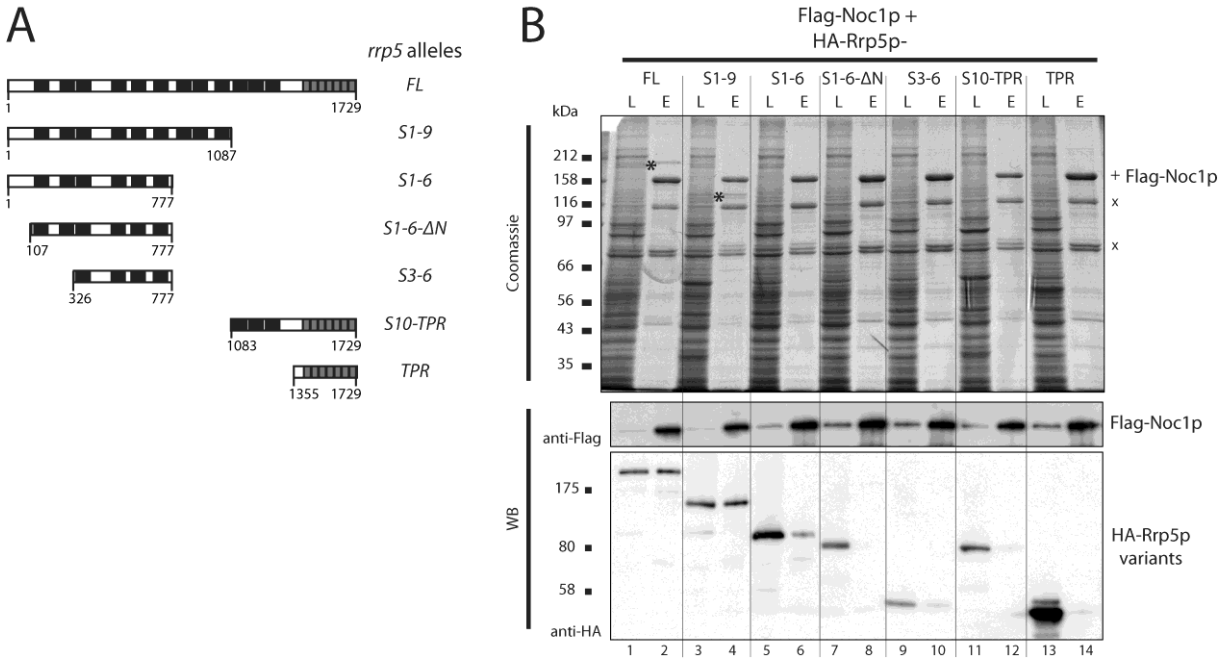

Fig. 3-6: Analyses of the interactions between Noc1p and truncated Rrp5p variants

A) Overview of the *rrp5* alleles analysed in this study and schematic presentation of the corresponding protein variants. The positions of the first and last amino acids relative to the full length protein (FL) are indicated. Black bars illustrate the S1 RNA binding motifs, grey bars the tetratricopeptide repeats, respectively (see section 2.2.7; adapted from (Eppens et al., 1999)). B) The indicated combinations of Flag-Noc1p and truncated HA-Rrp5p variants were co-expressed in SF21 insect cells infected with recombinant baculo viruses containing one of the plasmids K1658, K1727-1730, K1732 or K1733 (see section 5.1.4). Flag-Noc1p was purified with anti-Flag affinity matrix from lysates of 50 x 10^6 infected cells and eluted with buffer containing Flag peptide (section 5.2.7.1). Aliquots of the lysates (L) and eluates (E) were analysed by SDS-PAGE and Coomassie staining (upper panel; 0.04% L, 20% E) or Western Blotting using anti-Flag and anti-HA antibodies (lower panels; 0.006% L, 1 % E). Coomassie stained proteins were identified by mass spectrometry and indicated as follows: *: HA-Rrp5p variants; +: Flag-Noc1p; x: N-terminal Flag-Noc1p fragments.

The bait protein was generally well enriched and, as expected, full length HA-Rrp5p (FL) was efficiently co-purified (Fig. 3-6 B, lanes1+2). The longest N-terminal fragment of Rrp5p (S1-9, aa 1-1087) was equally well co-purified as Rrp5p-FL (Fig. 3-6 B, compare lanes 3/4 with 1/2), but co-purification of a shorter N-terminal fragment (S1-6; aa 1-777) was already severely reduced (Fig. 3-6 B, lanes 5/6 with 1/2). Further truncated N-terminal (S1-6ΔN, S3-6) or C-terminal Rrp5p fragments (S10-TPR, TPR) were not or very inefficiently co-purified with Flag-Noc1p (Fig. 3-6 B, lanes 7-14).

Hence it was concluded that the N-terminal part of Rrp5p (aa 1-1087), which is important for the function of Rrp5p in LSU maturation is required and sufficient to mediate a stable interaction with Noc1p.

3.3 Analyses of *in vivo* interactions of the Rrp5p/Noc1p/Noc2p module components with pre-ribosomes

3.3.1 Noc1p and Rrp5p are stably associated with similar 90S and pre-60S particles

After reconstitution of the Rrp5p/Noc1p/Noc2p complex and characterisation of its architecture, it should be analysed into which pre-ribosomes the module is incorporated *in vivo*. Previous studies analysing the protein composition of different pre-ribosomal particles indicated that Rrp5p and Noc1p are associated with early LSU precursors purified via Nsa3p, Ssf1p or Nop7p but not with later pre-ribosomes purified via Nsa1p (Nissan et al., 2002; Kressler et al., 2008). In addition, Noc1p and Noc2p sedimented together with 35S pre-rRNA on sucrose gradients at ~ 90S, and Rrp5p was shown to be part of U3 snoRNA and 35S pre-rRNA containing pre-ribosomal particles (see sections 2.2.5, 2.2.7). However, it remained unclear whether the function of Rrp5p in LSU and SSU biogenesis (Venema and Tollervey, 1996; Eppens et al., 1999) involves the interaction of Rrp5p with different populations of LSU and SSU precursor particles, respectively. Since detailed knowledge on the composition of Rrp5p- or Noc1p-bound pre-ribosomes was still lacking, we decided to perform a thorough comparative characterization of pre-ribosomes associated with Noc1p or Rrp5p.

Therefore, TAP-tag fusion proteins of Noc1p and Rrp5p were affinity purified from yeast cell extracts in a one-step procedure under mild buffer conditions to preserve pre-ribosomal particles (described in section 5.2.7.4). Western blot analysis showed that both Noc1p-TAP and Rrp5p-TAP were purified with similar efficiencies (Fig. 3-7J, compare signal intensities in lanes 2/5 and 3/6). To characterise co-purified pre-ribosomes on RNA level, total RNA was extracted from aliquots of the cell lysates and the purified fractions and analysed by Northern blotting or in primer extension reactions (Fig. 3-7, A-I). Consistent with a direct interaction of Noc1p and Rrp5p, these analyses showed that both proteins co-purified the same RNA species with very similar efficiencies. The most highly enriched RNA in both purifications was 27SA2 pre-rRNA (Fig. 3-7 B), the first specific pre-LSU RNA species resulting from processing of the common precursor rRNA at site A2 (see section 2.2.3). Co-purification of $27SB_{(L+S)}$ pre-rRNAs, the downstream processing intermediates, was much less efficient as judged by Northern blotting (Fig. 3-7 C) and primer extension (Fig. 3-7 D) analyses. This is in agreement with previous studies, which indicated that Noc1p and Rrp5p are part of early pre-60S particles (De Boer et al., 2006; Kressler et al., 2008), but depleted in intermediate pre-60S particles purified via Nsa1p (Kressler et al., 2008). Interestingly, the less abundant $27SB_L$ pre-rRNA was preferentially enriched in the Noc1p purification (Fig. 3-7 D, compare $27SB_L/27SB_S$ signal ratios in lanes 2, 5), indicating that different release mechanisms might play a role in the two alternative processing pathways yielding $27SB_L$ and $27SB_S$ pre-rRNAs. Furthermore, both Noc1p and Rrp5p co-purified with similar efficiencies 35S and 32S pre-rRNAs (Fig. 3-7 B), as well as U3 snoRNA (Fig. 3-7 A), in agreement with previous studies that indicated association of Noc1p and Rrp5p with 90S/SSU processome particles (Milkereit et al., 2001; Dragon et al., 2002; Grandi et al., 2002; Vos et al., 2004a). In contrast, RNA components of later pre-LSU (7S pre-rRNA, Fig. 3-7 E) or specific pre-SSU (20S pre-rRNA,

Fig. 3-7 H) particles were not efficiently enriched in either purification. Quantitation of the respective co-purification efficiencies showed that they were in the range of those for the mature 25S, 5.8S and 18S rRNAs (Fig. 3-7F, G, I) that were used to determine the internal background in these experiments.

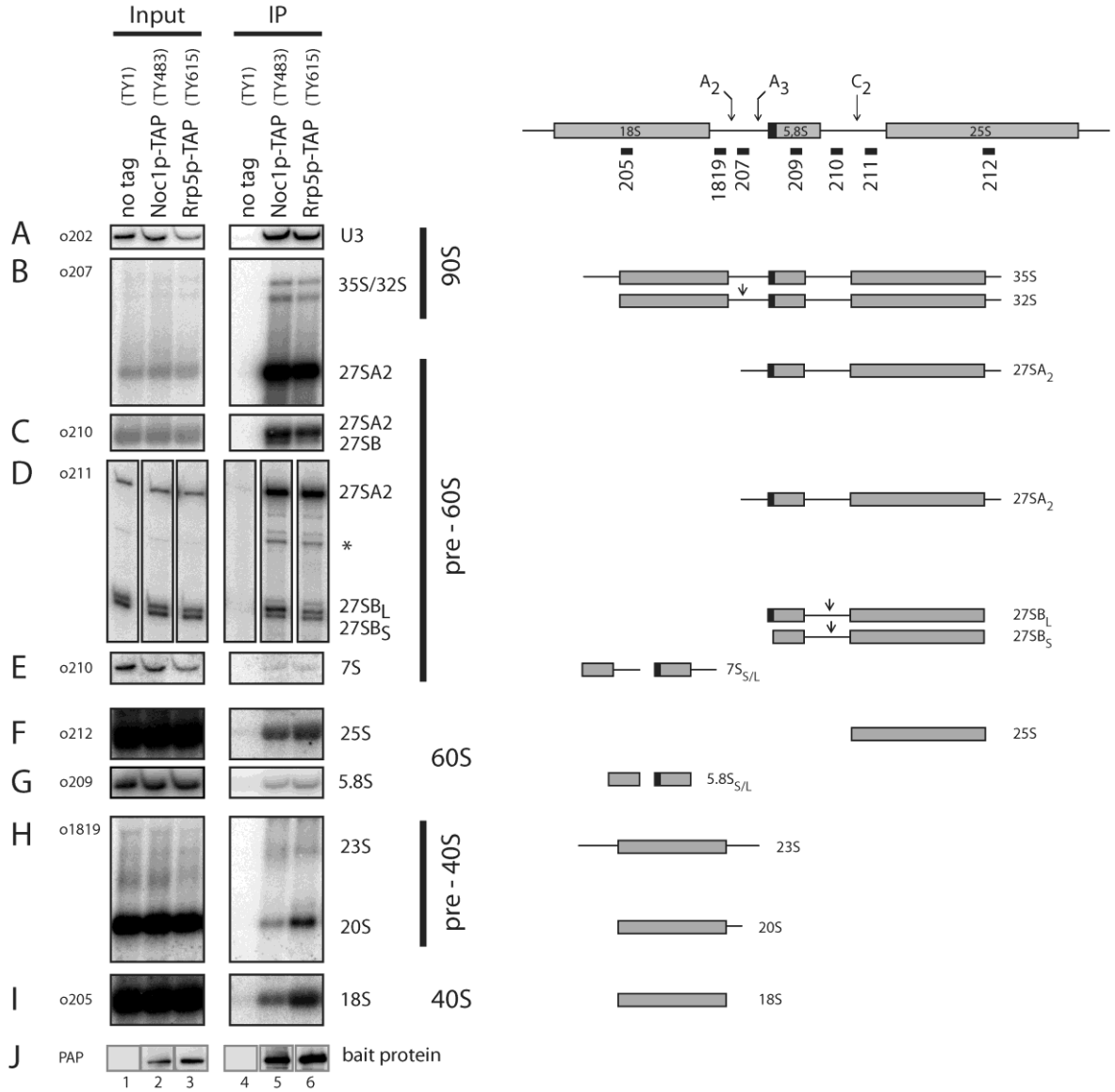

Fig. 3-7: Comparison of pre-ribosomal particles associated with Noc1p or Rrp5p

Yeast strains expressing chromosomally encoded Noc1p-TAP (TY483) or Rrp5p-TAP (TY615) and an untagged control strain (TY1) were grown to exponential phase (OD600 = 0.8) in rich medium. TAP-tagged proteins were affinity purified from cell extracts using IgG-coupled magnetic beads (section 5.2.7.4). After washing, the beads were split for the analysis of co-purified RNAs and proteins. RNA isolated from aliquots of cell extracts (Input) and precipitates (IP) was separated on acryl amide (A, E, G) or agarose (B, C, F, H, I) gels and analysed by Northern blotting. Alternatively, the isolated RNA was used as template in primer extension reactions (D) (section 5.2.5.8). Binding sites of the different probe (o202 – o1819) and the detected (pre-) rRNA species are schematically shown on the right. A signal potentially arising from 27SA3 pre-rRNA is marked by asterisk. Purification of the bait proteins was controlled by Western blotting (J) against the Protein A moiety of the TAP tag using PAP detection reagent. Equal signal intensities in Input and IP correspond to 2% and 11% precipitation efficiency in Northern (0.067 % In, 3.33 % IP) and Western blot (0.11 % In, 1% IP) analysis, respectively.

In summary, these results clearly indicated that Noc1p and Rrp5p are stably associated with highly overlapping populations of early pre-ribosomes. Since in *S. cerevisiae* a significant pool of the common precursor transcript (35S pre-RNA) is co-transcriptionally cleaved into 20S and 27SA2 pre-rRNAs (Osheim et al., 2004; Kos and Tollervey, 2010), co-precipitation of 27SA2 and 35S pre-rRNA implies that Noc1p and Rrp5p are recruited to the earliest LSU precursor particles.

To characterize in more detail the composition of the pre-ribosomes associated with Noc1p and Rrp5p, the proteins in the purified Noc1p-TAP and Rrp5p-TAP fractions were analysed by comparative mass spectrometry using iTRAQ reagents ((Ross et al., 2004; Merl et al., 2010); see section 5.2.7.6). In this way, co-purified proteins can not only be identified, but in addition, this method enables determination of the relative abundances of the identified proteins in two purifications. In these analyses (Fig. 3-8 shows the results of a representative purification), a specific set of around 30 LSU biogenesis factors was reproducibly identified (Fig. 3-8 A). Most of those factors were previously described to be required for early steps in LSU maturation, as the processing of the 5' end of 5.8S rRNA and production and/or stabilization of 27SB pre-rRNA (e. g. Rix7p, Ssf1p, Ebp2p, Rrp1p, Ytm1p, Erb1p, Rlp7p, Nop7p, Nsa3p, Brx1p, Nop4p, Rrs1p, Dbp9p; see section 2.2.6 for details and references). In contrast, no biogenesis factors characteristic for later pre-60S or pre-40S particles (e.g. Rea1p, Arx1p, Nmd3p, Rix1p, Ipi1p, Ipi3p, Drg1p, Lsg1p or Efl1p, Rio2p, Ltv1p; see sections 2.2.5/6) were identified, consistent with the low levels of 20S and 7S pre-rRNAs in the Noc1p and Rrp5p purifications (Fig. 3-7 E + H). However, around 20 components of the 90S/SSU processome particle, including C/D box and H/ACA box snoRNP components, were reproducibly identified in the purified Noc1p-TAP and Rrp5p-TAP fractions (Fig. 3-8 B), in agreement with the observed co-purification of 35S, 32S pre-rRNAs and U3 snoRNA with both proteins (Fig 3-8 A + B). Interestingly, peptides of several subunits of Pol-I, which transcribes the 35S rRNA gene, were also identified in both purifications. Comparison of the relative abundances of the co-purified proteins identified in the Noc1p-TAP and Rrp5p-TAP fractions did not show a clear enrichment of any protein in the one or the other purification (iTRAQ ratios ~ 0.5 – 1.5; see Fig. 3-8 A+B). However, Rrp5p was clearly overrepresented in the Rrp5p-TAP fraction (Fig. 3-8 A), which might indicate the existence of a cellular pool of Rrp5p that is not involved in Noc1p-related interactions with pre-ribosomes. Alternatively, module bound Rrp5p could be less stably associated with pre-ribosomes than Noc1p, and hence preferentially be released during the purification procedure.

In summary, these results showed that Noc1p and Rrp5p are associated with pre-ribosomes that are very similar in their RNA composition (U3 snoRNA; 35S, 32S, 27SA2, 27SB pre-rRNAs), as well as in their content of SSU processome components and early LSU ribosome biogenesis factors. This allows the conclusion that Noc1p and Rrp5p interact as a protein complex with the common 90S precursor of the large and the small ribosomal subunits, and with subsequent early pre-60S particles. However, it remained unclear whether the specific function of Rrp5p in SSU biogenesis is achieved in a complex with Noc1p and Noc2p or by a second population of Rrp5p independent of Noc1p/Noc2p.

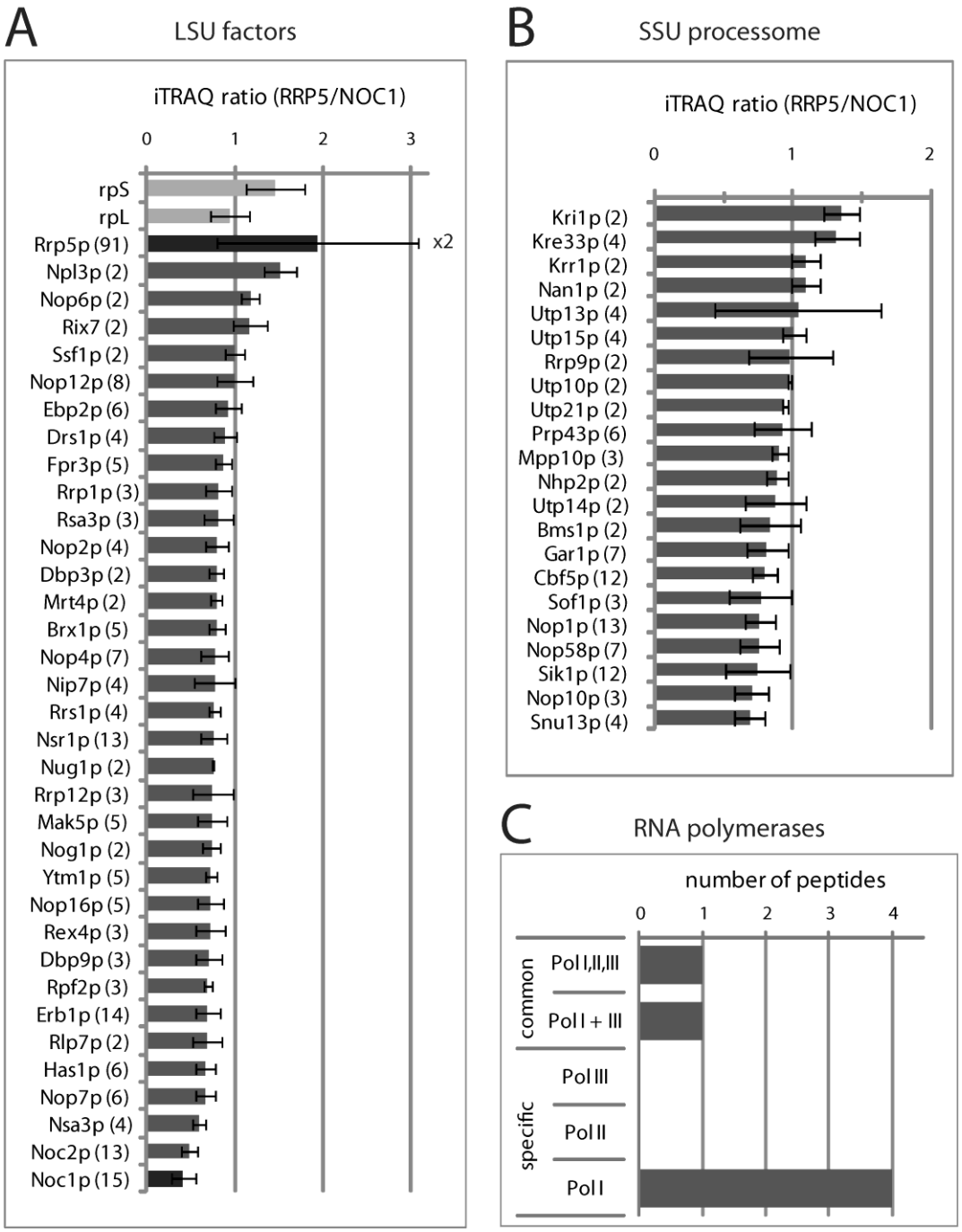

Fig. 3-8: Comparative proteome analysis of pre-ribosomes associated with Noc1p and Rrp5p

Proteins from aliquots of Noc1p-TAP and Rrp5p-TAP purifications (see Fig. 3-7) were digested using trypsin and the resulting peptides were labelled with iTRAQ(R) reagents 116 (Noc1p purification) and 117 (Rrp5p purification), subsequently pooled, separated by reversed phase nano HPLC and spotted on a MALDI-MS/MS target (see section 5.2.7.6 for experimental details). The top 8 peptides of the MS run in each spot were selected for fragmentation in MS/MS mode to determine the identity of the peptide and the ratio of the iTRAQ reporter group signal intensities (117/116). For proteins identified with more than one peptide with an ion score confidence interval (c.i) > 95% the average iTRAQ ratio (117/116 := RRP5/NOC1) was calculated. LSU biogenesis factors (A) and SSU processome components (B) identified in both purifications are listed according to their average iTRAQ ratio (error bars are standard deviations of the average ratios; numbers of identified peptides are indicated in brackets). The average iTRAQ ratios of ribosomal proteins of the large (rpL) and the small (rpS) subunit identified with more than one peptide are shown in (A). C) Peptide count analysis of RNA polymerase subunits identified in both purifications. Only peptides of Pol-I specific subunits (A12.2, A49, A135, A190) and of common subunits (AC40, ABC23) were identified with a c.i. score of more than 95% (one peptide each, iTRAQ ratios ~ 1).

3.3.2 *In vivo* interaction studies of truncated Rrp5p variants with pre-ribosomal particles

To further characterise the interaction of Rrp5p with pre-ribosomal particles, and to address the question if different populations of Rrp5p act in the LSU and SSU biogenesis pathways, the association of different truncated Rrp5p variants with pre-ribosomes was analysed. Based on previous studies, showing that distinct N- and C-terminally truncated Rrp5p variants provide the function of Rrp5p in SSU and LSU maturation in trans (Torchet et al., 1998; Eppens et al., 1999; Torchet and Hermann-Le Denmat, 2000), yeast strains were constructed in which chromosomal deletion of *RRP5* is complemented by ectopic expression of different combinations of trans-complementing *rrp5-ΔX* alleles (*rrp5-S1-9-GFP/rrp5-S10-TPR-TAP* (TY2304), *rrp5-S1-9-GFP/rrp5-TPR-TAP* (TY2305), *rrp5-S1-9-TAP/rrp5-TPR-GFP* (TY2306); Fig. 3-9 A) or of full length *RRP5-TAP* (TY2307). The different Rrp5p-TAP variants were purified from the respective cell extracts under the same mild conditions as described above to preserve pre-ribosomal particles (described in section 5.2.7.4).
All bait proteins were expressed in similar amounts and were purified with similar efficiencies as judged by Western blot (Fig. 3-9 B). To determine the association of the different Rrp5p variants with pre-ribosomal particles, total RNA was isolated from aliquots of the cell extracts and the purified fractions, and analysed by Northern blotting and primer extension reactions (Fig. 3-9 C). Consistent with previous studies (Torchet et al., 1998; Eppens et al., 1999), cellular levels of mature rRNAs were similar in the trans-complementing strains (TY2304-2306) and the control strain expressing full length Rrp5p (TY2307; Fig. 3-9 C i-iv, compare lanes 1-4), except a change in $5.8S_L/5.8S_S$ ratios in strain TY2304. However, pre-rRNA processing was significantly altered in the trans-complementing strains (Fig. 3-9 C v-x). When Rrp5p-S1-9/Rrp5p-TPR variants were co-expressed (TY2305, TY2306), 32S pre-rRNA was strongly accumulated, 27SA2 and 20S pre-rRNAs could hardly be detected and large amounts of 21S pre-rRNA were present (Fig. 3-9 C vi, viii, x, compare lanes 2-4). Primer extension analysis indicated that levels of 27SA3 were slightly elevated compared with the control strain, whereas 27SB pre-rRNAs levels were similar as in the control strain and ratios of $27SB_L/27SB_S$ were not changed (Fig. 3-9 C viii, compare lanes 2-4). The additional stop in primer extension reactions arises most likely from methylation of nucleotides A1779 and A1780 of the 18S rRNA in accumulated 32S pre-rRNA ((Lafontaine et al., 1995, 1998); see also Torchet et al. (2000) and discussion therein). These results are in agreement with previous studies indicating that in strains depending on the Rrp5p-S1-9/Rrp5p-TPR or Rrp5p-ΔS10-12 variants, 32S pre-rRNA is cleaved at site A3 rather than at site A2 and that 27SA3 pre-rRNA could be processed at site B1L (Torchet et al., 1998; Torchet and Hermann-Le Denmat, 2000; Vos et al., 2004b). In contrast, the yeast strain depending on co-expression of Rrp5p-S1-9/Rrp5p-S10-TPR (TY2304) showed similar levels of 35S, 32S, 20S and 27SB pre-rRNAs as the control strain, but no 27SA2 pre-rRNA was detectable and ratios of $27SB_L/27SB_S$ pre-rRNAs were elevated (Fig. 3-9 C vi-vii, x, compare lanes 1+4). This indicated that processing at sites A0, A1 and A2 resulting in 20S and 27SA2 pre-rRNA occurred normally in this strain, but that the subsequent conversion of 27SA2 into 27SB pre-rRNA was significantly accelerated with preference for the $B1_L$ pathway.

Accordingly, Rrp5p could play a role in the structural organization of the 5' end of the 27SA2 pre-rRNA and thereby contribute to its stability and the regulation of the mode of processing.

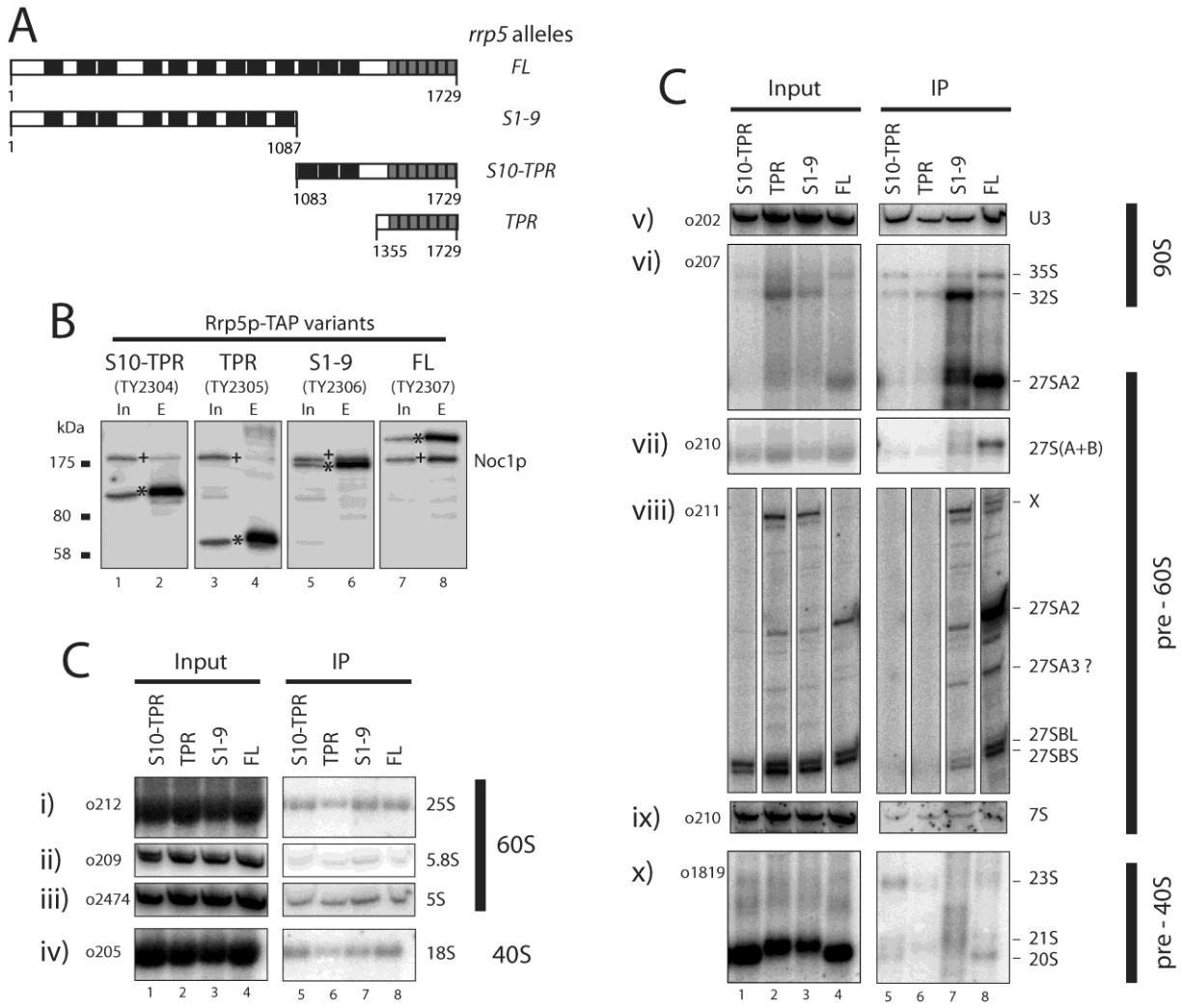

Fig. 3-9: Analyses of the interactions of truncated Rrp5p variants with pre-ribosomal particles

Yeast strains in which genomic deletion of *RRP5* is either rescued by expression of ectopically encoded Rrp5p-FL-GFP (TY2307; FL), or by the split co-expression of the Rrp5p fragments Rrp5p-S1-9-GFP/Rrp5p-S10-TPR-TAP (TY2304; S10-TPR), Rrp5p-S1-9-GFP/Rrp5p-TPR-TAP (TY2305; TPR) or Rrp5p-S1-9-TAP/Rrp5p-TPR-GFP (TY2306; S1-9) were grown in YPDA medium to exponential phase (OD600 = 0.8-1.0). The different *rrp5* alleles are schematically shown in (A) (see Fig. 3-6 for details). Rrp5p-TAP variants were purified from cell lysates using IgG-coupled magnetic beads. After washing, the beads were split for the analysis of co-purified RNAs and proteins, respectively. B) Precipitated proteins were eluted under basic conditions and aliquots of the cell lysates (In) and eluates (E) were analysed by Western Blotting using rabbit anti-Noc1p antibodies to detect both Noc1p (+) and the Protein-A moiety of the Rrp5p-TAP variants (*). C) RNAs isolated from aliquots of cell extracts (Input) and precipitates (IP) were separated on agarose (i, iv, vi, vii, x) or acryl amide (ii, iii, v, ix) gels and analysed by Northern Blotting using the indicated probes (o202 – o2474; for binding sites see Fig. 3-7). Alternatively, the isolated RNA was used as template in primer extension reactions using o211 as primer (viii). Bands corresponding to mature rRNAs and major pre-rRNA species are indicated. X marks an additional stop in primer extension reactions that most likely arises from methylation of nucleotides A1779 and A1780 of the 18S rRNA in accumulated 32S pre-rRNA, which does normally not occur in wild type strains before A2 cleavage has taken place (see main text for details). Equal signal intensities in Input and IP correspond to 11% and 4% precipitation efficiency in Western (0.11 % In, 1% IP) and Northern blot (0.067% In, 1.67% IP) analysis, respectively.

Analysis of the RNAs in the purified fractions showed that Rrp5p-FL co-purified RNA components of 90S and pre-60S particles (U3 sno-rRNA, 35S, 32S, 27SA2, 27SB pre-rRNAs; Fig. 3-9 C v-x, compare lanes 4, 8) with similar efficiencies as described above (Fig.

3-7). However, direct comparison with purifications of the truncated Rrp5p variants was complicated by the different steady state levels of pre-rRNAs in the trans-complementing strains. Among the truncated Rrp5p variants, Rrp5p-S1-9 co-purified the highest amounts of the analysed RNAs (Fig. 3-9 C v-x, compare overall signal intensities in lanes 5-8), consistent with *in vitro* studies indicating high affinity RNA interaction of Rrp5p-S1-9 but not of Rrp5p-S10-TPR (Young and Karbstein, 2011). Nevertheless, U3 snoRNA and 35S pre-rRNAs were co-purified with Rrp5p-S1-9 and Rrp5p-S10-TPR with similar efficiencies as with Rrp5p-FL, and less efficient, but still significant with Rrp5p-TPR (Fig. 3-9 C i-vi, compare signal ratios IP/Input of U3, 35S with those of mature rRNAs). In contrast, significant amounts of pre-LSU specific RNAs (27SA2, 27SB pre-rRNAs) were only detected in the Rrp5p-S1-9 purification (Fig. 3-9 C vi-viii), suggesting that both N- and C-terminal Rrp5p variants are associated with common 90S pre-ribosomes, but only the N-terminal S1-9 variant is segregated into pre-60S particles. Consistently, and in agreement with the experiments shown in Fig. 3-6, Noc1p was co-purified with Rrp5p-S1-9 with similar efficiencies as with Rrp5p-FL (Fig. 3-9 B, compare lanes 5/6 and 7/8). Only minor amounts of Noc1p were detected in Rrp5p-S10-TPR and -TPR purifications (Fig. 3-9 B, lanes 2, 4), which might indicate a weak interaction of these Rrp5p variants with pre-ribosomes containing Noc1p.

In summary, these results indicated that Rrp5p could have two (or more) interaction interfaces with pre-ribosomes, potentially upstream and downstream of the A2 processing site in the ITS1 region as suggested by Young and Karbstein (2011). These interaction interfaces most likely participate differentially in the LSU and SSU specific functions of Rrp5p, respectively.

3.3.3 *In vivo* interaction studies of Noc1p variants with pre-ribosomal particles

3.3.3.1 Noc1p domain assignment and generation of *noc1* alleles lacking different domains

In order to gain further insights into the interaction of Noc1p with pre-ribosomal particles and with the other module components Noc2p and Rrp5p, a similar domain mapping approach should be employed as for Rrp5p. As so far only very limited information was available concerning functional domains of Noc1p (Edskes et al., 1998; Milkereit et al., 2001), sequences of Noc1p proteins from six different species from yeast to human were compared to identify conserved regions within the protein (Fig. 3-10). In agreement with previous analyses showing that the N-terminal (aa 1-228) and C-terminal (aa 899-1025) parts of Noc1p are not essential for growth in yeast (Edskes et al., 1998), these regions showed a low degree of conservation and were defined as domains D1 and D7. The region covering amino acids 726-795, which includes the ‘NOC domain’ (aa 726-770) that is conserved throughout species in Noc1p, Noc3p and Noc4p proteins (see section 2.2.7; (Milkereit et al., 2001, 2003)), showed the highest degree of conservation and was defined as domain D5. In consequence, the relatively low conserved downstream region (aa 796-898) was defined as domain D6. Domains D2, D3 and D4 were assigned based on blocks of highly conserved amino acids separated by stretches of lower conservation (Fig. 3-10).

Fig. 3-10: Definition of different Noc1p domains based on amino acid conservation determined by multiple sequence alignment

(see next page)

Fig. 3-10 (continued from previous page): The sequences of Noc1p from *Saccharomyces cerevisiae* (*S.c.*), *Schizosaccharomyces pombe* (*S.p.*), *Caenorhabditis elegans* (*C.e.*), *Drosophila melanogaster* (*D.m.*), *Mus musculus* (*M.m.*) and *Homo sapiens* (*H.s.*) were compared using the program AlignX (Clustal W based) from the Vector NTI software package and the blosum62mt2 matrix. The resulting consensus sequence (cons.) is shown. Colour code: red letter on yellow ground: identical amino acid (aa) in all sequences; blue on cyan: identical aa in at least 50% of sequences; black on green: similar aa in at least 50% of sequences; green on white: residue weakly similar to consensus residue; black on white: residue not similar to consensus residue. The previously described NOC domain (Milkereit et al., 2001) is marked as dashed box and predicted nuclear localisation signals using the program predictNLS (https://www.predictprotein.org) are underlined in red. Positions of mutated amino acids in the *noc1-6* and *noc1-7* alleles are indicated by black and red dashes, respectively. The assigned domains D1 – D7 (see main text for details) are indicated on the right, the domain boundaries are marked by black lines and the number of the last amino acid is indicated. Lower panel) The average similarity of the aligned sequences to the consensus sequence was determined for each residue using AlignX (based on similarity scores of 1, 0.5, 0.2 and 0 for identical, similar, weakly similar and not similar aa) and the average value of blocks spanning 10 aa was blotted against the position of the centre of the block. The assigned domains are indicated below the graph including the ratio of absolutely conserved to total amino acids per domain.

Sequencing of the *noc1-6* and *noc1-7* alleles described above (section 3.1.1) showed that both alleles contain numerous mutations, but most of those affect non conserved residues and are located in the non-essential domains D1 and D7 of Noc1p (Fig. 3-10), whereas no mutations were found in D5, underlining the importance of the NOC domain. Only two highly conserved amino acids were mutated in each allele, locating to D2 in *noc1-6* and to D3 and D4 in *noc1-7*. As these alleles showed slightly different growth and pre-rRNA processing phenotypes (Fig. 3-1), the respective domains might have different functions and thus appeared to be particularly interesting for interaction studies of truncated Noc1p variants.
Therefore, a library of n*oc1-ΔX* alleles in which one or more domains are deleted (Fig. 3-11 A) were generated by PCR and cloned into a yeast shuttle vector under control of a constitutive promoter to enable expression of the respective Noc1p-ΔX variants with an N-terminal Protein A tag in yeast cells (see section 5.2.4.14; plasmids are listed in section 5.1.4). To determine if and which *protA-noc1-ΔX* alleles are able to complement for deletion of *NOC1*, a NOC1-shuffle strain (TY772) was transformed with the respective plasmids and growth was analysed on plates containing 5-FOA (see section 5.2.2.5 for details). Only transformation with plasmids encoding ProtA-Noc1p-FL, -Δ1, -Δ7 and –Δ1,7 variants yielded colonies on FOA containing plates (data not shown), and the resulting strains grew on selection plates lacking leucin, but not on plates lacking uracil (Fig. 3-11 B). Accordingly, and consistent with previous studies (Edskes et al., 1998), only domains D1 and D7 are dispensable for the essential function of Noc1p. However, strains depending on the respective *protA-noc1-ΔX* alleles were not able to grow at higher temperature (37°C) and deletion of D7 caused growth defects even at lower temperatures, which was enhanced by additional deletion of D1 (Fig. 3-11 B), indicating that some functions of Noc1p are already impaired in these mutants.

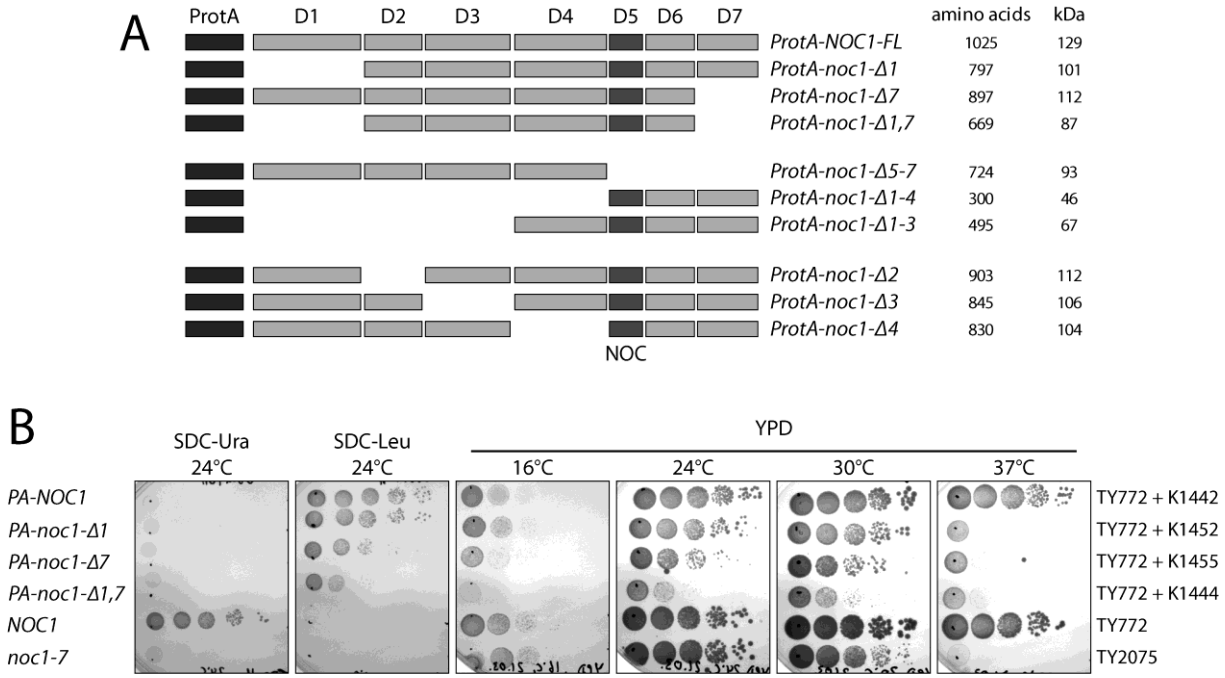

Fig. 3-11: The N- and C-terminal domains of Noc1p are not essential for growth

A) The indicated *noc1* alleles that lack one or more domains (see Fig. 3-10) were generated by PCR and cloned into the plasmid pNOP-PA (V17) carrying the LEU2 auxotrophy marker (see section 5.2.4.14 for experimental details). The resulting plasmids (K1442-1444, K1452-1458; listed in section 5.1.4) allow constitutive expression of Protein A tagged Noc1p variants in yeast cells. The number of Noc1p amino acids in the corresponding protein variants and the calculated mass including the Protein A epitope tag (115 aa) are indicated. B) A genomic *noc1Δ* yeast strain (TY772) expressing NOC1 from a plasmid carrying the URA3 auxotrophy marker, was transformed with one of the plasmids K1442-1444, K1452-1458 and grown on SDC-Leu plates at 24°C for 5 days. Colonies were streaked onto FOA containing SDC-Leu plates incubated at 24°C for 5 days (see section 5.2.2.5 for details). Resulting colonies, which were only obtained from cells transformed with plasmids K1442, K1444, K1452 or K1455, were grown in YPDA medium at 24°C to exponential phase. For growth tests, 1 OD of cells was resuspended in 1 ml sterile H_2O and 10-fold serial dilutions thereof were spotted on the indicated plates and incubated for three days at the indicated temperatures. The parental strain (TY772) and a temperature sensitive *noc1-7* strain (TY2075) were included as controls.

3.3.3.2 Analysis of the association of truncated Noc1p variants with Noc2p, Rrp5p and rRNA precursors

Next, the *in vivo* association of the ProtA-Noc1p-ΔX variants with pre-ribosomes was analysed to investigate whether different domains are important for specific interactions of Noc1p. To prevent that wild type Noc1p competes with the ProtA-Noc1p-ΔX variants for potential interaction partners, the different variants were expressed in a pGAL-*NOC1* strain (TY2154), in which expression of Noc1p can be switched off (see section 3.1.2). In addition, TY2154 expresses genomically encoded Rrp5p-Myc, Noc2p-GFP and Noc3p-HA fusion proteins to allow detection in Western blotting analyses. To deplete wild type Noc1p, cultures were grown in glucose containing full medium for 22h at 24°C. These conditions turned out to be optimal to achieve efficient depletion of Noc1p but to maintain relatively high levels of pre-rRNAs and to enable detection of weak interactions.

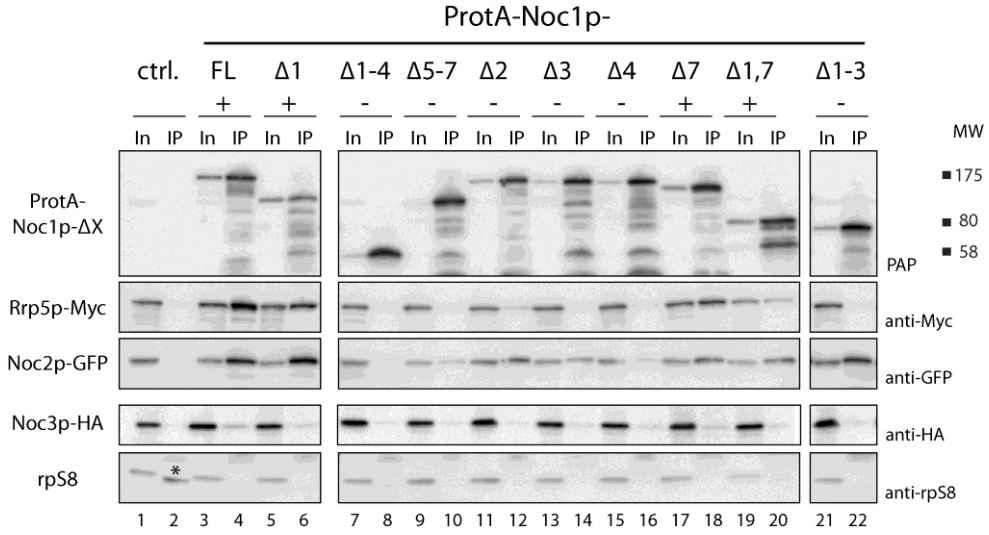

Fig. 3-12: Analyses of the interactions of ProtA-Noc1p-ΔX variants with Noc2p and Rrp5p

Yeast strain TY2154, which expresses genomically encoded Rrp5p-Myc, Noc2p-GFP and Noc3p-HA fusion proteins and in which *NOC1* is under control of the galactose inducible/glucose repressible GAL1/10 promoter (for details see sections 5.1.1 and 5.2.2.4/5), was transformed with plasmids encoding the indicated ProtA-Noc1p-ΔX variants (K1442-1444, K1452-1458; '+' and '-' indicates complementing and not complementing Noc1p variants, respectively) or the corresponding empty vector V17 (ctrl.), and cultivated in selective medium (SGCA-Leu, 24°C). Cells were shifted to glucose containing full medium (YPDA) and incubated for 22h at 24°C to deplete untagged wild type Noc1p from the cells (final OD600 = 0.7 – 1.1). ProtA-Noc1p-ΔX variants were affinity purified from cell extracts using IgG sepharose (see section 5.2.7.5 for experimental details). After washing, the beads were split for the analysis of co-purified proteins and RNAs (see Fig. 3-13). Proteins in the cell extracts (Input) and the purified fractions (IP) were separated by SDS-PAGE and analysed by Western blotting using PAP detection reagent or the indicated anti-bodies. rpS8 was used as a specificity control for the purification. All samples were derived from the same experiment and analysed on the same membrane. Equal signal intensities in Input and IP correspond to 1% purification efficiency. A band arising from a 21.5 kDa polypeptide with N-terminal Prot-A tag that is expressed from the empty vector is marked by asterisk and positions of marker proteins are indicated on the right.

The ProtA-Noc1p-ΔX variants were purified from cell extracts under mild conditions (described in section 5.2.7.5), and proteins in the cell extracts and the purified fractions were analysed by Western blotting to monitor expression and (co-)purification of the bait proteins and of the interaction partners Noc2p and Rrp5p. In general, the ProtA-Noc1p-ΔX variants were expressed in similar levels as ProtA-Noc1p-FL (Fig. 3-12, Input lanes), albeit the non-complementing variants appeared to be slightly less abundant. All bait proteins were efficiently enriched after purification, but substantial amounts of bait protein fragments were also detected in the purified fractions (including ProtA-Noc1p-FL) (Fig. 3-12, compare signals in Input and IP lanes). It remained unclear whether this was due to degradation during the purification procedure or if cellular degradation intermediates were purified, which might arise from elevated levels of ProtA-Noc1p variants resulting from their ectopic expression from the non-native p*NOP1* promoter. ProtA-Noc1p-FL, as expected, co-purified efficiently Noc2p and Rrp5p from cell extracts, but not Noc3p (Fig. 3-12, lanes 3, 4). All complementing variants (ProtA-Noc1p-Δ1, -Δ7, -Δ1,7) also co-purified Noc2p and Rrp5p, but in part with reduced efficiencies, especially in case of ProtA-Noc1p-Δ1,7 (Fig. 3-12, lanes 5, 6, 17-20). Besides, Noc2p was efficiently enriched with ProtA-Noc1p-Δ1-3 and, to a lesser extent, also with ProtA-Noc1p-Δ2, -Δ3, but not or just inefficiently with further N-terminally truncated (-Δ1-4, -Δ4) or C-terminally truncated (-Δ5-7) Noc1p variants (Fig. 3-12, lanes 7-16, 21, 22). In

contrast, of all non-complementing Noc1p variants only ProtA-Noc1p-Δ2 showed some co-purification of Rrp5p (Fig. 3-12, lanes 7-16, 21, 22).
These analyses indicated that domains D1-D3 and D7 of Noc1p are dispensable for stable interaction with Noc2p, suggesting that the region surrounding the 'NOC domain' (D4-D5/(D6), aa 531-795/(898)) might be sufficient therefor. This is reminiscent of the interaction of Noc4p with Nop14p/Noc5p that was shown to be mediated by the C-terminal part (aa 316-553) of Noc4p, which also contains the 'NOC domain' (Kühn et al., 2009). In contrast, the interaction of Noc1p with Rrp5p apparently requires additional elements in Noc1p, as only domains D1 and D7 were individually dispensable for stable interaction with Rrp5p, whereas combined deletion of D1 and D7, as well as further truncations of Noc1p significantly weakened this interaction. Accordingly, stable interaction of Noc1p with Rrp5p might involve several contact sites all over the Noc1p primary sequence or require a folding state of Noc1p that cannot be achieved in the truncated variants. Alternatively, Noc1p variants not co-purifying Rrp5p might not be imported into the nucleus. Bioinformatical analysis using the program predictNLS (https://www.predictprotein.org; Rost laboratory) identified a potential nuclear localisation sequence (NLS) that is partially conserved and located in domain D7 of yeast Noc1p (Fig. 3-10). However, as domain D7 is not essential for growth (Fig. 3-11 B; (Edskes et al., 1998)), this cannot be the exclusive nuclear import mechanism for Noc1p. Accordingly, Noc1p could be co-imported with other proteins, but the obvious candidates Noc2p and Rrp5p do not contain a predicted NLS, either. Alternatively, Noc1p could contain a hidden NLS in one of its essential domains, but as the intracellular localisation of the ProtA-Noc1p-ΔX alleles was not analysed in this work, this question remains elusive.

To investigate the association of ProtA-Noc1p-ΔX variants with pre-ribosomes, RNA was isolated from aliquots of cell extracts and the purified fractions, and analysed by Northern blotting and primer extension reactions. Strains expressing non-complementing ProtA-Noc1p-ΔX variants showed very similar pre-rRNA processing phenotypes as the control strain transformed with an empty plasmid, which in general resembled the ones described in Fig. 3-3. However, the effects on pre-rRNA levels were less severe, probably due to growth at lower temperature resulting in slower Noc1p depletion kinetics and/or reduced turnover of aberrant pre-ribosomes.Levels of LSU precursor rRNAs (27SA2, 27SB) were reduced when compared to the strain expressing ProtA-Noc1p-FL (Fig. 3-14 A, compare signals in lanes 1, 3, 7, 9, 13, 15, 21), but the ratios between $27SB_L$ and $27SB_S$ appeared to be unaffected (Fig. 3-14 B, lanes 1, 3, 11). In contrast, levels of 35S pre-rRNA were elevated and accumulated relative to 27S pre-rRNAs, (Fig. 3-14 B, compare 35S/27S signal ratios in Input lanes). Effects on 7S and 20S pre-rRNAs and levels of mature rRNAs were also very similar to those described in Fig. 3-3 (data not shown). Notably, only expression of ProtA-Noc1p-Δ1, but not of –Δ7 and –Δ1,7 variants, resulted in similar pre-rRNA levels as in the ProtA-Noc1p-FL strain (Fig. 3-13 A, compare lanes 3, 5, 17, 19), indicating that rRNA processing is partially impaired in those strains. As observed before for Noc1p-TAP (Fig. 3-7), ProtA-Noc1p-FL co-purified most efficiently 27SA2 pre-rRNA, but also 35S, 32S and 27SB pre-rRNAs, with a preference for the $27SB_L$ species (Fig. 3-13 A + B, lanes 3, 4). All complementing Noc1p variants co-purified the same pre-rRNA species as ProtA-Noc1p-FL, although with lower

efficiencies, especially in case of ProtA-Noc1p-Δ1,7 (Fig. 3-13 A (lanes 5, 6, 17 – 20) + B (lanes 5-10). Of all non-complementing Noc1p variants, only ProtA-Noc1p-Δ2 showed minor co-purification of pre-rRNAs (Fig. 3-13 A + B, lanes 11, 12), indicating that domain D2 is not required for nuclear import of Noc1p, whereas this cannot be excluded for domains D3-D6 at this point. Thus, co-purification of pre-rRNA and Rrp5p was correlated in all analysed ProtA-Noc1p-ΔX variants, indicating that Noc1p might be indirectly associated with pre-ribosomes/pre-rRNA via Rrp5p. Alternatively, robust interactions with both Rrp5p and pre-rRNA might involve overlapping domains within the essential part of Noc1p. Finally, failure of nuclear import of the truncated variants might interfere with establishment of interactions with both Rrp5p and pre-rRNA.

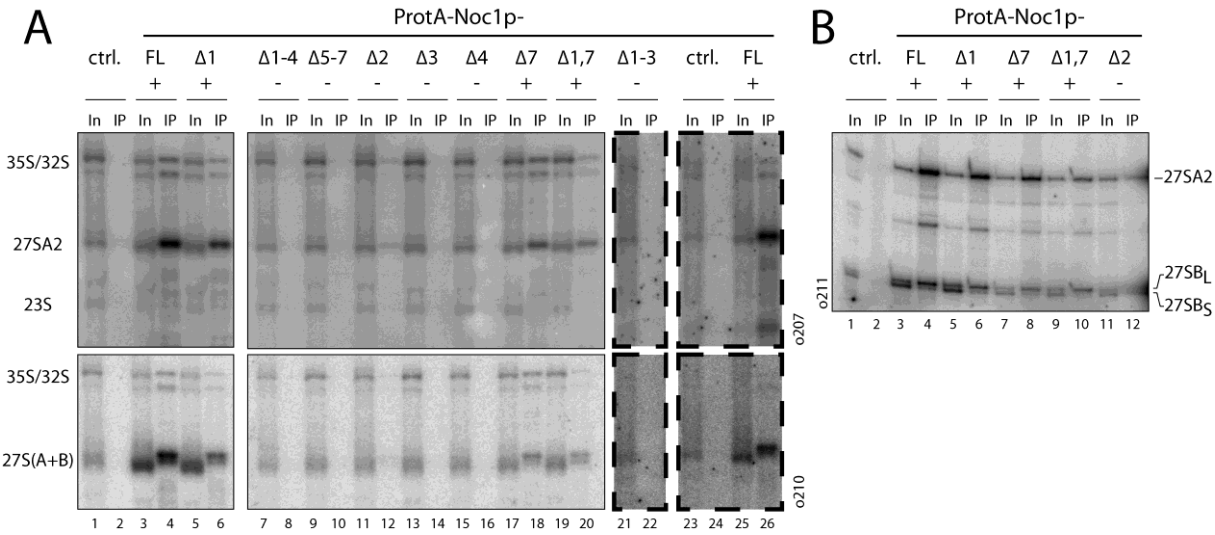

Fig. 3-13: Analyses of the interactions of ProtA-Noc1p-ΔX variants with pre-rRNA

A) RNAs isolated from aliquots of cell lysates (In) and purified fractions (IP) obtained from the experiment described in Fig. 3-12 were separated on agarose gels and analysed by Northern blotting by subsequent hybridization using the indicated probes (o207, o210; binding sites are depicted in Fig. 3-7). Except for ProtA-Noc1p-Δ1-3, which was derived from a separate purification including the empty vector and the ProtA-Noc1p-FL controls (dashed boxes), all samples were analysed on the same gel. B) From selected samples, the isolated RNA was used as template in primer extension reactions using oligo o211 as primer to detect the different 5' ends of 27S pre-rRNAs.

In summary, these experiments indicated that for all *protA-noc1-ΔX* alleles that cause growth defects or do not allow growth, pre-rRNA processing is disturbed and the corresponding protein variants are impaired in their interaction with Noc2p and/or Rrp5p and pre-ribosomal particles. This suggests that formation of the Rrp5p/Noc1p/Noc2p module as well as its association with pre-ribosomes is a prerequisite for correct pre-rRNA processing and thus required for ribosome synthesis and cell growth.

3.3.4 Analysis of the binding hierarchy of the Rrp5p/Noc1p/Noc2p module components to pre-ribosomes

Interaction studies of truncated Noc1p variants showed that for all analysed ProtA-Noc1p-ΔX variants the association with pre-rRNAs and Rrp5p was correlated (section 3.3.3.2) and analogous studies with truncated Noc2p variants indicated correlation of pre-rRNA, Rrp5p and Noc1p co-purification with ProtA-Noc2p-ΔX variants (Hierlmeier, 2008 (diploma thesis)). Furthermore, Rrp5p was described to have RNA binding activity and to interact with specific sequences of the ITS1 region of 35S pre-rRNA *in vitro* (De Boer et al., 2006; Young and Karbstein, 2011), raising the possibility that binding of the Rrp5p/Noc1p/Noc2p module to pre-ribosomes *in vivo* might occur via direct RNA interaction of Rrp5p. To test this, the binding hierarchy of the module components to pre-ribosomes was analysed.

Therefore, yeast strains were constructed in which *RRP5* is under control of the endogenous or the conditional GAL1/10 promoter and *NOC1* (TY2302, TY2343) or *NOC2* (TY2303, TY2301) are genomically fused to the TAP-tag. In addition, yeast strains were generated that express genomically encoded Rrp5p-TAP fusion protein and in which *NOC1* (TY2499, TY2501) or *NOC2* (TY2500, TY2502) are under control of the endogenous or the *GAL1/10* promoter. These strains were grown for 10h, 18h or 24h in glucose containing medium to shut off expression of Rrp5p, Noc1p or Noc2p, respectively, and the TAP-tagged bait proteins were purified from the respective cell extracts under mild conditions to preserve pre-ribosomal particles (described in section 5.2.7.5).

To determine the association of the bait proteins with pre-ribosomes, RNA was isolated from aliquots of the cell extracts and the purified fractions and analysed by Northern blotting. As described above in detail (section 3.1.2, Fig. 3-3), depletion of Rrp5p, Noc1p and Noc2p resulted in severely reduced levels of pre-LSU rRNA species, accompanied by the appearance of aberrant pre-rRNA fragments in case of Rrp5p depletion (Fig. 3-14 A, B, C, compare Input lanes of WT and p*GAL* strains). However, levels of 35S pre-rRNA were similar as in the corresponding non-depleted control strains, which was a prerequisite to determine association of the bait proteins with pre-ribosomal particles.

Fig. 3-14: Analysis of the binding hierarchy of the Rrp5p/Noc1p/Noc2p module components to pre-ribosomal particles (next page)

Yeast strains expressing chromosomally encoded Noc1p-TAP (TY2302/TY2343) or Noc2p-TAP (TY2303/TY2301) in which the *RRP5* gene is either under control of the endogenous (WT) or the inducible *GAL 1/10* promoter (p*GAL*) were cultivated for 10h and 18h in glucose containing rich medium (YPDA; final OD600 = 0.5 – 1). Analogous experiments were carried out with strains expressing chromosomally encoded Rrp5p-TAP with *NOC1* (TY2499/TY2501) or *NOC2* (TY2500/TY2502) under the control of the endogenous (WT) or the GAL 1/10 promoter. These strains were cultivated for 10h,18h and 24h in glucose containing rich medium (final OD600 = 0,5 – 1). The respective background strains expressing no tagged protein (TY1, TY616), which served as controls, were cultivated for 18h in glucose containing rich medium. TAP-tagged proteins were affinity purified from cell extracts using IgG sepharose (section 5.2.7.5). After washing, the beads were split for the analysis of co-purified RNAs and proteins. RNAs isolated from aliquots of cell extracts (Input) and immuno-purified fractions (IP) were separated on acrylamide or agarose gels and analysed by Northern blotting by subsequent hybridization using the indicated probes (o202 – o1819; binding sites are depicted in Fig. 3-7). All input and IP samples of the purification of one bait protein in the different strains were analysed on the same gel. Purification of the bait proteins was controlled by Western Blotting (WB) against the ProteinA moiety of the TAP tag using anti-ProteinA antibody. Equal signal intensities in Input and IP correspond to 2% and 1.5% purification efficiency in Northern Blots of agarose and acrylamide gels, respectively. In Western Blots, equal signal intensities in Input and IP correspond to 20% (Rrp5-TAP), 33% (Noc1-TAP) and 17% (Noc2-TAP) purification efficiencies. Aberrant pre-rRNA fragments resulting from depletion of biogenesis factors are indicated (X). A) Depletion of Rrp5p; B) Depletion of Noc1p; C) Depletion of Noc2p; D) untagged control strains.

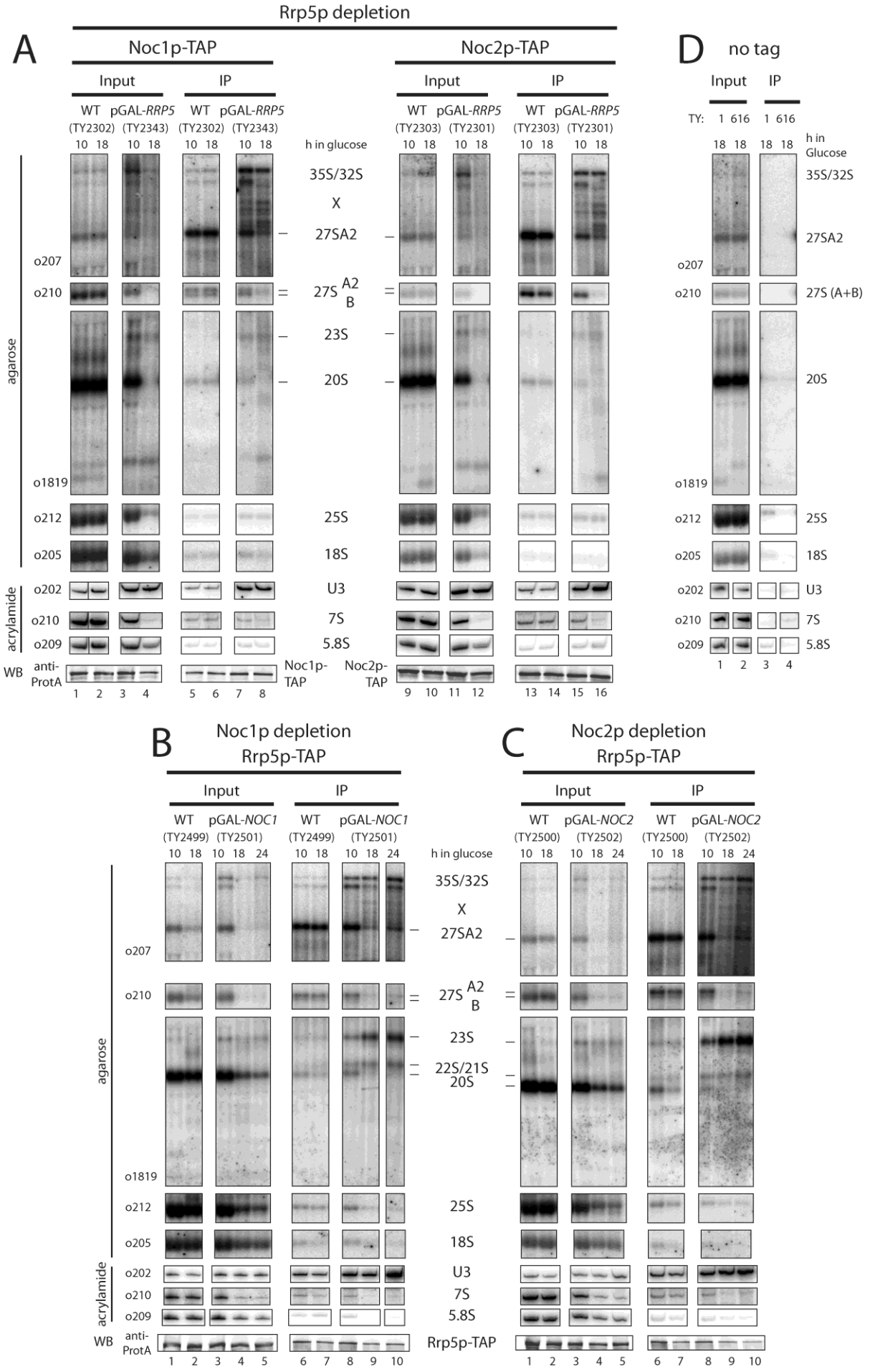
A
Rrp5p depletion
Noc1p-TAP
Noc2p-TAP
Input
IP
WT (TY2302)
pGAL-RRP5 (TY2343)
WT (TY2303)
pGAL-RRP5 (TY2301)
h in glucose
35S/32S
X
27SA2
27S A2 B
23S
20S
25S
18S
U3
7S
5.8S
o207
o210
o1819
o212
o205
o202
o209
agarose
acrylamide
WB
anti-ProtA
Noc1p-TAP
Noc2p-TAP
D
no tag
TY:
Input
IP
h in Glucose
27S (A+B)
B
Noc1p depletion
Rrp5p-TAP
WT (TY2499)
pGAL-NOC1 (TY2501)
C
Noc2p depletion
Rrp5p-TAP
WT (TY2500)
pGAL-NOC2 (TY2502)
22S/21S
Rrp5p-TAP

Noc1p-TAP co-purified U3 snoRNA, 35S, 32S, 27SA2 and 27SB pre-rRNAs from extracts of cells not depleted of Rrp5p with similar efficiencies as described above (compare Fig. 3-14 A and Fig. 3-7). Notably, from extracts of cells depleted of Rrp5p, 35S pre-rRNA and U3 snoRNA were even more efficiently co-purified with Noc1p-TAP (Fig 3-15 A, compare signal ratios of lane 6/2 with 8/4), and several aberrant pre-rRNA fragments resulting from Rrp5p depletion were also efficiently enriched in the Noc1p purification (Fig. 3-15 A, bands marked with X). From extracts of cells expressing Rrp5p, Noc2p-TAP co-purified not only U3 snoRNA, 35S, 32S, 27SA2 pre-rRNAs in similar efficiencies as Noc1p-TAP, but also substantial amounts of 27SB pre-rRNAs and some 7S pre-rRNA (Fig 3-15 A, compare lanes 9 and 13 with 1 and 5), consistent with the association of a Rrp5p/Noc1p/Noc2p complex with early, and a Noc2p/Noc3p complex with intermediate pre-60S particles. Similar as observed for Noc1p, Noc2p-TAP co-purified even more efficiently U3 snoRNA and 35S pre-rRNA as well as aberrant pre-rRNA fragments after depletion of Rrp5p (Fig 3-15 A, compare signal ratios of lane 14/10 with 16/12). Altogether, these results indicated that Noc1p and Noc2p can bind independent of Rrp5p to pre-ribosomal particles containing U3 snoRNA and 35S pre-rRNA or fragments thereof.

From extracts of cells expressing Noc1p and Noc2p, Rrp5p-TAP co-purified the same RNA species (U3 snoRNA, 35S, 32S, 27SA2 and 27SB pre-rRNAs) in similar efficiencies as described above (compare Fig 3-15 B, C lanes 1/6 with Fig. 3-7). After depletion of Noc1p or Noc2p, U3 snoRNA, 35S and 23S pre-rRNAs were even more efficiently enriched in the Rrp5p purification (Fig. 3-14 B, C, compare signal ratios of lanes 2/7, 4/9, 5/10) indicating Noc1p/Noc2p independent recruitment of Rrp5p to pre-ribosomes and a possible prolonged dwelling time of Rrp5p in the corresponding RNPs. Notably, a significant population of Rrp5p was associated with pre-ribosomes containing 23S pre-rRNA, possibly by direct interaction with pre-rRNA between processing sites A2 and A3 (De Boer et al., 2006; Young and Karbstein, 2011). In addition, several aberrant pre-rRNA fragments were specifically enriched in the Rrp5p purification (Fig. 3-14 B, C, bands marked with X), underlining inaccurate processing and/or destabilisation of pre-rRNAs in absence of Noc1p and Noc2p.

In summary, these results suggested that LSU precursors that are depleted of either Noc1p, Noc2p or Rrp5p are specifically sensitive to pre-rRNA degradation pathways, and indicated that the Rrp5p/Noc1p/Noc2p module has several binding sites on pre-ribosomes.

3.3.5 Comparative analysis of the effect of Rrp5p and Noc1p on the recruitment of the UTP-C complex to pre-ribosomes

The experiments described so far strongly suggested that a Rrp5p/Noc1p/Noc2p module is associated with 90S and early pre-60S particles and contributes to the stability of these LSU precursors. However, it remained unclear if the specific function of Rrp5p in SSU biogenesis such as impact on A0, A1, A2 processing (Venema and Tollervey, 1996) or recruitment of the UTP-C complex to pre-ribosomes (Pérez-Fernández et al., 2007), are achieved in the context of the Rrp5p/Noc1p/Noc2p module or by a separate, Noc1p/Noc2p independent population of Rrp5p. To address this question, the effect of Rrp5p and Noc1p on the UTP-C recruitment was compared in a similar approach as described above. Therefore, yeast

strains were constructed in which the UTP-C component Utp22p is expressed as TAP-tag fusion protein and in which *RRP5* (TY2322, TY2318) or *NOC1* (TY2417, TY2418) are under control of the endogenous or the conditional *GAL1/10* promoter. Strains were cultivated in glucose containing medium for 10, 18 or 24h to deplete Rrp5p or Noc1p, respectively, and Utp22p-TAP was purified from the cell extracts. Analysis of the RNAs in the cell extracts and the purified fractions by Northern blotting showed that the expected rRNA processing phenotypes were established in strains depleted of Rrp5p or Noc1p (Fig. 3-15 A+B, compare Input lanes of WT and pGAL strains; for details, see sections 3.1.2 and 3.3.4).

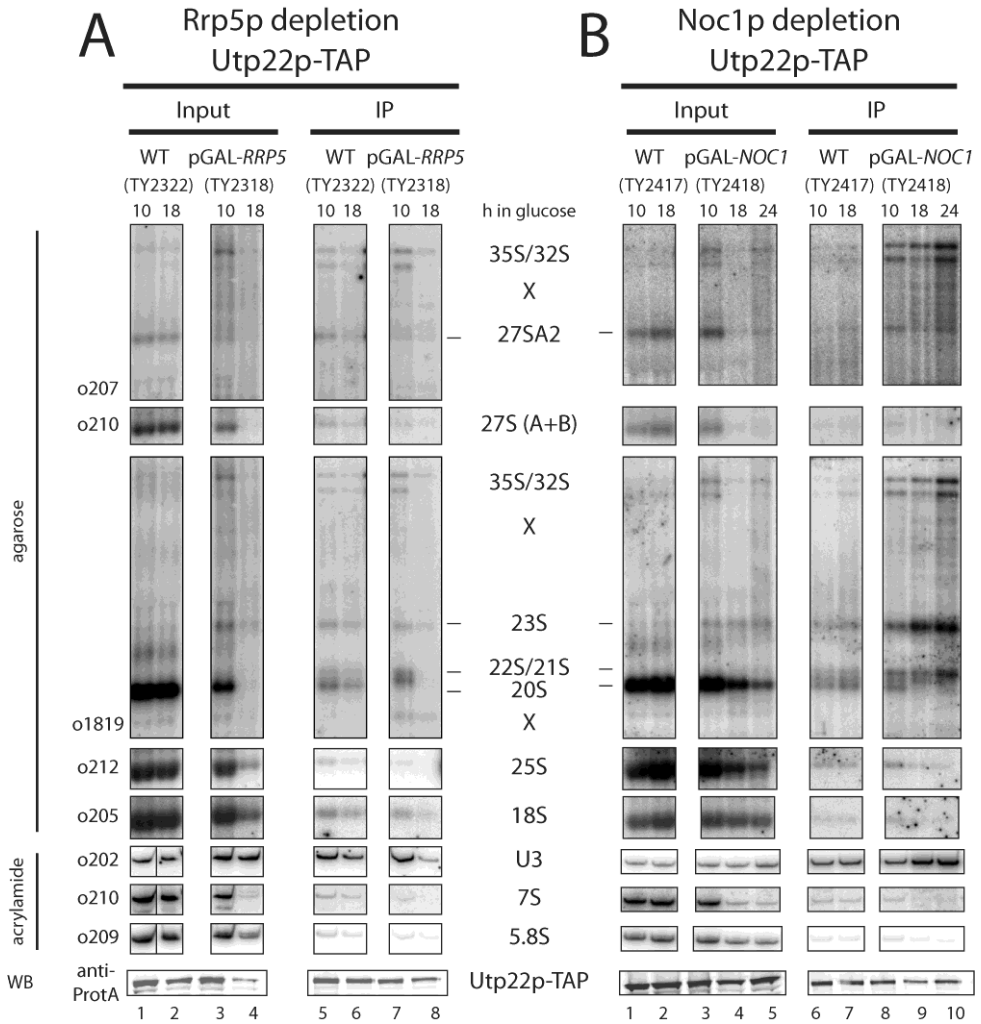

Fig. 3-15: Analysis of the effects of Rrp5p and Noc1p on the binding of the UTP-C component Utp22p to pre-ribosomal particles

Analogous experiments as described in Fig. 3-14 were carried out with strains expressing chromosomally encoded Utp22p-TAP with *RRP5* (TY2322/TY2318) or *NOC1* (TY2417/TY2418) under the control of the endogenous (WT) or the *GAL 1/10* promoter. A) Depletion of Rrp5p. B) Depletion of Noc1p. Equal signal intensities in Input and IP correspond to 2% and 1.5% purification efficiency in Northern Blots of agarose and acrylamide gels, respectively. In Western Blots, equal signal intensities in Input and IP correspond to 50% purification efficiencies.

As expected, Utp22p-TAP co-purified most efficiently U3 snoRNA, 35S, 32S as well as 23S, 22S and 21S pre-rRNAs from cells expressing Rrp5p and Noc1p (Fig. 3-15 A (compare lanes 1/5, 2/6) + B (compare lanes 1/6, 2/7)). These results confirmed the association of Utp22p/UTP-C with 90S pre-ribosomes and indicated its association with particles arising

from processing of site A3 prior to processing of sites A0-A2 (Grandi et al., 2002; Pérez-Fernández et al., 2007). After *in vivo* depletion of Rrp5p, co-purification efficiency for U3 snoRNA was significantly reduced. On the other hand, co-purification of 35S pre-rRNA was hardly affected, and a non-canonical pre-rRNA fragment migrating faster than 18S rRNA specifically co-purified with Utp22p-TAP (Fig. 3-15 A, compare lanes 2/6, 4/8). These experiments indicated that Rrp5p is required for stable binding of Utp22p (and the UTP-C complex) to 90S pre-ribosomes containing U3 snoRNA. However, Utp22p apparently shows residual, Rrp5p-independent affinity to pre-ribosomal particles containing the entire 35S pre-rRNA or fragments of it. Accordingly, the latter could represent non-productive pre-ribosomes.

In contrast, after *in vivo* depletion of Noc1p, U3 snoRNA, 35S, 32S and 23S pre-rRNAs co-purified with Utp22p-TAP with significantly increased efficiencies (Fig. 3-15 B, compare lanes 2/7, 4/9, 5/10), strongly indicating Noc1p independent binding of Utp22p to pre-ribosomes and a possible prolonged dwelling time of Utp22p in the corresponding RNPs. Notably, after depletion of Rrp5p, but not of Noc1p, total cellular levels of Utp22p were apparently reduced (Fig. 3-15 A+B, compare lanes 1-4 and 1-5 of WB), whereas the ratio of free Utp22p versus pre-ribosome associated Utp22p seemed to be increased (Fig 3-16 A, compare ratios of Utp22-TAP signal (WB) to overall pre-rRNA signal (o207, o210, o1819) in lanes 6 and 8), suggesting that free Utp22p might be unstable and get degraded.

In summary, these experiments provided clear evidence that Noc1p is not required for the function of Rrp5p in the recruitment of the UTP-C complex to pre-ribosomes.

3.4 Evidence for co-transcriptional recruitment of Rrp5p, Noc1p and Noc2p to pre-ribosomes

3.4.1 Noc1p and Rrp5p are part of RNA polymerase I transcribed chromatin

In the proteome analyses of fractions co-purified with Noc1p-TAP and Rrp5p-TAP, several Pol-I specific subunits (A12.2, A49, A135, A190) and shared Pol-I/(II/)III subunits (AC40, ABC23) were identified (Fig. 3-8 C; one peptide each with iTRAQ ratios ~ 1), but no subunits specific for Pol-II or Pol-III. Since Pol-I synthesizes the primary pre-rRNA transcript, this observation provided first evidence that recruitment of Rrp5p and Noc1p to pre-ribosomal particles could occur co-transcriptionally.

Remarkably, comparative proteome analyses of chromatin associated with Pol-I or Pol-II identified Rrp5p and Noc1p as specific components of Pol-I transcribed chromatin (Fig. 16; data generously provided by J. Perez-Fernandez and A. Bruckmann; adapted from (Hierlmeier et al., 2012)). In these experiments, Pol-I and Pol-II were purified from the chromatin fractions of cells treated with formaldehyde using Protein A fusion proteins of the Pol-I subunit Rpa135p and the Pol-II subunit Rpb2p. Proteins in the purified fractions were analysed by comparative mass spectrometry using iTRAQ reagents and the results of six independent experiments were subjected to statistical analyses using clustering algorithms to identify specific components of Pol-I and Pol-II transcribed chromatin (Fig. 3-16 A). These analyses resulted in five groups of proteins that are either preferentially enriched in the Pol-I

(cluster A + B) or the Pol-II purification (cluster D + E) or equally abundant in both purifications (cluster C). Cluster C contained some common components of Pol-I and Pol-II chromatin (e.g. shared subunits Rpo26p, Rpc10p) and general chromatin components (Rvb1p, Rsc8p) as well as a large number of obviously unspecific contaminants (e.g. ribosomal proteins, chaperones, components of the cytoskeleton). Cluster D and E contained five Pol-II specific subunits as well as Pol-II elongation factors (e.g. Spt5p, Spt6p) and proteins involved in co-transcriptional mRNA metabolism (e.g. Yra1p, Sub2p), but only few putative contaminants like chaperones (Hsp82p, Ssb1p) (Fig. 3-16 E + F).

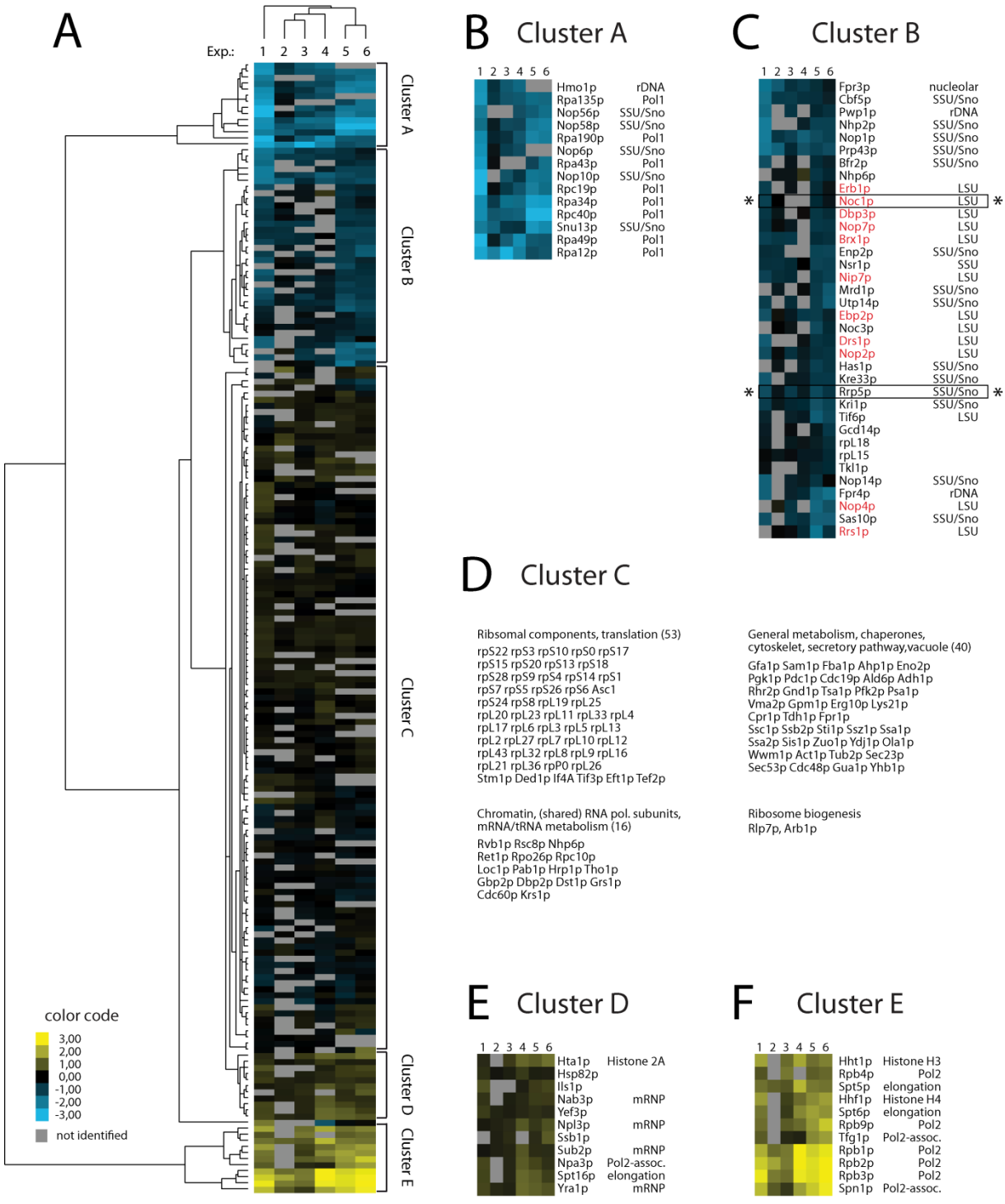

Fig. 3-16 A specific set of LSU and SSU biogenesis factors is part of RNA polymerase-I transcribed chromatin (previous page)

(Figure from (Hierlmeier et al., 2012); data generously provided by J. Perez-Fernandez and A. Bruckmann)
Yeast strains expressing chromosomally encoded Protein A fusion proteins of the Pol-I subunit Rpa135p (TY2423) or the Pol-II subunit Rpb2p (TY2424) were grown in rich medium to exponential phase (OD600 ~ 0.5 – 0.8) and cross linked using formaldehyde. Chromatin fractions were prepared and the bait proteins were purified using IgG coupled magnetic beads (see section 5.2.7.9 for experimental details). The co-purified proteins were subjected to comparative mass spectrometric analysis using iTRAQ reagents. For proteins identified with at least one peptide with an ion score confidence interval of more than 95%, the (average) iTRAQ ratio (Pol-II vs. Pol-I purification) was calculated to determine the relative abundance of the respective protein in the Pol-I purification compared to the Pol-II purification. The results of six independent experiments were subjected to statistical analysis using clustering algorithms to determine groups of proteins specifically associated with Pol-I or Pol-II transcribed chromatin. Only proteins identified in at least 4 out of 6 experiments were included. A) Overview of the cluster analysis of six independent comparative Pol-II/Pol-I purifications with the five main clusters indicated on the right. The color code for the log2 transformed iTRAQ ratios of Pol-II vs. Pol-I purifications is indicated. grey: protein not identified in this experiment; blue: enriched in Pol-I purifications; yellow: enriched in Pol-II purifications; black: equally abundant in Pol-I and Pol-II purifications. B, C, E, F) Detailed view of the clusters A, B, D and E, respectively, including a classification of the identified proteins. rDNA: shown to co-immunoprecipitate rDNA; Pol1: Pol-I subunit; SSU/Sno: part of SSU-processome/90S pre-ribosome or snoRNPs involved in ribosome biogenesis; LSU: Large ribosomal subunit biogenesis factor; mRNP: part of co-transcriptionally formed mRNP; elongation: Pol-II elongation factor; Pol2-assoc.: shown to associate with Pol-II. LSU biogenesis factors are shown in red if they were already identified in the Noc1p/Rrp5p proteome analyses shown in Fig. 3-8. Identified components of the Rrp5p-Noc1p-Noc2p module are highlighted (*). D) Proteins in cluster C are classified and listed according to their physiological function. The numbers of identified proteins are indicated in brackets.

In contrast, cluster A contained eight Pol-I specific subunits, a protein associated with rDNA (Hmo1p (Merz et al., 2008)) as well as five components of snoRNPs and/or the SSU processome, supposed to be co-transcriptionally recruited to rRNA (Fig. 3-16 B). Accordingly, the purified Rpa135p-TAP and Rpb2p-TAP fractions were specifically enriched for protein components characteristic for Pol-I and Pol-II transcribed chromatin, respectively. In agreement with that, cluster B contained some proteins described to be associated with rDNA chromatin (Pwp1p (Suka et al., 2006), Fpr4p (Kuzuhara and Horikoshi, 2004)), as well as twelve additional components of the SSU processome, but only few putative contaminants (e.g. Tkl1p, rpL15, rpL18) (Fig. 3-16 C). Notably, in addition to Noc1p and Rrp5p, twelve other biogenesis factors of the large ribosomal subunit were also found in cluster B, and eleven of those have also been identified as components of pre-ribosomes associated with Noc1p and Rrp5p (Fig. 3-8). Apparently, the sensitivity of this approach was limited, as not all Pol-I and Pol-II subunits or SSU processome components could be detected, and consistently some LSU ribosome biogenesis factors like Noc2p may have been missed in these analyses.
In summary, these results indicated that Noc1p and Rrp5p as well as a specific set of early acting LSU biogenesis factors are part of Pol-I transcribed chromatin suggesting that these factors are co-transcriptionally recruited to nascent pre-rRNA.

3.4.2 Rrp5p, Noc1p and Noc2p are associated with specific parts of rDNA chromatin

To test in a more direct way if Rrp5p, Noc1p and Noc2p are part of rDNA chromatin, the association of these proteins with rDNA was analysed in chromatin immunopurification (ChIP) experiments using yeast strains that express TAP-tag fusion proteins of Rrp5p, Noc1p and Noc2p, respectively. In addition, two strains expressing either TAP-tag fusion proteins of the UTP-A component Utp4p, which was described to bind co-transcriptionally to pre-

ribosomes (Dragon et al., 2002; Wery et al., 2009), or of Nog2p, a LSU biogenesis factor associated with pre-60S particles of later maturation states (Saveanu et al., 2001; see also section 2.2.6), were included as controls in these experiments.

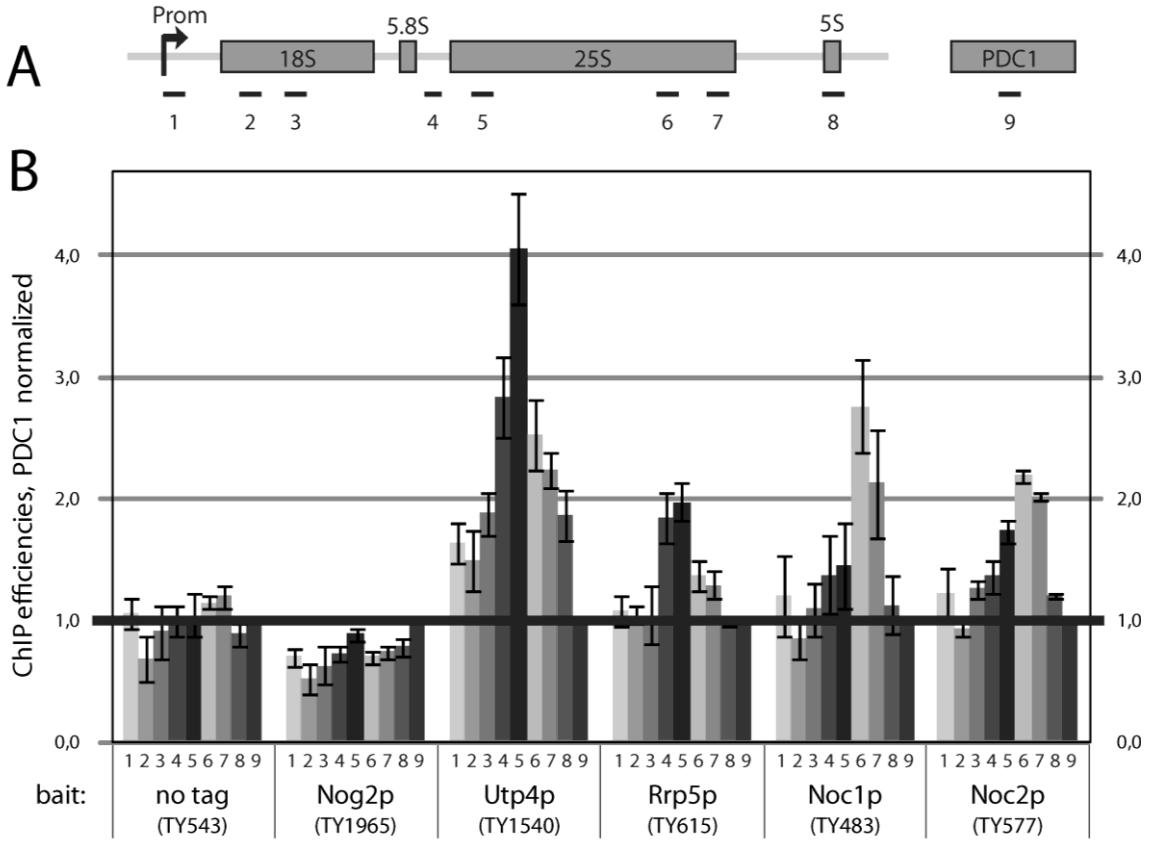

Fig. 3-17 Analysis of the association of Rrp5p, Noc1p and Noc2p with 35S rDNA chromatin

A) Primer pair positions on the rRNA gene to perform quantitative PCR (qPCR) analysis of Chromatin immunoprecipitation (ChIP) experiments. The relative positions of the rDNA amplicons analysed by qPCR (1-8) are indicated. For normalisation, an amplicon in the PDC1 gene (9) was used. B) ChIP experiments were performed with yeast strains in which Noc1p (TY483), Noc2p (TY577), Rrp5p (TY615), Utp4p (TY1540) or Nog2p (TY1965) are expressed as tandem affinity purification (TAP) tag fusion proteins, and with a control strain expressing no tagged protein (TY543). Cells were grown in YPDA medium at 30°C to exponential phase (OD600 = 0.5-0.7) and cross linked using formaldehyde (final concentration 1%) for 15' at 30°C. ChIP analysis was performed as described in section 5.2.7.7. The amounts of specific DNA fragments present in the input and retained on the beads were determined by qPCR with primer pairs amplifying the regions 1-8 of the rDNA de picted in the schematic representation and of the PDC1 gene (primer pair 9). In each experiment the precipitation efficiencies (% IP (rDNA)) for the respective amplified DNA regions were calculated and normalised to the PDC1 precipitation efficiencies (% IP (rDNA) / % IP (PDC1)). The graph shows the average of three biological replicates including standard deviations. A black line depicts the internal background as a result of the normalisation to the precipitated PDC1 DNA.

The bait proteins were purified from the chromatin fractions of formaldehyde treated cells (described in section 5.2.7.7), and DNA in the chromatin and the purified fractions was analysed by qPCR to determine co-purification efficiencies of different DNA regions (section 5.2.4.7). Therefore, seven primer pairs amplifying different regions of the Pol-I transcribed 35S rDNA were employed (Fig. 3-17 A), as well as primer pairs amplifying regions of the Pol-III transcribed 5S rDNA or the Pol-II transcribed PDC1 locus, respectively, that were used to determine the internal background of unspecifically co-purified DNA in each purification.

Consistent with previous studies (Wery et al., 2009), Utp4p-TAP co-purified specifically DNA spanning the ITS2 region and at the 5' end of the 25S rRNA coding region of rDNA (Fig. 3-17 B, compare amplicons 4-7 with 8 and 9). Notably, 5S rDNA was significantly more enriched than PDC1 DNA in this purification, which might be due to increased non-specific crosslinking of Utp4p to nucleolar chromatin. In contrast, none of the analysed DNA regions was specifically enriched in the Nog2p-TAP purification or in the untagged control. Similar as Utp4p, Rrp5p-TAP specifically enriched DNA spanning the ITS2 region and the 5' end of the 25S rRNA coding region of rDNA, albeit with reduced efficiencies when related to the PDC1 background. However, enrichment over the 5S background was similar in both cases (Fig3-18 B, compare amplicons 4-7 with 8 and 9). In contrast, Noc1p-TAp and Noc2p-TAP co-purified specifically DNA regions encoding the 3' end of 25S rRNA, indicating association of Noc1p, Noc2p and Rrp5p with specific parts of 35S rDNA chromatin.

As the association of UTP-A and UTP-B components with rDNA chromatin was reported to be mediated by the nascent Pol-I transcript (Wery et al., 2009), this might also be the case for Noc1p, Noc2p and Rrp5p.To test this, analogous ChIP experiments were performed as described above, except that the chromatin fractions were split before the purification step and subjected to RNase or mock treatment (described in section 5.2.7.8). Furthermore, a strain expressing the Pol-I subunit Rpa135p as Protein A fusion protein (TY2423) was included as additional control.

qPCR analyses of the purifications from mock treated chromatin showed for all biogenesis factors the same pattern of specifically associated rDNA with similar enrichment over the PDC1 background as described above (Fig. 3-18 A, '-RNase' sets; compare with Fig. 3-17 B). As expected, the Pol-I subunit Rpa135p co-purified DNA all over the 35S rDNA locus including the promoter region, but not of the 5S or PDC1 region. In addition, Rpa135p co-purified rDNA with substantial higher efficiencies than the ribosome biogenesis factors (Fig. 3-18 A, compare amplicons 1-7 with 8/9 in '-RNAse' sets).

After RNase treatment of the chromatin, Rpa135p co-purified specifically the same 35S rDNA regions as in the mock treated sample, consistent with direct, RNA independent interaction of Pol-I with rDNA, however with severely reduced efficiencies (Fig. 3-18 A, compare '+RNAse' and '-RNAse' sets). In agreement with that, Western blot analyses of proteins in the chromatin and purified fractions indicated that also the purification efficiency of Rpa135p was reduced in these conditions (Fig. 3-18 B, compare signal ratios of lanes 5/3 and 6/4). This suggested that the population of the bait protein that is accessible to affinity purification was strongly reduced after RNase treatment of the chromatin fraction, possibly due to formation of aggregates (J. Griesenbeck, unpublished observations).

In contrast, none of the analysed rDNA regions was more efficiently enriched than the PDC1 DNA in purifications of Noc1p-TAP, Noc2p-TAP, Rrp5p-TAP or Utp4p-TAP from chromatin treated with RNase, suggesting RNA dependent association of these ribosome biogenesis factors with rDNA chromatin (Fig. 3-18 A, compare '+RNase' sets). However, only Rrp5p-TAP and Utp4p-TAP were purified in similar efficiencies from untreated and RNase treated chromatin (Fig. 3-18 B, compare signal ratios of lanes 23/21, 24/22 and 29/27, 30/28), whereas for unclear reasons Noc1p-TAP and Noc2p-TAP could hardly be detected in the

purified fractions from RNase treated chromatin (Fig. 3-18 B, compare lanes 11, 12 and 17, 18), which prevented clear interpretation of the qPCR data in these cases.

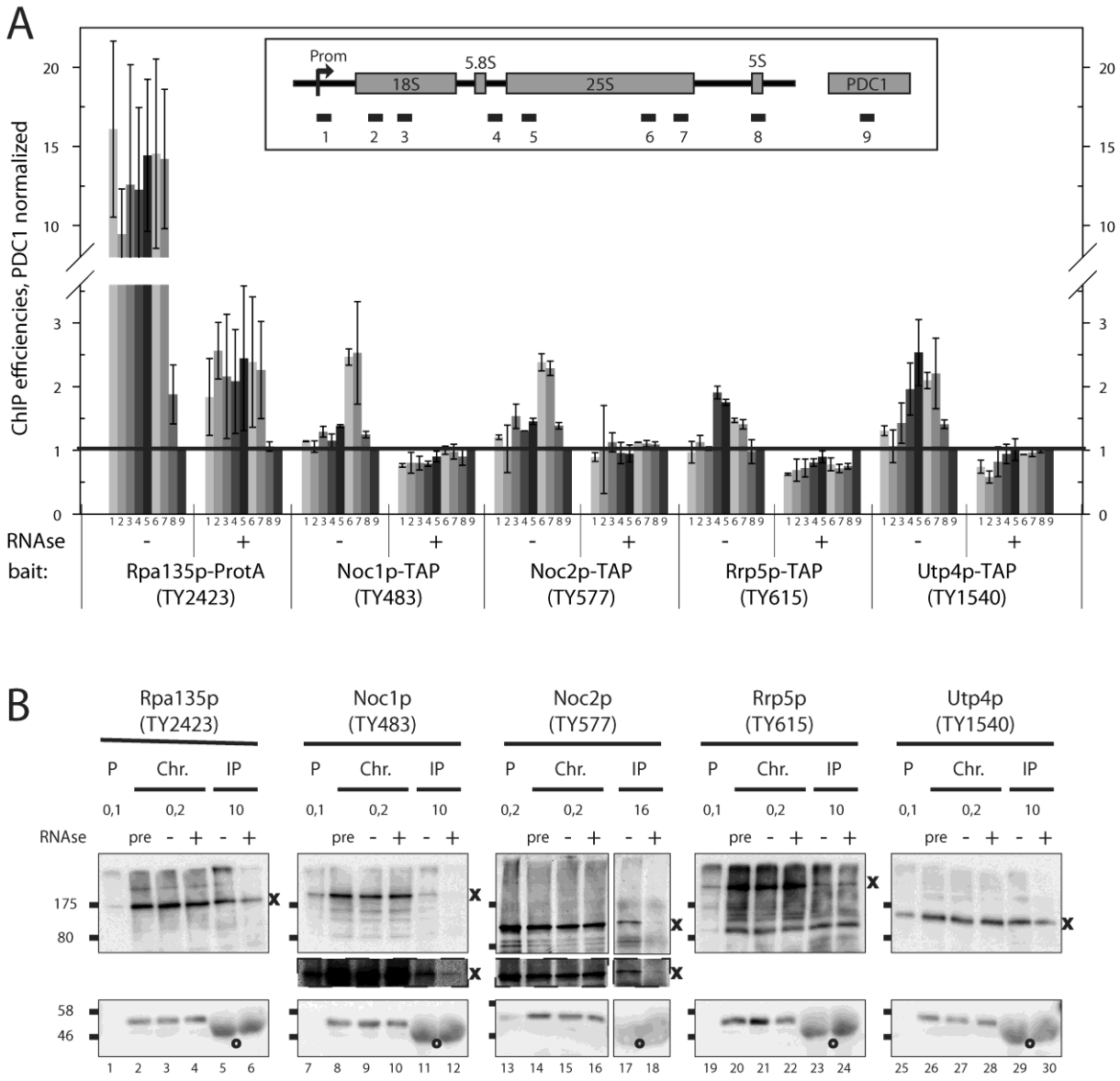

Fig. 3-18: Analysis of RNA dependent association of Rrp5p, Noc1p and Noc2p with 35S rDNA chromatin

A) ChIP experiments were performed with the indicated strains as in Fig. 3-17, with the exception that the chromatin fractions were subjected to RNAse A and T1 ('+') or mock treatment ('-') prior to immunoprecipitation (see section 5.2.7.8 for details). The amounts of specific DNA fragments present in the input and retained on the beads were determined by qPCR using the same primer pairs in Fig. 3-17. In each experiment the precipitation efficiencies (% IP (rDNA)) for the respective amplified DNA regions were calculated and normalised to the PDC1 precipitation efficiencies (% IP (rDNA) / % IP (PDC1)). The graph shows the average of two biological replicates including standard deviations. A black line depicts the internal background as a result of the normalisation to the precipitated PDC1 DNA. B) The yield of immunoprecipitated Pol-I and biogenesis factors in ChIP experiments with and without RNase treatment was analysed by Western blotting. Relative amounts to the chromatin input per IP of the insoluble material after sonication (P), the soluble chromatin fraction (Chr) without (pre) or after incubation at 25°C with (+) or without (-) RNAses, and the precipitated material (IP) from RNAse treated (+) or untreated (-) chromatin are indicated. Upper panels: The bait proteins were detected with anti-ProtA antibody and a fluorophor coupled secondary antibody (TY577) or with PAP detection reagent (all other cases) (see section 5.2.6.7 for details). The bands of the TAP-tagged proteins are marked (x). Dashed boxes show a digitally enhanced view of the same blot. Lower panel: Tubulin was detected as a loading control. Rabbit IgG chains detected in the IP lanes by cross reaction of the secondary antibody are indicated (°).

Accordingly, these experiments could only provide evidence that Rrp5p and Utp4p are associated with rDNA chromatin in an RNA dependent manner, strongly suggesting co-transcriptional recruitment of these proteins to nascent pre-rRNA. This is also likely to be the case for Noc1p and Noc2p, but remains to be experimentally validated.

4 Discussion

4.1 Rrp5p, Noc1p and Noc2p form a protein complex that is associated with the earliest LSU precursor particles

Previous studies indicated that the LSU biogenesis factors Noc1p and Noc2p form a protein complex (Milkereit et al., 2001) that might in addition interact with Rrp5p, a biogenesis factor required for both LSU and SSU maturation, independent of pre-ribosomal particles (Merl et al., 2010). In this work, a protein complex consisting of the proteins Noc1p, Noc2p and Rrp5p could be reconstituted from recombinantly expressed proteins, and low resolution images of the purified complex could be obtained. Architectural analyses showed that Noc1p can establish direct interactions with Noc2p and Rrp5p (Fig. 3-4) and thus enables formation of a bridged hetero-trimeric protein complex. Notably, the N-terminal part of Rrp5p, which is crucial for the function of Rrp5p in LSU maturation, is required and sufficient for stable interaction with Noc1p (Fig. 3-6), suggesting that the Rrp5p/Noc1p/Noc2p module might act as an entity in biogenesis of the large ribosomal subunit.

In agreement with that, *in vivo* all module components were similarly stably associated with the first specific LSU precursor particles containing 27SA2 pre-rRNA (Fig. 3-7, 3-14) resulting from pre-rRNA processing within the ITS1 sequence, which frequently occurs co-transcriptionally in yeast (Kos and Tollervey, 2010). In addition, Rrp5p, Noc1p and Noc2p were also part of common 90S pre-ribosomes containing 35S pre-rRNA and U3 snoRNA (Fig. 3-7, 3-14), consistent with the observed co-sedimentation of Noc1p and Noc2p with 35S pre-rRNA at ~ 90S (Milkereit et al., 2001) and co-precipitation of U3 snoRNA with human Noc2p/NIR (Wu et al., 2012). As it was previously suggested for Rrp5p (De Boer et al., 2006), release of Rrp5p and Noc1p from pre-ribosomal particles occurred concomitant with or immediately after downstream pre-rRNA processing events yielding 27SB pre-rRNAs, and apparently involved different mechanisms in the alternative B1L and B1S processing pathways (Fig. 3-7). In contrast, Noc2p was also stably associated with intermediate pre-60S particles containing 27SB pre-rRNA (Fig. 3-14), most likely in complex with Noc3p (Milkereit et al., 2001; Nissan et al., 2002). However, it remained elusive if Noc2p stays associated with pre-ribosomes when Noc1p and Rrp5p are released, or if the Rrp5p/Noc1p/Noc2p module leaves (*en bloc*) and a Noc2p/Noc3p complex enters these particles. Consistent with the co-purified RNA species, in proteome analyses of pre-ribosomes purified via Noc2p (U. Ohmayer, manuscript in preparation; J. Ossowski, 2010 (diploma thesis); M. Sauert, 2010 (diploma thesis)), a similar set of early acting LSU biogenesis factors was identified as in pre-ribosomes purified via Rrp5p or Noc1p (Fig. 3-8), and in addition several biogenesis factors described to be specifically associated with intermediate pre-60S particles containing 27SB pre-rRNA (e.g. Noc3p, Nsa1p, Sbp4p (Kressler et al., 2008; García-Gómez et al., 2011b)). In contrast to the Rrp5p and Noc1p purifications (Fig. 3-8), only few SSU processome components were identified in the Noc2p purifications. This is probably due to limitations in sensitivity in the mass spectrometric analyses, since the ratio of 90S pre-ribosomes to pre-

60S particles in Noc2p purifications is much smaller than in Noc1p and Rrp5p purifications as judged by RNA analyses (Fig. 3-14).

In summary, these results strongly suggest that the Rrp5p/Noc1p/Noc2p module is already incorporated into 90S pre-ribosomes and stays associated with the first specific LSU precursor particles after cleavage in the internal transcribed spacer 1.The same scenario probably also applies for other LSU biogenesis factors that were identified in pre-ribosomes associated with Noc1p and Rrp5p, and that were also shown to co-purify some U3 snoRNA or 35S pre-rRNA (e.g. Brix1p, Ebp2 (Shimoji et al., 2012), Ssf1p (Fatica et al., 2002), Nop7p (Harnpicharnchai et al., 2001), Nsa3p (Nissan et al., 2002)), raising an apparent contradiction to previous analyses suggesting that 90S pre-ribosomes are largely devoid of LSU biogenesis factors (Grandi et al., 2002). However, these findings are in agreement with the hypothesis that several 90S/SSU processome particles of different composition and maturation state are present in the cell (see (Granneman and Baserga, 2004) for a detailed discussion). Accordingly, one population of common 90S particles contains 35S pre-rRNA as well as SSU processome components and LSU biogenesis factors. After pre-rRNA processing within the ITS1 region precursor, which occurs in yeast with fast kinetics (Kos and Tollervey, 2010), these are segregated into the specific pre-40S and pre-60S particles, respectively. As a consequence, particles purified via SSU processome components (Fig. 3-15; Grandi et al., 2002) comprise a mixture of early, common 90S pre-ribosomes and predominantly later, specific SSU processome particles (containing 23S, 22S, 21S pre-rRNAs), which explains the observed apparent lack of LSU biogenesis factors in 90S pre-ribosomes. Analogously, LSU biogenesis factors like Noc1p and Noc2p co-purify predominantly pre-60S rRNA and other LSU biogenesis factors and only minor amounts of 35S pre-rRNA and SSU processome components.

Components of the SSU processome can co-transcriptionally bind to nascent pre-rRNA (Wery et al., 2009), resulting in compaction of the RNA and formation of knob like structures at the ends of the nascent transcripts, which can be visualised by electron microscopy and are referred to as ‘terminal balls’ or ‘SSU knobs’ (Miller and Beatty, 1969, Mougey et al., 1993; Dragon et al., 2002; Osheim et al., 2004). In exponentially growing yeast cells, ~ 70% of the nascent transcripts are co-transcriptional processed in the ITS1 region, resulting in loss of the ‘SSU knobs’ (Osheim et al., 2004; Kos and Tollervey, 2010). Subsequently, new structures termed ‘LSU knobs’ are formed on the nascent pre-60S rRNA that are supposed to result from co-transcriptional binding of LSU biogenesis factors to pre-rRNA ((Osheim et al., 2004); see Fig. 2-9).

Several experiments described here provided evidence that Rrp5p, Noc1p and Noc2p can co-transcriptionally bind to the nascent pre-rRNA. First, Rrp5p, Noc1p and Noc2p co-purified not only U3 snoRNA, but also (numerous) protein components of the SSU processome that are supposed to be co-transcriptionally recruited to pre-rRNA (see above). Second, Rrp5p and Noc1p co-purified several subunits of Pol-I (Fig. 3-8), and were identified as specific components of Pol-I transcribed chromatin (Fig. 3-16). Third, Rrp5p, Noc1p and Noc2p were associated with specific regions of the 35S rDNA, which in case of Rrp5p could be shown to be sensitive to RNase treatment (Fig. 3-17, 3-18). Accordingly, Rrp5p, Noc1p and Noc2p are good candidates to be components of the ‘LSU knobs’. Notably, the size of the reconstituted

complex (particles of ~ 8 & 12nm diameter, Fig. 3-5) is smaller than the size of the 'LSU knobs' (~ 15-20 nm diameter (Osheim et al., 2004)). This indicates that other LSU factors that are part of pre-ribosomes co-purified with Noc1p and Rrp5p and which were identified as components of Pol-I transcribed chromatin (Fig. 3-16) and/or to co-purify 35S pre-rRNA or U3 snoRNA (see above) could also be part of the 'LSU knobs', as previously suggested for Nop53p (Granato et al., 2008) and Nop15p (Wery et al., 2009).

4.2 The function of Rrp5p, Noc1p and Noc2p in ribosome biogenesis

4.2.1 Formation of the Rrp5p/Noc1p/Noc2p module is required for the stability of LSU precursor particles

Analyses of pre-rRNA processing phenotypes in yeast cells in which the function of Noc1p or Noc2p was impaired due to the use of temperature sensitive alleles confirmed that the function of Noc1p and Noc2p is specific for the LSU maturation pathway, as formation of 25S and 5.8SrRNAs, but not of 18S rRNA was inhibited (Fig. 3-1; (Edskes et al., 1998; Milkereit et al., 2001)). Furthermore, these experiments and steady state analyses of pre-rRNA processing phenotypes after *in vivo* depletion of Noc1p or Noc2p (Fig. 3-3), showed severely reduced levels of all LSU specific precursor RNAs but no direct effect on the levels of the common 35S pre-rRNA. These results indicated that Noc1p and Noc2p are required for the formation of stable pre-60S particles, which are otherwise prone to degradation. A similar destabilization of pre-60S particles was observed after *in vivo* depletion of Rrp5p (Fig. 3-3), albeit accompanied by equally reduced 20S levels, consistent with the described function of Rrp5p in LSU and SSU biogenesis (Venema and Tollervey, 1996). Accordingly, association with the Rrp5p/Noc1p/Noc2p module appears to be essential for the stability of early LSU precursor particles. In agreement with that, characterisation of several truncated *noc1-ΔX* alleles showed that perturbation of any interaction of Noc1p with Noc2p, Rrp5p or pre-rRNA is accompanied by defects in pre-rRNA processing, destabilisation of pre-rRNAs and impaired growth (Fig. 3-11, 3-12, 3-13).

Analyses of the binding hierarchy of the module components to pre-ribosomes showed that Noc1p and Noc2p are still associated with U3 snoRNA, 35S pre-rRNA and fragments thereof after *in vivo* depletion of Rrp5p (Fig. 3-14). Analogously, Rrp5p was still associated with U3 snoRNA, 35S pre-rRNA and fragments thereof after *in vivo* depletion of Noc1p and Noc2p (Fig. 3-14). These findings indicated that the Rrp5p/Noc1p/Noc2p module has several interaction interfaces on pre-ribosomes, possibly by direct binding of pre-rRNA as described for Rrp5p in *in vitro* systems (De Boer et al., 2006; Young and Karbstein, 2011). In agreement with these reports, a major *in vivo* interaction site for Rrp5p is likely to be located in the ITS1 region between processing sites A2 and A3, as Rrp5p was stably associated with 27SA2 but not 27SB pre-rRNA in wild type cells, and as Rrp5p co-purified efficiently 23S, but not 20S pre-rRNA from cells depleted of Noc1p or Noc2p (Fig. 3-14). In this way, Rrp5p could modulate the local structure of the ITS1 region to enable subsequent processing steps and to regulate their order as previously discussed (Fig. 3-9; (Torchet and Hermann-Le

Denmat, 2000; Eppens et al., 2002; Bax et al., 2006a)). This could explain the impact of Rrp5p on both A2 and A3 site cleavage (Venema and Tollervey, 1996), although no direct interactions of Rrp5p with the respective endonucleases (Rcl1p, RNase MRP) are apparent (Horn et al., 2011) or have been described so far. The existence of (an) additional binding site(s) on pre-rRNA upstream of the A2 processing site (Young and Karbstein, 2011) was supported by the observation that C-terminal fragments of Rrp5p co-purified significant amounts of 35S pre-rRNA, but no specific LSU precursor rRNAs (Fig. 3-9).

In contrast to Rrp5p, RNA binding activity of Noc1p and Noc2p has not been analysed to date. However, as Noc1p and Noc2p are associated with very early pre-ribosomes, it is not unlikely that these proteins establish direct contacts with pre-rRNA. Furthermore, recombinantly expressed and purified human Noc1p/CBF showed specific DNA binding activity *in vitro* (Lum et al., 1990), suggesting that Noc1p could have a general affinity for nucleic acids. Potential binding sites for Noc1p/Noc2p are expected to be downstream of the A3 processing site, as neither Noc1p nor Noc2p co-purified significant amounts of 23S pre-rRNA from cells depleted of Rrp5p (Fig. 3-14), and/or downstream of the B1L/S processing sites, as Noc1p was specifically associated with $27SB_L$ pre-rRNA (Fig. 3-7). Consistently, depletion of Noc1p and Noc2p showed no direct or specific effects on A2 or A3 site cleavage, respectively (Fig. 3-3, 3-13). As the binding interdependency of Noc1p and Noc2p to pre-ribosomes was not directly addressed, it remained unclear if one or both proteins make contacts to pre-ribosomes/pre-rRNA. However, the combined results of the experiments analysing the *in vivo* interactions of truncated Noc1p variants (Fig. 3-12, 3-13) and the association of Noc1p with pre-ribosomes after depletion of Rrp5p (Fig. 3-14) provided indirect evidence that Noc1p could interact with pre-ribosomes/pre-rRNA independent of Noc2p. First, deletion of domain D2 just slightly affected the interaction of Noc1p with Noc2p, whereas the interactions with Rrp5p and pre-rRNA were severely weakened, but still detectable, indicating that ProtA-Noc1p-Δ2 is localized to the nucleolus. Second, Rrp5p was not required for the association of Noc1p with pre-rRNA. Accordingly, interaction with Noc2p is not sufficient for stable association of Noc1p with pre-rRNA, suggesting a direct interaction between Noc1p and pre-ribosomes/pre-rRNA. Analogous studies with truncated Noc2p variants indicated that the interaction of Noc2p with Noc1p and with pre-ribosomes is not strictly correlated, either (Hierlmeier, 2008 (diploma thesis)). Therefor, both Noc1p and Noc2p could establish (weak) direct interactions with pre-ribosomes/pre-rRNA resulting in stable association of the Noc1p/Noc2p sub-module with pre-ribosomes. Future experiments will be required to determine if and how Noc1p and Noc2p bind to pre-rRNA (see section 4.3).

In summary, these results suggested that the Rrp5p/Noc1p/Noc2p module can establish an extensive interaction network with the earliest pre-60S particles, and could thereby contribute to the structural organisation of these particles similar as it was suggested for the'A3 factors' (see section 2.2.6; (Granneman et al., 2011; Sahasranaman et al., 2011)). In this way, or merely by covering different regions of pre-rRNAs, the respective RNA species could be protected from undesired access of, and degradation by endo- and exonucleases to enable the formation of stable LSU precursors. This function of the Rrp5p/Noc1p/Noc2p module is likely to be shared with, or to be achieved in cooperation with other LSU biogenesis factors

that are part of Noc1p and Rrp5p associated pre-ribosomes and whose depletion results in a similar destabilisation of all LSU precursor RNAs (e.g. Ssf1p (Fatica et al., 2002), Dbp9p (Daugeron et al., 2001), Rrs1p (Tsuno et al., 2000), Nop4p (Bergès et al., 1994)). A common function of early acting LSU biogenesis factors is also supported by the observation that in corresponding yeast mutant strains residual non-degraded pre-60S particles fail to leave the nucleolar compartment as described for Noc1p and Noc2p (Milkereit et al., 2001; Gadal et al., 2002b; Fatica et al., 2003; Miles et al., 2005), albeit the mechanism of this retention remains unclear.

It was reported that overexpression of the conserved 'NOC domain', found in Noc1p, Noc3p and Noc4p, prevents cell growth and leads to nuclear accumulation of pre-60S particles, but has no apparent effect on levels of 35S, 27S and 20S pre-rRNAs (Milkereit et al., 2001). Accordingly, it was suggested that the 'NOC domain' might mediate the interaction of pre-ribosomes with an intra-nuclear transport system. Although this is one possible scenario, the results presented here provide another potential explanation. As the region of Noc1p containing the 'NOC domain' appeared to be important for the interaction with Noc2p (and Rrp5p) (Fig. 3-12), overexpression of the 'NOC domain' could interfere with the formation of the Noc1p/Noc2p submodule and/or the Rrp5p/Noc1p/Noc2p module, without directly affecting the association of module components with pre-ribosomes. Accordingly, the single proteins could still cover different pre-rRNA regions and thus prevent access of nucleases and stabilise pre-ribosomes/pre-rRNAs. However, the Rrp5p/Noc1p/Noc2p module could then no longer contribute to the structural organisation of the pre-ribosomes, thereby preventing further maturation steps, e.g. conversion of 27SA2 to 27SB pre-rRNA, and concomitant transport through the nucleolus. Since the pre-rRNA processing phenotypes after overexpression of the 'NOC domain' was not analysed in detail, this effect may have been overlooked. It should be noted that such a retention model of immature or aberrant pre-ribosomes was also suggested by Milkereit and colleagues as an alternative explanation for the nucleolar accumulation of LSU precursors after inactivation of Noc1p and Noc2p (Milkereit et al., 2001). Future experiments will be necessary to distinguish between these options.

Finally, structural organisation of pre-60S particles could facilitate binding of other biogenesis factors and/or r-proteins that are required for subsequent maturation steps, in a similar way as suggested for the SSU maturation pathway. There, the binding hierarchy of early acting biogenesis factors (e.g. UTP-A, UTP-B, UTP-C complexes, U3 snoRNP, Noc4p/Nop15p etc., see section 2.2.5; (Dosil and Bustelo, 2004; Gallagher et al., 2004; Pérez-Fernández et al., 2007, 2011), as well as their impact on r-protein assembly (Jakob et al., 2012), has been extensively studied, resulting in a well defined map describing their binding interdependencies. Analogous studies should help to determine the binding hierarchy of LSU factors to the earliest pre-60S particles and to determine their functions. As described in detail in the introduction (section 2.2.6), the 'A3 factors' have a specific function in generation of the $27SB_S$ pre-rRNA but do not affect levels of 27SA2 pre-rRNA (except for Erb1p (Pestov et al., 2001)), and contribute to the assembly of some r-proteins (Sahasranaman et al., 2011). Furthermore, recruitment of the 'A3 factors' to pre-ribosomes was described to depend on previous assembly of the r-proteins rpL7 and rpL8, whereas this was not the case

for Rrp5p, Noc1p and Noc2p (Jakovljevic et al., 2012). Accordingly, binding of the Rrp5p/Noc1p/Noc2p module might be an upstream requirement for the assembly of r-proteins and the recruitment of the 'A3 factors'.
Since all three proteins are conserved from yeast to human, and as human Noc2p/NIR and hRrp5p/NFBP affect ribosome biogenesis (see section 2.2.7; (Sweet et al., 2008; Wu et al., 2012), the function of the module may also be conserved in evolution.

4.2.2 The function of Rrp5p in the maturation of the small ribosomal subunit

In contrast to Noc1p and Noc2p (section 4.2.1), Rrp5p is not only required to form stable pre-60S particles, but has an additional function in the maturation of the small ribosomal subunit, as processing at sites A0, A1 and A2 is impaired in absence of Rrp5p (Venema and Tollervey, 1996). The functions in LSU and SSU maturation are separated into the N- and C-terminal part of Rrp5p, respectively, and can be provided *in trans* by expressing the respective truncated Rrp5p variants (Torchet et al., 1998; Eppens et al., 1999). Congruently, the N-terminal part of Rrp5p was required and sufficient to mediate stable interaction with Noc1p (Fig. 3-6), and was associated with 90 S particles and also with pre-60S particles (Fig. 3-9), whereas the C-terminal part did not interact with Noc1p and was apparently only associated with 90S pre-ribosomes (Fig. 3-6, 3-9). Furthermore, Rrp5p was described to be required for the recruitment of the UTP-C complex to pre-ribosomes (Pérez-Fernández et al., 2007), which could be confirmed with a different experimental approach in this work (Fig. 3-15). In contrast, analogous experiments indicated that Noc1p is not required for binding of UTP-C to pre-ribosomes (Fig. 3-15), underlining that Noc1p does not primarily affect SSU maturation.
In summary, these results showed that formation of the Rrp5p/Noc1p/Noc2p module is not required for the function of Rrp5p in SSU maturation, suggesting that this function is provided by 'free' Rrp5p not being part of the module. Although comparison of pre-ribosomes co-purified with Noc1p and Rrp5p strongly suggested that Rrp5p is stably associated with pre-ribosomes in the context of the module (section 4.1), some results indicated that such a population of 'free' Rrp5p could weakly or transiently be associated with pre-ribosomes, either prior to or overlapping with module bound Rrp5p. First, Rrp5p was purified in large excess from cell extracts relative to Noc1p and other biogenesis factors (Fig. 3-8). Second, after treatment of cells with cross-linking reagents, Rrp5p was associated with similar rDNA regions (ITS2, 5' end of 25S rDNA) as components of the SSU processome (Fig. 3-17; (Wery et al., 2009)), whereas Noc1p and Noc2p were associated with the 3' region of 25S rDNA, similar as the LSU biogenesis factor Nop15p (Fig. 3-17; (Wery et al., 2009)). These specific patterns of rDNA association were suggested to result from gradual compaction of the SSU knobs and LSU knobs along the 35S rDNA with the most highly compacted particles being close to 5' and 3' ends of 25S rDNA, respectively (Wery et al., 2009). Third, the C-terminal part of Rrp5p, which provides the function in SSU maturation, was associated with 90S pre-ribosomes but not with pre-60S particles (Fig. 3-9).
Accordingly, pre-ribosomes could be associated with a population of 'free' Rrp5p, and different scenarios are conceivable, how this Rrp5p population could act in ribosome

biogenesis: (i) The same Rrp5p molecule could first act in SSU maturation, stay associated with the pre-ribosomal particle, and subsequently recruit Noc1p/Noc2p and act in LSU biogenesis in the context of the module. (ii) A population of 'free' Rrp5p could exclusively act in SSU maturation, whereas a Rrp5p/Noc1p/Noc2p module could provide the function in LSU maturation. However, the former one appears to be more likely, as there is good evidence that Rrp5p stably interacts with the ITS1 region of pre-rRNA between processing sites A2 and A3, which could establish an RNA folding state that enables processing at these sites, and could contribute to the stability and/or life time of 27SA2 pre-rRNA (discussed in detail in section 4.2.1). Accordingly, exchange of different Rrp5p populations associated with this pre-rRNA region is unlikely, and as processing of site A2 and A3 is required for SSU and LSU maturation, respectively, this suggests that the same population of Rrp5p acts in both pathways. Alternatively, two populations of Rrp5p could act in SSU biogenesis, one recruiting UTP-C and facilitating A0, A1 cleavage, and another one stably binding between A2 and A3 and facilitating A2, and subsequently, A3 processing.

4.2.3 A model for the binding of Rrp5p, Noc1p and Noc2p to pre-ribosomes

Based on the results discussed above in detail, the following model is proposed how binding of Rrp5p, Noc1p and Noc2p to pre-ribosomes could occur *in vivo*. Initially, Rrp5p can co-transcriptionally and independent of Noc1p and Noc2p bind to nascent pre-40S rRNA, probably weakly and upstream of the A2 processing site, and subsequently recruit the UTP-C complex into evolving SSU processome particles (SSU knobs). After formation of the SSU processome, pre-rRNA processing at sites A0, A1 and A2 can occur co-transcriptionally while Pol-I transcribes the 5' region of 25S rDNA. This results in separation of the SSU-processome components from pre-60S rRNA, but probably not of Rrp5p, as Rrp5p can make stable RNA contacts between A2 and A3 and is required for processing of A2 and A3. At this stage, Noc1p and Noc2p can be recruited to the nascent pre-60S rRNA, possibly via interaction of Rrp5p with Noc1p, and establish direct contacts to pre-rRNA (downstream of $B1_L$). This results in formation of the Rrp5p/Noc1p/Noc2p module and enables the structural organisation of the pre-60S rRNA and the formation of the 'LSU knobs', most likely in cooperation with other co-transcriptionally recruited LSU biogenesis factors. After transcription of the 25S rDNA has been completed, LSU precursors containing 27SA2 pre-rRNA and amongst others the Rrp5p/Noc1p/Noc2p module components are released.
In case that no co-transcriptional cleavage occurs, Rrp5p, Noc1p and Noc2p probably bind in the same order to the nascent transcript or, alternatively, to released 35S pre-rRNA, resulting in common 90S pre-ribosomes associated with the Rrp5p/Noc1p/Noc2p module. After processing at site A2, the module is segregated into the LSU maturation pathway. Accordingly, in this situation at least some functions of Rrp5p in SSU biogenesis (A2 processing) would be achieved in the context of the module.
A sequential assembly of the Rrp5p/Noc1p/Noc2p module members with pre-ribosomes would explain (i) why Rrp5p and Noc1p co-purified pre-ribosomes of very similar composition, although Rrp5p has a distinct function in SSU maturation, which does not require formation of the Rrp5p/Noc1p/Noc2p module, (ii) why Rrp5p was purified in excess

relative to Noc1p and other biogenesis factors and (iii) why Rrp5p was associated with similar rDNA regions as SSU processome components, in contrast to Noc1p or Noc2p.
However, this model requires that the module is disassembled after its function in LSU maturation has been completed, at least into Rrp5p and a Noc1p/Noc2p submodule. As Noc1p co-purified slightly more efficiently 27SB pre-rRNA than Rrp5p did (Fig. 3-7), this could be the case. Nevertheless, this is not directly compatible with (i) the apparent existence of the Rrp5p/Noc1p/Noc2p module in cells in which ribosome biogenesis is shut down (Merl et al., 2010), and (ii) efficient reconstitution of the module in the heterologous expression system (Fig. 3-4). One possible explanation for this apparent discrepancy would be that structural rearrangements within the pre-ribosome concomitant with or immediately after formation of the 27SB pre-rRNA (as discussed in section 2.2.6) could disrupt the Rrp5p/Noc1p interaction. Thus Rrp5p would be released prior to Noc1p/Noc2p from the pre-60S particle, and could immediately bind to another nascent 35S pre-rRNA molecule. In analogy, subsequently released Noc1p/Noc2p, either as submodule or as single proteins, would be rapidly recruited to pre-ribosomes containing Rrp5p. Alternatively, the same recycling pathway could occur by post-transcriptional modification of one or more module components. For instance, phosphorylation of Rrp5p in pre-60S particles could reduce its affinity to Noc1p and cause its release from the respective pre-rRNPs, while dephosphorylation of Rrp5p could occur in the context of the SSU processome, allowing subsequent recruitment of Noc1/Noc2p. Accordingly, when ribosome biogenesis is impaired, i.e. in absence of pre-ribosomal particles, the populations of free Rrp5p and Noc1p/Noc2p would increase. In the former case, this would directly allow formation of the module independent of pre-ribosomes, whereas in the latter, prior dephosphorylation of free Rrp5p by the respective phosphatase would be expected to be required therefor. Both scenarios are also compatible with the reconstitution of the module from recombinantly expressed proteins. Future experiments analysing the release mode and the modification state of the module components will be required to test this model and to identify potential modification enzymes.

4.3 Outlook

In this work, a reconstituted Rrp5p/Noc1p/Noc2p complex could be isolated in high purity and visualized in low resolution by electron microscopy. Obviously, future work should aim to obtain higher resolution images, e.g. by cryo-EM, to determine the structure of the complex in more detail. The ultimate goal should of course be crystallisation of the complex and determination of its structure by X-ray crystallography. Structural studies will also help to better understand the architecture of the module in regard of the stoichiometry of its components. Here, it could be shown that Noc1p interacts with Noc2p and the N-terminal part of Rrp5p to form a hetero-trimeric complex. Furthermore, analyses of *in vivo* interactions of truncated Noc1p variants (Fig. 3-12) indicated that the region of Noc1p surrounding its ‘NOC domain’ could be sufficient for interaction with Noc2p, supporting the suggestion that the ‘NOC domain’ might be a general protein-protein interaction motif whose binding specificity can be modulated by few amino acids (Kühn et al., 2009). These aspects should

be further investigated using recombinantly (co-)expressed proteins by analysing pairwise interactions between different truncated protein variants and the effect of point mutations on specific interactions.

Furthermore, the RNA binding activity of the Rrp5p/Noc1p/Noc2p module and its components should be addressed. Detailed *in vitro* studies were performed with Rrp5p (Young and Karbstein, 2011), indicating strong, unspecific affinity of the N-terminal part and weak, but specific affinity of the C-terminal part for model RNAs. Analogous studies should help to investigate if Noc1p and/or Noc2p can interact with RNAs and if so, to determine the important protein domains and RNA motifs or structures. In addition, comparison of the RNA binding properties of the complex and the single proteins, as well as analyses of a potential RNA folding activity of the module and its components will help to better understand the binding mode of the module *in vivo,* and to verify if the module can contribute to the structural organisation of pre-ribosomes. In a complementary approach, the *in vivo* RNA binding sites of Rrp5p, Noc1p and Noc2p should be analysed, for instance using the CRAC method (Granneman et al., 2009).

Finally, a potential impact of Rrp5p, Noc1p and Noc2p on the recruitment of other biogenesis factors or on the assembly of r-proteins remains elusive. To address this question, the composition of pre-ribosomes in cells depleted of one of the module components could be analysed in comparison to the wild type situation to determine if specific factors or r-proteins are absent, but clearly, such experiments will be complicated by the destabilisation of the early pre-60S particles in this situation. In combination with analogous experiments after depletion of other early associated LSU biogenesis factors it should be possible to obtain a detailed map of the binding events in the earliest pre-60S particles, similar as for the SSU processome.

5 Material and Methods

5.1 Material

5.1.1 Yeast strains

TY	name	genotype	origin
1	BSY420	mat A, ade2-1, can1-100, his3200, leu2-3,112, trp1-1, ura3-1	Milkereit et al, 2001
23	noc2-1	mat alpha, ura3, his3, leu2 noc2::noc2-1	Amberg et al., 1992
71	noc3-1	mat alpha, ade2-1, can1-100, his3200, leu2-3,112, trp1-1, ura3-1, noc3::HIS3, pNOPPA-noc3-1 (LEU2)	Milkereit et al, 2001
206	BY4741	mat A, his31, leu20, met150, ura30	Euroscarf
483	BSY420 NOC1-TAP	mat A, ade2-1, can1-100, his3200, leu2-3,112, trp1-1, ura3-1, noc1:: NOC1-TAP-TRP1	Anja Ackermann
543	CG379	mat alpha, ade5-1, his7-2, leu2-3,-112, trp1-289, ura3-52	Cadwell et al., 1997
577	CG379 NOC2-TAP	mat alpha, ade5, his7-2, leu2-112, trp1-289, ura3-52, noc2:: NOC2-TAP-TRP1	Juliane Merl
615	RRP5-TAP	mat alpha, ADE2, ADE3, his3, leu2, trp1, ura3, rrp5::RRP5-TAP-TRP1	gift from J. Baßler, Heidelberg
616	RRP5 shuffle (YJV148)	mat A, ade2, his3, leu2, trp1, ura3, rrp5::HIS3, pURA3 RRP5 (URA3)	Venema and Tollervey, 1996
772	NOC1-Shuffle	mat alpha, ade2-1, can1-100, his3200, leu2-3,112, trp1-1, ura3-1, noc1::HIS3, YCplac33-pNOC1-NOC1 (URA3)	Milkereit et al, 2001
773	NOC2-Shuffle	mat alpha, ade2-1, can1-100, his3200, leu2-3,112, trp1-1, ura3-1, noc2::HIS3, YCplac33-pNOC2-NOC2 (URA3)	Milkereit et al, 2001
774	NOC3 shuffle	mat alpha, ade2-1, can1-100, his3200, leu2-3,112, trp1-1, ura3-1, noc3::HIS3, YCplac33-pNOC3-NOC3 (URA3)	Milkereit et al, 2001
775	pGAL-NOC1	mat alpha, ade2-1, can1-100, his3200, leu2-3,112, trp1-1, ura3-1, noc1::HIS3, YCplac22-pGAL-NOC1 (TRP1)	Ester Draken
776	pGAL-NOC2	mat alpha, ade2-1, can1-100, his3200, leu2-3,112, trp1-1, ura3-1, noc2::HIS3, YCplac22-pGAL-NOC2 (TRP1)	Ester Draken
1540	CG379 UTP4-TAP	mat alpha, ade5-1, his7-2, leu2-3,-112, trp1-289, ura3-52, utp4::UTP4-TAP-URA3	Steffen Jakob
1965	CG379 NOG2-TAP	mat alpha, ade5-1, his7-2, leu2-3,-112, trp1-289, ura3-52, nog2::NOG2-TAP-URA3	Juliane Merl
2068	noc1-6 (genomic)	mat alpha, ade2-1, can1-100, his3200, leu2-3,112, trp1-1, ura3-1, noc1::noc1-6	this study; derivate of TY772 by genomic integration of noc1-6 allele (PCR on K113 with o2073/o2074) at NOC1 locus

2069	noc1-7 (genomic)	mat alpha, ade2-1, can1-100, his3200, leu2-3,112, trp1-1, ura3-1, noc1::noc1-7	this study; derivate of TY772 by genomic integration of noc1-7 allele (PCR on K114 with o2073/o2074) at NOC1 locus
2070	noc1-6 (genomic) Rrp5-Myc	mat alpha, ade2-1, can1-100, his3200, leu2-3,112, trp1-1, ura3-1, noc1::noc1-6, rrp5::RRP5-Myc9-natNT2	this study; derivate of TY2068 by genomic integration of a tagging cassette (PCR on K1062 with o287/o288)
2071	noc1-6 (genomic) Rrp5-Myc Noc3-HA	mat alpha, ade2-1, can1-100, his3200, leu2-3,112, trp1-1, ura3-1, noc1::noc1-6, rrp5::RRP5-Myc9-natNT2, noc3::NOC3-HA3-hphNT1	this study; derivate of TY2070 by genomic integration of a tagging cassette (PCR on K1063 with o1901/o1902)
2072	noc1-6 (genomic) Rrp5-Myc Noc3-HA Noc2-GFP	mat alpha, ade2-1, can1-100, his3200, leu2-3,112, trp1-1, ura3-1, noc1::noc1-6, rrp5::RRP5-Myc9-natNT2, noc3::NOC3-HA3-hphNT1, noc2::NOC2-GFP-kanMX	this study; derivate of TY2071 by genomic integration of a tagging cassette (PCR on V47 with o908/o909)
2073	noc1-7 (genomic) Rrp5-Myc	mat alpha, ade2-1, can1-100, his3200, leu2-3,112, trp1-1, ura3-1, noc1::noc1-7, rrp5::RRP5-Myc9-natNT2	this study; derivate of TY2069 by genomic integration of a tagging cassette (PCR on K1062 with o287/o288)
2074	noc1-7 (genomic) Rrp5-Myc Noc3-HA	mat alpha, ade2-1, can1-100, his3200, leu2-3,112, trp1-1, ura3-1, noc1::noc1-7, rrp5::RRP5-Myc9-natNT2, noc3::NOC3-HA3-hphNT1	this study; derivate of TY2073 by genomic integration of a tagging cassette (PCR on K1063 with o1901/o1902)
2075	noc1-7 (genomic) Rrp5-Myc Noc3-HA Noc2-GFP	mat alpha, ade2-1, can1-100, his3200, leu2-3,112, trp1-1, ura3-1, noc1::noc1-7, rrp5::RRP5-Myc9-natNT2, noc3::NOC3-HA3-hphNT1, noc2::NOC2-GFP-kanMX	this study; derivate of TY2074 by genomic integration of a tagging cassette (PCR on V47 with o908/o909)
2079	NOC1-shuffle Rrp5-Myc	mat alpha, ade2-1, can1-100, his3200, leu2-3,112, trp1-1, ura3-1, noc1::HIS3, rrp5::RRP5-Myc9-natNT2, YCplac33-pNOC1-NOC1 (URA3)	this study; derivate of TY772 by genomic integration of a tagging cassette (PCR on K1062 with o287/o288)
2080	NOC1-shuffle Rrp5-Myc Noc3-HA	mat alpha, ade2-1, can1-100, his3200, leu2-3,112, trp1-1, ura3-1, noc1::HIS3, rrp5::RRP5-Myc9-natNT2, noc3::NOC3-HA3-hphNT1, YCplac33-pNOC1-NOC1 (URA3)	this study; derivate of TY2079 by genomic integration of a tagging cassette (PCR on K1063 with o1901/o1902)
2081	NOC1-shuffle Rrp5-Myc Noc3-HA Noc2-GFP	mat alpha, ade2-1, can1-100, his3200, leu2-3,112, trp1-1, ura3-1, noc1::HIS3, rrp5::RRP5-Myc9-natNT2, noc3::NOC3-HA3-hphNT1, noc2::NOC2-GFP-kanMX, YCplac33-pNOC1-NOC1 (URA3)	this study; derivate of TY2080 by genomic integration of a tagging cassette (PCR on V47 with o908/o909)
2154	pGAL-NOC1 Rrp5-Myc Noc3-HA Noc2-GFP	mat alpha, ade2-1, can1-100, his3200, leu2-3,112, trp1-1, ura3-1, noc1::HIS3, rrp5::RRP5-Myc9-natNT2, noc3::NOC3-HA3-hphNT1, noc2::NOC2-GFP-kanMX, YCplac22-pGAL-NOC1 (TRP1)	this study; derivate of TY2081 by plasmid shuffling with T33
2201	PA-NOC1	mat alpha, ade2-1, can1-100, his3200, leu2-3,112, trp1-1, ura3-1, noc1::HIS3, pNOPPA-Noc1-FL (LEU2)	this study; derivate of TY772 by plasmid shuffling with K1442

2202	PA-noc1-delta1	mat alpha, ade2-1, can1-100, his3200, leu2-3,112, trp1-1, ura3-1, noc1::HIS3, pNOPPA-noc1-delta1 (LEU2)	this study; derivate of TY772 by plasmid shuffling with K1452
2203	PA-noc1-delta7	mat alpha, ade2-1, can1-100, his3200, leu2-3,112, trp1-1, ura3-1, noc1::HIS3, pNOPPA-noc1-delta7 (LEU2)	this study; derivate of TY772 by plasmid shuffling with K1455
2204	PA-noc1-delta1,7	mat alpha, ade2-1, can1-100, his3200, leu2-3,112, trp1-1, ura3-1, noc1::HIS3, pNOPPA-noc1-delta1,7 (LEU2)	this study; derivate of TY772 by plasmid shuffling with K1444
2299	pGAL-RRP5	mat A, ade2, his3, leu2, trp1, ura3, rrp5::HIS3, YCplac22-pGAL-RRP5 (TRP1)	this study; derivate of TY616 by plasmid shuffling with K1517
2301	pGAL-RRP5 NOC2-TAP	mat A, ade2, his3, leu2, trp1, ura3, rrp5::HIS3, noc2::NOC2-TAP-URA3, YCplac22-pGAL-RRP5 (TRP1)	this study; derivate of TY2299 by genomic integration of a tagging cassette (PCR on V97 with o621/o622)
2302	RRP5 shuffle NOC1-TAP	mat A, ade2, his3, leu2, trp1, ura3, rrp5::HIS3, noc1::NOC1-TAP-TRP1, pURA3 RRP5 (URA3)	this study; derivate of TY616 by genomic integration of a tagging cassette (PCR on K132 with o177/o178)
2303	RRP5 shuffle NOC2-TAP	mat A, ade2, his3, leu2, trp1, ura3, rrp5::HIS3, noc2::NOC2-TAP-TRP1, pURA3 RRP5 (URA3)	this study; derivate of TY616 by genomic integration of a tagging cassette (PCR on K132 with o621/o622)
2304	rrp5-S10-TPR-TAP rrp5-S1-9-GFP	mat A, ade2, his3, leu2, trp1, ura3, rrp5::HIS3, pRS314-rrp5-S10-TPR-TAP (TRP1) pRS315-rrp5-S1-9-GFP (LEU2)	gift from J. Baßler, Heidelberg
2305	rrp5-deltaS-TAP rrp5-S1-9-GFP	mat A, ade2, his3, leu2, trp1, ura3, rrp5::HIS3, pRS314-rrp5-deltaS-TAP (TRP1) pRS315-rrp5-S1-9-GFP (LEU2)	gift from J. Baßler, Heidelberg
2306	rrp5-S1-9-TAP rrp5-deltaS-GFP	mat A, ade2, his3, leu2, trp1, ura3, rrp5::HIS3, pRS314-rrp5-deltaS-GFP (TRP1) pRS315-rrp5-S1-9-TAP (LEU2)	gift from J. Baßler, Heidelberg
2307	RRP5-TAP	mat A, ade2, his3, leu2, trp1, ura3, rrp5::HIS3, pRS315-RRP5-TAP (LEU2)	gift from J. Baßler, Heidelberg
2318	pGAL-RRP5 UTP22-TAP	mat A, ade2, his3, leu2, trp1, ura3, rrp5::HIS3, utp22::UTP22-TAP-URA3, YCplac22-pGAL-RRP5 (TRP1)	this study; derivate of TY2299 by genomic integration of a tagging cassette (PCR on V97 with o2261/o2262)
2322	RRP5-Shuffle UTP22-TAP	mat A, ade2, his3, leu2, trp1, ura3, rrp5::HIS3, utp22::UTP22-TAP-kanMX, pURA3 RRP5 (URA3)	this study; derivate of TY616 by genomic integration of a tagging cassette (PCR on V1890 with o2952/o2953)
2343	pGAL-RRP5 NOC1-TAP	mat A, ade2, his3, leu2, trp1, ura3, rrp5::HIS3, noc1::NOC1-TAP-URA3, YCplac22-pGAL-RRP5 (TRP1)	this study; derivate of TY2299 by genomic integration of a tagging cassette (PCR on V97 with o177/o178)
2417	NOC1-shuffle UTP22-TAP	mat alpha, ade2-1, can1-100, his3200, leu2-3,112, trp1-1, ura3-1, noc1::HIS3, utp22::UTP22-TAP-kanMX, YCplac33-pNOC1-NOC1 (URA3)	this study; derivate of TY772 by genomic integration of a tagging cassette (PCR on K1890 with o2952/o2953)

2418	pGAL-NOC1 UTP22-TAP	mat alpha, ade2-1, can1-100, his3200, leu2-3,112, trp1-1, ura3-1, noc1::HIS3, utp22::UTP22-TAP-kanMX, YCplac22-pGAL-NOC1 (TRP1)	this study; derivate of TY775 by genomic integration of a tagging cassette (PCR on K1890 with o2952/o2953)
2423	BY4741 A135-TEV-ProtA	mat A, his31 leu20 met150 ura30 rpa135::RPA135-TEV-ProtA-kanMX6	Jochen Gerber
2424	BY4741 Rpb2-TEV-ProtA	mat A, his31 leu20 met150 ura30 rpb2::RPB2-TEV-ProtA-kanMX6	Jochen Gerber
2499	NOC1-Shuffle RRP5-TAP	mat alpha, ade2-1, can1-100, his3200, leu2-3,112, trp1-1, ura3-1, noc1::HIS3, rrp5::RRP5-TAP-kanMX, YCplac33-pNOC1-NOC1 (URA3)	this study; derivate of TY772 by genomic integration of a tagging cassette (PCR on K1890 with o287/o288)
2500	NOC2-Shuffle RRP5-TAP	mat alpha, ade2-1, can1-100, his3200, leu2-3,112, trp1-1, ura3-1, noc2::HIS3, rrp5::RRP5-TAP-kanMX, YCplac33-pNOC2-NOC2 (URA3)	this study; derivate of TY773 by genomic integration of a tagging cassette (PCR on K1890 with o287/o288)
2501	pGAL-NOC1 RRP5-TAP	mat alpha, ade2-1, can1-100, his3200, leu2-3,112, trp1-1, ura3-1, noc1::HIS3, rrp5::RRP5-TAP-kanMX, YCplac22-pGAL-NOC1 (TRP1)	this study; derivate of TY2499 by plasmid shuffling with T33
2502	pGAL-NOC2 RRP5-TAP	mat alpha, ade2-1, can1-100, his3200, leu2-3,112, trp1-1, ura3-1, noc2::HIS3, rrp5::RRP5-TAP-kanMX, YCplac22-pGAL-NOC2 (TRP1)	this study; derivate of TY2500 by plasmid shuffling with T34

5.1.2 *E. coli* strains

name	genotype	origin
XL1blue	recA1, endA1, gyrA96 thi-1, hsdR17, supE44, relA1, lac [F´ proAB lacIqZΔM15 Tn10 (Tet_R)]	Stratagene
BW23473	Δ(argF-lac)169, ΔuidA3::pir+ , recA1, rpoS396(Am), endA9(del-ins)::FRT, rph-1, hsdR514, rob-1, creC510	Imre Berger
DH10Bac-eYFP	pMON7124 (bom+, tra-, mob-), bMON14272 – eYFP, F– mcrA (mrr-hsdRMS-mcrBC) 80lacZΔ M15 lacX74 recA1 endA1 araD139 (ara, leu)7697 galU galK – rpsL nupG	Imre Berger

5.1.3 SF21 insect cells

The SF21 cell line is developed from primary explants of pupal tissue from the insect Spodoptera frugiperda (Vaughn et al., 1977). Cells were purchased from Invitrogen.

5.1.4 Plasmids

K	name	features	origin	generation
V17	pNOPPA	CEN6 ARSH4 LEU2 pNOP1-ProteinA	gift from Ed Hurt	
V47	pYM12	Ori-ColE1 AmpR yEGFP-tag-kanMX-cassette	(Knop et al., 1999)	

V48	YCplac22GAL	CEN4 ARS1 TRP1 pGAL1/10	gift from M. Künzler	
V96	pBS1479	Ori-ColE1 AmpR TAP-tag-TRP1-cassette	(Rigaut et al., 1999)	
T17	YCplac33 NOC1	CEN4 ARS1 URA3 pNOC1-NOC1	(Milkereit et al., 2001)	
T19	YCplac33 NOC3	CEN4 ARS1 URA3 pNOC3-NOC3	(Milkereit et al., 2001)	
T33	YCplac22GAL-NOC1	CEN4 ARS1 TRP1 pGAL-NOC1	Philipp Milkereit	
T34	YCplac22GAL-NOC2	CEN4 ARS1 TRP1 pGAL-NOC2	Philipp Milkereit	
113	pNOPPA-noc1-6	CEN6 ARSH4 LEU2 pNOP1-PA-noc1-6	Philipp Milkereit	
114	pNOPPA-noc1-7	CEN6 ARSH4 LEU2 pNOP1-PA-noc1-7	Philipp Milkereit	
132	pBS1539	Ori-ColE1 AmpR TAP-tag-URA3-cassette	(Puig et al., 2001)	
1062	pYM21	Ori-ColE1 AmpR 9xMyc-tag-natNT2-cassette	(Janke et al., 2004)	
1063	pYM24	Ori-ColE1 AmpR 3xHA-tag-hphNT1-cassette	(Janke et al., 2004)	
1127	pUCDM	Ori-R6Kg ChlR loxP p10 polh	(Berger et al., 2004)	
1129	pSPL	Ori-R6Kg SpecR loxP p10 polh	(Fitzgerald et al., 2006)	
1130	pFL	Ori-ColE1 AmpR GentR loxP Tn7L/R p10 polh	(Fitzgerald et al., 2006)	
1212	pFL-Flag-TEV	Ori-ColE1 AmpR GentR loxP Tn7L/R p10 polh-FLAG-TEV	Juliane Merl	
1213	pFL-Flag-TEV-Noc2	Ori-ColE1 AmpR GentR loxP Tn7L/R p10 polh-NOC2	Juliane Merl	
1230	pUCDM-Noc1	Ori-R6Kg ChlR loxP p10 polh-NOC1	Juliane Merl	
1232	pFL-Flag-TEV-Noc2-pUCDM-Noc1	Ori-ColE1 Ori-R6Kg AmpR GentR ChlR loxP Tn7L/R p10 polh-NOC2, polh-NOC1	Juliane Merl	
1259	pSPL-6xHis-Rrp5	Ori-R6Kg SpecR loxP p10 polh-RRP5	Juliane Merl	
1442	pNOPPA-Noc1-FL	CEN6 ARSH4 LEU2 pNOP1-PA-NOC1	this study	yeast NOC1 was generated by PCR using oligos o2056 and o2064 and cloned into V17 via HindIII/XhoI

1443	pNOPPA-noc1-delta1-3	CEN6 ARSH4 LEU2 pNOP1-PA-noc1-delta1-3	this study	truncated allele of yeast NOC1 was generated by PCR using oligos o2059 and o2064 and cloned into V17 via HindIII/XhoI
1444	pNOPPA-noc1-delta1,7	CEN6 ARSH4 LEU2 pNOP1-PA-noc1-delta1,7	this study	truncated allele of yeast NOC1 was generated by PCR using oligos o2057 and o2063 and cloned into V17 via HindIII/XhoI
1445	pGEMT-easy-noc1-delta1	Ori-ColE1 AmpR	this study	truncated allele of yeast NOC1 was generated by PCR using oligos o2057 and o2064 and cloned into pGEMT-easy vector (Promega)
1446	pGEMT-easy-noc1-delta1-4	Ori-ColE1 AmpR	this study	truncated allele of yeast NOC1 was generated by PCR using oligos o2060 and o2064 and cloned into pGEMT-easy vector (Promega)
1447	pGEMT-easy-noc1-delta5-7	Ori-ColE1 AmpR	this study	truncated allele of yeast NOC1 was generated by PCR using oligos o2056 and o2061 and cloned into pGEMT-easy vector (Promega)
1448	pGEMT-easy-noc1-delta7	Ori-ColE1 AmpR	this study	truncated allele of yeast NOC1 was generated by PCR using oligos o2056 and o2063 and cloned into pGEMT-easy vector (Promega)
1449	pGEMT-easy-noc1-delta2	Ori-ColE1 AmpR	this study	internal deletion allele of yeast NOC1 was generated by SOE-PCR, using o2056/o2066 and o2065/o2064 to generate the 5' and 3' fragments, which were used as templates in a PCR with o2056/o2064. Product was cloned into pGEMT-easy vector (Promega)
1450	pGEMT-easy-noc1-delta3	Ori-ColE1 AmpR	this study	internal deletion allele of yeast NOC1 was generated by SOE-PCR, using o2056/o2068 and o2067/o2064 to generate the 5' and 3' fragments, which were used as templates in a PCR with o2056/o2064. Product was cloned into pGEMT-easy vector (Promega)
1451	pGEMT-easy-noc1-delta4	Ori-ColE1 AmpR	this study	internal deletion allele of yeast NOC1 was generated by SOE-PCR, using o2056/o2090 and o2069/o2064 to generate the 5' and 3' fragments, which were used as templates in a PCR with o2056/o2064. Product was cloned into pGEMT-easy vector (Promega)
1452	pNOPPA-noc1-delta1	CEN6 ARSH4 LEU2 pNOP1-PA-noc1-delta1	this study	truncated allele of yeast NOC1 was subcloned from K1445 into V17 via HindIII/XhoI
1453	pNOPPA-noc1-delta1-4	CEN6 ARSH4 LEU2 pNOP1-PA-noc1-delta1-4	this study	truncated allele of yeast NOC1 was subcloned from K1446 into V17 via HindIII/XhoI
1454	pNOPPA-noc1-delta5-7	CEN6 ARSH4 LEU2 pNOP1-PA-noc1-delta5-7	this study	truncated allele of yeast NOC1 was subcloned from K1447 into V17 via HindIII/XhoI

1455	pNOPPA-noc1-delta7	CEN6 ARSH4 LEU2 pNOP1-PA-noc1-delta7	this study	truncated allele of yeast NOC1 was subcloned from K1448 into V17 via HindIII/XhoI
1456	pNOPPA-noc1-delta2	CEN6 ARSH4 LEU2 pNOP1-PA-noc1-delta2	this study	truncated allele of yeast NOC1 was subcloned from K1449 into V17 via HindIII/XhoI
1457	pNOPPA-noc1-delta3	CEN6 ARSH4 LEU2 pNOP1-PA-noc1-delta3	this study	truncated allele of yeast NOC1 was subcloned from K1450 into V17 via HindIII/XhoI
1458	pNOPPA-noc1-delta4	CEN6 ARSH4 LEU2 pNOP1-PA-noc1-delta4	this study	truncated allele of yeast NOC1 was subcloned from K1451 into V17 via HindIII/XhoI
1476	pFL-Flag-TEV-Noc1	Ori-ColE1 AmpR GentR loxP Tn7L/R p10 polh-NOC1	this study	yeast NOC1 subcloned from K1230 into K1212 via SalI/XbaI
1500	pMA-RQ-3xHA-Thrombin	Ori-ColE1 AmpR START-3xHA-Thrombin-site cassette	Geneart	gene synthesis
1502	pSPL-3xHA-ThrombinSS	Ori-R6Kg SpecR loxP p10 polh-HA-Thrombin-site	M. Sauert/ this study	START-3xHA-Thrombin-site cassette subcloned from K1500 (BglII/PstI) in K1129 BamHI/PstI)
1503	pSPL-3xHA-Rrp5	Ori-R6Kg SpecR loxP p10 polh-RRP5	M. Sauert/ this study	yeast RRP5 subcloned from K1259 into K1502 via BamHI/PstI
1504	pFL-Flag-TEV-Noc2-pSPL-3xHA-Rrp5-pUCDM-Noc1	Ori-ColE1 Ori-R6Kg AmpR GentR ChlR SpecR loxP Tn7L/R p10 polh-NOC1, polh-NOC2, polh-RRP5	M. Sauert/ this study	in vitro cre-lox recombination of plasmids K1213, K1230 und K1503
1517	YCplac22GAL-RRP5	pGAL-RRP5 ARS1 CEN4 TRP1	this study	yeast RRP5 subcloned from K1503 into V48 via BamHI/PstI
1608	pGEMT-easy-noc1-delta1,2	Ori-ColE1 AmpR	this study	truncated allele of yeast NOC1 was generated by PCR using oligos o2058 and o2064 and cloned into pGEMT-easy vector (Promega)
1609	pGEMT-easy-noc1-D3-6	Ori-ColE1 AmpR	this study	truncated allele of yeast NOC1 was generated by PCR using oligos o2058 and o2063 and cloned into pGEMT-easy vector (Promega)
1610	pGEMT-easy-noc1-D4-6	Ori-ColE1 AmpR	this study	truncated allele of yeast NOC1 was generated by PCR using oligos o2059 and o2063 and cloned into pGEMT-easy vector (Promega)
1611	pGEMT-easy-noc1-delta5	Ori-ColE1 AmpR	this study	internal deletion allele of yeast NOC1 was generated by SOE-PCR, using o2056/o2070 and o2091/o2064 to generate the 5' and 3' fragments, which were used as templates in a PCR with o2056/o2064. Product was cloned into pGEMT-easy vector (Promega)
1612	pGEMT-easy-noc1-delta6	Ori-ColE1 AmpR	this study	internal deletion allele of yeast NOC1 was generated by SOE-PCR, using o2056/o2072 and o2071/o2064 to generate the 5' and 3' fragments, which were used as templates in a PCR with o2056/o2064. Product was cloned into pGEMT-easy vector (Promega)

1613	pNOPPA-noc1-delta1,2	CEN6 ARSH4 LEU2 pNOP1-PA-noc1-delta1,2	this study	truncated allele of yeast NOC1 was subcloned from K1608 into V17 via HindIII/XhoI
1614	pNOPPA-noc1-D3-6	CEN6 ARSH4 LEU2 pNOP1-PA-noc1-D3-6	this study	truncated allele of yeast NOC1 was subcloned from K1609 into V17 via HindIII/XhoI
1615	pNOPPA-noc1-D4-6	CEN6 ARSH4 LEU2 pNOP1-PA-noc1-D4-6	this study	truncated allele of yeast NOC1 was subcloned from K1610 into V17 via HindIII/XhoI
1616	pNOPPA-noc1-delta5	CEN6 ARSH4 LEU2 pNOP1-PA-noc1-delta5	this study	truncated allele of yeast NOC1 was subcloned from K1611 into V17 via HindIII/XhoI
1617	pNOPPA-noc1-delta6	CEN6 ARSH4 LEU2 pNOP1-PA-noc1-delta6	this study	truncated allele of yeast NOC1 was subcloned from K1612 into V17 via HindIII/XhoI
1624	pFL-Flag-TEV-RRP5	Ori-ColE1 AmpR GentR loxP Tn7L/R p10 polh-RRP5	this study	yeast RRP5 subcloned from K1259 into K1212 via BamHI/PstI
1658	pFL-Flag-TEV-NOC1-pSPL-3xHA-RRP5	Ori-ColE1 Ori-R6Kg AmpR GentR SpecR loxP Tn7L/R p10 polh-NOC1, polh-RRP5	this study	in vitro cre-lox recombination of plasmid K1476 and K1503
1663	pNOPPA-noc3-1	CEN6 ARSH4 LEU2 pNOP1-PA-noc3-1	(Milkereit et al., 2001)	
1677	pFL-Flag-TEV-NOC2-pSPL-3xHA-RRP5	Ori-ColE1 Ori-R6Kg AmpR GentR SpecR loxP Tn7L/R p10 polh-NOC2, polh-RRP5	this study	in vitro cre-lox recombination of plasmid K1212 and K1503
1692	pGEMT-easy-rrp5-S1-6+N	Ori-ColE1 AmpR	this study	truncated allele of yeast RRP5 was generated by PCR using oligos o1972 and o2900 and cloned into pGEMT-easy vector (Promega)
1693	pGEMT-easy-rrp5-S1-6	Ori-ColE1 AmpR	this study	truncated allele of yeast RRP5 was generated by PCR using oligos o2897 and o2900 and cloned into pGEMT-easy vector (Promega)
1694	pGEMT-easy-rrp5-S3-6	Ori-ColE1 AmpR	this study	truncated allele of yeast RRP5 was generated by PCR using oligos o2898 and o2900 and cloned into pGEMT-easy vector (Promega)
1695	pGEMT-easy-rrp5-S4-9	Ori-ColE1 AmpR	this study	truncated allele of yeast RRP5 was generated by PCR using oligos o2899 and o2901 and cloned into pGEMT-easy vector (Promega)
1696	pGEMT-easy-rrp5-S10-TPR	Ori-ColE1 AmpR	this study	truncated allele of yeast RRP5 was generated by PCR using oligos o2905 and o1973 and cloned into pGEMT-easy vector (Promega)
1697	pGEMT-easy-rrp5-TPR	Ori-ColE1 AmpR	this study	truncated allele of yeast RRP5 was generated by PCR using oligos o2906 and o1973 and cloned into pGEMT-easy vector (Promega)
1698	pSPL-3xHA-rrp5-S1-9+N	Ori-R6Kg SpecR loxP p10 polh-rrp5-S1-9	this study	truncated allele of yeast RRP5 was generated by PCR using oligos o1972 and o2901 and cloned into K1502 via BamHI/PstI

1699	pSPL-3xHA-rrp5-S1-6+N	Ori-R6Kg SpecR loxP p10 polh-rrp5-S1-6	this study	truncated allele of yeast RRP5 was subcloned from K1692 into K1502 via BamHI/PstI
1700	pSPL-3xHA-rrp5-S1-6	Ori-R6Kg SpecR loxP p10 polh-rrp5-S1-6-dN	this study	truncated allele of yeast RRP5 was subcloned from K1693 into K1502 via BamHI/PstI
1701	pSPL-3xHA-rrp5-S3-6	Ori-R6Kg SpecR loxP p10 polh-rrp5-S3-6	this study	truncated allele of yeast RRP5 was subcloned from K1694 into K1502 via BamHI/PstI
1702	pSPL-3xHA-rrp5-S4-9	Ori-R6Kg SpecR loxP p10 polh-rrp5-S4-9	this study	truncated allele of yeast RRP5 was subcloned from K1695 into K1502 via BamHI/PstI
1703	pSPL-3xHA-rrp5-S10-TPR	Ori-R6Kg SpecR loxP p10 polh-rrp5-S10-TPR	this study	truncated allele of yeast RRP5 was subcloned from K1696 into K1502 via BamHI/PstI
1704	pSPL-3xHA-rrp5-TPR	Ori-R6Kg SpecR loxP p10 polh-rrp5-TPR	this study	truncated allele of yeast RRP5 was subcloned from K1697 into K1502 via BamHI/PstI
1727	pSPL-3xHA-rrp5-S1-9+pFL-Flag-NOC1	Ori-ColE1 Ori-R6Kg AmpR GentR SpecR loxP Tn7L/R p10 polh-NOC1, polh-rrp5-S1-9	this study	in vitro cre-lox recombination of plasmid K1476 and K1698
1728	pSPL-3xHA-rrp5-S1-6+pFL-Flag-NOC1	Ori-ColE1 Ori-R6Kg AmpR GentR SpecR loxP Tn7L/R p10 polh-NOC1, polh-rrp5-S1-6	this study	in vitro cre-lox recombination of plasmid K1476 and K1699
1729	pSPL-3xHA-rrp5-S1-6-ΔN+pFL-Flag-NOC1	Ori-ColE1 Ori-R6Kg AmpR GentR SpecR loxP Tn7L/R p10 polh-NOC1, polh-rrp5-S1-6-ΔN	this study	in vitro cre-lox recombination of plasmid K1476 and K1700
1730	pSPL-3xHA-rrp5-S3-6+pFL-Flag-NOC1	Ori-ColE1 Ori-R6Kg AmpR GentR SpecR loxP Tn7L/R p10 polh-NOC1, polh-rrp5-S3-6	this study	in vitro cre-lox recombination of plasmid K1476 and K1701
1731	pSPL-3xHA-rrp5-S4-9+pFL-Flag-NOC1	Ori-ColE1 Ori-R6Kg AmpR GentR SpecR loxP Tn7L/R p10 polh-NOC1, polh-rrp5-S4-9	this study	in vitro cre-lox recombination of plasmid K1476 and K1702
1732	pSPL-3xHA-rrp5-S10-TPR+pFL-Flag-NOC1	Ori-ColE1 Ori-R6Kg AmpR GentR SpecR loxP Tn7L/R p10 polh-NOC1, polh-rrp5-S10-TPR	this study	in vitro cre-lox recombination of plasmid K1476 and K1703
1733	pSPL-3xHA-rrp5-TPR+pFL-Flag-NOC1	Ori-ColE1 Ori-R6Kg AmpR GentR SpecR loxP Tn7L/R p10 polh-NOC1, polh-rrp5-TPR	this study	in vitro cre-lox recombination of plasmid K1476 and K1704
1890	pYM13	Ori-ColE1 AmpR TAP-tag-kanMX-cassette	(Janke et al., 2004)	

5.1.5 Oligonucleotides

Probes for Northern blotting

oligo	name	sequence
202	U3-sno-254	CCAACTTGTCAGACTGCCATT
205	o2-18S	CATGGCTTAATCTTTGAGAC
207	o4-A2/A3	TGTTACCTCTGGGCCC
209	o6-5.8	TTTCGCTGCGTTCTTCATC
210	o7-E/C2	GGCCAGCAATTTCAAGTTA
211	o8-C1/C2	GAACATTGTTCGCCTAGA
212	o9-25S	CTCCGCTTATTGATATGC
1819	ext_ITS1_2	GTAAAAGCTCTCATGCTCTTGCC
2474	5S-rDNA	TTAACTACAGTTGATCGG

Primer for qPCR

oligo	name	sequence	amplicon
613	qPCR-PDC1-up	CATGATCAGATGGGGCTTGA	9
614	qPCR-PDC1-do	ACCGGTGGTAGCGACTCTGT	
710	M1	TGGAGCAAAGAAATCACCGC	7
711	M2	CCGCTGGATTATGGCTGAAC	
712	M3	GAGTCCTTGTGGCTCTTGGC	3
713	M4	AATACTGATGCCCCCGACC	
920	5S ChIP-F1	GCCATATCTACCAGAAAGCACC	8
921	5S ChIP-R1	GATTGCAGCACCTGAGTTTCG	
969	Prom ChIP-F2	TCATGGAGTACAAGTGTGAGGA	1
970	Prom ChIP-R1	TAACGAACGACAAGCCTACTC	
2011	qPCR6_for	CTTGGATGTGGTAGCCGTTT	2
2012	qPCR6_rev	TCGACCCTTTGGAAGAGATG	
2429	Laf 14 for	AAAGAAGACCCTGTTGAGCTTGA	6
2430	Laf 14 rev	GTATTTCACTGGCGCCGAA	
2481	rDNA8 Th fo	GGTGGTAAATTCCATCTAAAGCTAAATATT	5
2482	rDNA8 Th re	CACGTACTTTTTCACTCTCTTTTCAAA	
2864	IGS2-up-q	GCATGCCTGTTTGAGCGTC	4
2865	IGS2-do-q	CGACCGTACTTGCATTATACC	

Oligonucleotides used for genomic integration

oligo	name	sequence
177	noc1-TAP.f	ATCTGCCGACGATTATGCTCAATATTTAGATCAAGATTC AGACTCCATGGAAAAGAGAAG
178	noc1-TAP.r	TAATTTACAACACCGAAGTGTTTAGTTAATGTATTATTAT TTTTACGACTCACTATAGGG
287	RRP5-HA.forward	GCTACTGAGTATGTCGCTAGCCATGAATCTCAAAAAGCA GACGAACGTACGCTGCAGGTCGAC
288	RRP5-HA.reverse	AACTTAGCCATTTATATTACTTTACAGTTAAAAATCCATC AGGAAATCGATGAATTCGAGCTCG

621	Noc2-TAP FP	AAGTGATGATGACAACGAAGATGTTGAAATGTCAGACG CT TCCATGGAAAAGAGAAG
622	Noc2-TAP RP	CTATTGAATTCAAGACAAAAAATCAAATCTTGCTGAGTT GTACGACTCACTATAGGG
908	NOC2_S2	CTTAACTATTGAATTCAAGACAAAAAATCAAATCTTGCTG AGTTGATCGATGAATTCGAGCTCG
909	NOC2_S3	CTGGAAAGTGATGATGACAACGAAGATGTTGAAATGTC AGACGCTCGTACGCTGCAGGTCGAC
1901	Noc3_S3-forw	AAGGGGCTACGCTCTCTATCATCTAGATCTAAAGAGTGT TCTAAA-cgtacgctgcaggtcgac
1902	Noc3_S2-rev	TAACGATAATCGTGGCTCTTTATATACTTAATATATAGGA TCTAG-atcgatgaattcgagctcg
2073	Noc1-Integr_fw	gatattaaacctctccagtgtctttgttggtacagtaatcaaaaata atgagtgagaacaacggc
2074	Noc1-Integr_rev	ttaatttacaacaccgaagtgtttagttaatgtattattattttcta gtctgaatcttgatctaa
2261	Utp22-TAP-F	GAGATTGCTGCATTCGGGAATGACATGGTTATAAATTTT GAGACAGATTCCATGGAAAAGAGAAG
2262	Utp22-TAP-R	TTTAATATTATACAGATACTTCTAAAAGTTATGATTTTGTT GTTTATTTACGACTCACTATAGGG
2952	UTP22-S3-fw	ATGAGATTGCTGCATTCGGGAATGACATGGTTATAAATT TTGAGACAGATCGTACGCTGCAGGTCGAC
2953	UTP22-S2-REV	GCTGCTTTAATTATTTAATATTATACAGATACTTCTAAAA GTTATGATTTTGTTGTTTATT ATCGATGAATTCGAGCTCG

Oligonucleotides used for cloning

oligo	name	sequence
1972	Rrp5-BamHI_for	TTTTTTGGATCCATGGTAGCTTCCACCAAAAG
1973	Rrp5-PstI_rev	TTTTTTCTGCAGTTATTCGTCTGCTTTTTGAG
2056	Noc1-D1-f_Hind+S	gtact AAGCTT GTCGAC atgagtgagaacaacggcaa
2057	Noc1-D2-f_Hind+S	gtact AAGCTT GTCGAC ggacaaaatgatgatgttga
2058	Noc1-D3-f_Hind+S	gtact AAGCTT GTCGAC tctatgatgctaaacaagaa
2059	Noc1-D4-f_Hind+S	gtact AAGCTT GTCGAC aagggtaaacacggtggtaa
2060	Noc1-D5-f_Hind+S	gtact AAGCTT GTCGAC tacgacggccgcaagcgtga
2061	Noc1-D4-rev_XhoI	gtact CTCGAG cta ttccttccttttatgtccttgt
2062	Noc1-D5-rev_XhoI	gtact CTCGAG cta cttggcacttctgtagacaaatc
2063	Noc1-D6-rev_XhoI	gtact CTCGAG cta aacatctggtctcgatttaacca
2064	Noc1-D7-rev_XhoI	gtact CTCGAG cta gtctgaatcttgatctaaatatt
2065	Noc1-D3-delta2_f	ttccattggatcctcaagtt tctatgatgctaaacaagaa
2066	Noc1-D1-delta2_r	ttcttgtttagcatcataga aacttgaggatccaatggaa
2067	Noc1-D4-delta3_f	tcaaaaatcaacctggctta aagggtaaacacggtggtaa
2068	Noc1-D2-delta3_r	ttaccaccgtgtttaccctt taagccaggttgatttttga
2069	Noc1-D5-delta4_f	aaagaaagaagaactttaaa tacgacggccgcaagcgtga
2070	Noc1-D4-delta5_r	cctcttgctgtattggtctg ttccttccttttatgtcct
2071	Noc1-D7-delta6_f	ttgtctacagaagtgccaag gaagatgatagcgacgacag
2072	Noc1-D5-delta6_r	ctgtcgtcgctatcatcttc cttggcacttctgtagacaa
2090	Noc1-D3-delta4_r	tcacgcttgcggccgtcgta tttaaagttcttctttcttt
2091	Noc1-D6-delta5_f	aggacataaaaaggaaggaa cagaccaatacagcaagagg

2897	Rrp5-S1-BamHI_fw	ttTttttt ggatcc ATG ctaattgaacatgtcaactttaaaacg
2898	Rrp5-S3-BamHI_fw	ttTttttt ggatcc ATG attactcaaatctcctcaattgatg
2899	Rrp5-S4-BamHI_fw	ttTttttt ggatcc ATG aagtatctaagaacaaatgatattcc
2900	Rrp5-S6-PstI_rev	ttTttttt ctgcag TTA tttagcgtctttaatcagagaac
2901	Rrp5-S9-PstI_rev	ttTttttt ctgcag TTA aactttaattgtggacatatttatgtc
2905	Rrp5-S10-BamHI-fw	ttTttttt ggatcc ATG tccacaattaaagttggtgatgaa
2906	Rrp5-TPR-BamHI-fw	ttTttttt ggatcc ATG actgtggatcaactggaaaag

5.1.6 Chemicals

Chemicals were purchased at the highest available purity from Sigma-Aldrich, Merck, Fluka, Roth or J.T.Baker, except agarose electrophoresis grade (Invitrogen), bromine phenol blue (Serva), Ficoll (Serva) G418/Geneticin (Gibco), nourseothricin (Werner Bioagents), gentamycin (PAA), 5-FOA (Toronto Research Chemicals), X-GAL (Peqlab), milk powder (Sukofin), Nonidet P-40 substitute (NP40) (USB Corporation), Tris ultrapure (USB Corporation) and Tween 20 (Serva). Isotope labelled compounds were purchased from PerkinElmer (5',6'-[$_3$H] uracil), and Hartmann Analytic (γ-^{32}P-ATP).
Ingredients for growth media were purchased from BD Biosciences (Bacto Agar, Bacto Peptone, Bacto Tryptone and Bacto Yeast Extract), Q-Biogene, Bio101, Inc. or Sunrise Science Products (Complete supplement mixtures (CSM), Yeast nitrogen base (YNB), amino acids, adenine) and Sigma-Aldrich (D(+)-glucose, D(+)-galactose, amino acids and uracil).

5.1.7 Media and buffers

Unless stated otherwise, all solutions have been prepared in water that has a resistivity of 18.2 MΩ-cm and total organic content of less than five parts per billion. The pH values were measured at room temperature.

Medium	**Composition**
YPD (yeast extract, peptone, dextrose)	1% (w/v) yeast extract 2% (w/v) peptone 2% (w/v) glucose
YPDA (YPD plus adenine)	YPD + 100 mg/l adenine
YPDU (YPD plus uracil)	YPD + 2 mg/ml uracil
YPG (yeast extract, peptone, galactose)	1% (w/v) yeast extract 2% (w/v) peptone 2% (w/v) galactose
YPGA (YPG plus adenine)	YPG + 100 mg/l adenine
SCD (synthetic complete dextrose)	0.67% (w/v) YNB + nitrogen 0.062% (w/v) CSM-his-leu-trp 2% (w/v) glucose + 20 mg/l L-histidine + 100 mg/l L-leucine + 50 mg/l L-tryptophan
SCD-leu (SCD minus leucine)	0.67% (w/v) YNB + nitrogen 0.062% (w/v) CSM-his-leu-trp 2% (w/v) glucose + 20 mg/l L-histidine + 50 mg/l L-tryptophan

SCD-trp (SCD minus tryptophan)	0.67% (w/v) YNB + nitrogen 0.062% (w/v) CSM-his-leu-trp 2% (w/v) glucose + 20 mg/l L-histidine + 100 mg/l L-leucine
SCD-his (SCD minus histidine)	0.67% (w/v) YNB + nitrogen 0.062% (w/v) CSM-his-leu-trp 2% (w/v) glucose + 50 mg/l L-tryptophan + 100 mg/l L-leucine
SCD-ura (SCD minus uracil)	0.67% (w/v) YNB + nitrogen 0.062% (w/v) CSM-his-leu-ura 2% (w/v) glucose + 20 mg/l L-histidine + 100 mg/l L-leucine
SCG (synthetic complete galactose)	0.67% (w/v) YNB + nitrogen 0.062% (w/v) CSM-his-leu-trp 2% (w/v) galactose + 20 mg/l L-histidine + 100 mg/l L-leucine + 50 mg/l L-tryptophan
LB (luria broth)	1% (w/v) tryptone 0.5% (w/v) yeast extract 0.5% (w/v) NaCl
SOB (super optimal broth)	2% (w/v) tryptone 0.5% (w/v) yeast extract 0.5 g/l NaCl 0.19 g/l KCl 2.03 g/l $MgCl_2$ x 6 H2O pH 7.0 with NaOH

All media were autoclaved at 121°C for 20 minutes and subsequently stored at RT. To prepare plates, 2% (w/v) agar was added to the medium. SCG media lacking single amino acids were prepared analogous to SCD selection media. Antibiotics, 5-FOA and IPTG were added as stock solutions (see 'buffer' table) or as powder to the autoclaved medium after cooling to ~ 60°C. Working concentrations were 0.1% (w/v) 5-FOA, 200 µg/ml (geneticin), 300 µg/ml (hygromycin B), 100 µg/ml (nurseothricin), 100 µg/ml (ampicillin), 30 µg/ml (chloramphenicol), 50 µg/ml spectinomycin), 10 µg/ml (gentamycin), 10 µg/ml (tetracycline), 0.5 mM IPTG. Plates were stored at 4°C in the dark. X-GAL was plated onto LB+amp/tetra/genta/IPTG plates prior to use (80 µl of a 50 mg/ml stock solution in DMSO).

Medium for insect cell culture was purchased from Life technologies (Sf900 II SFM medium).

Buffer	Ingredients	Concentration
10x PBS	NaCl KCl KH_2PO_4 Na_2HPO_4 pH 7.4 with NaOH	1.37 M 27 mM 18 mM 0.1 M
1x PBST	NaCl KCl KH_2PO_4 Tween-20	0.137 M 2.7 mM 1.8 mM 0.05% (v/v)
4x lower tris (SDS-PAGE)	Tris SDS pH 8.8 with HCl	1.5 M 0.4% (w/v)
4x upper tris (SDS-PAGE)	Tris SDS bromophenol blue pH 6.8 with HCl	0.5 M 0.4% (w/v)
4x protein sample buffer (Laemmli buffer)	Tris pH 6.8 glycerol SDS β-mercaptoethanol bromophenol blue	0.25 M 40% (v/v) 8.4% (w/v) 0.57 M
HU buffer	Tris pH 6.8 SDS EDTA pH 8.0 β-mercaptoethanol urea bromophenol blue	0.2 M 5% (w/v) 1 mM 0.21 M 8 M
10x electrophoresis buffer	Tris glycine SDS	0.25 M 1.92 M 1% (w/v)
transfer buffer (Western Blot)	Tris glycine methanol	25 mM 192 mM 20% (v/v)
Poinceau staining solution	Poinceau S HOAc	0.5% (w/v) 1% (v/v)
Coomassie staining solution	Coomassie Brilliant Blue R 250 methanol HOAc	0.1% (w/v) 45% (v/v) 10% (v/v)
destaining solution	methanol HOAc	45% (v/v) 10% (v/v)
100x protease inhibitors (PIs)	benzamidine PMSF solvent: ethanol store at -20°C	0.2 M 0.1 M
10x DNA loading buffer	Tris-HCl pH 8.0 EDTA pH 8.0 glycerol bromophenol blue xylene cyanol	4 mM 0.4 mM 60% (v/v)
5x TBE buffer	Tris boric acid EDTA pH 8.0	445 mM 445 mM 10 mM
IRN buffer	Tris/HCl pH 8.0 NaCl EDTA pH 8.0	50 mM 0.5 M 20 mM
AE buffer	NaOAc pH 5.3 EDTA pH 8.0	50 mM 10 mM

RNA solubilization buffer (for agarose gel samples)	formamide (deionised) formaldehyde MOPS buffer store at -20°C	50% (v/v) 8% (v/v) 1x
RNA solubilization buffer (for acryl amide gel samples)	formamide (deionised) TBE check pH; should be pH 7 Xylen cyanol Bromphenol blue	80% (v/v) 0.1x
20x SSC	NaCl tri-sodium-citrate dihydrate pH 7.0 with HCl	3 M 0.3 M
10x MOPS buffer	sodium acetate trihydrate MOPS EDTA pH 8.0 pH 7.0 with NaOH	20 mM 0.2 M 10 mM
RNA hybridisation buffer	Formamide SSC SDS Denhard's solution	50% (v/v) 5x 0.5% (w/v) 5x
50x Denhard's solution	Ficoll (Typ 400) Polyvinylpyrrolidone (avg. MW 40000) BSA (Fraction V) store at -20°C	10mg/ml 10mg/ml 10mg/ml
5x Annealing buffer (PEX)	Tris/HCl pH 7.5 NaCl EDTA pH 8.0	50 mM 1.5 M 10 mM
1.25x RT-buffer (PEX)	Tris/HCl pH 8.4 DTT $MgCl_2$ dNTPs store at -20°C	12.5 mM 12.5 mM 7.5 mM 1.25 mM each
2x PEX loading buffer	formamide (deionised) EDTA pH 8.0 Xylen cyanol Bromphenol blue store at -20°C	95% (v/v) 20 mM
1x PEX loading buffer	2x PEX loading buffer H_2O	50% (v/v) 50% (v/v)
buffer A100	Tris/HCl pH 8 KCl $Mg(OAc)_2$ Protease inhibitors	20mM 200mM 5mM 1x
buffer A100 +T/T	Tris‑HCl pH 8 KCl $Mg(OAc)_2$ Protease inhibitors Triton X-100 Tween-20	20mM 200mM 5mM 1x 0.5% (w/v) 0.1% (w/v)
buffer AC	NH_4OAC $MgCl_2$ pH ad 7.4 with HOAc	100 mM 0.1 mM
ChIP Lysis buffer	HEPES pH 7.5 NaCl EDTA EGTA Triton X-100 Na-Desoxycholate (DOC)	50 mM 140 mM 5 mM 5 mM 1 % (w/v) 0.1 % (w/v)

ChIP Wash buffer I	HEPES pH 7.5 NaCl EDTA Triton X-100 Na-Desoxycholate (DOC)	50 mM 500 mM 2 mM 1 % (w/v) 0.1 % (w/v)
ChIP Wash buffer II	Tris/HCl pH 8.0 LiCl EDTA Nonidet P-40 alternative Na-Desoxycholate (DOC)	10 mM 250 mM 2 mM 0.5 % (w/v) 0.5 % (w/v)
RD buffer	glucose peptone malt extract yeast extract mannitol MgOAc store at -20°C	2% (w/v) 1% (w/v) 0.6% (w/v) 0.01% (w/v) 12% (w/v) 17.8 mM
TELit	Tris pH 8.0 LiOAc EDTA pH 8.0 pH 8.0 with HOAc	10 mM 100 mM 1 mM
LitSorb	sorbitol solvent: TELit sterile filtration	1 M
LitPEG	polyethylene glycol (PEG3350) solvent: TELit sterile filtration	40% (w/v)
Tfb-I	KAc $MnCl_2$ KCl glycerol pH 5,8 with 0,2 M HOAc sterile filtration	30 mM 50 mM 100 mM 15% (v/v)
Tfb-II	MOPS $CaCl_2$ KCl glycerol pH 7,0 with 1M NaOH sterile filtration	10 mM 75 mM 10 mM 15% (v/v)
ampicilin stock solution	ampicilin store at -20°C	100 mg/ml
chloramphenicol stock solution	chloramphenicol solvent: EtOH store at -20°C	30 mg/ml
spectinomycin stock solution	spectinomycin store at -20°C	50 mg/ml
tetracyclin stock solution	tetracyclin solvent: 70% (v/v) EtOH store at -20°C	10 mg/ml
gentamycin stock solution	gentamycin store at -20°C	10 mg/ml
IPTG stock solution	IPTG store at -20°C	1 M
DTT stock solution	DTT (dithiothreitol) store at -20°C	1 M

5.1.8 Enzymes

Enzyme	Origin
Antarctic Phosphatase	New England Biolabs (NEB)
Cre Recombinase	NEB
GoTaq Polymerase	Bio-Rad
Herculase II Fusion DNA Polymerase	Agilent
HotStarTaq DNA Polymerase	Qiagen
iProof High-Fidelity DNA Polymerase	Bio-Rad
M-MLV Reverse Transcriptase	Invitrogen
Proteinase K	Sigma-Aldrich
Restriction Endonucleases	New England Biolabs
RNase A	Invitrogen
RNase A/T1 cocktail	Ambion
T4 DNA Ligase	New England Biolabs
T4 Polynucleotide Kinase	NEB
Taq DNA Polymerase	New England Biolabs
Trypsin, sequencing grade	Roche

5.1.9 Antibodies

Antibody	Species	Dilution	Origin
α-rpS8	rabbit	1:5000	Georgio Dieci
α-Noc1 (serum) (to detect recombinant proteins)	rabbit	1:500	E. Kremmer, GSF München
α-Noc1 (affinity purified) (to detect endogenous proteins)	rabbit	1:200	E. Kremmer, GSF München
α-Noc2 (serum) (to detect recombinant proteins)	rabbitv	1:500	E. Kremmer, GSF München
α-Noc2 (affinity purified) (to detect endogenous proteins)	rabbit	1:100	E. Kremmer, GSF München
α-HA (3F10)	rat	1:5000	Roche
α-Myc (9E10)	mouse	1:200	E. Kremmer
α-Flag	rabbit	1:1000	Sigma-Aldrich
α-ProteinA	rabbit	1:10.000	Sigma-Aldrich
α-Tubulin	rat	1:1000	Abcam
α-GFP		1:1000	Roche
IRDye® 800CW Goat (polyclonal) Anti-Rabbit IgG (H+L),	goat	1:5000	LI-COR
α-mouse IgG (H+L) (peroxidase-conjugated)	goat	1:5000	Jackson IR/Dianova
α-rabbit IgG (H+L) (peroxidase-conjugated)	goat	1:5000	Jackson IR/Dianova
α-rat IgG+IgM (H+L) (peroxidase-conjugated)	goat	1:5000	Jackson IR/Dianova
PAP (peroxidase anti-peroxidase)	rabbit	1:5000	Sigma-Aldrich

5.1.10 Kits

Kit	Origin
Hot Star Taq qPCR kit	Qiagen
iTRAQ labelling kit	Life Technologies
peqGOLD Plasmid Miniprep Kits	Peqlab
QIAEX II gel extraction kit	Qiagen
QIAquick PCR Purification Kit	Qiagen

5.1.11 Consumables

Material	Origin
1 kb DNA ladder	New England Biolabs
100 bp DNA ladder	New England Biolabs
ANTI-FLAG M2 Affinity Gel	Sigma
BcMag™ Epoxy-Activated magnetic beads	Bioclone Inc.
BioMax MS Film	Sigma-Aldrich
Blotting papers MN 827 B	Millipore
BM Chemiluminescence Blotting Substrate (POD)	Roche
ColorPlus Prestained Protein Marker, Broad Range (7-175 kDa)	New England Biolabs
EN3HANCE Spray Surface Autoradiography Enhancer	PerkinElmer
Extra Thick Blot Paper	Bio-Rad
FLAG-Peptide	Sigma
FuGENE HD transfection reagent	Promega
glass beads (ø 0.75-1 mm)	Roth
IgG SepharoseTM 6 Fast Flow	GE Healthcare
Immobilion-P Membrane PVDF 0,45 µm	Millipore
Membrane Positive™	MP Biomedicals
Micro Bio-Spin 6 Columns	Bio-Rad
MobiCol microspin column	(MoBiTec
HYBOND ECL Nitrocellulose membrane	GE Healthcare
Protein Assay Dye Reagent Concentrate	Bio-Rad
Protein Marker, Broad Range (2-212 kDa)	New England Biolabs
rabbit IgG	Sigma-Aldrich
Salmon Sperm DNA (10 mg/ml)	Invitrogen
Ultima Gold Liquid scintillation cocktail	Perkin Elmer
SimplyBlueTM SafeStain	Invitrogen
SYBR Green	Roche
yeast genomic DNA (strain S288C)	Invitrogen
glycogen	Ambion

5.1.12 Equipment

Device	Manufacturer
4800 Proteomics Analyzer MALDI-TOF/TOF	Applied Biosystems
Avanti J-26 XP centrifuge	Beckman Coulter
AxioCam MR CCD camera	Zeiss
Axiovert 200M microscope	Zeiss
Biofuge Fresco refrigerated tabletop centrifuge	Hereaus
Biofuge Pico tabletop centrifuge	Hereaus
C412 centrifuge	Jouan
Centrikon T-324 centrifuge	Kontron Instruments

CT422 refrigerated centrifuge	Jouan
Electrophoresis system model 45-2010-i	Peqlab Biotechnologie GmbH
Trans Blot Cell	Biorad
FLA-3000 phosphor imager	Fujifilm
FPLC-System (Pumps P-500; Controller LCC-501+; Fraction Collector FRAC-100)	Pharmacia Biotech
Gel Max UV transilluminator	Intas
IKA-Vibrax VXR	IKA
Incubators	Memmert
LAS-3000 chemiluminescence imager	Fujifilm
MicroPulser electroporation apparatus	Bio-Rad
NanoDrop ND-1000 spectrophotometer	Peqlab Biotechnologie GmbH
Odyssey Infrared Imaging System	LI-COR
PCR Sprint thermocycler	Hybaid
Philips CM12 electron microscope	FEI Electron Optics
Power Pac 3000 power supplies	Bio-Rad
Rotor-Gene 3000	Corbett Research
Roto-Shake Genie	Scientific Industries
Shake incubators Multitron / Minitron	Infors
slow-scan-CCD-Kamera, Model 0124	TVIPS Tietz
SMART System	Pharmacia Biotech
Sonifier 250	Branson
Speed Vac Concentrator	Savant
Superose 12 PC 3.2/30	GE Healthcare
Thermomixer compact	Eppendorf
Trans-Blot SD Semi-Dry Transfer Cell	Bio-Rad
Ultrospec 3100pro spectrophotometer	Amersham
Vacuum blotter	Biorad
Drystar	H. Hoelzel
XCell SureLock Mini-Cell electrophoresis system	Invitrogen

5.1.13 Software

Software	Producer
4000 Series Explorer v.3.6	Applied Biosystems
Acrobat 7.0 Professional v.7.0.9	Adobe
Axiovision V 4.7.1.0	Zeiss
Data Explorer v.4.5 C	Applied Biosystems
GPS Explorer v.3.5	Applied Biosystems
Illustrator CS3	Adobe
Image Reader FLA-3000 V1.8	Fujifilm
Image Reader LAS-3000 V2.2	Fujifilm
Mascot	Matrix Science
Microsoft Office 2007	Microsoft
Multi Gauge V3.0	Fujifilm
ND-1000 v.3.5.2	Peqlab Biotechnologie GmbH
Photoshop CS v.8.0.1	Adobe
Rotor-Gene 6000	Corbett Research
SigmaPlot	Systat
VectorNTI	Invitrogen

5.2 Methods

5.2.1 Heterologous protein expression in SF21 insect cells using recombinant baculo viruses

The baculo virus/SF21 insect cell expression system enables co-expression of recombinant proteins in the context of eukaryotic cells. In this way, reconstitution of eukaryotic protein complexes is often more easily achieved than by co-expression of the respective proteins in *E.coli* or by *in vitro* assembly from single, independently expressed and purified proteins. In this work, the MultiBac system (Berger et al., 2004; Fitzgerald et al., 2006) was used to generate recombinant baculo viruses encoding combinations of different yeast genes.

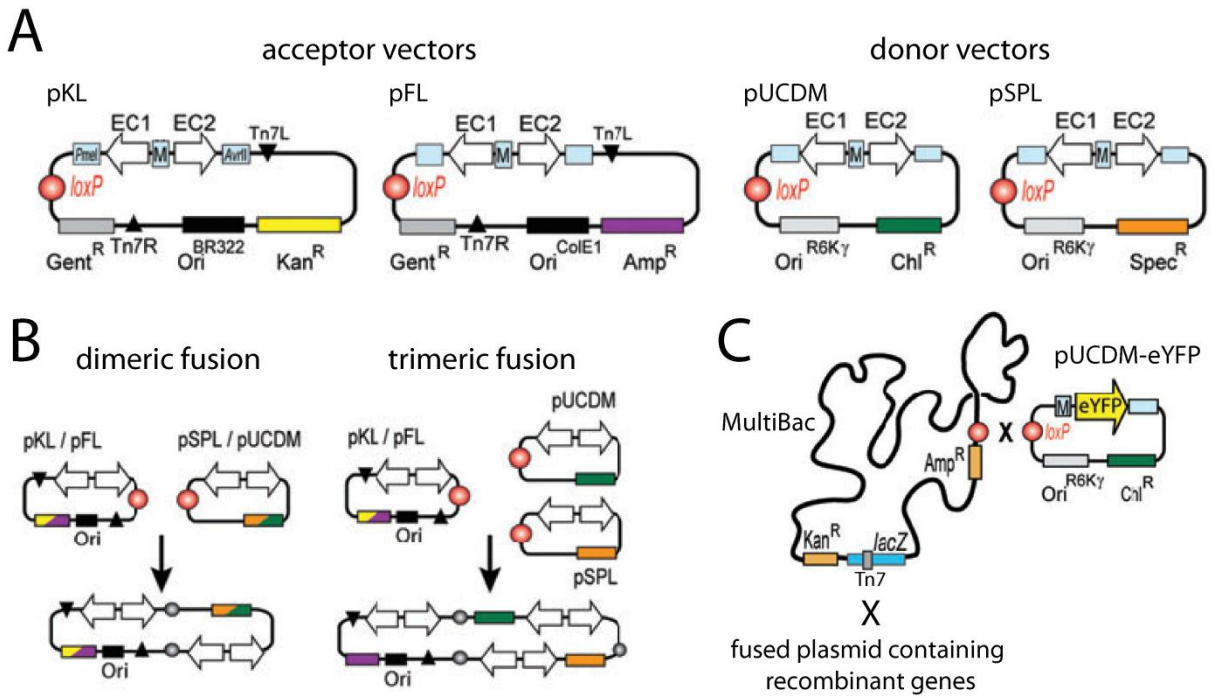

Fig. 5-1: Overview of the MultiBac system

A) All transfer vectors contain two strong baculo viral promoter sequences (polh, p10) followed by multiple cloning sites (expression cassettes EC1, EC2), as well as the LoxP recombination site and different resistance markers (GentR, KanR, AmpR, ChlR, SpecR). Only the acceptor vectors pKL and pFL contain Tn7 transposon elements required for the integration into the bacmid (see below). B) The transfer vectors can be fused using the Cre-Lox system and the resulting fusion plasmids can be selected by the respective combinations of antibiotics. C) Schematic presentation of the modified baculoviral genome (bacmid) containing resistance markers, a LoxP recombination site into which a plasmid containing the eYFP gene is integrated, and Tn7 transposition sequences. Since the latter are part of the lacZ gene encoding the enzyme β-galactosidase, integration of fusion plasmids into the bacmid via Tn7 transposition can be monitored by blue/white colony screening. Modified from Fitzgerald et al., 2006.

Briefly, this system employs a four step strategy to generate the recombinant viruses (Fig. 5-1). First, the genes of interest are inserted by standard cloning techniques into one of four transfer vectors (pSPL, pUCDM, pFL, pKL) under control of a strong viral promoter. Second, the plasmids are fused *in vitro* by site specific recombination at LoxP sites using the enzyme Cre-recombinase to combine different genes on one plasmid. Third, the fused plasmid is integrated *in vivo* into a modified viral genome (bacmid) via Tn7 transposition sites present in pFL and pKL vectors. This is achieved by transformation of the respective plasmid into the *E. coli* strain DH10MultiBac-eYFP, which carries the bacmid and a helper plasmid pMON7124 encoding the DNA recombinase Tn7 transposase (see Bac-to-Bac® Baculovirus Expression

System manual; Invitrogen). Finally, the recombinant bacmid is isolated from the *E. coli* cells and transfected into SF21 insect cells, which subsequently produce recombinant baculo viruses. After amplification of the virus stock, the viruses are used to infect cultures of SF21 cells resulting in expression of the recombinant proteins in insect cells. To monitor transfection and infection of insect cells, the bacmid contains in addition the gene encoding a fluorescent protein (eYFP).

5.2.1.1 SF21 insect cell culture

Maintenance cultures of SF21 insect cells were cultivated in suspension in Sf900 II SFM medium (life technologies) at 27°C on an orbital shaker (Heidolph Unimax 2010, 100 rpm) and diluted daily to a density of 0.5 x 10^6 cells per ml.
For long term storage, aliquots of 60 x 10^6 cells were harvested by centrifugation (130 x g, 10 min, RT), resuspended in 1 ml Sf900 II SFM medium supplemented with 30% foetal calf serum (FCS) and 10% sterile DMSO and rapidly frozen in cold (-20°C) isopropanol. After 24h at -20°C, the cells are either stored at -80°C (up to several months) or in liquid nitrogen (long term storage).

5.2.1.2 Combination of genes and integration into the viral genome

The coding regions of yeast NOC1, NOC2 and RRP5 (or truncated versions thereof) were amplified by PCR and inserted by standard cloning techniques (section 5.2.4.14) into the plasmids pUCDM, pFL, pSPL or derivatives thereof. PCR primers and resulting plasmids are listed in sections 5.1.5 and 5.1.4, respectively. Fusion plasmids containing combinations of genes were obtained by *in vitro* Cre-Lox recombination (section 5.2.4.12) of the respective plasmids. The fusion plasmids were transformed into *E. coli* DH10-MultiBac-eYFP cells (section 5.2.3.4) to integrate the plasmids into the viral genome. After blue/white colony screening on LB+Amp+Tetra+Genta+IPTG+X-GAL plates, the recombinant bacmids were isolated (section 5.2.3.7) and transfected into SF21 cells (section 5.2.1.3).

5.2.1.3 Transfection of SF21 insect cells

To 20 µl of bacmid DNA solution (section 5.2.3.7), 300 µl of Sf900 II SFM medium (life technologies) and 10 µl of FuGene transfection reagent (Promega) were added, carefully mixed by stirring and incubated for 30 min at RT. For each bacmid to be transfected, 1x10^6 SF21 cells were seeded in each of two wells of a 6-well plate and incubated for 30 min to let cells adhere to the bottom. The supernatant was removed and 3 ml of fresh Sf900 II SFM medium was added to each well, followed by addition of 160 µl of the bacmid/medium/FuGene mix to each well. Cells were incubated at 27°C and transfection was monitored by fluorescence microscopy. After 48 – 60 h the supernatant containing the recombinant baculo viruses (V0 stock) was harvested and stored at 4°C in the dark.

5.2.1.4 Amplification of recombinant baculo viruses

Recombinant baculo viruses were amplified by infecting 50 ml SF21 cultures (0.5x10^6 cells/ml) with 50-200 µl of the V0 stock (section 5.2.1.3) followed by incubation at 27°C with shaking (100 rpm). Cell density was monitored daily at the same time, and as long cells were doubling, cultures were diluted to 50 ml of 0.5x10^6 cells/ml. After growths arrest (< 1x 10^6 cells/ml when counted), cultures were incubated another 24 h at 27°C. Cells were pelleted (130x g, 10 min, RT) and the supernatant containing the amplified virus (V1 stock) was stored at 4°C in the dark. Infection of the cells was monitored by fluorescence microscopy. The volume of V0 stock used for virus amplification was adjusted to achieve growth arrest after 2 - 4 days.

5.2.1.5 Expression of recombinant proteins in SF21 insect cells

200 ml SF21 cell culture (1 x 10^6 cells/ml) in 1 l Erlmeyer flasks were infected with 5 ml of V1 virus (section 5.2.1.4) and incubated for 48h at 27°C resulting in a cell density ~ 0.9-1.2 x 10^6 cells/ml. Infection of the cells was monitored by fluorescence microscopy. Cells were harvested in aliquots of 50 x 10^6 cells. After centrifugation (130x g, 10 min, room temperature), cell pellets were flash frozen in liquid nitrogen and stored at -20°C.

5.2.2 Work with *Saccharomyces cerevisiae*

5.2.2.1 Cultivation of yeast strains

Strains of the yeast *Saccharomyces cerevisiae* were cultivated using standard microbiological methods (Amberg et al., 2005). Liquid cultures were grown in the appropriate medium (section 5.1.7) usually at 30°C, except for temperature-sensitive mutants (24°C) or for temperature-shift experiments (24°C, 37°C). Cell growth was monitored by measuring the optical density at 600 nm (OD600). For cultivation on solid agar plates containing the appropriate medium, single colonies or small aliquots of glycerol stocks were streaked out using sterile disposable inoculation loops in order to obtain colonies derived from single yeast cells. Plates were incubated upside down at the respective temperatures for 1-5 days. Short-term storage of yeast strains was accomplished by keeping the agar plates at 4°C.

5.2.2.2 Preparation of competent yeast cells

50 ml of a exponentially growing yeast culture (OD600 ~ 0.5-0.7) were harvested by centrifugation for 5 min at 4000 rpm and RT. Cells were washed with 25 ml sterile H_2O and 5 ml LitSorb before resuspending in 360 µl LitSorb. 40 µl of Salmon Sperm DNA, which were incubated for 5 min at 99°C and immediately chilled on ice, were added to the cell suspension. After mixing, 50 µl aliquots were transferred to 0.5 ml tubes and stored at -80°C.

5.2.2.3 Transformation of competent yeast cells

An aliquot of competent yeast cells (section 5.2.2.2) was thawed on ice. DNA to be transformed (100 ng of plasmid DNA or 5-10 µg of linear DNA for integration into the genome) was added and the sample was mixed. After addition of six volumes of LitPEG, the suspension was mixed thoroughly and incubated for 30 min at RT on a turning wheel. Sterile DMSO was added to the sample (1/9 of the total volume), followed incubation at 42°C for 15 min and centrifugation for 1 min at 3000 rpm and RT. When selecting for auxotrophic markers (*e.g. TRP1*, *LEU2*, *URA3*), the cell pellet was directly resuspended in 100 µl sterile H_2O and plated on SCD- or SCG-plates lacking the corresponding amino acid. If selection for antibiotic resistance (*e.g.* geneticin, hygromycin B) was required, the cell pellet was resuspended in 5 ml YPD or YPG and incubated for 2-3 generation times at 30°C (24°C for temperature sensitive strains) while shaking to allow the expression of the marker before plating on the respective selection media (section 5.1.7). Since selection for antibiotic resistance often results in a high number of transient transformants, these plates were replica-plated on fresh selection media to identify positive clones.

5.2.2.4 Generation of strains expressing affinity tag fusion proteins

Yeast strains expressing endogenously encoded hemagglutinin (HA), Myc, GFP, Protein A or tandem affinity purification (TAP) tag fusion proteins were constructed by transformation of PCR based (section 5.2.4.6) tagging cassettes and homologous recombination as described (Puig et al., 2001, Knop et al., 1999), using different auxotrophy or resistance markers for selection. The plasmids and oligonucleotides used are listed in section 5.1.4 and 5.1.5, respectively. Resulting strains are listed in section 5.1.1.

5.2.2.5 Yeast plasmid shuffle

The plasmid shuffle (Sikorski and Boeke, 1991) yeast strain TY772 (NOC1-shuffle) was used to test if truncated *noc1-ΔX* alleles can complement the essential function of *NOC1*. In this strain, the chromosomal copy of *NOC1* is knocked out with the *HIS3* marker gene and the deletion is complemented by a wild-type copy of *NOC1* on a plasmid containing the counter-selectable *URA3* auxotrophy marker. The mutant alleles were introduced on another plasmid (V17) carrying a different selection marker (*LEU2*), and the cells were cultivated on SCD-Leu plates at 24°C. If the mutant allele is able to complement the chromosomal deletion, the plasmid containing the wild-type copy can be lost during cultivation. To select for clones which have lost the wild type plasmid, single colonies were streaked on SCD-Leu plates containing 5-FOA (5-Fluoro-orotic acid), which facilitates counter selection against cells carrying a functional *URA3* gene. *URA3* encodes the enzyme orotidin-5'-phosphate decarboxylase of the uracil-biosynthesis pathway which also converts 5-FOA into the toxic 5-fluorouracil (Boeke et al., 1984, 1987). Resulting clones were controlled for (i) the presence of the mutant vector, (ii) the loss of the wild-type plasmid and (iii) the maintenance of the chromosomal deletion via the respective auxotrophic markers. Single clones were further cultivated on YPD plates to obtain the mutant strains listed in section 5.1.1.
Plasmid shuffling was also applied to generate strains that express *RRP5*, *NOC1* and *NOC2* under control of the galactose inducible, glucose repressible *GAL1/10* promoter (pGAL). To this end, the plasmid shuffle yeast strains TY616 (RRP5-shuffle), TY772 (NOC1-shuffle) and TY773 (NOC2-shuffle) were transformed with plasmids K1517 (pGAL-*RRP5*; *TRP1*), K37 (pGAL-*NOC1*; *TRP1*) or K11 (pGAL-*NOC2*; *TRP1*), respectively, grown on SGC-trp plates and followed by counter selection on 5-FOA containing SGC-trp plates. Single clones were controlled for (i) the presence of the mutant vector, (ii) the loss of the wild-type plasmid and (iii) the maintenance of the chromosomal deletion via the respective auxotrophic markers, as well as for galactose dependent cell growth. Single clones were further cultivated on YPG plates to obtain the mutant strains listed in section 5.1.1.
A modified plasmid shuffling protocol was applied to generate strains depending on chromosomally encoded temperature sensitive *noc1* alleles. To this end, *noc1* alleles were amplified from the respective plasmids by PCR (section 5.2.4.6) using primers that introduce flanking sequences (~ 50 nucleotides) homologous to the chromosomal regions upstream and downstream of the START and STOP codon of *NOC1*. The purified PCR products were transformed into TY772 (section 5.2.2.3) followed by incubation in SCD liquid medium at 24°C for at least 3 generation times (or over night) to allow homologous recombination of the PCR product into the endogenous *NOC1* locus and loss of the wild type plasmid. For counter selection, cells were subsequently grown on 5-FOA containing SCD plates at 24°C. Single clones were controlled for (i) the loss of the wild-type plasmid and (ii) the loss of the chromosomal deletion via the respective auxotrophic markers, and (iii) temperature sensitive growth. Single clones were further cultivated on YPD plates at 24°C to obtain the mutant strains listed in section 5.1.1.

5.2.2.6 Spot test analysis of yeast strains

Overnight cultures of the yeast strains to be tested were diluted to OD600 = 0.1 with sterile H_2O. 7-10 µl of this cell suspension and of serial 1:10, 1:100, 1:1,000 and 1:10,000 dilutions in sterile H_2O were spotted on the appropriate test plates (section 5.1.7). Growth phenotypes were monitored after incubation for 2-4 days at 16°C, 24°C, 30°C, and 37°C, respectively.

5.2.2.7 Growth kinetic analysis of yeast strains

Cultures of the yeast strains to be tested were grown to stationary phase overnight. From these pre-cultures fresh cultures were inoculated to OD600 = 0.1 in the appropriate medium (section 5.1.7) and growth at the desired temperature was monitored by measuring the OD600 mostly in 1 h intervals. Since the strains were always kept in the exponential growth phase (OD600 ~ 0.1-0.7) by dilution with the respective medium, the dilution factor had to be taken into account for the calculation of the growth kinetics.

5.2.2.8 Long-term storage of yeast strains

2 ml of an overnight culture of the yeast strain to be stored were mixed with 1 ml sterile 50% (v/v) glycerol and separated into two aliquots. Glycerol stocks were stored at -80°C.

5.2.2.9 Crosslinking of yeast cells with formaldehyde

Exponentially growing cells from 45 ml liquid culture were crosslinked by adding 1.25 ml 37% (v/v) formaldehyde and subsequent incubation for additional 15 min at the respective growth temperature while shaking. Crosslinking was quenched by adding 2.5 ml 2.5 M glycine. The culture was further incubated at growth temperature for additional 5 min. Cells were harvested by centrifugation in a 50 ml tube for 3 min at 3000 rpm and 4°C. The cell pellet was washed with cold water, transferred to a 1.5 ml tube, and frozen in liquid nitrogen before storage at -20°C.

5.2.3 Work with *Escherichia coli*

5.2.3.1 Cultivation of bacterial strains

Liquid cultures were grown in LB medium supplemented with the required antibiotics (section 5.1.7) at 37°C. Cell growth was monitored by measuring the optical density at 600 nm (OD600). For cultivation on solid agar plates containing LB medium and the required antibiotics, single colonies or small aliquots of glycerol stocks were streaked out using sterile disposable inoculation loops in order to obtain colonies derived from single bacterial cells. Plates were incubated upside down at 37°C for 1 day. Short-term storage of bacterial strains was accomplished by keeping the agar plates at 4°C.

5.2.3.2 Preparation of electrocompetent bacterial cells

In general, the *E. coli* strain XL1-Blue was used as a host for amplification of plasmid DNA, except for derivatives of pUCDM (K1127) or pSPL (K1129), which were propagated in the BW23473 strain, as these plasmids contain a replication origin derived from R6Kγ and hence require a host expressing the *pir* gene for propagation (Metcalf et al., 1994).
In order to increase the efficiency of plasmid DNA uptake, competent cells for electroporation were prepared. Cells were grown in 400 ml SOB medium (section 5.1.7) at 37°C to mid-log phase (OD600 ~ 0.35-0.6), chilled on ice for 15 min, and centrifuged for 10 min at 6000 rpm and 4°C. To reduce the ionic strength of the cell suspension, cells were washed three times with cold sterile H_2O and once with sterile 10% (v/v) glycerol. After resuspending the cells in 1.5 ml sterile 10% (v/v) glycerol, 50 µl aliquots were transferred to 1.5 ml tubes and stored at -80°C.

5.2.3.3 Transformation of competent bacterial cells by electroporation

An aliquot of electrocompetent bacterial cells (section 5.2.3.2) was thawed on ice. DNA to be transformed (1 ng of plasmid DNA or 2 µl of a ligation sample) was added and the sample was mixed. After pipetting the suspension into a cold 0.2 cm electroporation cuvette, pulsing was performed with program EC2 in a MicroPulser electroporation apparatus. Immediately

after the pulse, 1 ml LB medium (section 5.1.7) was added and the sample was transferred to a 1.5 ml tube following incubation for 30-60 min at 37°C. 100 µl of the cell suspension were plated on LB supplemented with the required antibiotics and incubated overnight at 37°C. The residual cells were centrifuged for 1 min at 5000 rpm and RT. About 900 µl of the supernatant were discarded and the pellet was resuspended in the remaining liquid, plated as above, and incubated overnight at 37°C.

5.2.3.4 Preparation of chemocompetent bacterial cells

200 ml SOB medium (section 5.1.7) were inoculated from a stationary *E. coli* culture to an OD 600 = 0.2 and incubated at 37°C to a final OD600 ~ 0.5 – 0.6. Cells were harvested in 50 ml Falcon tubes by centrifugation (4500 rpm, 10 min, 4°C). Each cell pellet was resuspended in 15 ml cold Tfb-I buffer, incubated on ice for 20 min and centrifuged as above. The cell pellets were resuspended and combined in a total volume of 4 ml cold Tfb-II buffer and incubated on ice for 20 min. 100 µl aliquots of the cell suspension were stored at – 80°C.

5.2.3.5 Transformation of chemocompetent bacterial cells by heat shock

An aliquot of chemocompetent bacterial cells (section 5.2.3.4) was thawed on ice. DNA to be transformed (10 - 100 ng of plasmid DNA) was added the sample was mixed and incubated on ice for 5 min. After a heat shock step (42°C, 40 sec), the samples was incubated on ice for another 3 min. Subsequently, 1 ml LB medium (section 5.1.7) was added and the sample was incubated for 30-60 min at 37°C in case of transformation of XL1-Blue or BW23473 cells. When *E. coli* strain DH10MultiBac-eYFP was transformed to integrate plasmids carrying yeast genes in the baculoviral genome (bacmid) (section 5.2.1.2), cells were incubated at 37°C for 8 h or overnight. 100 µl of the cell suspension were plated on LB supplemented with the required antibiotics and incubated overnight at 37°C. The residual cells were centrifuged for 1 min at 5000 rpm and RT. About 900 µl of the supernatant were discarded and the pellet was resuspended in the remaining liquid, plated as above and incubated overnight at 37°C. For blue/white colony screening of transformed DH10MultiBac-eYFP cells, the plates were in addition supplemented with IPTG and X-GAL. Single clones were restreaked on LB-plates containing the required antibiotics, IPTG and X-GAL to assure correct integration of the transformed plasmid into the bacmid.

5.2.3.6 Purification of plasmid DNA from *E. coli* (mini-preparation)

Plasmid DNA was isolated from 3-5 ml *E. coli* cultures with the peqGOLD Plasmid Miniprep Kit (Peqlab) according to the manufacturer's instructions. Briefly, cells were lysed, and plasmid DNA was isolated from the lysate by DNA trapping on a matrix. The plasmid DNA was further washed with an alcohol-based solution, and eluted from the matrix with sterile water.

5.2.3.7 Bacmid preparation from *E. coli*

Recombinant bacmids containing (combinations of) yeast genes were isolated from DH10MultiBac-eYFP cells transformed with the respective plasmids after blue/white colony screening (section 5.2.3.5). To this end, 4 ml LB medium containing Tetracyclin (10 µg/ml), Gentamycin (10 µg/ml) and Ampicillin (100 µg/ml) were inoculated with a single colony and incubated at 37°C overnight. 3 ml of cell culture were harvested in 15 ml Falcon tubes by centrifugation (4500 rpm, 5 min, RT). For cell lysis, solutions 1, 2 and 3 of the peqGOLD Plasmid Miniprep Kit (Peqlab) were used. The cell pellet was resuspended in 300 µl of Solution 1 and transferred to a 1.5 ml reaction tube. To lyse the cells, 300 µl of Solution 2 were added, the tube was carefully inverted and the sample was incubated for 3 min at RT. After addition of 300 µl Solution 3, the tube was carefully inverted and cell debris was

removed by centrifugation (13000 rpm, 10 min, RT). The supernatant was transferred in a new reaction tube and centrifuged again (13000 rpm, 5 min, RT). The supernatant (~700 – 750 µl) was transferred in a new reaction tube and 700 µl isopropanol were added, followed by centrifugation (13000 rpm, 10 min, RT) to precipitate the DNA. The supernatant was discarded and the DNA pellet was washed once with 200 µl cold 70% EtOH. After centrifugation (13000 rpm, 5 min, 4°C), the supernatant was completely removed and the pellet air dried for ~ 15 - 30 min in the sterile hood. Finally, the bacmid DNA was dissolved in 30 µl sterile H2O by gentle stirring.

5.2.3.8 Long-term storage of *E. coli* strains containing recombinant bacmids

1 ml of the overnight culture used for bacmid isolation (section 5.2.3.7) was mixed with 0.5 ml sterile 50% (v/v) glycerol and stored at -80°C.

5.2.4 Work with DNA

5.2.4.1 Native agarose gel electrophoresis

Native agarose gel electrophoresis was used to separate DNA fragments. Depending on the fragment size, electrophoresis was performed with gels composed of 0.8%, 1% or 1.2% (w/v) agarose and 0.5x TBE buffer (section 5.1.7) and containing 0.1 µg/ml ethidium bromide. 0.5x TBE was used as electrophoresis buffer and gels were run at 100-150 V. For length determination, 0.5 µg of a DNA standard (1 kb ladder or 100 bp ladder) was used in a concentration of 50 µg/ml in 1x DNA loading buffer. DNA fragments were visualized by exposing the gel to UV light (254 nm).

5.2.4.2 Purification of DNA fragments from agarose gel

DNA fragments of interest were cut out from agarose gels (section 5.2.4.1) and eluted using the QIAEX II gel extraction kit (Qiagen) following the instructions provided by the manufacturer.

5.2.4.3 Phenol-chloroform extraction

The same volume of a phenol:chloroform:isoamyl alcohol-mixture (25:24:1; Roth) was added to the sample. The samples were mixed by vortexing for two times 20 sec. After centrifugation for 5 min at 13000 rpm and RT, an aliquot of the upper, aqueous phase was transferred to a 1.5 ml tube.

5.2.4.4 Ethanol precipitation of DNA

If samples did not yet contain at least 0.25M salt, an equal volume of IRN buffer (section 5.1.7) was added to the sample. DNA was precipitated by addition of 2.5 volumes of 100% ethanol; to precipitate small amounts of DNA, glycogen (5µl of 20mg/ml stock solution) was supplemented. Samples were kept at -20°C for at least 1 hour. DNA was pelleted at 13000 rpm for 20 minutes at 4°C. To remove excess salt, the pellet was washed with ice-cold 70% ethanol. The supernatant was discarded, the pellet air-dried and dissolved in TE or water.

5.2.4.5 DNA quantification using UV spectroscopy

Concentration of pure DNA samples was measured by UV spectroscopy at 260 nm (1 OD260 = 50 µg/ml) using a NanoDrop ND-1000 spectrophotometer. To determine contamination with proteins, absorbance was concomitantly measured at 280 nm. The ratio of OD260/OD280 of pure DNA is between 1.8 and 2.0.

5.2.4.6 Polymerase Chain Reaction (PCR)

The annealing temperatures for all primers used in PCR (section 5.1.5) were estimated with the program 'calc11' (http://www.promega.com/techserv/tools/biomath/calc11.htm).
DNA fragments for integration in the yeast genome were amplified using GoTaq polymerase (Biorad) in 100µl reactions (50-100 ng template plasmid DNA, 0.5 µM of reverse and forward primers, 0.2 mM each dNTP, 5 U GoTaq). To account for the long integration primers that have only short hybridization sequences on the template plasmids, two-stage PCRs were performed. Annealing temperatures and amplification times were individually adjusted according to the manufacturer's manual. A typical PCR program was 1 cycle 95°C for 3 min, 10 cycles 95°C for 30 sec, 46°C for 30 sec, 72°C for 2.5 min, 25 cycles 95°C for 30 sec, 65°C for 30 sec, 72°C for 2.5 min, 1 cycle 72°C for 7 min.
For amplification of DNA fragments used for cloning, proofreading PCR was performed using Herculase II fusion polymerase (Agilent) with yeast genomic DNA (~ 500 ng) or plasmid DNA (~ 50 ng) as templates in 50µl reactions (0.25 µM of reverse and forward primers, 0.25 mM each dNTP). Annealing temperatures and amplification times were individually adjusted according to the manufacturer's manual.
Mutant *rrp5* or *noc1* alleles with deletions of 5' or 3' sequences were generated using primers that introduce a new START or STOP codon, respectively. Mutant *noc1* alleles with deletions of internal sequences were generated by spliced overlap extension PCR (SOE-PCR; Ho et al., 1989). Briefly, the respective 5' and 3' parts of the gene were initially amplified by separate PCRs. The primers were designed in way that the reverse primer of the 5' fragment overlaps with the 5' end of the 3' fragment, and vice versa for the forward primer of the 3' fragment. The resulting PCR products were purified (see below) and employed as templates in a new PCR using the forward primer of the 5' fragment and the reverse primer of the 3' fragment to generate the internal deletion construct.
5% of each PCR was analysed by agarose gel electrophoresis (section 5.2.4.1) and subsequently purified with Qiaquick PCR purification kit (Qiagen) according to the manufacturer or precipitated with ethanol (section 5.2.4.4) for cloning or integration, respectively.

5.2.4.7 Quantitative real-time Polymerase Chain Reaction (qPCR)

Quantitative real-time PCR was used to measure amounts a specific DNA fragment with high accuracy. The amount of DNA present at the end of each single PCR cycle was detected by measuring the fluorescence of SYBR Green. SYBR Green is a dye that exhibits fluorescence when bound to double-stranded DNA, but not in solution. Therefore, the intensity of the fluorescence signal allows direct measurement of the actual amount of DNA present in the sample. Quantitative real-time PCR reactions were performed in 0.1 ml tubes, the reaction volume was 20 µl. The reaction contained 4 µl of DNA sample and 16 µl of master mix. The master mix contained 4 pmol of both the forward and the reverse primer, 0.25 µl of a 1:400000 SYBR Green stock solution in DMSO, 0.4 U HotStarTaq DNA Polymerase and a premix. The premix was composed of $MgCl_2$ (final concentration in the reaction: 2.5 mM), dNTPs (final concentration in the reaction: 0.2 mM) and 10x PCR buffer (Quiagen) (final concentration in the reaction: 1x). Quantitative real-time PCR was performed in a Rotor-Gene 3000 machine. The data were analysed with Rotor-Gene V6000.

5.2.4.8 Adenylation of PCR products

Proofreading polymerases yield blunt ended PCR products. However, for subsequent ligation into the pGEMT easy vector system (Promega), a 3' A overhang is required, which can be introduced by Taq Polymerase. To this end, ethanol precipitated (section 5.2.4.4) PCR

product was incubated in a 30 µl reaction containing 0.25 mM dATP, 1x Thermo-Pol buffer (NEB) and 2.5 U Taq polymerase (NEB) for 5 min at 72°C. The adenylated PCR product was subsequently purified using the QIAquick PCR Purification Kit (Quiagen) according to the manual.

5.2.4.9 Digestion of DNA with restriction endonucleases

A variety of restriction endonucleases were used to digest DNA in order to prepare defined DNA fragments for cloning or to check for presence and correct orientation of inserted DNA fragments. Restriction endonucleases were used as suggested by the manufacturer. After digestion, the DNA fragments were separated on agarose gels (5.2.4.1) and for cloning the desired fragment was purified from the gel (section 5.2.4.2).

5.2.4.10 Dephosphorylation of DNA fragments

Religation of the target plasmid can interfere with efficient ligation of the desired insert DNA into the plasmid. This problem can be minimized by dephosphorylation of the plasmid DNA after restriction enzyme digest. Digested plasmid DNA (section 5.2.4.2) was incubated in 1x Antarctic phosphatase buffer (NEB) with 5 U Antarctic phosphatase at 37°C for 1 h, followed by incubation at 65°C for 5 min to inactivate the enzyme. The dephosphorylated plasmid DNA was directly used for ligation reactions without further purification.

5.2.4.11 DNA ligation + pGEMT vector

In order to clone DNA sequences into yeast/bacterial plasmids, the quantity of purified DNA fragments digested with restriction endonucleases was measured by UV spectroscopy (section 5.2.4.5). A fivefold molar excess of insert DNA compared to the plasmid DNA fragment was incubated in a 20 µl ligation reaction using 400 U T4 DNA ligase (NEB) for 2 h at RT or overnight at 16°C. 2 µl of the ligation reaction were used for transformation of competent bacterial cells (section 5.2.3.3).
Cloning of adenylated PCR products into the pGEMT vector system (Promega) was done according to the manual using a 3:1 molar excess of insert to vector DNA.

5.2.4.12 *in vitro* cre-fusion of plasmids

Plasmids containing the LoxP recombination site can be fused by site specific recombination using the enzyme cre-recombinase (Sternberg and Hamilton, 1981; Liu et al., 1998). Therefore, equimolar amounts of plasmids (~200 ng of the smaller plasmids) were incubated in a total of 10 µl in 1x cre recombination buffer (NEB) with 1 U Cre recombinase (NEB) for 15 - 30 min at 37°C. Plasmid amounts and incubation times were adjusted to prevent multi plasmid fusions. After inactivation of the enzyme (10 min, 70°C), 2 µl of the reaction were transformed into electrocompetent *E. coli* cells (section 5.2.3.3) and selected on LB plates containing the required antibiotics. Plasmids were isolated from the resulting colonies (section 5.2.3.6) and analysed by restriction enzyme digestion (5.2.4.9).

5.2.4.13 DNA sequencing and oligonucleotide synthesis

DNA sequencing was performed by GENEART/Life technologies and the service of primer synthesis was provided by Eurofins MWG Operon. Oligonucleotides used in this work are listed in section 5.1.5.

5.2.4.14 Plasmid construction

To generate plasmids encoding yeast genes for the expression in *S. cerevisiae* or for the integration into baculo viral genomes (5.2.1), the respective genes were amplified by PCR (section 5.2.4.6) from yeast genomic DNA or from plasmid DNA using primers that introduce recognition sites for restriction endonucleases. The purified PCR products were digested with

the respective enzymes (section 5.2.4.9) and ligated into the target vector (section 5.2.4.11), which was digested with the same enzymes and dephosphorylated (section 5.2.4.10) to prevent plasmid relegation. Alternatively, the PCR products were adenylated (section 5.2.4.8) and ligated into the pGEMT easy vector. Plasmids isolated from single colonies (section 5.2.3.6) obtained from *E. coli* cells transformed (section 5.2.3.3) with the ligation reaction were analysed by restriction enzyme digest. Resulting candidate plasmids were verified by DNA sequencing (section 5.2.4.13). If applicable, the genes were subcloned from the pGEMT vector into the target plasmids. Plasmids generated in this work are listed in section 5.1.4.

5.2.5 Work with RNA

5.2.5.1 RNA extraction

RNA extractions were essentially performed as described previously (Schmitt et al., 1990). Samples from which RNA should be extracted (cell pellets, aliquots of cell lysates, affinity purified material) were resuspended or diluted in 500 µl AE buffer (section 5.1.7) and mixed with 500 µl phenol equilibrated in AE buffer and 50 µl of 10% (w/v) SDS. The samples were incubated in a thermomixer for 7 min at 1400 rpm and 65°C and afterwards chilled on ice for 3 min. After centrifugation for 2 min at 13000 rpm and RT, 3x 150 µl of the aqueous phase was collected and mixed with 500 µl phenol equilibrated in AE buffer by vortexing. The samples were again centrifuged and 3x 120 µl of the supernatant were mixed with 500 µl chloroform by vortexing. Phases were separated by centrifugation and the RNA in 3x 100 µl of the supernatant was precipitated by addition of 750 µl NaOAc-EtOH mix (composed of 1 volume 3 M NaOAc pH 5.3 and 25 volumes of ethanol) and incubation for at least 30 min at -20°C. In case that RNA should subsequently be analysed in different gel systems, the sample was split in appropriate ratios (usually 1/3 for acryl amide, 2/3 for agarose gels) prior to incubation at -20°C. The precipitated RNA was dissolved in MOPS (for agarose gels) and TBE (for acryl amide gels) based solubilisation buffer (section 5.1.7), respectively, denatured by incubation for 15 min at 65°C, and stored at -20°C.

5.2.5.2 Denaturing agarose gel electrophoresis of high molecular weight RNA

Denaturing agarose gel electrophoresis was used to separate RNA species longer than 1000 bases. In this work electrophoresis was routinely performed with gels composed of 1.2% (w/v) agarose, 2% (v/v) formaldehyde, and 1x MOPS buffer (section 5.1.7) containing 0.5 µg/ml ethidium bromide. The electrophoresis buffer was composed of 1x MOPS buffer and 2% (v/v) formaldehyde. Gels were run for 14-16 h at 40 V.

5.2.5.3 Denaturing acryl amide gel electrophoresis of low molecular weight RNA

Denaturing acryl amide gel electrophoresis was used to separate RNA species between 100 and 500 bases. In this work electrophoresis was routinely performed with gels composed of 6% (w/v) acryl amide (acryl amide: bis-acryl amide 37.5:1), 7 M urea and 0.5x TBE (section 5.1.7). The electrophoresis buffer was 0.5x TBE. Gels were run for 75 – 90 min at 150 V.

5.2.5.4 Northern Blotting (Vacuum transfer)

RNAs separated on agarose gels (section 5.2.5.2) were transferred and immobilised on positively charged membranes (Positive™ MPBiomedicals) using different methods (see also section 5.2.4.5). In either case, the RNAs were cross-linked to the membranes by 1 min exposition to UV light (254/312 nm). Vacuum transfer was used for nonradioactive RNA samples. Prior to transfer, the agarose gels were washed once for 5 min in milli-Q water, once 20 min in 0.05 M NaOH to partially hydrolyse the RNAs and facilitate the transfer of

larger RNAs, and were further equilibrated 20 min in 10xSSC (section 5.1.7). The RNAs were transferred from the gel onto the positively charged membrane (Positive™ MP-Biomedicals) applying a vacuum of 5 bar for 90 min using a vacuum blotter (Biorad).

5.2.5.5 Northern Blotting (Passive capillary transfer)

Passive capillary transfer was used for tritium labelled RNA samples (section 5.2.5.9). Prior to transfer, agarose gels were treated as described in section 5.2.5.4. Transfer of the RNAs from the agarose gel to the membrane was then achieved over-night by drawing the transfer buffer (10xSSC) from the reservoir upward through the gel into a stack of pumping paper. The RNAs were eluted from the gel and deposited onto the positively charged membrane with the help of the buffer stream.

5.2.5.6 Northern Blot (electro transfer)

RNAs separated on acryl amide gels (section 5.2.5.3) were transferred and immobilised on positively charged membranes (Positive™ MPBiomedicals) by electro transfer. Prior to transfer, the gels were stained with 0.5 µg/ml ethidium bromide solution in 0.5x TBE (section 5.1.7) for 15 min. The RNAs were transferred from the gel onto the positively charged membrane in 0.5x TBE using a wet tank blotting apparatus (Biorad) and applying a voltage of 50 V for 90 min. Subsequently, the RNAs were cross-linked to the dried membrane by 1 min exposition to UV light (254/312nm).

5.2.5.7 Radioactive probe labelling and detection

Different RNA species immobilised on solid supports can be detected using specific DNA probes. Probes used in this work are listed in section 5.1.5. 5' ends of all oligo-probes were labelled with ^{32}P. 100 pmol of oligo-probe were incubated with 50 mCi of γ-^{32}P-ATP (Hartmann Analytik), in 1x PNK buffer (NEB) and 10 U of T4 polynucleotide kinase (NEB) in a total volume of 15 µl for 30 - 45 min at 37°C. Reactions were stopped by addition of 1ml of 0.5M EDTA pH 8. After addition of 50 µl H_2O, labelled probes were purified from non-incorporated nucleotides using a size exclusion column (Spin6-Biorad). Incorporated radioactivity was estimated by counting 1 µl of purified labelled probes using a scintillation counter (1600TR-Packard). Membranes carrying the RNAs to be isolated (sections 5.2.5.4, 5.2.5.6) were pre-hybridised at least 1 h at 30°C in RNA hybridisation buffer (section 5.1.7). Membranes were then incubated at 30°C over night after addition of 1-2x10^6 cpm of radiolabelled probe per blot. The membranes were washed twice 15 min in 2x SSC at 30°C. Signals were acquired exposing the membrane to a Phosphoimager screen (Fujifilm). Screens were read out with the FLA-3000 phosphor imager (Fujifilm) and data were analysed with the Multigauge V3.0 software (Fujifilm).

5.2.5.8 Primer extension analysis (PEX)

Primer extension analyses employ a reverse transcription reaction to determine the 5' end of RNA molecules. Reactions were performed essentially as described (Venema et al., 1998) using 5' ^{32}P-labelled antisense oligonucleotides (section 5.1.5) and RNAs dissolved in TBE based buffer (section 5.2.5.1) and appropriately diluted in H_2O as templates. Normally, RNA amounts according to 0.05-0.1 OD of cells, to cell lysates of 0.1 µg total protein content or to 0.2-0.5 % of precipitated material were used as template in primer extension reactions. 2-5 µl of the diluted RNA sample were incubated with 2 µl of the radiolabelled oligonucleotide (5.2.5.7) in 1x PEX annealing buffer (section 5.1.7) in total volume of 10 µl for 5 min at 80°C to denature the RNA, followed by 90 min incubation at 46°C to anneal the oligonucleotide. After addition of 40 µl 1.25x RT buffer, 20 U rRNasin (Promega) and 100 U M-MLV reverse transcriptase (Invitrogen), reverse transcription was carried out for 40 min at 46°C. The

reaction was stopped and template RNA was degraded by addition of 6 µl 1 M NaOH and 1 µl 0.5 M EDTA (pH 8.0) and incubation at 56°C for 30-60 min. After addition of 6 µl 1 M HCl, 2 µl glycogen (2 mg/ml, Ambion), 30 µl 7.5 M NH_4OAc and 250 µl EtOH, cDNA was precipitated over night at -20°C. After centrifugation (13,000 rpm, 20 min, 4°C) the DNA pellet was washed once with 100 µl cold 70% EtOH, dried at 80°C for 3 min and dissolved in 10 µl 1x PEX loading buffer by incubation at 80°C for 3 min. cDNA was separated on gels containing 6% (w/v) acryl amide (acryl amide: bis-acryl amide 37.5:1), 7 M urea and 1x TBE. The electrophoresis buffer was 1x TBE. Gels were run for 7-8 h at 350 V, dried for 2 h at 80°C and signals were acquired exposing the gel to a Phosphoimager screen (Fujifilm). Screens were read out with the FLA-3000 phosphor imager (Fujifilm) and data were analysed with the Multigauge V3.0 software (Fujifilm).

5.2.5.9 Analysis of neo-synthesised rRNA

Cells were grown overnight in YPDA medium at 24°C, diluted to OD600 ~ 0.1 in fresh YPDA (50 ml) medium and cultivated at 24°C to an OD600 ~ 0.3 - 0.4. Subsequently, cultures were shifted to 37°C. For each sample 1 OD600 of cells was harvested (2000 rpm, 3 min, RT) and resuspended in buffer RD (section 5.1.7). 20 µCi of 5',6'-^{3}H uracil (Perkin Elmer) was added and the cells were incubated at 37°C for 15 min ('pulse'). For the 'chase' samples, one volume of preheated YPDU (containing 2 mg/ml unlabeled uracil) was added and cells were incubated either for additional 15 or 30 min at 37°C. Immediately after the treatment, samples were chilled on ice and centrifuged for 1 min at 13000 rpm and 4°C. The supernatants were discarded and the cell pellets were stored at -20°C. Total RNA was extracted (section 5.2.5.1) and dissolved in MOPS and TBE based buffer, respectively. The incorporated activity was determined using scintillation cocktail (Perkin Elmer) in a scintillation counter (1600TR-Packard) and aliquots of RNA corresponding to same amounts of incorporated activity were separated by denaturing agarose (section 5.2.5.2) or acryl amide (section 5.2.5.2) gel electrophoresis. Subsequently, RNA was transferred to a membrane (Positive TM, MP-Biomedicals) as described (sections 5.2.5.5, 5.2.5.6). To visualize radiolabeled RNA, the membrane was sprayed with a liquid enhancer (EN3HANCE spray surface, Perkin Elmer) and subjected to autoradiography (BioMax MS film, FUJI).

5.2.6 Work with proteins

5.2.6.1 Determination of protein concentration

Protein concentrations were determined using the Bio-Rad Protein Assay which is based on the method by Bradford (Bradford, 1976). Briefly, 1-5 µl of the protein solution to be tested were mixed with 1 ml protein assay dye after diluting the reagent to the working concentration according to the instructions of the manufacturer. The approximate protein concentrations in µg/µl were calculated by dividing the absorbance at 595 nm by the sample volume and multiplying with the factor 23 which was determined using a BSA standard curve.

5.2.6.2 TCA precipitation

The volume of the protein sample to be analyzed was adjusted to 100 µl with cold H_2O prior to mixing with 10 µl cold 100% (w/v) TCA and 2 µl 2% (w/v) DOC (Bensadoun and Weinstein, 1976). After incubation for 30 min at 4°C, the precipitated proteins were pelleted by centrifugation for 15 min at 13000 rpm and 4°C. The supernatant was discarded and the pellet was solubilised in an adequate volume of SDS sample buffer (section 5.1.7). The pH of the sample was neutralized using NH_3 gas, if necessary. Proteins were denatured by incubating the sample for 5 min at 95°C for subsequent separation by SDS-PAGE.

5.2.6.3 Methanol-chloroform precipitation

Protein precipitation for subsequent mass spectrometric analyses was performed using the methanol-chloroform precipitation method (Wessel and Flügge, 1984). The volume of the sample was adjusted to 150 µl with H_2O, followed by the addition of four volumes of methanol (600 µl), one volume of chloroform (150 µl), and three volumes of H_2O (450 µl). After each of these steps the sample was mixed well by vortexing. After incubation for 5 min at 4°C, the sample was centrifuged for 5 min at 13000 rpm and 4°C. The supernatant was discarded without disturbing the interphase which contains the precipitated proteins. Upon addition of another three volumes of methanol (450 µ) and vortexing, the sample was incubated for 5 min at 4°C before centrifugation for 5 min at 13000 rpm and 4°C. The supernatant was completely removed and the protein pellet dried for 10 min in a Speed Vac Concentrator.

5.2.6.4 Denaturing protein extraction

Yeast cell pellets (1-2 OD600) were resuspended in 1 ml cold H_2O, mixed with 150 µl pre-treatment solution (1.85 M NaOH, 1 M β-mercaptoethanol), and incubated for 15 min at 4°C. Proteins were precipitated with 150 µl 55% (w/v) TCA for 15 min at 4°C and pelleted by centrifugation for 10 min at 13000 rpm and 4°C. The supernatant was discarded and the pellet was resuspended in 25 - 50 µl HU buffer (section 5.1.7). The pH of the sample was neutralized using NH_3 gas, if necessary. Proteins were solubilised by incubating the sample for 10 min at 65°C for subsequent separation by SDS-PAGE.

5.2.6.5 SDS-polyacrylamide gel electrophoresis (SDS-PAGE)

Proteins were separated according to their molecular weight using the vertical discontinuous SDS-polyacrylamide gel electrophoresis method by Laemmli (Laemmli, 1970). The discontinuous system used in this work consisted of a lower separating gel composed of 8% or 10% acrylamide, 375 mM Tris-HCl pH 8.8, and 0.1% (w/v) SDS and an upper stacking gel composed of 4% acrylamide, 125 mM Tris-HCl pH 6.8, and 0.1% (w/v) SDS. Gels were run for ~1.5 h at 50 mA and 180 V in 1x electrophoresis buffer. Molecular weights of the different proteins were estimated using protein markers of known molecular weight.

5.2.6.6 Western Blot

Proteins separated by SDS-PAGE (section 5.2.6.5) were transferred to a PVDF or to a nitrocellulose membrane using a Trans-Blot SD Semi-Dry Transfer Cell. The gel and the PVDF membrane, pre-treated with methanol, were placed in the transfer cell between two piles of three blotting papers soaked with transfer buffer (section 5.1.7). In case of transfer to a nitrocellulose membrane, gel and membrane were pre-treated with transfer buffer. Transfer was performed for 1 h at 24 V. To control the blotting of the proteins before immunodetection (section 5.2.6.7), the total protein content was reversibly stained with Poinceau S by incubating the membrane in Poinceau staining solution for 2 min and subsequent destaining with H_2O until the protein bands were visible.

5.2.6.7 Detection of proteins by chemiluminescence or fluorescence

To avoid unspecific binding of the antibodies, the membrane (5.2.6.6) was blocked with non-related proteins from bovine milk prior to specific immunodetection of proteins by incubating the membrane in 5% (w/v) milk powder in 1x PBST on a shaker for 1 h at RT or overnight at 4°C. The antibodies were diluted to an adequate working concentration (section 5.1.9) in 1% (w/v) milk powder in 1x PBST. Incubations were performed in 50 ml tubes on a turning wheel for 1 h (primary antibodies) or 30 min (secondary antibodies) at RT. Following each antibody incubation step, the membrane was washed in 1x PBST for three times 10 min on a shaker.

In order to detect the specifically bound antibodies, the membrane was normally incubated for 1 min at RT with 1 ml BM Chemiluminescence Blotting Substrate (POD; Roche) which was prepared according to the instructions of the manufacturer. This reagent contains hydrogen peroxide and luminal, which is a substrate for the horseradish peroxidase conjugated to the secondary antibodies. The light, which is emitted during this reaction at the corresponding specific positions on the membrane, was detected with a LAS-3000 chemiluminescence imager using Image Reader LAS-3000 V2.2 followed by quantitative analysis using Multi Gauge V3.0 (Fujifilm).
Alternatively, a secondary antibody coupled to a fluorophor (LICOR, 926-32211) was used to detect Protein A tagged proteins. In this case, proteins were transferred to nitrocellulose membranes, which exhibit significantly lower background fluorescence than PVDF membranes. Incubation with the secondary antibody and subsequent washing steps were performed in the dark. Protein signals were visualized using Odyssey Infrared Imaging System (LI-COR) followed by quantitative analysis using Multi Gauge V3.0 (Fujifilm).

5.2.6.8 Coomassie staining

Polyacrylamide gels (5.2.6.5) were stained with Coomassie Brilliant Blue R-250 in order to visualize the total protein content. Briefly, the gel was incubated in Coomassie staining solution for 1 h on a shaker at RT. Destaining was performed by incubating the gel in destaining solution (section 5.1.7) or H_2O for 3-4x 30 min until protein bands showed up significantly over the background staining. Optionally, the gel was dried in a vacuum gel dryer system for 2 h at 80°C or bands were excised for subsequent protein identification using mass spectrometry (section 5.2.6.9).

5.2.6.9 Protein identification using MALDI-TOF/TOF mass spectrometry

Protein bands of interest were excised from Coomassie-stained gels (section 5.2.6.9) and digested in gel with modified sequencing grade trypsin essentially as described (Shevchenko et al., 1996, 2006). Briefly, the excised pieces were cut into small cubes and subsequently washed with 50 mM NH_4HCO_3, 50 mM NH_4HCO_3/25% (v/v) acetonitrile, 25% (v/v) actetonitrile, and 50% (v/v) acetonitrile followed by lyophilization. The dried gel cubes were rehydrated with an equal volume of trypsin in 70mM NH_4HCO_3 (final concentration: 4 µg trypsin per 100 µl gel) for 30 min at RT. After addition of another volume of 50 mM NH_4HCO_3 and incubation for 16 h at 37°C, the resulting tryptic peptides were eluted by diffusion upon shaking the gel cubes two times for 1 h in two volumes of 100 mM NH_4HCO_3 and once for 1 h in two volumes of 100 mM NH_4HCO_3/35% acetonitrile at 37°C. The supernatants of these elution steps were pooled in a 1.5 ml tube and the solvents removed by lyophilization. The extracted peptides were solubilised in 5 µl matrix solution (2 mg/ml α-cyano-4-hydroxycinnamic acid (CHCA), 50% (v/v) acetonitrile, 0.1% (v/v) TFA) and manually spotted on the MALDI target plate. Peptide mass fingerprints (PMF) and MS/MS analyses were performed on a 4800 Proteomics Analyzer MALDI-TOF/TOF mass spectrometer (ABI) operated in positive ion reflector mode and evaluated by searching the NCBInr protein sequence database with Mascot implemented in GPS Explorer v.3.5 (ABI).

5.2.7 Additional biochemical methods

5.2.7.1 Affinity purification of recombinantly expressed FLAG-tag fusion proteins

Cell pellets according to 50 x 10^6 infected SF21 cells were thawed on ice and resuspended in 40 ml ice cold A100+T/T buffer (20 mM Tris–HCl pH 8, 100 mM KCl, 5 mM $Mg(OAc)_2$, 2 mM Benzamidine, 1 mM PMSF, 0.5% Triton-X100, 0.1% Tween-20). Cells were lysed by sonication in a cooling bath using Branson Sonifier 250 (output 5, duty cycle 40%, 30 sec

pulse, 30 sec cooling, 6 repeats) and cell debris was removed by centrifugation (4°C, 20 min, 3300 x g). The cleared cell lysate was incubated with 50 µl anti-FLAG M2 affinity gel (Sigma-Aldrich), equilibrated with buffer A100+T/T, for 2h at 4°C on a turning wheel. After centrifugation (4°C, 1 min, 130 x g), the supernatant was removed and the beads were washed with buffer A100+T/T in batch mode (3x 10 ml, 3x 1ml). To elute the FLAG-tag fusion protein, the beads were incubated with 100 µl buffer A100+T/T containing 300 µg/ml FLAG peptide (Sigma-Aldrich) for 2h at 4°C on a turning wheel. Finally, the beads were removed from the eluate by centrifugation (4°C, 1 min, 16,000 x g) through a MobiCol microspin column (MoBiTec).

5.2.7.2 Gel filtration chromatography

Affinity purified protein complexes were analyzed using the Smart System (Pharmacia Biotech) and a Superose6 PC 3.2/30 gel filtration column (GE Healthcare) equilibrated with buffer A100 (20 mM Tris–HCl pH 8, 200 mM KCl, 5 mM $Mg(OAc)_2$, 2 mM Benzamidine, 1 mM PMSF, 0.1% Tween-20) supplemented with 0.1% Tween-20. Samples were loaded using a 50 µl loop and separated over the column at 4°C with a flow rate of 20 µl/min. After the void volume had passed, 50 µl fractions were collected.

5.2.7.3 Electron microscopy

Protein complex (~ 50 µg/ml) was adsorbed to glow-discharged carbon film for 10 s, followed by staining with a 1% (w/v) uranyl acetate solution for two times 10 s. Images of the complex were recorded with a Philips CM12 (FEI Electron Optics) electron microscope (120 keV, magnification 28,000). Images were taken with a Slow-scan-CCD-Kamera (Modell 0124, TVIPS Tietz) (1024 x 1024 pixels).

5.2.7.4 Affinity purification using IgG coupled magnetic beads

The cell pellet corresponding to 1 l yeast culture with OD600 = 0.8-1.2 was resuspended in 1.5 ml of cold A100 buffer (20 mM Tris–HCl pH 8, 100 mM KCl, 5 mM $Mg(OAc)_2$, 2 mM Benzamidine, 1 mM PMSF), supplemented with 0.04 U/ml RNasin, per gramm of cell pellet. 800 µl aliquots of this cell suspension were divided to 2 ml reaction tubes containing 1.4 ml glass beads (Ø 0.75–1 mm). Cells were disrupted on an IKA Vibrax VXR basic shaker with 2200 rpm at 4°C for 15 min, followed by 5 min on ice. This procedure was repeated twice. The cell lysate was cleared from cell debris by two centrifugation steps (4°C, 5 min, 16000 x g; 4°C, 10 min, 16000 x g). The protein concentration of the cleared lysate was determined using the Bradford assay (section 5.2.6.1). Triton X-100 (0.5% final concentration) and Tween 20 (0.1% final concentration) was added to the cell lysate. Equal protein amounts of cell lysates (typically 1.1 ml with 30-40 mg of total protein) were incubated for 1 hour at 4°C with 100 µl of IgG (rabbit serum, I5006-100MG, Sigma) coupled magnetic beads slurry (1 mm BcMag, FC-102, Bioclone) equilibrated in A100 buffer containing 0.5% Triton X-100 and 0.1% Tween. The beads were washed four times with 700 µl cold A100+T/T buffer. After the fourth washing step, an aliquot of 20% of the beads was separated for the analysis of co-purified RNA. The remaining beads were washed twice with 700 µl AC buffer (100 mM NH_4OAc pH 7.4, 0.1 mM $MgCl_2$) to remove remaining salt from the sample. Bound proteins were eluted twice with 500 µl of freshly prepared 500 mM NH_4OH solution for 20 min at RT. Both eluate fractions were pooled, an aliquot of 10% was separated for SDS-PAGE analysis and the remaining eluate was lyophilised over night.

5.2.7.5 Affinity purification using IgG coupled sepharose beads

Cell lysates were prepared as described above (section 5.2.7.4). Equal protein amounts of cell lysates (typically 800 µl with 10 mg of total protein) were incubated for 1-2 hours at 4°C

with 60 µl of IgG sepharose slurry (GE Healthcare, 52-2083-00 AH) equilibrated in buffer A100+T/T. The beads were washed twice with 1 ml, five times with 2 ml and twice with 10 ml cold A100+T/T buffer in a 10 ml column. After washing, the beads were split for analysis of purified protein (25%) and co-purified RNA (75%).

5.2.7.6 Comparative MALDI TOF/TOF mass spectrometry using iTRAQ reagents

The lyophilised protein samples were resuspended in 20µl dissolution buffer (iTRAQ™ labelling kit (Life Technologies) and reduced with 5mM Tris-(2-carboxyethyl)phosphine at 60°C for 1h. Cysteins were blocked with 10mM methyl-methanethiosulfonate (MMTS) at room temperature for 10min. After trypsin digestion for 20h at 37°C, tryptic peptides of the purifications of interest were labelled with different combinations of the four iTRAQ™ reagents according to the manual. The differentially labelled peptides were combined and lyophilized.

The combined differentially labelled peptides were dissolved for 2h in 0.1%TFA and loaded on a nano-flow HPLC-system (Dionex) harbouring a C18-Pep-Mep column (LC-Packings). The peptides were separated by a gradient of 5% to 95% of buffer B (80% acetonitrile/0.05% TFA) and fractions were mixed with 5 volumes of CHCA (alpha-cyano-4-hydroxy cinnamic acid; Sigma) matrix (2mg/ml in 70% acetonitrile/0.1%TFA) and spotted online via the Probot system (Dionex) on a MALDI-target.

MS/MS analyses were performed on an Applied Biosystems 4800 Proteomics Analyzer. MALDI-TOF/TOF mass spectrometer operated in positive ion reflector mode and evaluated by searching the NCBInr protein sequence database with the Mascot search engine (Matrix Science) implemented in the GPS Explorer software (Applied Biosystems). Laser intensity was adjusted according to laser condition and sample concentration. The ten most intense peptide peaks per spot detected in the MS mode were further fragmented yielding the respective MS/MS spectra.

Only proteins identified by peptides with a Confidence Interval > 95% were included in the analysis. The peak area for iTRAQ reporter ions were interpreted and corrected by the GPS-Explorer software (Applied Biosystems) and Excel (Microsoft). An average iTRAQ ratio of all peptides of a given protein was calculated and outliers were deleted by manual evaluation.

Hierarchical clustering analysis of datasets derived from several experiments was performed with cluster 3.0 software (Eisen et al., 1998) using the ‘‘log2 transform data’’ and the ‘‘median center arrays’’ settings for data adjustment and the Euclidean distance and centroid linkage settings for gene and array clustering. Java Treeview was used for cluster visualization (see http://www.eisenlab.org/eisen/?page_id = 42).

5.2.7.7 Chromatin immunoprecipitation (ChIP)

ChIP was performed mainly as described (Hecht and Grunstein, 1999). Formaldehyde fixed cells (section 5.2.2.9) from 50ml of an exponentially growing yeast culture were washed (1 min, 13000 rpm, 4°C) with 1ml of cold ChIP lysis buffer (section 5.1.7) and suspended in 350µl of ChIP lysis buffer. Glass beads (Ø 0.75-1.0 mm, Roth) were added and cells were disrupted on a VXR basic IKA Vibrax orbital shaker for 3x15min with 2200 rpm at 4°C with 10 min cooling steps on ice in between. Cell lysates were transferred into a 15 ml tube, adjusted to 1 ml with ChIP lysis buffer and sonicated in a cooling bath using Branson Sonifier 250 (Output 3, duty cycle constant; 6 times 10 pulses of ~1 sec, 30 sec cooling between each cycle). This procedure yielded an average DNA fragment size of 500 bp. Cell debris was removed by centrifugation (20 min, 13000 rpm, 4°C). The chromatin extracts were split into three aliquots. 40µl of each aliquot served as an input control, 200 µl of each aliquot were incubated for 2 h at 4°C with 125 µl IgG-Sepharose slurry (GE Healthcare, 52-2083-00 AH) to enrich the TAP- tagged proteins. After immunoprecipitation, the beads were washed three

times with ChIP lysis buffer, twice with ChIP washing buffer I and twice with ChIP washing buffer II followed by a final washing step with TE buffer. 250 µl of buffer IRN were added to the beads (IPs) and to the input samples.
For DNA isolation, Input and IP samples were treated with 2 µl of RNase A (20 mg/ml), mixed, and incubated at 37°C for 1 h. 10µl of 10% SDS and 2 µl of Proteinase K (20 mg/ml) were added, mixed, and samples were incubated for 1 h at 56°C. Formaldehyde crosslink was reverted by incubation at 65°C over night. DNA was extracted with phenol–chloroform–isoamyl alcohol (section 5.2.4.3). 1 volume of IRN and 2.5 volumes of ethanol were added and DNA was precipitated at −20°C for at least 20 min. DNA was collected by centrifugation at 16,000 x g for 20 min at 4°C. DNA was dried for 5–10min at room temperature and resuspended in 50 µl of TE buffer.
Relative DNA amounts present in Input and IP were determined by quantitative PCR (section 5.2.4.7) using a RotorGene 3000 system (Corbett Research) and the comparative analysis software module. Primer pairs used for amplification are listed in section 5.1.5. Input DNA was diluted 1:500, and IP DNA was diluted 1:20 in H_2O prior to analysis. All samples were analysed in triplicate qPCR reactions to ensure accuracy of the data. For each amplicon in each purification, the precipitation efficiencies (% IP (rDNA)) were calculated and normalised to the PDC1 precipitation efficiencies (% IP (rDNA) / % IP (PDC1)).

5.2.7.8 ChIP after RNase treatment of chromatin

ChIP experiments after RNase treatment of the chromatin fractions were essentially performed as described in section 5.2.7.7. Yeast strains were grown in 120 ml rich medium at 30°C to exponential phase (OD600 = 0.5-0.7), subsequently cross linked using formaldehyde (final concentration 1%) for 15' at 30°C and harvested in two aliquots of 50 ml each. From each cell pellet, the chromatin extract was prepared and chromatin fractions from the same strains were pooled. Subsequently, two aliquots of the pooled fractions were treated either with 10 U of RNase A and 400 U of RNase T1 (RNase A/T1 cocktail, Ambion) or an equivalent volume of lysis buffer. After incubating at 25°C for 40 min, input samples of the RNase treated and untreated chromatin were taken and immunopurification of the remaining solution was performed as described above. After the last washing step, an aliquot of the precipitated material (10% or 20%) was prepared for Western blot analysis. Samples for Western blot analysis were incubated in 1x Laemmli protein sample buffer (section 5.1.7) at 95°C for 15 min to reverse the formaldehyde cross link. DNA workup and analysis by qPCR was performed as described in section 5.2.7.7.

5.2.7.9 Chromatin immunoprecipitation and analysis of co-purified proteins (pChIP)

pChIP was performed as described (Hierlmeier et al., 2012). Yeast cells were grown at 30°C in 500 ml YPD medium to mid exponential phase (OD600 = 0.5-0.8) and treated with formaldehyde (0.5 % final concentration, 10 min, 30°C). After quenching of excess formaldehyde with Tris-glycine solution (10 mM final concentration, 5 min, 30°C), cells were harvested (10 min, 4°C, 2200 x g) and washed twice with 40 ml of ice cold PBS (4°C, 5 min, 2000 x g) and once with cold lysis buffer (50mM HEPES-KOH (pH 7.5), 200mM NaCl, 0.5mM EDTA, 1% Triton, 0.1% Na-Deoxycholate, 0.1% SDS, 2 mM Benzamidine, 1 mM PMSF). The cell pellet was resuspended in 1.5 ml lysis buffer per gram of cells. 500µl aliquots were mixed with 500µl glass beads (diameter 0.75 to 1.0 mm; Roth) and cells were disrupted on an IKA Vibrax VXR basic shaker (4ºC, 2200 rpm) for 4 cycles of 10 min with a 2 min cooling step in between. Extracts were centrifuged (5 min, 4ºC, 850 x g), the supernatant was collected and adjusted to 1 ml final volume with lysis buffer. Sonification was performed in a cooling bath using a Branson Sonifier 250 for 5 cycles of 10 pulses (Microtip limit 3, 90%

Duty cycle) with a 30 sec cooling step in between. Sonicated extract was centrifuged (10 min, 4ºC, 18000 x g) and the supernatant was collected and used in the affinity purification.
Equal volumes of cell lysates were incubated over night at 4°C on a turning wheel with 200 µl of IgG (rabbit serum, I5006-100MG, Sigma) coupled magnetic beads slurry (1 mm BcMag, FC-102, Bioclone) equilibrated in lysis buffer. The beads were washed four times with lysis buffer and two times with AC buffer (100 mM NH_4OAc pH 7.4, 0.1 mM $MgCl_2$) for 5 min each at 4ºC on a turning wheel. Bound proteins were eluted twice with 500 µl of freshly prepared 500 mM NH_4OH solution for 20 min at RT. Eluates were combined and lyophilized and subjected to comparative mass spectrometric analysis (section 5.2.7.6).

6 References

Adams, C.C., Jakovljevic, J., Roman, J., Harnpicharnchai, P., and Woolford, J.L., Jr (2002). Saccharomyces cerevisiae nucleolar protein Nop7p is necessary for biogenesis of 60S ribosomal subunits. RNA *8*, 150–165.

Allmang, C., Kufel, J., Chanfreau, G., Mitchell, P., Petfalski, E., and Tollervey, D. (1999a). Functions of the exosome in rRNA, snoRNA and snRNA synthesis. EMBO J. *18*, 5399–5410.

Allmang, C., Mitchell, P., Petfalski, E., and Tollervey, D. (2000). Degradation of ribosomal RNA precursors by the exosome. Nucleic Acids Res *28*, 1684–1691.

Allmang, C., Petfalski, E., Podtelejnikov, A., Mann, M., Tollervey, D., and Mitchell, P. (1999b). The yeast exosome and human PM–Scl are related complexes of 3′ → 5′ exonucleases. Genes Dev *13*, 2148–2158.

Amberg, D.C., Burke, D.J., and Strathern, J.N. (2005). Methods in Yeast Genetics: A Cold Spring Harbor Laboratory Course Manual, 2005 Edition (Cold Spring Harbor Laboratory).

Amberg, D.C., Goldstein, A.L., and Cole, C.N. (1992). Isolation and characterization of RAT1: an essential gene of Saccharomyces cerevisiae required for the efficient nucleocytoplasmic trafficking of mRNA. Genes Dev. *6*, 1173–1189.

Andersen, J.S., Lyon, C.E., Fox, A.H., Leung, A.K.L., Lam, Y.W., Steen, H., Mann, M., and Lamond, A.I. (2002). Directed Proteomic Analysis of the Human Nucleolus. Current Biology *12*, 1–11.

Ban, N., Nissen, P., Hansen, J., Moore, P.B., and Steitz, T.A. (2000). The complete atomic structure of the large ribosomal subunit at 2.4 A resolution. Science *289*, 905–920.

Bargis-Surgey, P., Lavergne, J.-P., Gonzalo, P., Vard, C., Filhol-Cochet, O., and Reboud, J.-P. (1999). Interaction of elongation factor eEF-2 with ribosomal P proteins. European Journal of Biochemistry *262*, 606–611.

Bassler, J., Kallas, M., Pertschy, B., Ulbrich, C., Thoms, M., and Hurt, E. (2010). The AAA-ATPase Rea1 drives removal of biogenesis factors during multiple stages of 60S ribosome assembly. Mol. Cell *38*, 712–721.

Baudin-Baillieu, A., Tollervey, D., Cullin, C., and Lacroute, F. (1997). Functional analysis of Rrp7p, an essential yeast protein involved in pre-rRNA processing and ribosome assembly. Mol Cell Biol *17*, 5023–5032.

Bax, R., Raué, H.A., and Vos, J.C. (2006a). Slx9p facilitates efficient ITS1 processing of pre-rRNA in Saccharomyces cerevisiae. RNA *12*, 2005–2013.

Bax, R., Vos, H.R., Raué, H.A., and Vos, J.C. (2006b). Saccharomyces cerevisiae Sof1p Associates with 35S Pre-rRNA Independent from U3 snoRNA and Rrp5p. Eukaryot Cell *5*, 427–434.

Van Beekvelt, C.A., De Graaff-Vincent, M., Faber, A.W., Van't Riet, J., Venema, J., and Raué, H.A. (2001). All three functional domains of the large ribosomal subunit protein L25 are required for both early and late pre-rRNA processing steps in Saccharomyces cerevisiae. Nucleic Acids Res. *29*, 5001–5008.

Beltrame, M., and Tollervey, D. (1992). Identification and functional analysis of two U3 binding sites on yeast pre-ribosomal RNA. EMBO J. *11*, 1531–1542.

Beltrame, M., and Tollervey, D. (1995). Base pairing between U3 and the pre-ribosomal RNA is required for 18S rRNA synthesis. EMBO J. *14*, 4350–4356.

Bensadoun, A., and Weinstein, D. (1976). Assay of proteins in the presence of interfering materials. Anal. Biochem. *70*, 241–250.

Ben-Shem, A., Garreau de Loubresse, N., Melnikov, S., Jenner, L., Yusupova, G., and Yusupov, M. (2011). The structure of the eukaryotic ribosome at 3.0 Å resolution. Science *334*, 1524–1529.

Ben-Shem, A., Jenner, L., Yusupova, G., and Yusupov, M. (2010). Crystal structure of the eukaryotic ribosome. Science *330*, 1203–1209.

Berger, I., Fitzgerald, D.J., and Richmond, T.J. (2004). Baculovirus expression system for heterologous multiprotein complexes. Nat. Biotechnol. *22*, 1583–1587.

Bergès, T., Petfalski, E., Tollervey, D., and Hurt, E.C. (1994). Synthetic lethality with fibrillarin identifies NOP77p, a nucleolar protein required for pre-rRNA processing and modification. EMBO J *13*, 3136–3148.

Bernstein, K.A., Gallagher, J.E.G., Mitchell, B.M., Granneman, S., and Baserga, S.J. (2004). The small-subunit processome is a ribosome assembly intermediate. Eukaryotic Cell *3*, 1619–1626.

Boeke, J.D., LaCroute, F., and Fink, G.R. (1984). A positive selection for mutants lacking orotidine-5'-phosphate decarboxylase activity in yeast: 5-fluoro-orotic acid resistance. Mol. Gen. Genet. *197*, 345–346.

Boeke, J.D., Trueheart, J., Natsoulis, G., and Fink, G.R. (1987). 5-Fluoroorotic acid as a selective agent in yeast molecular genetics. Meth. Enzymol. *154*, 164–175.

De Boer, P., Vos, H.R., Faber, A.W., Vos, J.C., and Raué, H.A. (2006). Rrp5p, a trans-acting factor in yeast ribosome biogenesis, is an RNA-binding protein with a pronounced preference for U-rich sequences. RNA *12*, 263–271.

Borovjagin, A.V., and Gerbi, S.A. (2000). The spacing between functional Cis-elements of U3 snoRNA is critical for rRNA processing. J. Mol. Biol. *300*, 57–74.

Bradatsch, B., Katahira, J., Kowalinski, E., Bange, G., Yao, W., Sekimoto, T., Baumgärtel, V., Boese, G., Bassler, J., Wild, K., et al. (2007). Arx1 functions as an unorthodox nuclear export receptor for the 60S preribosomal subunit. Mol. Cell *27*, 767–779.

Bradatsch, B., Leidig, C., Granneman, S., Gnädig, M., Tollervey, D., Böttcher, B., Beckmann, R., and Hurt, E. (2012). Structure of the pre-60S ribosomal subunit with nuclear export factor Arx1 bound at the exit tunnel. Nat. Struct. Mol. Biol. *19*, 1234–1241.

Bradford, M.M. (1976). A rapid and sensitive method for the quantitation of microgram quantities of protein utilizing the principle of protein-dye binding. Anal. Biochem. *72*, 248–254.

Brand, R.C., Klootwijk, J., Van Steenbergen, T.J., De Kok, A.J., and Planta, R.J. (1977). Secondary methylation of yeast ribosomal precursor RNA. Eur. J. Biochem. *75*, 311–318.

Briggs, M.W., Burkard, K.T., and Butler, J.S. (1998). Rrp6p, the yeast homologue of the human PM-Scl 100-kDa autoantigen, is essential for efficient 5.8 S rRNA 3' end formation. J. Biol. Chem. *273*, 13255–13263.

Bycroft, M., Hubbard, T.J., Proctor, M., Freund, S.M., and Murzin, A.G. (1997). The solution structure of the S1 RNA binding domain: a member of an ancient nucleic acid-binding fold. Cell *88*, 235–242.

Cadwell, C., Yoon, H.J., Zebarjadian, Y., and Carbon, J. (1997). The yeast nucleolar protein Cbf5p is involved in rRNA biosynthesis and interacts genetically with the RNA polymerase I transcription factor RRN3. Mol. Cell. Biol. *17*, 6175–6183.

Carter, A.P., Clemons, W.M., Brodersen, D.E., Morgan-Warren, R.J., Wimberly, B.T., and Ramakrishnan, V. (2000). Functional insights from the structure of the 30S ribosomal subunit and its interactions with antibiotics. Nature *407*, 340–348.

Cavaillé, J., Nicoloso, M., and Bachellerie, J.P. (1996). Targeted ribose methylation of RNA in vivo directed by tailored antisense RNA guides. Nature *383*, 732–735.

Cech, T.R. (2000). Structural biology. The ribosome is a ribozyme. Science *289*, 878–879.

Chakraborty, A., Uechi, T., and Kenmochi, N. (2011). Guarding the “translation apparatus”: defective ribosome biogenesis and the p53 signaling pathway. Wiley Interdiscip Rev RNA *2*, 507–522.

Chen, W., Bucaria, J., Band, D.A., Sutton, A., and Sternglanz, R. (2003). Enp1, a yeast protein associated with U3 and U14 snoRNAs, is required for pre-rRNA processing and 40S subunit synthesis. Nucleic Acids Res. *31*, 690–699.

Chu, S., Archer, R.H., Zengel, J.M., and Lindahl, L. (1994). The RNA of RNase MRP is required for normal processing of ribosomal RNA. Proc. Natl. Acad. Sci. U.S.A. *91*, 659–663.

Cole, S.E., LaRiviere, F.J., Merrikh, C.N., and Moore, M.J. (2009). A convergence of rRNA and mRNA quality control pathways revealed by mechanistic analysis of nonfunctional rRNA decay. Mol. Cell *34*, 440–450.

Combs, D.J., Nagel, R.J., Ares, M., and Stevens, S.W. (2006). Prp43p Is a DEAH-Box Spliceosome Disassembly Factor Essential for Ribosome Biogenesis. Mol. Cell. Biol. *26*, 523–534.

De la Cruz, J., Kressler, D., Rojo, M., Tollervey, D., and Linder, P. (1998). Spb4p, an essential putative RNA helicase, is required for a late step in the assembly of 60S ribosomal subunits in Saccharomyces cerevisiae. RNA *4*, 1268–1281.

Daugeron, M.C., Kressler, D., and Linder, P. (2001). Dbp9p, a putative ATP-dependent RNA helicase involved in 60S-ribosomal-subunit biogenesis, functionally interacts with Dbp6p. RNA *7*, 1317–1334.

Deisenroth, C., and Zhang, Y. (2010). Ribosome biogenesis surveillance: probing the ribosomal protein-Mdm2-p53 pathway. Oncogene *29*, 4253–4260.

Dez, C., Dlakić, M., and Tollervey, D. (2007). Roles of the HEAT repeat proteins Utp10 and Utp20 in 40S ribosome maturation. RNA *13*, 1516–1527.

Dez, C., Froment, C., Noaillac-Depeyre, J., Monsarrat, B., Caizergues-Ferrer, M., and Henry, Y. (2004). Npa1p, a component of very early pre-60S ribosomal particles, associates with a subset of small nucleolar RNPs required for peptidyl transferase center modification. Mol. Cell. Biol. *24*, 6324–6337.

Dez, C., Houseley, J., and Tollervey, D. (2006). Surveillance of nuclear-restricted pre-ribosomes within a subnucleolar region of Saccharomyces cerevisiae. EMBO J *25*, 1534–1546.

Dosil, M., and Bustelo, X.R. (2004). Functional characterization of Pwp2, a WD family protein essential for the assembly of the 90 S pre-ribosomal particle. J. Biol. Chem. *279*, 37385–37397.

Dragon, F., Gallagher, J.E.G., Compagnone-Post, P.A., Mitchell, B.M., Porwancher, K.A., Wehner, K.A., Wormsley, S., Settlage, R.E., Shabanowitz, J., Osheim, Y., et al. (2002). A large nucleolar U3 ribonucleoprotein required for 18S ribosomal RNA biogenesis. Nature *417*, 967–970.

Dunbar, D.A., Dragon, F., Lee, S.J., and Baserga, S.J. (2000). A nucleolar protein related to ribosomal protein L7 is required for an early step in large ribosomal subunit biogenesis. PNAS *97*, 13027–13032.

Dunbar, D.A., Wormsley, S., Agentis, T.M., and Baserga, S.J. (1997). Mpp10p, a U3 small nucleolar ribonucleoprotein component required for pre-18S rRNA processing in yeast. Mol Cell Biol *17*, 5803–5812.

Dutca, L.M., Gallagher, J.E.G., and Baserga, S.J. (2011). The initial U3 snoRNA:pre-rRNA base pairing interaction required for pre-18S rRNA folding revealed by in vivo chemical probing. Nucleic Acids Res. *39*, 5164–5180.

Edskes, H.K., Ohtake, Y., and Wickner, R.B. (1998). Mak21p of Saccharomyces cerevisiae, a homolog of human CAATT-binding protein, is essential for 60 S ribosomal subunit biogenesis. J. Biol. Chem. *273*, 28912–28920.

Eisen, M.B., Spellman, P.T., Brown, P.O., and Botstein, D. (1998). Cluster analysis and display of genome-wide expression patterns. Proc. Natl. Acad. Sci. U.S.A. *95*, 14863–14868.

El Hage, A., Koper, M., Kufel, J., and Tollervey, D. (2008). Efficient termination of transcription by RNA polymerase I requires the 5' exonuclease Rat1 in yeast. Genes Dev. *22*, 1069–1081.

Eppens, N.A., Faber, A.W., Rondaij, M., Jahangir, R.S., Van Hemert, S., Vos, J.C., Venema, J., and Raué, H.A. (2002). Deletions in the S1 domain of Rrp5p cause processing at a novel site in ITS1 of yeast pre-rRNA that depends on Rex4p. Nucleic Acids Res. *30*, 4222–4231.

Eppens, N.A., Rensen, S., Granneman, S., Raué, H.A., and Venema, J. (1999). The roles of Rrp5p in the synthesis of yeast 18S and 5.8S rRNA can be functionally and physically separated. RNA *5*, 779–793.

Faber, A.W., Dijk, M.V., Raué, H.A., and Vos, J.C. (2002). Ngl2p is a Ccr4p-like RNA nuclease essential for the final step in 3'-end processing of 5.8S rRNA in Saccharomyces cerevisiae. RNA *8*, 1095–1101.

Faber, A.W., Vos, H.R., Vos, J.C., and Raué, H.A. (2006). 5'-end formation of yeast 5.8SL rRNA is an endonucleolytic event. Biochem. Biophys. Res. Commun. *345*, 796–802.

Fang, F., PHILLIPS, S., and BUTLER, J.S. (2005). Rat1p and Rai1p function with the nuclear exosome in the processing and degradation of rRNA precursors. RNA *11*, 1571–1578.

Fath, S., Kobor, M.S., Philippi, A., Greenblatt, J., and Tschochner, H. (2004). Dephosphorylation of RNA polymerase I by Fcp1p is required for efficient rRNA synthesis. J. Biol. Chem. *279*, 25251–25259.

Fatica, A., Cronshaw, A.D., Dlakić, M., and Tollervey, D. (2002). Ssf1p prevents premature processing of an early pre-60S ribosomal particle. Mol. Cell *9*, 341–351.

Fatica, A., Oeffinger, M., Dlakić, M., and Tollervey, D. (2003). Nob1p Is Required for Cleavage of the 3′ End of 18S rRNA. Mol. Cell. Biol. *23*, 1798–1807.

FATICA, A., OEFFINGER, M., TOLLERVEY, D., and BOZZONI, I. (2003). Cic1p/Nsa3p is required for synthesis and nuclear export of 60S ribosomal subunits. RNA *9*, 1431–1436.

Fayet-Lebaron, E., Atzorn, V., Henry, Y., and Kiss, T. (2009). 18S rRNA processing requires base pairings of snR30 H/ACA snoRNA to eukaryote-specific 18S sequences. EMBO J *28*, 1260–1270.

Ferreira-Cerca, S., Pöll, G., Gleizes, P.-E., Tschochner, H., and Milkereit, P. (2005). Roles of eukaryotic ribosomal proteins in maturation and transport of pre-18S rRNA and ribosome function. Mol. Cell *20*, 263–275.

Ferreira-Cerca, S., Pöll, G., Kühn, H., Neueder, A., Jakob, S., Tschochner, H., and Milkereit, P. (2007). Analysis of the in vivo assembly pathway of eukaryotic 40S ribosomal proteins. Mol. Cell *28*, 446–457.

Fitzgerald, D.J., Berger, P., Schaffitzel, C., Yamada, K., Richmond, T.J., and Berger, I. (2006). Protein complex expression by using multigene baculoviral vectors. Nat. Methods *3*, 1021–1032.

Fournier, M.J., and Maxwell, E.S. (1993). The nucleolar snRNAs: catching up with the spliceosomal snRNAs. Trends Biochem. Sci. *18*, 131–135.

Freed, E.F., Prieto, J.-L., McCann, K.L., McStay, B., and Baserga, S.J. (2012). NOL11, implicated in the pathogenesis of North American Indian childhood cirrhosis, is required for pre-rRNA transcription and processing. PLoS Genet. *8*, e1002892.

Gadal, O., Labarre, S., Boschiero, C., and Thuriaux, P. (2002a). Hmo1, an HMG-box protein, belongs to the yeast ribosomal DNA transcription system. EMBO J. *21*, 5498–5507.

Gadal, O., Strauss, D., Kessl, J., Trumpower, B., Tollervey, D., and Hurt, E. (2001). Nuclear export of 60s ribosomal subunits depends on Xpo1p and requires a nuclear export sequence-containing factor, Nmd3p, that associates with the large subunit protein Rpl10p. Mol. Cell. Biol. *21*, 3405–3415.

Gadal, O., Strauss, D., Petfalski, E., Gleizes, P.-E., Gas, N., Tollervey, D., and Hurt, E. (2002b). Rlp7p is associated with 60S preribosomes, restricted to the granular component of the nucleolus, and required for pre-rRNA processing. J. Cell Biol. *157*, 941–951.

Gallagher, J.E.G., Dunbar, D.A., Granneman, S., Mitchell, B.M., Osheim, Y., Beyer, A.L., and Baserga, S.J. (2004). RNA polymerase I transcription and pre-rRNA processing are linked by specific SSU processome components. Genes Dev. *18*, 2506–2517.

Ganot, P., Bortolin, M.L., and Kiss, T. (1997). Site-specific pseudouridine formation in preribosomal RNA is guided by small nucleolar RNAs. Cell *89*, 799–809.

García-Gómez, J.J., Babiano, R., Lebaron, S., Froment, C., Monsarrat, B., Henry, Y., and De la Cruz, J. (2011a). Nop6, a component of 90S pre-ribosomal particles, is required for 40S ribosomal subunit biogenesis in Saccharomyces cerevisiae. RNA Biol *8*, 112–124.

García-Gómez, J.J., Lebaron, S., Froment, C., Monsarrat, B., Henry, Y., and De la Cruz, J. (2011b). Dynamics of the Putative RNA Helicase Spb4 during Ribosome Assembly in Saccharomyces cerevisiae ▽. Mol Cell Biol *31*, 4156–4164.

Geerlings, T.H., Vos, J.C., and Raué, H.A. (2000). The final step in the formation of 25S rRNA in Saccharomyces cerevisiae is performed by 5'-->3' exonucleases. RNA *6*, 1698–1703.

Gerbasi, V.R., Weaver, C.M., Hill, S., Friedman, D.B., and Link, A.J. (2004). Yeast Asc1p and mammalian RACK1 are functionally orthologous core 40S ribosomal proteins that repress gene expression. Mol. Cell. Biol. *24*, 8276–8287.

Gonzalo, P., and Reboud, J.-P. (2003). The puzzling lateral flexible stalk of the ribosome. Biology of the Cell *95*, 179–193.

Granato, D.C., Machado-Santelli, G.M., and Oliveira, C.C. (2008). Nop53p interacts with 5.8S rRNA co-transcriptionally, and regulates processing of pre-rRNA by the exosome. FEBS J. *275*, 4164–4178.

Grandi, P., Rybin, V., Bassler, J., Petfalski, E., Strauss, D., Marzioch, M., Schäfer, T., Kuster, B., Tschochner, H., Tollervey, D., et al. (2002). 90S pre-ribosomes include the 35S pre-rRNA, the U3 snoRNP, and 40S subunit processing factors but predominantly lack 60S synthesis factors. Mol. Cell *10*, 105–115.

Granneman, S., and Baserga, S.J. (2004). Ribosome biogenesis: of knobs and RNA processing. Exp. Cell Res. *296*, 43–50.

Granneman, S., Gallagher, J.E.G., Vogelzangs, J., Horstman, W., Van Venrooij, W.J., Baserga, S.J., and Pruijn, G.J.M. (2003). The human Imp3 and Imp4 proteins form a ternary complex with hMpp10, which only interacts with the U3 snoRNA in 60-80S ribonucleoprotein complexes. Nucleic Acids Res. *31*, 1877–1887.

Granneman, S., Kudla, G., Petfalski, E., and Tollervey, D. (2009). Identification of protein binding sites on U3 snoRNA and pre-rRNA by UV cross-linking and high-throughput analysis of cDNAs. Proc. Natl. Acad. Sci. U.S.A. *106*, 9613–9618.

Granneman, S., Petfalski, E., Swiatkowska, A., and Tollervey, D. (2010). Cracking pre-40S ribosomal subunit structure by systematic analyses of RNA-protein cross-linking. EMBO J. *29*, 2026–2036.

Granneman, S., Petfalski, E., and Tollervey, D. (2011). A cluster of ribosome synthesis factors regulate pre-rRNA folding and 5.8S rRNA maturation by the Rat1 exonuclease. EMBO J *30*, 4006–4019.

Greber, B.J., Boehringer, D., Montellese, C., and Ban, N. (2012). Cryo-EM structures of Arx1 and maturation factors Rei1 and Jjj1 bound to the 60S ribosomal subunit. Nature Structural & Molecular Biology *19*, 1228–1233.

Haeusler, R.A., and Engelke, D.R. (2006). Spatial organization of transcription by RNA polymerase III. Nucleic Acids Res *34*, 4826–4836.

Harnpicharnchai, P., Jakovljevic, J., Horsey, E., Miles, T., Roman, J., Rout, M., Meagher, D., Imai, B., Guo, Y., Brame, C.J., et al. (2001). Composition and functional characterization of yeast 66S ribosome assembly intermediates. Mol. Cell *8*, 505–515.

Hecht, A., and Grunstein, M. (1999). Mapping DNA interaction sites of chromosomal proteins using immunoprecipitation and polymerase chain reaction. Meth. Enzymol. *304*, 399–414.

Henras, A.K., Soudet, J., Gérus, M., Lebaron, S., Caizergues-Ferrer, M., Mougin, A., and Henry, Y. (2008). The post-transcriptional steps of eukaryotic ribosome biogenesis. Cell. Mol. Life Sci. *65*, 2334–2359.

Henry, Y., Wood, H., Morrissey, J.P., Petfalski, E., Kearsey, S., and Tollervey, D. (1994). The 5' end of yeast 5.8S rRNA is generated by exonucleases from an upstream cleavage site. EMBO J. *13*, 2452–2463.

Herbert Spring, M.F.T. Structural and biochemical studies of the primary nucleus of two green algal species, Acetabularia mediterranea and Acetabularia major. In: Cytobiologie (1974) 10, 1-65.

Hernandez-Verdun, D., Roussel, P., Thiry, M., Sirri, V., and Lafontaine, D.L.J. (2010). The nucleolus: structure/function relationship in RNA metabolism. Wiley Interdisciplinary Reviews: RNA *1*, 415–431.

Heyne, K., Willnecker, V., Schneider, J., Conrad, M., Raulf, N., Schüle, R., and Roemer, K. (2010). NIR, an inhibitor of histone acetyltransferases, regulates transcription factor TAp63 and is controlled by the cell cycle. Nucleic Acids Res. *38*, 3159–3171.

Hierlmeier, T. (2008). In vivo Charakterisierung von Noc1/Noc2 und Noc2/Noc3 Interaktionen (Diplomarbeit)

Hierlmeier, T., Merl, J., Sauert, M., Perez-Fernandez, J., Schultz, P., Bruckmann, A., Hamperl, S., Ohmayer, U., Rachel, R., Jacob, A., et al. (2012). Rrp5p, Noc1p and Noc2p form a protein module which is part of early large ribosomal subunit precursors in S. cerevisiae. Nucl. Acids Res.

Ho, J.H., and Johnson, A.W. (1999). NMD3 encodes an essential cytoplasmic protein required for stable 60S ribosomal subunits in Saccharomyces cerevisiae. Mol. Cell. Biol. *19*, 2389–2399.

Ho, J.H.-N., Kallstrom, G., and Johnson, A.W. (2000). Nmd3p Is a Crm1p-Dependent Adapter Protein for Nuclear Export of the Large Ribosomal Subunit. J Cell Biol *151*, 1057–1066.

Ho, S.N., Hunt, H.D., Horton, R.M., Pullen, J.K., and Pease, L.R. (1989). Site-directed mutagenesis by overlap extension using the polymerase chain reaction. Gene *77*, 51–59.

Hoareau-Aveilla, C., Fayet-Lebaron, E., Jády, B.E., Henras, A.K., and Kiss, T. (2012). Utp23p is required for dissociation of snR30 small nucleolar RNP from preribosomal particles. Nucleic Acids Res *40*, 3641–3652.

Holub, P., Lalakova, J., Cerna, H., Pasulka, J., Sarazova, M., Hrazdilova, K., Arce, M.S., Hobor, F., Stefl, R., and Vanacova, S. (2012). Air2p is critical for the assembly and RNA-binding of the TRAMP complex and the KOW domain of Mtr4p is crucial for exosome activation. Nucleic Acids Res. *40*, 5679–5693.

Van Hoof, A., Lennertz, P., and Parker, R. (2000). Three conserved members of the RNase D family have unique and overlapping functions in the processing of 5S, 5.8S, U4, U5, RNase MRP and RNase P RNAs in yeast. EMBO J. *19*, 1357–1365.

Horn, D.M., Mason, S.L., and Karbstein, K. (2011). Rcl1 Protein, a Novel Nuclease for 18 S Ribosomal RNA Production. J Biol Chem *286*, 34082–34087.

Horsey, E.W., Jakovljevic, J., Miles, T.D., Harnpicharnchai, P., and Woolford, J.L., Jr (2004). Role of the yeast Rrp1 protein in the dynamics of pre-ribosome maturation. RNA *10*, 813–827.

Houseley, J., LaCava, J., and Tollervey, D. (2006). RNA-quality control by the exosome. Nat. Rev. Mol. Cell Biol. *7*, 529–539.

Houseley, J., and Tollervey, D. (2009). The many pathways of RNA degradation. Cell *136*, 763–776.

Huang, J., Brito, I.L., Villén, J., Gygi, S.P., Amon, A., and Moazed, D. (2006). Inhibition of homologous recombination by a cohesin-associated clamp complex recruited to the rDNA recombination enhancer. Genes Dev. *20*, 2887–2901.

Hublitz, P., Kunowska, N., Mayer, U.P., Müller, J.M., Heyne, K., Yin, N., Fritzsche, C., Poli, C., Miguet, L., Schupp, I.W., et al. (2005). NIR is a novel INHAT repressor that modulates the transcriptional activity of p53. Genes Dev. *19*, 2912–2924.

Hughes, J.M. (1996). Functional base-pairing interaction between highly conserved elements of U3 small nucleolar RNA and the small ribosomal subunit RNA. J. Mol. Biol. *259*, 645–654.

Hughes, J.M., and Ares, M., Jr (1991). Depletion of U3 small nucleolar RNA inhibits cleavage in the 5' external transcribed spacer of yeast pre-ribosomal RNA and impairs formation of 18S ribosomal RNA. EMBO J. *10*, 4231–4239.

Hung, N.-J., and Johnson, A.W. (2006). Nuclear Recycling of the Pre-60S Ribosomal Subunit-Associated Factor Arx1 Depends on Rei1 in Saccharomyces cerevisiae. Mol Cell Biol *26*, 3718–3727.

Hung, N.-J., Lo, K.-Y., Patel, S.S., Helmke, K., and Johnson, A.W. (2008). Arx1 Is a Nuclear Export Receptor for the 60S Ribosomal Subunit in Yeast. Mol. Biol. Cell *19*, 735–744.

Ide, S., Miyazaki, T., Maki, H., and Kobayashi, T. (2010). Abundance of ribosomal RNA gene copies maintains genome integrity. Science *327*, 693–696.

Imbriano, C., Bolognese, F., Gurtner, A., Piaggio, G., and Mantovani, R. (2001). HSP-CBF Is an NF-Y-dependent Coactivator of the Heat Shock Promoters CCAAT Boxes. J. Biol. Chem. *276*, 26332–26339.

Ito, T., Chiba, T., Ozawa, R., Yoshida, M., Hattori, M., and Sakaki, Y. (2001). A comprehensive two-hybrid analysis to explore the yeast protein interactome. Proc. Natl. Acad. Sci. U.S.A. *98*, 4569–4574.

Jackson, R.J., Hellen, C.U.T., and Pestova, T.V. (2010). The mechanism of eukaryotic translation initiation and principles of its regulation. Nat. Rev. Mol. Cell Biol. *11*, 113–127.

Jacq, B. (1981). Sequence homologies between eukaryotic 5.8S rRNA and the 5' end of prokaryotic 23S rRNa: evidences for a common evolutionary origin. Nucleic Acids Res *9*, 2913–2932.

Jakob, S., Ohmayer, U., Neueder, A., Hierlmeier, T., Perez-Fernandez, J., Hochmuth, E., Deutzmann, R., Griesenbeck, J., Tschochner, H., and Milkereit, P. (2012). Interrelationships between yeast ribosomal protein assembly events and transient ribosome biogenesis factors interactions in early pre-ribosomes. PLoS ONE *7*, e32552.

Jakovljevic, J., Ohmayer, U., Gamalinda, M., Talkish, J., Alexander, L., Linnemann, J., Milkereit, P., and Woolford, J.L., Jr (2012). Ribosomal proteins L7 and L8 function in concert with six A_3 assembly factors to propagate assembly of domains I and II of 25S rRNA in yeast 60S ribosomal subunits. RNA *18*, 1805–1822.

Janke, C., Magiera, M.M., Rathfelder, N., Taxis, C., Reber, S., Maekawa, H., Moreno-Borchart, A., Doenges, G., Schwob, E., Schiebel, E., et al. (2004). A versatile toolbox for PCR-based tagging of yeast genes: new fluorescent proteins, more markers and promoter substitution cassettes. Yeast *21*, 947–962.

Jenner, L., Melnikov, S., De Loubresse, N.G., Ben-Shem, A., Iskakova, M., Urzhumtsev, A., Meskauskas, A., Dinman, J., Yusupova, G., and Yusupov, M. (2012). Crystal structure of the 80S yeast ribosome. Curr. Opin. Struct. Biol. *22*, 759–767.

Karbstein, K. (2011). Inside the 40S ribosome assembly machinery. Curr Opin Chem Biol *15*, 657–663.

Kass, S., Tyc, K., Steitz, J.A., and Sollner-Webb, B. (1990). The U3 small nucleolar ribonucleoprotein functions in the first step of preribosomal RNA processing. Cell *60*, 897–908.

Kawauchi, J., Mischo, H., Braglia, P., Rondon, A., and Proudfoot, N.J. (2008). Budding yeast RNA polymerases I and II employ parallel mechanisms of transcriptional termination. Genes Dev. *22*, 1082–1092.

Keener, J., Dodd, J.A., Lalo, D., and Nomura, M. (1997). Histones H3 and H4 are components of upstream activation factor required for the high-level transcription of yeast rDNA by RNA polymerase I. Proc. Natl. Acad. Sci. U.S.A. *94*, 13458–13462.

Kemmler, S., Occhipinti, L., Veisu, M., and Panse, V.G. (2009). Yvh1 is required for a late maturation step in the 60S biogenesis pathway. J. Cell Biol. *186*, 863–880.

Kempers-Veenstra, A.E., Oliemans, J., Offenberg, H., Dekker, A.F., Piper, P.W., Planta, R.J., and Klootwijk, J. (1986). 3'-End formation of transcripts from the yeast rRNA operon. EMBO J *5*, 2703–2710.

Keys, D.A., Lee, B.S., Dodd, J.A., Nguyen, T.T., Vu, L., Fantino, E., Burson, L.M., Nogi, Y., and Nomura, M. (1996). Multiprotein transcription factor UAF interacts with the upstream element of the yeast RNA polymerase I promoter and forms a stable preinitiation complex. Genes Dev. *10*, 887–903.

Keys, D.A., Vu, L., Steffan, J.S., Dodd, J.A., Yamamoto, R.T., Nogi, Y., and Nomura, M. (1994). RRN6 and RRN7 encode subunits of a multiprotein complex essential for the initiation of rDNA transcription by RNA polymerase I in Saccharomyces cerevisiae. Genes Dev. *8*, 2349–2362.

King, T.H., Liu, B., McCully, R.R., and Fournier, M.J. (2003). Ribosome structure and activity are altered in cells lacking snoRNPs that form pseudouridines in the peptidyl transferase center. Mol. Cell *11*, 425–435.

Knop, M., Siegers, K., Pereira, G., Zachariae, W., Winsor, B., Nasmyth, K., and Schiebel, E. (1999). Epitope tagging of yeast genes using a PCR-based strategy: more tags and improved practical routines. Yeast *15*, 963–972.

Kos, M., and Tollervey, D. (2010). Yeast pre-rRNA processing and modification occur cotranscriptionally. Mol. Cell *37*, 809–820.

Kressler, D., Hurt, E., and Bassler, J. (2010). Driving ribosome assembly. Biochim. Biophys. Acta *1803*, 673–683.

Kressler, D., Roser, D., Pertschy, B., and Hurt, E. (2008). The AAA ATPase Rix7 powers progression of ribosome biogenesis by stripping Nsa1 from pre-60S particles. J. Cell Biol. *181*, 935–944.

Krogan, N.J., Peng, W.-T., Cagney, G., Robinson, M.D., Haw, R., Zhong, G., Guo, X., Zhang, X., Canadien, V., Richards, D.P., et al. (2004). High-definition macromolecular composition of yeast RNA-processing complexes. Mol. Cell *13*, 225–239.

Krokowski, D., Tchórzewski, M., Boguszewska, A., and Grankowski, N. (2005). Acquisition of a stable structure by yeast ribosomal P0 protein requires binding of P1A–P2B complex: In vitro formation of the stalk structure. Biochimica Et Biophysica Acta (BBA) - General Subjects *1724*, 59–70.

Kruiswijk, T., Planta, R.J., and Krop, J.M. (1978). The course of the assembly of ribosomal subunits in yeast. Biochim. Biophys. Acta *517*, 378–389.

Kudla, G., Granneman, S., Hahn, D., Beggs, J.D., and Tollervey, D. (2011). Cross-linking, ligation, and sequencing of hybrids reveals RNA-RNA interactions in yeast. Proc. Natl. Acad. Sci. U.S.A. *108*, 10010–10015.

Kühn, H., Hierlmeier, T., Merl, J., Jakob, S., Aguissa-Touré, A.-H., Milkereit, P., and Tschochner, H. (2009). The Noc-domain containing C-terminus of Noc4p mediates both formation of the Noc4p-Nop14p submodule and its incorporation into the SSU processome. PLoS ONE *4*, e8370.

Kulkens, T., Riggs, D.L., Heck, J.D., Planta, R.J., and Nomura, M. (1991). The yeast RNA polymerase I promoter: ribosomal DNA sequences involved in transcription initiation and complex formation in vitro. Nucleic Acids Res. *19*, 5363–5370.

Kuzuhara, T., and Horikoshi, M. (2004). A nuclear FK506-binding protein is a histone chaperone regulating rDNA silencing. Nat. Struct. Mol. Biol. *11*, 275–283.

LaCava, J., Houseley, J., Saveanu, C., Petfalski, E., Thompson, E., Jacquier, A., and Tollervey, D. (2005). RNA Degradation by the Exosome Is Promoted by a Nuclear Polyadenylation Complex. Cell *121*, 713–724.

Laemmli, U.K. (1970). Cleavage of structural proteins during the assembly of the head of bacteriophage T4. Nature *227*, 680–685.

Lafontaine, D., Delcour, J., Glasser, A.L., Desgrès, J., and Vandenhaute, J. (1994). The DIM1 gene responsible for the conserved m6(2)Am6(2)A dimethylation in the 3'-terminal loop of 18 S rRNA is essential in yeast. J. Mol. Biol. *241*, 492–497.

Lafontaine, D., Vandenhaute, J., and Tollervey, D. (1995). The 18S rRNA dimethylase Dim1p is required for pre-ribosomal RNA processing in yeast. Genes Dev. *9*, 2470–2481.

Lafontaine, D.L., Preiss, T., and Tollervey, D. (1998). Yeast 18S rRNA dimethylase Dim1p: a quality control mechanism in ribosome synthesis? Mol. Cell. Biol. *18*, 2360–2370.

Lalo, D., Steffan, J.S., Dodd, J.A., and Nomura, M. (1996). RRN11 encodes the third subunit of the complex containing Rrn6p and Rrn7p that is essential for the initiation of rDNA transcription by yeast RNA polymerase I. J. Biol. Chem. *271*, 21062–21067.

Lamanna, A.C., and Karbstein, K. (2009). Nob1 binds the single-stranded cleavage site D at the 3'-end of 18S rRNA with its PIN domain. Proc. Natl. Acad. Sci. U.S.A. *106*, 14259–14264.

Lamanna, A.C., and Karbstein, K. (2011). An RNA conformational switch regulates pre-18S rRNA cleavage. J. Mol. Biol. *405*, 3–17.

Lamb, J.R., Tugendreich, S., and Hieter, P. (1995). Tetratrico peptide repeat interactions: to TPR or not to TPR? Trends Biochem. Sci. *20*, 257–259.

Lang, W.H., Morrow, B.E., Ju, Q., Warner, J.R., and Reeder, R.H. (1994). A model for transcription termination by RNA polymerase I. Cell *79*, 527–534.

Lang, W.H., and Reeder, R.H. (1993). The REB1 site is an essential component of a terminator for RNA polymerase I in Saccharomyces cerevisiae. Mol. Cell. Biol. *13*, 649–658.

Lang, W.H., and Reeder, R.H. (1995). Transcription termination of RNA polymerase I due to a T-rich element interacting with Reb1p. Proc. Natl. Acad. Sci. U.S.A. *92*, 9781–9785.

LaRiviere, F.J., Cole, S.E., Ferullo, D.J., and Moore, M.J. (2006). A late-acting quality control process for mature eukaryotic rRNAs. Mol. Cell *24*, 619–626.

Lebaron, S., Froment, C., Fromont-Racine, M., Rain, J.-C., Monsarrat, B., Caizergues-Ferrer, M., and Henry, Y. (2005). The splicing ATPase prp43p is a component of multiple preribosomal particles. Mol. Cell. Biol. *25*, 9269–9282.

Lebaron, S., Schneider, C., Van Nues, R.W., Swiatkowska, A., Walsh, D., Böttcher, B., Granneman, S., Watkins, N.J., and Tollervey, D. (2012). Proofreading of pre-40S ribosome maturation by a translation initiation factor and 60S subunits. Nat. Struct. Mol. Biol. *19*, 744–753.

Lebreton, A., Rousselle, J.-C., Lenormand, P., Namane, A., Jacquier, A., Fromont-Racine, M., and Saveanu, C. (2008). 60S ribosomal subunit assembly dynamics defined by semi-quantitative mass spectrometry of purified complexes. Nucleic Acids Res. *36*, 4988–4999.

Lebreton, A., Saveanu, C., Decourty, L., Rain, J.-C., Jacquier, A., and Fromont-Racine, M. (2006). A functional network involved in the recycling of nucleocytoplasmic pre-60S factors. J. Cell Biol. *173*, 349–360.

Leeds, N.B., Small, E.C., Hiley, S.L., Hughes, T.R., and Staley, J.P. (2006). The Splicing Factor Prp43p, a DEAH Box ATPase, Functions in Ribosome Biogenesis. Mol Cell Biol *26*, 513–522.

Léger-Silvestre, I., Trumtel, S., Noaillac-Depeyre, J., and Gas, N. (1999). Functional compartmentalization of the nucleus in the budding yeast Saccharomyces cerevisiae. Chromosoma *108*, 103–113.

Li, H.D., Zagorski, J., and Fournier, M.J. (1990). Depletion of U14 small nuclear RNA (snR128) disrupts production of 18S rRNA in Saccharomyces cerevisiae. Mol. Cell. Biol. *10*, 1145–1152.

Liang, W.Q., and Fournier, M.J. (1995). U14 base-pairs with 18S rRNA: a novel snoRNA interaction required for rRNA processing. Genes Dev. *9*, 2433–2443.

Liang, X., Liu, Q., and Fournier, M.J. (2007). rRNA modifications in an intersubunit bridge of the ribosome strongly affect both ribosome biogenesis and activity. Mol. Cell *28*, 965–977.

Liang, X.-H., Liu, Q., and Fournier, M.J. (2009). Loss of rRNA modifications in the decoding center of the ribosome impairs translation and strongly delays pre-rRNA processing. RNA *15*, 1716–1728.

Liu, Q., Li, M.Z., Leibham, D., Cortez, D., and Elledge, S.J. (1998). The univector plasmid-fusion system, a method for rapid construction of recombinant DNA without restriction enzymes. Curr. Biol. *8*, 1300–1309.

Lo, K.-Y., Li, Z., Bussiere, C., Bresson, S., Marcotte, E.M., and Johnson, A.W. (2010). Defining the pathway of cytoplasmic maturation of the 60S ribosomal subunit. Mol. Cell *39*, 196–208.

Lo, K.-Y., Li, Z., Wang, F., Marcotte, E.M., and Johnson, A.W. (2009). Ribosome stalk assembly requires the dual-specificity phosphatase Yvh1 for the exchange of Mrt4 with P0. J Cell Biol *186*, 849–862.

Long, E.O., and Dawid, I.B. (1980). Repeated Genes in Eukaryotes. Annual Review of Biochemistry *49*, 727–764.

Lum, L.S., Hsu, S., Vaewhongs, M., and Wu, B. (1992). The hsp70 gene CCAAT-binding factor mediates transcriptional activation by the adenovirus E1a protein. Mol Cell Biol *12*, 2599–2605.

Lum, L.S., Sultzman, L.A., Kaufman, R.J., Linzer, D.I., and Wu, B.J. (1990). A cloned human CCAAT-box-binding factor stimulates transcription from the human hsp70 promoter. Mol. Cell. Biol. *10*, 6709–6717.

Lygerou, Z., Allmang, C., Tollervey, D., and Séraphin, B. (1996). Accurate processing of a eukaryotic precursor ribosomal RNA by ribonuclease MRP in vitro. Science *272*, 268–270.

McKnight, S.L., and Miller Jr., O.L. (1976). Ultrastructural patterns of RNA synthesis during early embryogenesis of Drosophila melanogaster. Cell *8*, 305–319.

Méreau, A., Fournier, R., Grégoire, A., Mougin, A., Fabrizio, P., Lührmann, R., and Branlant, C. (1997). An in vivo and in vitro structure-function analysis of the Saccharomyces cerevisiae U3A snoRNP: protein-RNA contacts and base-pair interaction with the pre-ribosomal RNA. J. Mol. Biol. *273*, 552–571.

Merl, J., Jakob, S., Ridinger, K., Hierlmeier, T., Deutzmann, R., Milkereit, P., and Tschochner, H. (2010). Analysis of ribosome biogenesis factor-modules in yeast cells depleted from pre-ribosomes. Nucleic Acids Res. *38*, 3068–3080.

Merz, K., Hondele, M., Goetze, H., Gmelch, K., Stoeckl, U., and Griesenbeck, J. (2008). Actively transcribed rRNA genes in S. cerevisiae are organized in a specialized chromatin associated with the high-mobility group protein Hmo1 and are largely devoid of histone molecules. Genes Dev. *22*, 1190–1204.

Metcalf, W.W., Jiang, W., and Wanner, B.L. (1994). Use of the rep technique for allele replacement to construct new Escherichia coli hosts for maintenance of R6K gamma origin plasmids at different copy numbers. Gene *138*, 1–7.

Meyer, A.E., Hoover, L.A., and Craig, E.A. (2010). The Cytosolic J-protein, Jjj1, and Rei1 Function in the Removal of the Pre-60 S Subunit Factor Arx1. J Biol Chem *285*, 961–968.

Miles, T.D., Jakovljevic, J., Horsey, E.W., Harnpicharnchai, P., Tang, L., and Woolford, J.L., Jr (2005). Ytm1, Nop7, and Erb1 form a complex necessary for maturation of yeast 66S preribosomes. Mol. Cell. Biol. *25*, 10419–10432.

Milkereit, P., Gadal, O., Podtelejnikov, A., Trumtel, S., Gas, N., Petfalski, E., Tollervey, D., Mann, M., Hurt, E., and Tschochner, H. (2001). Maturation and intranuclear transport of pre-ribosomes requires Noc proteins. Cell *105*, 499–509.

Milkereit, P., Strauss, D., Bassler, J., Gadal, O., Kühn, H., Schütz, S., Gas, N., Lechner, J., Hurt, E., and Tschochner, H. (2003). A Noc complex specifically involved in the formation and nuclear export of ribosomal 40 S subunits. J. Biol. Chem. *278*, 4072–4081.

Milkereit, P., and Tschochner, H. (1998). A specialized form of RNA polymerase I, essential for initiation and growth-dependent regulation of rRNA synthesis, is disrupted during transcription. EMBO J. *17*, 3692–3703.

Miller, O.L., and Beatty, B.R. (1969). Visualization of Nucleolar Genes. Science *164*, 955–957.

Mitchell, P., Petfalski, E., Shevchenko, A., Mann, M., and Tollervey, D. (1997). The Exosome: A Conserved Eukaryotic RNA Processing Complex Containing Multiple 3′→5′ Exoribonucleases. Cell *91*, 457–466.

Morrissey, J.P., and Tollervey, D. (1993). Yeast snR30 is a small nucleolar RNA required for 18S rRNA synthesis. Mol Cell Biol *13*, 2469–2477.

Mougey, E.B., O'Reilly, M., Osheim, Y., Miller, O.L., Jr, Beyer, A., and Sollner-Webb, B. (1993). The terminal balls characteristic of eukaryotic rRNA transcription units in chromatin spreads are rRNA processing complexes. Genes Dev. *7*, 1609–1619.

Musters, W., Knol, J., Maas, P., Dekker, A.F., Van Heerikhuizen, H., and Planta, R.J. (1989). Linker scanning of the yeast RNA polymerase I promoter. Nucleic Acids Res. *17*, 9661–9678.

Ni, J., Tien, A.L., and Fournier, M.J. (1997). Small nucleolar RNAs direct site-specific synthesis of pseudouridine in ribosomal RNA. Cell *89*, 565–573.

Nissan, T.A., Bassler, J., Petfalski, E., Tollervey, D., and Hurt, E. (2002). 60S pre-ribosome formation viewed from assembly in the nucleolus until export to the cytoplasm. EMBO J. *21*, 5539–5547.

Nissan, T.A., Galani, K., Maco, B., Tollervey, D., Aebi, U., and Hurt, E. (2004). A pre-ribosome with a tadpole-like structure functions in ATP-dependent maturation of 60S subunits. Mol. Cell *15*, 295–301.

Van Nues, R.W., Rientjes, J.M., Van der Sande, C.A., Zerp, S.F., Sluiter, C., Venema, J., Planta, R.J., and Raué, H.A. (1994). Separate structural elements within internal transcribed spacer 1 of Saccharomyces cerevisiae precursor ribosomal RNA direct the formation of 17S and 26S rRNA. Nucleic Acids Res. *22*, 912–919.

Oakes, M., Aris, J.P., Brockenbrough, J.S., Wai, H., Vu, L., and Nomura, M. (1998). Mutational analysis of the structure and localization of the nucleolus in the yeast Saccharomyces cerevisiae. J. Cell Biol. *143*, 23–34.

Oeffinger, M., Dlakic, M., and Tollervey, D. (2004). A pre-ribosome-associated HEAT-repeat protein is required for export of both ribosomal subunits. Genes Dev. *18*, 196–209.

Oeffinger, M., Leung, A., Lamond, A., Tollervey, D., and Lueng, A. (2002). Yeast Pescadillo is required for multiple activities during 60S ribosomal subunit synthesis. RNA *8*, 626–636.

Oeffinger, M., and Tollervey, D. (2003). Yeast Nop15p is an RNA-binding protein required for pre-rRNA processing and cytokinesis. EMBO J. *22*, 6573–6583.

Oeffinger, M., Zenklusen, D., Ferguson, A., Wei, K.E., El Hage, A., Tollervey, D., Chait, B.T., Singer, R.H., and Rout, M.P. (2009). Rrp17p is a eukaryotic exonuclease required for 5' end processing of Pre-60S ribosomal RNA. Mol. Cell *36*, 768–781.

Ogle, J.M., Brodersen, D.E., Clemons, W.M., Jr, Tarry, M.J., Carter, A.P., and Ramakrishnan, V. (2001). Recognition of cognate transfer RNA by the 30S ribosomal subunit. Science *292*, 897–902.

Ogle, J.M., Murphy, F.V., Tarry, M.J., and Ramakrishnan, V. (2002). Selection of tRNA by the ribosome requires a transition from an open to a closed form. Cell *111*, 721–732.

Osheim, Y.N., French, S.L., Keck, K.M., Champion, E.A., Spasov, K., Dragon, F., Baserga, S.J., and Beyer, A.L. (2004). Pre-18S ribosomal RNA is structurally compacted into the SSU processome prior to being cleaved from nascent transcripts in Saccharomyces cerevisiae. Mol. Cell *16*, 943–954.

Osheim, Y.N., French, S.L., Sikes, M.L., and Beyer, A.L. (2009). Electron microscope visualization of RNA transcription and processing in Saccharomyces cerevisiae by Miller chromatin spreading. Methods Mol. Biol. *464*, 55–69.

Ossowski, J. (2010). Analysen zur *in vivo* Assemblierung ribosomaler Proteine im Zuge der Reifung der großen ribosomalen Untereinheit in der Bäckerhefe *S.cerevisiae*. Diplomarbeit

Panse, V.G., and Johnson, A.W. (2010). Maturation of Eukaryotic Ribosomes: Acquisition of Functionality. Trends Biochem Sci *35*, 260–266.

Paule, M.R., and White, R.J. (2000). Transcription by RNA polymerases I and III. Nucleic Acids Res *28*, 1283–1298.

Pérez-Fernández, J., Martín-Marcos, P., and Dosil, M. (2011). Elucidation of the assembly events required for the recruitment of Utp20, Imp4 and Bms1 onto nascent pre-ribosomes. Nucleic Acids Res. *39*, 8105–8121.

Pérez-Fernández, J., Román, A., De Las Rivas, J., Bustelo, X.R., and Dosil, M. (2007). The 90S preribosome is a multimodular structure that is assembled through a hierarchical mechanism. Mol. Cell. Biol. *27*, 5414–5429.

Pertschy, B., Schneider, C., Gnädig, M., Schäfer, T., Tollervey, D., and Hurt, E. (2009). RNA helicase Prp43 and its co-factor Pfa1 promote 20 to 18 S rRNA processing catalyzed by the endonuclease Nob1. J. Biol. Chem. *284*, 35079–35091.

Pestov, D.G., Stockelman, M.G., Strezoska, Z., and Lau, L.F. (2001). ERB1, the yeast homolog of mammalian Bop1, is an essential gene required for maturation of the 25S and 5.8S ribosomal RNAs. Nucleic Acids Res. *29*, 3621–3630.

Petes, T.D. (1979). Yeast ribosomal DNA genes are located on chromosome XII. Proc. Natl. Acad. Sci. U.S.A. *76*, 410–414.

Petfalski, E., Dandekar, T., Henry, Y., and Tollervey, D. (1998). Processing of the precursors to small nucleolar RNAs and rRNAs requires common components. Mol. Cell. Biol. *18*, 1181–1189.

Peyroche, G., Milkereit, P., Bischler, N., Tschochner, H., Schultz, P., Sentenac, A., Carles, C., and Riva, M. (2000). The recruitment of RNA polymerase I on rDNA is mediated by the interaction of the A43 subunit with Rrn3. EMBO J. *19*, 5473–5482.

Philippsen, P., Thomas, M., Kramer, R.A., and Davis, R.W. (1978). Unique arrangement of coding sequences for 5 S, 5.8 S, 18 S and 25 S ribosomal RNA in Saccharomyces cerevisiae as determined by R-loop and hybridization analysis. J. Mol. Biol. *123*, 387–404.

Planta, R.J., and Mager, W.H. (1998). The list of cytoplasmic ribosomal proteins of Saccharomyces cerevisiae. Yeast *14*, 471–477.

Pöll, G., Braun, T., Jakovljevic, J., Neueder, A., Jakob, S., Woolford, J.L., Jr, Tschochner, H., and Milkereit, P. (2009). rRNA maturation in yeast cells depleted of large ribosomal subunit proteins. PLoS ONE *4*, e8249.

Prescott, E.M., Osheim, Y.N., Jones, H.S., Alen, C.M., Roan, J.G., Reeder, R.H., Beyer, A.L., and Proudfoot, N.J. (2004). Transcriptional termination by RNA polymerase I requires the small subunit Rpa12p. Proc. Natl. Acad. Sci. U.S.A. *101*, 6068–6073.

Prieto, J.-L., and McStay, B. (2007). Recruitment of factors linking transcription and processing of pre-rRNA to NOR chromatin is UBF-dependent and occurs independent of transcription in human cells. Genes Dev. *21*, 2041–2054.

Puig, O., Caspary, F., Rigaut, G., Rutz, B., Bouveret, E., Bragado-Nilsson, E., Wilm, M., and Séraphin, B. (2001). The tandem affinity purification (TAP) method: a general procedure of protein complex purification. Methods *24*, 218–229.

Ramakrishnan, V., and Moore, P.. (2001). Atomic structures at last: the ribosome in 2000. Current Opinion in Structural Biology *11*, 144–154.

Raška, I., Shaw, P.J., and Cmarko, D. (2006). Structure and function of the nucleolus in the spotlight. Current Opinion in Cell Biology *18*, 325–334.

Reiter, A., Hamperl, S., Seitz, H., Merkl, P., Perez-Fernandez, J., Williams, L., Gerber, J., Németh, A., Léger, I., Gadal, O., et al. (2012). The Reb1-homologue Ydr026c/Nsi1 is required for efficient RNA polymerase I termination in yeast. EMBO J. *31*, 3480–3493.

Retèl, J., Van den Bos, R.C., and Planta, R.J. (1969). Characteristics of the methylation in vivo of ribosomal RNA in yeast. Biochim. Biophys. Acta *195*, 370–380.

Rigaut, G., Shevchenko, A., Rutz, B., Wilm, M., Mann, M., and Séraphin, B. (1999). A generic protein purification method for protein complex characterization and proteome exploration. Nat. Biotechnol. *17*, 1030–1032.

Rodríguez-Mateos, M., García-Gómez, J.J., Francisco-Velilla, R., Remacha, M., De la Cruz, J., and Ballesta, J.P.G. (2009). Role and dynamics of the ribosomal protein P0 and its related trans-acting factor Mrt4 during ribosome assembly in Saccharomyces cerevisiae. Nucleic Acids Res *37*, 7519–7532.

Ross, P.L., Huang, Y.N., Marchese, J.N., Williamson, B., Parker, K., Hattan, S., Khainovski, N., Pillai, S., Dey, S., Daniels, S., et al. (2004). Multiplexed protein quantitation in Saccharomyces cerevisiae using amine-reactive isobaric tagging reagents. Mol. Cell Proteomics *3*, 1154–1169.

Saffer, L.D., and Miller, O.L. (1986). Electron microscopic study of Saccharomyces cerevisiae rDNA chromatin replication. Mol. Cell. Biol. *6*, 1148–1157.

Sahasranaman, A., Dembowski, J., Strahler, J., Andrews, P., Maddock, J., and Woolford, J.L., Jr (2011). Assembly of Saccharomyces cerevisiae 60S ribosomal subunits: role of factors required for 27S pre-rRNA processing. EMBO J. *30*, 4020–4032.

Sauert, M. (2010). Studien zur *in vivo* Assemblierung der großen ribosomalen Untereinheit der Bäckerhefe *Saccharomyces cerevisiae.* Diplomarbeit

Saveanu, C., Bienvenu, D., Namane, A., Gleizes, P.E., Gas, N., Jacquier, A., and Fromont-Racine, M. (2001). Nog2p, a putative GTPase associated with pre-60S subunits and required for late 60S maturation steps. EMBO J. *20*, 6475–6484.

Saveanu, C., Namane, A., Gleizes, P.-E., Lebreton, A., Rousselle, J.-C., Noaillac-Depeyre, J., Gas, N., Jacquier, A., and Fromont-Racine, M. (2003). Sequential protein association with nascent 60S ribosomal particles. Mol. Cell. Biol. *23*, 4449–4460.

Saveanu, C., Rousselle, J.-C., Lenormand, P., Namane, A., Jacquier, A., and Fromont-Racine, M. (2007). The p21-activated protein kinase inhibitor Skb15 and its budding yeast homologue are 60S ribosome assembly factors. Mol. Cell. Biol. *27*, 2897–2909.

Savino, R., and Gerbi, S.A. (1990). In vivo disruption of Xenopus U3 snRNA affects ribosomal RNA processing. EMBO J. *9*, 2299–2308.

Schäfer, T., Strauss, D., Petfalski, E., Tollervey, D., and Hurt, E. (2003). The path from nucleolar 90S to cytoplasmic 40S pre-ribosomes. EMBO J. *22*, 1370–1380.

Scheer, U., and Benavente, R. (1990). Functional and dynamic aspects of the mammalian nucleolus. Bioessays *12*, 14–21.

Schmeing, T.M., and Ramakrishnan, V. (2009). What recent ribosome structures have revealed about the mechanism of translation. Nature *461*, 1234–1242.

Schmitt, M.E., Brown, T.A., and Trumpower, B.L. (1990). A rapid and simple method for preparation of RNA from Saccharomyces cerevisiae. Nucleic Acids Res. *18*, 3091–3092.

Schmitt, M.E., and Clayton, D.A. (1993). Nuclear RNase MRP is required for correct processing of pre-5.8S rRNA in Saccharomyces cerevisiae. Mol. Cell. Biol. *13*, 7935–7941.

Schneider, D.A., French, S.L., Osheim, Y.N., Bailey, A.O., Vu, L., Dodd, J., Yates, J.R., Beyer, A.L., and Nomura, M. (2006). RNA polymerase II elongation factors Spt4p and Spt5p play roles in transcription elongation by RNA polymerase I and rRNA processing. Proc. Natl. Acad. Sci. U.S.A. *103*, 12707–12712.

Segerstolpe, A., Lundkvist, P., Osheim, Y.N., Beyer, A.L., and Wieslander, L. (2008). Mrd1p binds to pre-rRNA early during transcription independent of U3 snoRNA and is required for compaction of the pre-rRNA into small subunit processomes. Nucleic Acids Res. *36*, 4364–4380.

Seiser, R.M., Sundberg, A.E., Wollam, B.J., Zobel-Thropp, P., Baldwin, K., Spector, M.D., and Lycan, D.E. (2006). Ltv1 is required for efficient nuclear export of the ribosomal small subunit in Saccharomyces cerevisiae. Genetics *174*, 679–691.

Sengupta, J., Bussiere, C., Pallesen, J., West, M., Johnson, A.W., and Frank, J. (2010). Characterization of the nuclear export adaptor protein Nmd3 in association with the 60S ribosomal subunit. J Cell Biol *189*, 1079–1086.

Sentenac, A. (1985). Eukaryotic RNA Polymerase. Critical Reviews in Biochemistry and Molecular Biology *18*, 31–90.

Sharma, K., and Tollervey, D. (1999). Base pairing between U3 small nucleolar RNA and the 5' end of 18S rRNA is required for pre-rRNA processing. Mol. Cell. Biol. *19*, 6012–6019.

Shevchenko, A., Tomas, H., Havlis, J., Olsen, J.V., and Mann, M. (2006). In-gel digestion for mass spectrometric characterization of proteins and proteomes. Nat Protoc *1*, 2856–2860.

Shevchenko, A., Wilm, M., Vorm, O., and Mann, M. (1996). Mass spectrometric sequencing of proteins silver-stained polyacrylamide gels. Anal. Chem. *68*, 850–858.

Shimoji, K., Jakovljevic, J., Tsuchihashi, K., Umeki, Y., Wan, K., Kawasaki, S., Talkish, J., Woolford, J.L., and Mizuta, K. (2012). Ebp2 and Brx1 function cooperatively in 60S ribosomal subunit assembly in Saccharomyces cerevisiae. Nucleic Acids Res *40*, 4574–4588.

Siddiqi, I.N., Dodd, J.A., Vu, L., Eliason, K., Oakes, M.L., Keener, J., Moore, R., Young, M.K., and Nomura, M. (2001). Transcription of chromosomal rRNA genes by both RNA polymerase I and II in yeast uaf30 mutants lacking the 30 kDa subunit of transcription factor UAF. EMBO J. *20*, 4512–4521.

Siekevitz, P. (1952). Uptake of Radioactive Alanine in Vitro into the Proteins of Rat Liver Fractions. J. Biol. Chem. *195*, 549–565.

Sikorski, R.S., and Boeke, J.D. (1991). In vitro mutagenesis and plasmid shuffling: from cloned gene to mutant yeast. Meth. Enzymol. *194*, 302–318.

Sonenberg, N., and Hinnebusch, A.G. (2009). Regulation of translation initiation in eukaryotes: mechanisms and biological targets. Cell *136*, 731–745.

Soudet, J., Gélugne, J.-P., Belhabich-Baumas, K., Caizergues-Ferrer, M., and Mougin, A. (2010). Immature small ribosomal subunits can engage in translation initiation in Saccharomyces cerevisiae. EMBO J *29*, 80–92.

Stark, H., Rodnina, M.V., Wieden, H.-J., Zemlin, F., Wintermeyer, W., and Van Heel, M. (2002). Ribosome interactions of aminoacyl-tRNA and elongation factor Tu in the codon-recognition complex. Nat. Struct. Biol. *9*, 849–854.

Steffan, J.S., Keys, D.A., Vu, L., and Nomura, M. (1998). Interaction of TATA-binding protein with upstream activation factor is required for activated transcription of ribosomal DNA by RNA polymerase I in Saccharomyces cerevisiae in vivo. Mol. Cell. Biol. *18*, 3752–3761.

Sternberg, N., and Hamilton, D. (1981). Bacteriophage P1 site-specific recombination. I. Recombination between loxP sites. J. Mol. Biol. *150*, 467–486.

Strunk, B.S., Loucks, C.R., Su, M., Vashisth, H., Cheng, S., Schilling, J., Brooks, C.L., Karbstein, K., and Skiniotis, G. (2011). Ribosome Assembly Factors Prevent Premature Translation Initiation by 40S Assembly Intermediates. Science *333*, 1449–1453.

Strunk, B.S., Novak, M.N., Young, C.L., and Karbstein, K. (2012). A translation-like cycle is a quality control checkpoint for maturing 40S ribosome subunits. Cell *150*, 111–121.

Suka, N., Nakashima, E., Shinmyozu, K., Hidaka, M., and Jingami, H. (2006). The WD40-repeat protein Pwp1p associates in vivo with 25S ribosomal chromatin in a histone H4 tail-dependent manner. Nucleic Acids Res. *34*, 3555–3567.

Sweet, T., Khalili, K., Sawaya, B.E., and Amini, S. (2003). Identification of a novel protein from glial cells based on its ability to interact with NF-kappaB subunits. J. Cell. Biochem. *90*, 884–891.

Sweet, T., Sawaya, B.E., Khalili, K., and Amini, S. (2005). Interplay between NFBP and NF-kappaB modulates tat activation of the LTR. J. Cell. Physiol. *204*, 375–380.

Sweet, T., Yen, W., Khalili, K., and Amini, S. (2008). Evidence for involvement of NFBP in processing of ribosomal RNA. J. Cell. Physiol. *214*, 381–388.

Talkish, J., Zhang, J., Jakovljevic, J., Horsey, E.W., and Woolford, J.L. (2012). Hierarchical recruitment into nascent ribosomes of assembly factors required for 27SB pre-rRNA processing in Saccharomyces cerevisiae. Nucl. Acids Res. *40*, 8646–8661.

Tang, L., Sahasranaman, A., Jakovljevic, J., Schleifman, E., and Woolford, J.L. (2008). Interactions among Ytm1, Erb1, and Nop7 Required for Assembly of the Nop7-Subcomplex in Yeast Preribosomes. Mol Biol Cell *19*, 2844–2856.

Thomson, E., and Tollervey, D. (2010). The Final Step in 5.8S rRNA Processing Is Cytoplasmic in Saccharomyces cerevisiae. Mol. Cell. Biol. *30*, 976–984.

Tollervey, D. (1987). A yeast small nuclear RNA is required for normal processing of pre-ribosomal RNA. EMBO J. *6*, 4169–4175.

Tollervey, D., and Guthrie, C. (1985). Deletion of a yeast small nuclear RNA gene impairs growth. EMBO J. *4*, 3873–3878.

Torchet, C., and Hermann-Le Denmat, S. (2000). Bypassing the rRNA processing endonucleolytic cleavage at site A2 in Saccharomyces cerevisiae. RNA *6*, 1498–1508.

Torchet, C., Jacq, C., and Hermann-Le Denmat, S. (1998). Two mutant forms of the S1/TPR-containing protein Rrp5p affect the 18S rRNA synthesis in Saccharomyces cerevisiae. RNA *4*, 1636–1652.

Trapman, J., and Planta, R.J. (1975). Detailed analysis of the ribosomal RNA synthesis in yeast. Biochim. Biophys. Acta *414*, 115–125.

Trendelenburg, M. (1974). Morphology of ribosomal RNA cistrons in oocytes of the water beetle, Dytiscus marginalis L. Chromosoma *48*,.

Trendelenburg, M.F., and Gurdon, J.B. (1978). Transcription of cloned Xenopus ribosomal genes visualised after injection into oocyte nuclei. Nature *276*, 292–294.

Trumtel, S., Léger-Silvestre, I., Gleizes, P.-E., Teulières, F., and Gas, N. (2000). Assembly and Functional Organization of the Nucleolus: Ultrastructural Analysis of Saccharomyces cerevisiae Mutants. Mol Biol Cell *11*, 2175–2189.

Tschochner, H., and Hurt, E. (2003). Pre-ribosomes on the road from the nucleolus to the cytoplasm. Trends in Cell Biology *13*, 255–263.

Tsuno, A., Miyoshi, K., Tsujii, R., Miyakawa, T., and Mizuta, K. (2000). RRS1, a conserved essential gene, encodes a novel regulatory protein required for ribosome biogenesis in Saccharomyces cerevisiae. Mol. Cell. Biol. *20*, 2066–2074.

Turner, A.J., Knox, A.A., Prieto, J.-L., McStay, B., and Watkins, N.J. (2009). A novel small-subunit processome assembly intermediate that contains the U3 snoRNP, nucleolin, RRP5, and DBP4. Mol. Cell. Biol. *29*, 3007–3017.

Tycowski, K.T., Smith, C.M., Shu, M.D., and Steitz, J.A. (1996). A small nucleolar RNA requirement for site-specific ribose methylation of rRNA in Xenopus. Proc. Natl. Acad. Sci. U.S.A. *93*, 14480–14485.

Udem, S.A., and Warner, J.R. (1973). The cytoplasmic maturation of a ribosomal precursor ribonucleic acid in yeast. J. Biol. Chem. *248*, 1412–1416.

Ulbrich, C., Diepholz, M., Bassler, J., Kressler, D., Pertschy, B., Galani, K., Böttcher, B., and Hurt, E. (2009). Mechanochemical removal of ribosome biogenesis factors from nascent 60S ribosomal subunits. Cell *138*, 911–922.

Vanacova, S., and Stefl, R. (2007). The exosome and RNA quality control in the nucleus. EMBO Rep. *8*, 651–657.

Vanácová, S., Wolf, J., Martin, G., Blank, D., Dettwiler, S., Friedlein, A., Langen, H., Keith, G., and Keller, W. (2005). A new yeast poly(A) polymerase complex involved in RNA quality control. PLoS Biol. *3*, e189.

Vanrobays, E., Gélugne, J.-P., Caizergues-Ferrer, M., and Lafontaine, D.L.J. (2004). Dim2p, a KH-domain protein required for small ribosomal subunit synthesis. RNA *10*, 645–656.

Vaughn, J.L., Goodwin, R.H., Tompkins, G.J., and McCawley, P. (1977). The establishment of two cell lines from the insect Spodoptera frugiperda (Lepidoptera; Noctuidae). In Vitro *13*, 213–217.

Venema, J., Planta, R.J., and Raué, H.A. (1998). In vivo mutational analysis of ribosomal RNA in Saccharomyces cerevisiae. Methods Mol. Biol. *77*, 257–270.

Venema, J., and Tollervey, D. (1996). RRP5 is required for formation of both 18S and 5.8S rRNA in yeast. EMBO J. *15*, 5701–5714.

Venema, J., and Tollervey, D. (1999). Ribosome synthesis in Saccharomyces cerevisiae. Annu. Rev. Genet. *33*, 261–311.

Venema, J., Vos, H.R., Faber, A.W., Van Venrooij, W.J., and Raué, H.A. (2000). Yeast Rrp9p is an evolutionarily conserved U3 snoRNP protein essential for early pre-rRNA processing cleavages and requires box C for its association. RNA *6*, 1660–1671.

Vos, H.R., Bax, R., Faber, A.W., Vos, J.C., and Raué, H.A. (2004a). U3 snoRNP and Rrp5p associate independently with Saccharomyces cerevisiae 35S pre-rRNA, but Rrp5p is essential for association of Rok1p. Nucleic Acids Res. *32*, 5827–5833.

Vos, H.R., Faber, A.W., De Gier, M.D., Vos, J.C., and Raué, H.A. (2004b). Deletion of the three distal S1 motifs of Saccharomyces cerevisiae Rrp5p abolishes pre-rRNA processing at site A(2) without reducing the production of functional 40S subunits. Eukaryotic Cell *3*, 1504–1512.

Warner, J.R. (1999). The economics of ribosome biosynthesis in yeast. Trends in Biochemical Sciences *24*, 437–440.

Wegierski, T., Billy, E., Nasr, F., and Filipowicz, W. (2001). Bms1p, a G-domain-containing protein, associates with Rcl1p and is required for 18S rRNA biogenesis in yeast. RNA *7*, 1254–1267.

Wery, M., Ruidant, S., Schillewaert, S., Leporé, N., and Lafontaine, D.L.J. (2009). The nuclear poly(A) polymerase and Exosome cofactor Trf5 is recruited cotranscriptionally to nucleolar surveillance. RNA *15*, 406–419.

Wessel, D., and Flügge, U.I. (1984). A method for the quantitative recovery of protein in dilute solution in the presence of detergents and lipids. Anal. Biochem. *138*, 141–143.

Wild, T., Horvath, P., Wyler, E., Widmann, B., Badertscher, L., Zemp, I., Kozak, K., Csucs, G., Lund, E., and Kutay, U. (2010). A protein inventory of human ribosome biogenesis reveals an essential function of exportin 5 in 60S subunit export. PLoS Biol. *8*, e1000522.

Wilson, D.N., and Nierhaus, K.H. (2005). Ribosomal proteins in the spotlight. Crit. Rev. Biochem. Mol. Biol. *40*, 243–267.

Wimberly, B.T., Brodersen, D.E., Clemons, W.M., Morgan-Warren, R.J., Carter, A.P., Vonrhein, C., Hartsch, T., and Ramakrishnan, V. (2000). Structure of the 30S ribosomal subunit. Nature *407*, 327–339.

Wu, J., Zhang, Y., Wang, Y., Kong, R., Hu, L., Schuele, R., Du, X., and Ke, Y. (2012). Transcriptional repressor NIR functions in the ribosome RNA processing of both 40S and 60S subunits. PLoS ONE *7*, e31692.

Yamamoto, R.T., Nogi, Y., Dodd, J.A., and Nomura, M. (1996). RRN3 gene of Saccharomyces cerevisiae encodes an essential RNA polymerase I transcription factor which interacts with the polymerase independently of DNA template. EMBO J. *15*, 3964–3973.

Yao, W., Lutzmann, M., and Hurt, E. (2008). A versatile interaction platform on the Mex67-Mtr2 receptor creates an overlap between mRNA and ribosome export. EMBO J. *27*, 6–16.

Yao, W., Roser, D., Köhler, A., Bradatsch, B., Bassler, J., and Hurt, E. (2007). Nuclear export of ribosomal 60S subunits by the general mRNA export receptor Mex67-Mtr2. Mol. Cell *26*, 51–62.

Yeh, L.C., Thweatt, R., and Lee, J.C. (1990). Internal transcribed spacer 1 of the yeast precursor ribosomal RNA. Higher order structure and common structural motifs. Biochemistry *29*, 5911–5918.

Young, C.L., and Karbstein, K. (2011). The roles of S1 RNA-binding domains in Rrp5's interactions with pre-rRNA. RNA *17*, 512–521.

Yusupov, M.M., Yusupova, G.Z., Baucom, A., Lieberman, K., Earnest, T.N., Cate, J.H., and Noller, H.F. (2001). Crystal structure of the ribosome at 5.5 A resolution. Science *292*, 883–896.

Zagorski, J., Tollervey, D., and Fournier, M.J. (1988). Characterization of an SNR gene locus in Saccharomyces cerevisiae that specifies both dispensible and essential small nuclear RNAs. Mol. Cell. Biol. *8*, 3282–3290.

Zhang, J., Harnpicharnchai, P., Jakovljevic, J., Tang, L., Guo, Y., Oeffinger, M., Rout, M.P., Hiley, S.L., Hughes, T., and Woolford, J.L. (2007). Assembly factors Rpf2 and Rrs1 recruit 5S rRNA and ribosomal proteins rpL5 and rpL11 into nascent ribosomes. Genes Dev *21*, 2580–2592.

Zhang, Y., Sikes, M.L., Beyer, A.L., and Schneider, D.A. (2009). The Paf1 complex is required for efficient transcription elongation by RNA polymerase I. Proc. Natl. Acad. Sci. U.S.A. *106*, 2153–2158.

Zhang, Y., Smith, A.D., 4th, Renfrow, M.B., and Schneider, D.A. (2010). The RNA polymerase-associated factor 1 complex (Paf1C) directly increases the elongation rate of RNA polymerase I and is required for efficient regulation of rRNA synthesis. J. Biol. Chem. *285*, 14152–14159.

7 Abbreviations

aa	amino acid
AmpR	resistance marker for ampicillin
APS	ammonium persulfate
ATP	adenosine triphosphate
bp	base pair(s)
ChIP	chromatin immunoprecipitation
ChlR	resistance marker for chloramphenicol
co-IP	co-immunoprecipitation
cryo-EM	cryo-electron microscopy
Da	Dalton
DNA	desoxyribonucleic acid
dNTP	2-desoxyribonucleotide 5' triphosphate
EDTA	ethylene diamine tetra acetate
EGTA	ethylene glycol tetraacetic acid
ETS	external transcribed spacer
g	gram(s)
GentR	resistance marker for gentamycin,
GFP	green fluorescent protein
h	hour(s)
HA	hemagglutinin
In	Input
IP	immunoprecipitation
IPTG	isopropyl-thiogalactoside
iTRAQ	isobaric tag for relative and absolute quantitation
ITS 1/2	internal transcribed spacer 1/2
k	kilo
kb	kilo base pair(s)
l	liter(s)
LB	luria broth
loxP	Cre-lox recombination site
LSU	large ribosomal subunit
lys	lysate
M	molar (mol/l)
MALDI	matrix-assisted laser desorption/ionisation
mg	milligram(s)
min	minute(s)
ml	milliliter(s)
mRNA	messenger RNA
MS	mass spectrometry
MS/MS	tandem mass spectrometry
MW	molecular weight
NB	Northern blotting
nm	nanometer(s)
OD	optical density
PAGE	poly acryl amide electrophoresis
PA/ProtA	Protein A

PCR	polymerase chain reaction
PEG	poly ethylene glycol
PEX	primer extension reaction
pGAL	GAL1/10 promoter
pH	negative decadic logarithm of [H+]
Pol-I	RNA polymerase I
Pol-II	RNA polymerase II
Pol-III	RNA polymerase III
polh	baculoviral promoter
p10	baculoviral promoter
qPCR	quantitative PCR
rDNA	ribosomal DNA
RNA	ribonucleic acid
RNP	ribonucleoprotein complex
rpm	rotations per minute
r-protein	ribosomal protein
rpL	ribosomal protein of the large subunit
rpS	ribosomal protein of the small subunit
rRNA	ribosomal RNA
RT	room temperature
s	second(s)
S	sedimentation coefficient
SCD	synthetic complete medium containing glucose
SCG	synthetic complete medium containing galactose
SDS	sodium dodecyl sulfate
snoRNA	small nucleolar ribonucleic acid
snoRNP	small nucleolar ribonucleoprotein
SOE-PCR	spliced overlap extension PCR
SpecR	resistance marker for spectinomycin
SSU	small ribosomal subunit
S1	S1 RNA binding motif
TAP tag	tandem affinity purification tag
Taq	Thermus aquaticus
TCA	tri-chloro acetic acid
TEMED	tetramethylethylenediamine
Tn7L/R	Tn7 transposition sequences
TOF	time of flight
TPR	tetratricopeptide repeat
Tris	tris(hydroxy methyl) amino methane
ts	temperature sensitive
U	unit(s)
WB	Western blotting
wt	wild-type
X-Gal	5-bromo-4-chloro-3-indolyl-beta-D-galactopyranoside
YFP	yellow fluorescent protein
YPD	full medium containing glucose
YPG	full medium containing galactose
µ	micro

8 Table of Figures

9 Publications

Hierlmeier, T., Merl, J., Sauert, M., Perez-Fernandez, J., Schultz, P., Bruckmann, A., Hamperl, S., Ohmayer, U., Rachel, R., Jacob, A., et al. (2012). Rrp5p, Noc1p and Noc2p form a protein module which is part of early large ribosomal subunit precursors in S. cerevisiae. Nucl. Acids Res.

Kühn*, H., Hierlmeier*, T., Merl, J., Jakob, S., Aguissa-Touré, A.-H., Milkereit, P., and Tschochner, H. (2009). The Noc-domain containing C-terminus of Noc4p mediates both formation of the Noc4p-Nop14p submodule and its incorporation into the SSU processome. PLoS ONE *4*, e8370.

Ohmayer*, U., Perez-Fernandez*, J., Hierlmeier*, T., Pöll, G., Williams, L., Griesenbeck, J., Tschochner, H., and Milkereit, P. (2012). Local tertiary structure probing of ribonucleoprotein particles by nuclease fusion proteins. PLoS ONE *7*, e42449.

Jakob, S., Ohmayer, U., Neueder, A., Hierlmeier, T., Perez-Fernandez, J., Hochmuth, E., Deutzmann, R., Griesenbeck, J., Tschochner, H., and Milkereit, P. (2012). Interrelationships between yeast ribosomal protein assembly events and transient ribosome biogenesis factors interactions in early pre-ribosomes. PLoS ONE *7*, e32552.

Merl*, J., Jakob*, S., Ridinger, K., Hierlmeier, T., Deutzmann, R., Milkereit, P., and Tschochner, H. (2010). Analysis of ribosome biogenesis factor-modules in yeast cells depleted from pre-ribosomes. Nucleic Acids Res. *38*, 3068–3080.

*: these authors contributed equally to this work

10 Acknowledgements / Danksagung

Zu guter Letzt möchte ich mich ganz herzlich bei allen bedanken, die zum Gelingen dieser Arbeit beigetragen haben:

Mein Dank gilt vor allem Prof. Dr. Herbert Tschochner für die Möglichkeit an seinem Lehrstuhl zu promovieren, für die interessante Themenstellung und für die ausgezeichnete Betreuung während der Doktorarbeit, die neben der wissenschaftlichen Ausbildung auch noch Zusatzkurse im alpinen Bereich beinhaltete.

Im Besonderen möchte ich mich auch bei Dr. Philipp Milkereit für die zahlreichen Diskussionen bedanken, die nicht nur wertvolle Vorschläge und Anregungen für den Fortgang der Arbeit lieferten, sondern auch maßgeblich dazu beitrugen eine kritische Sichtweise zu entwickeln.

Vielen Dank auch an Dr. Joachim Griesenbeck und alle anderen aktuellen und früheren Mitglieder der „Selbsthilfegruppe Noc-Proteine/Ribosomenbiogenese“, die stets mit Rat und Tat zur Seite standen. Insbesondere seien hier Dr. Juliane Merl und Martina Sauert erwähnt, deren Arbeiten den Grundstein für die Rekonstitution und Charakterisierung des Rrp5p/Noc1p/Noc2p Moduls legten.

Bei Dr. Jorge Perez-Fernandez und Dr. Astrid Bruckmann möchte ich mich für die Bereitstellung der Proteomanalysen von Polymerase-assoziertem Chromatin bedanken.

Mein Dank gilt auch Dr. Jochen Baßler für sein Mentorat und die Zusammenarbeit bei der Publikation der Ergebnisse dieser Arbeit.

Auch allen anderen Mitgliedern des „House of the Ribosome“ sei gedankt für ein freundschaftliches und hilfsbereites Arbeitsumfeld.

Ganz herzlich möchte ich mich bei meiner Labornachbarin Gisela Pöll dafür bedanken, dass sie oft Nachsicht walten ließ, wenn im Eifer der Forschung das Chaos überhandnahm, sowie für den nie versiegenden Nachschub an Kuchen und anderen Köstlichkeiten, und für die Einführung in die Blaubeerreviere.

Besonderer Dank gilt meinem Vater, der mich stets voll und ganz unterstützt hat und ohne den meine gesamte Ausbildung so nicht möglich gewesen wäre.

Abschließend ein großes Dankeschön an meine Freundin Kathleen, die meist Verständnis für lange Labortage oder Schreibtischzeiten aufbrachte, zur rechten Zeit allerdings auch einschritt und daran erinnerte, dass daneben noch andere Dinge wichtig sind.